ABSTRACT

Title of Thesis: IMPACT OF BREAKWATERS ON SEDIMENT CHARACTERISTICS AND SUBMERGED AQUATIC VEGETATION

Nicole Barth, Master of Science, 2011

Thesis directed by: Assistant Professor Cindy M. Palinkas
Associate Professor Evamaria W. Koch
Horn Point Laboratory

This study examined the impact of breakwaters, with varying ages (1-19 y) and in 3 salinity regions of Chesapeake Bay, on sediment characteristics and submerged aquatic vegetation (SAV). Sediment and SAV characteristics were determined at an adjacent-exposed and a breakwater-protected site in 24 locations. A mesocosm experiment was also conducted to evaluate SAV response to 4 organic-content treatments for 3 SAV species (*Ruppia maritima, Vallisneria americana* and *Zannichellia palustris*).

Breakwater effects on sedimentation were site-specific, some sites, having no apparent effect, while others where sandy shoreline erosion was dominant, an increase in grain size and sedimentation rate was observed. At other sites breakwaters facilitated fine-sediment deposition. SAV responses in the mesocosms, were highly variable with organic content. Therefore, SAV biomass in breakwater-protected area was related to the amount and type of sediments that the breakwater retained. Site evaluations should be conducted before breakwater construction if SAV colonization is desired.

IMPACT OF BREAKWATERS ON SEDIMENT CHARACTERISTICS AND SUBMERGED AQUATIC VEGETATION

by

Nicole Barth

Thesis submitted to the Faculty of the Graduate School of the

University of Maryland, College Park in partial fulfillment

of the requirements for the degree of

Master of Science

2011

Advisory Committee:

Assistant Professor Cindy M. Palinkas – Co-advisor
Associate Professor Evamaria W. Koch – Co-advisor
Dr. Deborah J. Shafer

Acknowledgements

I cannot thank Donna and Kevin enough for all of your support, encouragement, and laughs that kept me going! I could not have done this without you and your friendships mean a great deal to me! Thanks to my parents for your love and support, my love of marine and environmental science grew from many family camping trips. I could not have completed the field and laboratory work without the help of Dale, Bern, Taylor, Annie, and all my friends and family that gave of their time to help! Thanks to my committee, Cindy, Eva, and Debbie, I appreciate your guidance and support through this process. The maintenance department at Horn Point Laboratory was also a huge help and I appreciate you all very much! Thanks to Horn Point Laboratory for this wonderful experience and the Army Corps of Engineers for funding the project.

Table of Contents

List of Tables

List of Figures

Chapter 1

INTRODUCTION

Shoreline erosion is a worldwide problem with 70% of the world's beaches retreating over the past century, and with less than 10% prograding (Bird, 1993). Although sea-level rise (SLR) plays a major role in shoreline erosion, increased urbanization and human actions, such as offshore dredging, dam construction, and the destruction of submerged aquatic vegetation (SAV), marshes and dunes, have compounded the problem (Living Shorelines Summit, 2006). Erosion rates vary globally and are site specific. For example, along the coast of Oregon, USA, sea bluffs experiencing uplift show low erosion rates, but bluffs experiencing little uplift have greater rates of erosion (Komar and Shih, 1993).

In the USA, the areas experiencing highest relative SLR, extensive shoreline erosion, and accelerated shoreline hardening are the marshes along the Mississippi River delta as well as the Chesapeake Bay (Titus and Richman, 2001). From 1940 to 1980, relative SLR in Chesapeake Bay has been 2.5-3.6 mm/year (Hicks et al., 1983; Davis, 1987), a rate that is projected to increase 2-5 times by 2100 (Titus and Narayanan, 1995). There are areas within the Chesapeake Bay experiencing rises twice the global rate (1.8 mm/y; Kearney et al., 2002; Church and White, 2006) due to local land subsidence of 0.6-2.6 mm/y (Holdahl and Morrison, 1974; Davis, 1987).

Currently, approximately one-third of Chesapeake Bay's 18,800 km of shoreline is classified as eroding, with rates up to 20-40 cm/year (Chesapeake Bay Program, 2005), depending on local wave characteristics, fetch, and sediment composition (Wray et al.,

1995). Chesapeake Bay islands experience some of the highest rates of erosion. The upland islands Barren, James and Poplar Islands, have lost 76%, 89%, and 88% of their area, respectively: low-lying marsh islands such as Bloodsworth, Smith, and South Marsh Islands have been reduced by 16%-28%, in the last 140 years (Wray et al., 1995). In some instances, entire islands within the Bay have disappeared; in some locations steps are being taken to prevent this disappearance (e.g., Tangier Island; Kearney and Stevenson, 1991; Mills et al., 2005 and Poplar Island; Dalal et al., 1999). Although coastal protection (rip rap) has reduced erosion at Hoopers Island; it has still diminished by 25% in the last 140 years (Wray et al., 1995).

Shoreline erosion has led to an increase in shoreline hardening-structures worldwide. In some areas, these structures cover a large portion of the shoreline. For example, over 50% of the Italian coast is hardened (Bacchiocchi and Airoldi, 2003), and more than 70% is hardened in Barnegat Bay, NJ and San Diego, CA (Lathrop, et al., 1997; Davis et al., 2002). Most of the land (85%) along Chesapeake Bay shorelines is privately owned (Chesapeake Bay Program, 2005), and property owners generally seek to protect their shoreline. Approximately 25% of the Chesapeake Bay shoreline (mainstem and tributaries) is hardened, and some sub-watersheds are >50% armored (Berman et al., 2000).

Shoreline-protection techniques can be non-structural, structural, or a combination of the two (Bulleri and Chapman, 2010). Structural methods use materials like rocks, wood, and cement to reduce erosion and include seawalls/bulkheads, revetments, breakwaters, groins, and sills/perched beaches. According to the US Army Corps of Engineers (USACE) Coastal Engineering Manual (2008), seawalls or bulkheads are

vertical retaining walls that hold back land from falling into the water. Rip rap is a common type of revetment, which is a material minimally affected by erosion (e.g., boulders) and is placed on a sloping bank to stabilize it. Breakwaters are constructed parallel to the shoreline and reduce erosion by reducing wave energy. Groins work in a similar fashion but are constructed perpendicular to the shoreline. Low-lying sills can be built to trap sand behind them, creating a beach that is elevated above its original level, also known as a perched beach.

The effects of shoreline hardening structures on physical processes are relatively well known. For example, scour is increased around pilings, and bulkheads increase wave energy seaward of the structure, increasing erosion of the seabed (Neelamani and Sandhya, 2004). Bulkheads also retain terrestrial sediments, starving the landward area (Nordstrom et al., 2009). In contrast, the ecological consequences of hardening shorelines have only received attention relatively recently (French, 1997; Loreau et al., 2002; Airoldi et al., 2005; Martin et al., 2005; Moschella et al., 2005; Birben et al., 2007; Gislason et al., 2009; Martins et al., 2009). In general, the introduction of rocky substrate, such as the material used in many coastal structures, alters the benthic habitat and fragments the coast (Moschella et al., 2005). Species diversity shifts as rocky substrate replaces the soft bottom habitat (Loreau et al., 2002). Mud is typically characterized by burrowing, deposit-feeding organisms, while sandy sediments tend to have mobile, suspension-feeding organisms (Martins et al., 2009) and rocky areas are dominated more by algae and marine animals (Moschella et al., 2005).

The intended effect of breakwaters is to reduce wave energy, by intercepting incident waves and causing them to break or reflect (Stamos and Hajj, 2001). This

reduction of energy reduces shoreline erosion and facilitates sediment deposition landward of the structure, resulting in higher sedimentation rates (Chasten et al., 1994). The specific ecosystem response to the substrate alteration when breakwaters are built however, is dependent on many factors (Birben et al., 2007) and is typically site specific (Airoldi et al., 2005). The presence of breakwaters may lead to changes in sediment characteristics (Martins et al., 2009), as they tend to cause decreasing sediment grain size, increasing sediment organic content, and changing redox conditions landward of the structure (Martin et al., 2005; Zhang and Feng, 2010). The exchange of sediment and biota between shore and deeper water is disrupted (Martins et al., 2009) as is the sediment supply to natural coastal defenses such as dunes, beaches and marshes (French, 1997). Breakwaters also tend to trap sediment landward of the structure, increasing sediment accumulation rates (SARs). SARs tend to be highest when breakwater segments are shorter and closer to shore (Birben et al., 2007).

Non-structural methods of protecting shorelines involving vegetative planting to stabilize the substrate (Living Shorelines Summit, 2006) have gained appreciation in recent years. As of October 1, 2008, "The Living Shoreline Protection Act" requires property owners in the Chesapeake Bay area to use nonstructural shoreline stabilization where feasible, which should characterize ~90% of Chesapeake Bay shorelines (Annotated Code of Maryland's Environmental Article Section 16-201, 2008).

Protecting shorelines is important however, protection techniques should be executed in a way to minimize impacts to the surrounding ecosystems, especially those that are already suffering great losses, such as SAV (Orth and Moore, 1983; Orth and Moore, 1984). SAV beds are one of the most important ecosystems in the Chesapeake

Bay, as they serve as habitat for fish, crabs, waterfowl, and many other organisms (Corona et al., 2000; Lazzari and Stone, 2006; Rybicki and Landwehr, 2007; Ma et al., 2010). SAV beds can also attenuate waves (Fonseca and Cahalan, 1992) and reduce current velocity (Fonseca et al., 1981; Gambi et al., 1990; Peterson et al., 2004), leading to a reduction of sediment resuspension and erosion (Fonseca and Fisher, 1986; Koch, 1999; Gacia and Duarte, 2001; Widdows et al., 2008). However, SAV populations have suffered major declines globally, (Waycott et al., 2009; Short et al., 2011), including the Chesapeake Bay (Orth and Moore, 1983; Orth and Moore, 1984; Orth et al., 2008).

Restoration efforts in Chesapeake Bay are attempting to bring SAV back to historical levels but have been met with mixed results (Orth et al., 2002; Shafer and Bergstrom, 2010). Recent improvements in restoration techniques have been made (Ailstock et al., 2010; Busch et al., 2010; Hengst et al., 2010; Koch et al., 2010; Leschen et al., 2010; Moore et al., 2010; Pan et al., 2011). Even so, there is still room for improvement in the site-selection process for large-scale restoration projects.

Light is the main parameter limiting SAV distribution (Kemp et al., 1984), yet SAV do not always grow successfully in areas where this habitat requirement has been met. Parameters other than light may also play a major role in SAV distribution (Koch, 2001). For example, in Florida's Indian River Lagoon, only 50% of the variation in seagrass distribution was attributed to light attenuation, with the rest being influenced by wave action, sediment grain size and toxicity, substrate reflectance, epiphytic growth on shoots, and competition with algae (Steward et al., 2005). Waves limit the upper (shallow-water) distribution depth of the seagrass *Posidonia oceanica* (Infantes, 2009),

and sediment characteristics have been shown to play a major role in the restoration of *Zostera marina* in Boston Harbor (Leschen et al., 2010).

Breakwaters are viewed as an alternative to direct hardening for the protection of relatively exposed shorelines (Hardaway and Gunn, 2010), but not much is known about their impacts on biota, especially SAV. An evaluation of the effect of 20 breakwaters on SAV within the Chesapeake Bay, using aerial photography, determined that SAV coverage in the area surrounding the breakwater (i.e., in the breakwater-protected and the adjacent-exposed areas) was influenced by region-wide processes rather than the existence of the breakwater (Karrh, 2000). Of the 20 breakwaters, 8 had small increases in SAV coverage, which was attributed to reduced wave action by the breakwater. In 5 breakwater locations, a minor decrease of SAV was observed. The overall conclusion of the study was that breakwaters have no effect on SAV presence; however, actual SAV density, species composition, or biomass were not measured (Karrh, 2000). In a later modeling study SAV growth potential was predicted to increase by 0.3% (2.5 shoots m^{-2} d^{-1}) when breakwaters attenuate waves and reduce sediment resuspension, resulting in less turbid water (Smith et al., 2009).

Increased sediment deposition due to a reduction in physical energy by breakwaters leads to changes in the sediment characteristics (Martins et al., 2009). We hypothesize that SAV distribution in breakwater-protected areas is affected by this change in sediment characteristics. SAV also reduce water flow causing an increase in sediment deposition (Kenworthy et al., 1982; Ward et al., 1984; Gacia et al., 1999; Bos et al., 2007; Hendriks et al., 2008). This decrease in flow, when combined with the

reduction in wave energy from a breakwater, leads to a more rapid deposition of fine-grained and organic material (Martin et al., 2005).

Sediment characteristics that may affect SAV growth and distribution include grain size, organic content, and porewater geochemistry (Short, 1987; Silva et al., 2009). In Boston Harbor, the seagrass *Z. marina* was successfully restored at sites with <35% silt/clay but failed in areas with > 57% silt/clay (Leschen et al., 2010). However, Krause-Jensen et al. (2011) determined 13% silt/clay to be a threshold value for *Z. marina*, in Danish coastal waters. Thus, these sediment requirements are likely to be species- and site-specific. For example, plants growing in quiescent waters may be more tolerant of fine and organic sediments, as they are less likely to be uprooted (Wicks et al., 2009). Additionally, sediments may become too coarse and hinder recolonization of the substrate, as was observed after dredging caused an increase in tidal wave penetration in Ria de Aveiro, Portugal, therefore increasing erosion of fine sediments (Silva et al, 2009). The potential for regional differences in SAV response to sediment characteristic thresholds is great, as are differences across the salinity gradient.

As the amount of fine particles in SAV beds increases, so does the sediment organic content, since these two characteristics are closely correlated (Silva et al., 2009). As with sediment grain size, sediment organic content is also considered limiting for SAV growth and distribution. A threshold of >5% organic matter has been suggested for SAV in general (Barko and Smart, 1983), but this value is also likely to be species- and site-specific and may differ between field and laboratory observations. Approximately 20% organic content limited *Myriophyllum spicatum* L. and *Hydrilla verticillata* growth in a greenhouse experiment (Barko and Smart, 1986). In another experiment, *H.*

verticillata grew better in sediments containing 2.3% organic matter than sediments containing 0.3% organic matter when grown in mixed cultures with *Vallisneria americana* (Ye et al., 2009). However, *V. americana* has been observed growing in sediments ranging from 0.3 to 44.1% organic-matter content in the field (Kreiling et al., 2007; Makkay et al., 2008; Moore et al., 2010). This broad range of values suggests that SAV are rather plastic in their response to sediment characteristics and/or that plants have site-specific responses to local sediments. Sediment habitat requirements for SAV in the Chesapeake Bay have not yet been determined.

The purpose of this study is to assess the effect of breakwaters on SAV via changes in sediment characteristics over time. The specific objectives are to: 1) determine long-term (pre-construction) and short-term (post-construction) sedimentation rates in breakwater-protected and adjacent exposed areas; 2) compare and contrast present SAV distribution and sediment characteristics (i.e., organic matter and grain size) in the rhizosphere at breakwaters with varying ages in the Chesapeake Bay; 3) assess the effect of varying sediment grain size and organic content on growth of 4 species of SAV found in the Chesapeake Bay (*Ruppia maritima, Potamogeton perfoliatus, Vallisneria americana,* and *Zannichellia palustris*), 3 of which are commonly used for restoration. These data will be used to make recommendations regarding the construction of breakwaters that minimize negative effects on SAV or possibly even enhance SAV growth.

The general hypothesis states that for a short period (few years) following construction, breakwaters enhance SAV distribution, but hinder their growth at a later time due to changes in sediment characteristics in the breakwater-protected area.

More specific hypotheses are:

Hypothesis 1: Sedimentation rates in breakwater-protected areas are greater than in adjacent wave-exposed areas. This is thought to occur because breakwaters reduce current and wave energy, allowing suspended fine particles to settle out of the water (Smith et al., 2009).

Hypothesis 2: SAV biomass is highest in sediments with ≤ 35% mud (silt and clay). A previous study in Chincoteague Bay found that 90% of the seagrasses *Zostera marina* and *Ruppia maritima* are found where sediments contain <35% mud at water depths of <2 m (Koch et al., in prep).

Hypothesis 3: SAV biomass is highest in sediments with less than 5% organic matter. A previous study has shown that >5% organic matter has a negative effect on SAV (Barko and Smart, 1983; 6 species were studied, however; this threshold may not apply to other species or in different salinity regimes).

Hypothesis 4: SAV biomass is greater in the breakwater-protected areas of younger breakwaters (<5 y) than in the adjacent-exposed areas. Protected areas of older breakwaters (>5 y) will have less SAV biomass than the adjacent-exposed area. Koch postulates that breakwaters provide a relatively quiescent environment that initially benefits SAV; however, over time, the deposition of fine sediments landward of the breakwater eventually leads to plant death (Koch, personal communication).

Chapter 2

Determining the influence of breakwaters on nearshore sedimentation in Chesapeake Bay: methods and observations

INTRODUCTION

Shoreline protection is becoming increasingly important, especially in response to accelerated shoreline erosion due to sea-level rise. Increased urbanization and anthropogenic activities, such as offshore dredging, dam construction, and the destruction of submerged aquatic vegetation (SAV) beds, marshes and dunes, have compounded the problem (Living Shorelines Summit, 2006), resulting in retreat of ~70% of the world's beaches over the past century (Bird, 1993). In the USA, the areas experiencing highest relative sea-level rise, extensive shoreline erosion, and accelerated shoreline hardening are the marshes along the Mississippi River delta and the Chesapeake Bay (Titus and Richman, 2001). Relative sea-level rise in Chesapeake Bay from 1940 to 1980 was 2.5-3.6 mm/y (Hicks et al., 1983; Davis 1987), a rate that is projected to increase 2-5 times by 2100 (Titus and Narayanan, 1995) due to land subsidence of 0.6-2.6 mm/y (Holdahl and Morrison, 1974; Davis, 1987). Currently, ~1/3 of Chesapeake Bay's 18,800 km of shoreline is classified as eroding, with rates up to 20-40 cm/y (Chesapeake Bay Program, 2005). These high rates of erosion have led to an increase in shoreline-hardening structures, especially since most (85%) of the Chesapeake shoreline is privately owned. Approximately 25% of the Chesapeake (mainstem and tributaries) shoreline is hardened; some sub-watersheds are >50% armored (Berman et al., 2000).

Shoreline-protection techniques can vary (Bulleri and Chapman, 2010), and while the effects of shoreline-hardening structures on physical processes are relatively well known, the ecological consequences of hardening shorelines have only received attention fairly recently (French, 1997; Loreau et al., 2002; Airoldi et al., 2005; Martin et al., 2005; Moschella et al., 2005; Birben et al., 2007). The intended effect of breakwaters is to reduce wave energy, by intercepting incident waves and causing them to break or reflect (Stamos and Hajj, 2001). This reduction of energy reduces shoreline erosion and facilitates sediment deposition landward of the structure, resulting in higher sedimentation rates (Chasten et al., 1994). The presence of breakwaters may also lead to changes in sediment characteristics (Martin et al., 2005), allowing finer-grained and more organic material to settle (Martin et al., 2005; Zhang and Feng, 2011). This change in sediment character may have implications for the benthic community, especially SAV, which in addition to water column habitat requirements (i.e., sufficient light) likely also has substrate requirements (Koch, 2001). While potential substrate requirements have only recently been explored, previous work has suggested that these requirements include the presence of a sufficiently thick sand layer (Wicks et al., 2009), relatively coarse material (<35% silt and clay; Leschen et al., 2010), and sedimentation rates high enough to bury seeds before germination (Palinkas and Koch, in review). Substrate requirements may also differ across salinity gradients and among species.

The overall goal of this study is to better understand the potential changes to both sediment character (grain size, organic content) and accumulation rates induced by breakwater construction. To accomplish this goal, trends at nearshore sites adjacent to 24 segmented, offshore breakwaters throughout Chesapeake Bay are first examined to

establish regional trends. Then, the evolution of the sedimentary record in the breakwater-protected areas is examined to assess possible changes.

MATERIALS AND METHODS

Field methods

Locations were selected for the study using aerial photography available at the Virginia Institute of Marine Science (VIMS; Orth et al., 2009; annual reports 1989-present). The photographs were examined for the presence of offshore, segmented breakwaters in areas with SAV within the last 20 years. Based on these criteria, 24 locations were chosen for study, representing a range of salinities (0-25) and ages (1-19 y; Table 2.1; Figure 2.1).

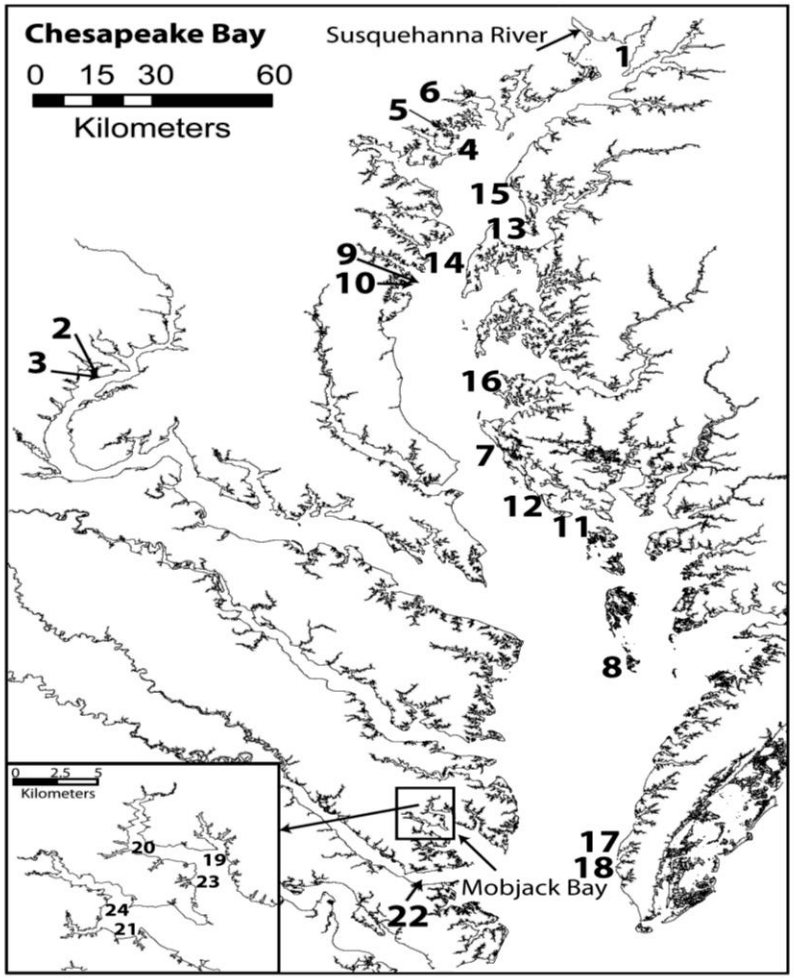

Figure 2.1. Map of breakwater study locations in Chesapeake Bay. Numbers correspond to location names listed in Table 2.1. At this scale, some locations appear to overlap (e.g., Mayo North and South, #9 and 10). Inset shows expanded view of locations in Mobjack Bay.

Table 2.1. Study locations and breakwater ages at the time of sampling. Most sediment cores were collected in 2009, except Elk Neck, Brannock Bay, Hoopers Island, and Bishops Head, which were sampled in 2008. Locations are divided by salinity region as defined by the Chesapeake Bay Program (CBP, 2004) and characterized by the values in parentheses. Within each salinity region, locations are listed by ascending age. (*A 36-cm sand layer is present at the top of the core that likely deposited between 2005 and 2007 and is not included in the sedimentation-rate calculation (Palinkas et al., 2010; Barth, 2011).

# (Fig. 1)	Location	Age (y)	Depth of Breakwater Influence
	Tidal fresh/oligohaline (0-5)		
1	Elk Neck	3	8
2	Mason Neck1	7	4
3	Mason Neck2	8	16
4	Hart-Miller Island	10	9
5	Sue Creek	15	8
6	Red Eyed Yacht Club	15	16
	Mesohaline (5-18)		
7	Taylors Island	1	1
8	Tangier Island	2	1
9	Mayo North	9	8
10	Mayo South	11	6
11	Bishops Head	11	22
12	Hoopers Island	14	23
13	Eastern Neck	15	108*
14	Highland Beach	18	32
15	Gratitude	19	10
16	Brannock Bay	19	30
	Polyhaline (18-25)		
17	Cape Charles Bay Creek	3	2.5
18	Cape Charles Public Beach	7	10
19	Mobjack Bay	7	32
20	Mobjack Bay5	8	10
21	Mobjack Bay7	8	16
22	Yorktown	16	30
23	Mobjack Bay3	17	32
24	Schley	18	29

Two vibracores (7-cm diameter, ~3-m length) were collected at each study site – one in the protected area landward of the breakwater (referred to as "breakwater-protected" throughout the paper) and one at the same water depth in the adjacent wave-exposed area (referred to as "adjacent-exposed"). A companion push core (5-cm diameter, ~20-cm long) was taken at the site of each vibracore to capture relatively undisturbed surface sediment. The vibracores were returned to the laboratory and frozen (-13ºC) in a vertical position until further analysis. Push cores were sectioned into 1-cm increments immediately upon returning to the lab. Prior to analysis, frozen vibracores were thawed, cut in half lengthwise, and sectioned into 1- (upper 20 cm) and 2-cm (rest of the core) increments. Sediments were then analyzed for grain size, organic matter, and the presence of naturally occurring radioisotopes (^{7}Be, ^{234}Th, ^{210}Pb, ^{137}Cs).

Laboratory methods

Sediment grain size was analyzed by wet-sieving samples through a 64-µm mesh to separate the sand and mud fractions. The mud fraction (<64 µm) was placed in a 0.05% sodium metaphosphate solution, placed in an ultrasonic bath, and then analyzed by a SediGraph 5120. Particles >64 µm (i.e., sand and gravel) were placed in a pre-weighed pan, dried for 24 h and then dry-sieved from 1-4 phi (500-64 µm) in ¼-phi increments (phi = $-\log_2$ (particle diameter in mm)). The mud and sand data were then joined to obtain the complete grain-size distribution for each sample, and the median diameter was calculated using MatLab. Samples for organic-content analysis were initially dried at 60º C until a constant weight was reached. Dried sediment was then combusted in a muffle furnace at 450º C for 4 h to determine the organic content (Erftemeijer and Koch, 2001).

Long-term (~100 y) sediment accumulation rates were determined by analyzing vibracore sediment for ^{210}Pb (half-life 22.3 y). ^{210}Pb is a decay product of ^{238}U; sources of ^{210}Pb to nearshore sediments include precipitation, runoff, and decay of its effective parent ^{226}Ra (Bruland et al., 1974). ^{210}Pb has previously been used in the Chesapeake Bay and its tributaries, and observed sediment accumulation rates typically range 0.2-1.0 cm/y (Brush et al., 1982; Yarbro et al. 1983; Marcus and Kearney, 1991; Arnold et al., 2000). ^{210}Pb activities were determined following the methods of Palinkas and Nittrouer (2006). Approximately 3 g of sediment were dried and spiked with a known amount of ^{209}Po. The samples were then digested in 15.8N HNO_3 and 6N HCl. ^{209}Po and ^{210}Po were electroplated onto silver planchets and then counted using alpha spectroscopy with a Canberra Alpha Analyst. Because ^{210}Pb preferentially absorbs to fine particles (Goodbred and Kuehl, 1998), activities in profiles at sites with significant grain-size variations and/or strong fining-upwards trends (which would produce an apparent increase in activity with depth) were normalized to the corresponding mud content. Accumulation rates were calculated as in Jaeger et al. (1998), assuming steady-state sedimentation and constant initial activity of ^{210}Pb. ^{210}Pb-derived sediment accumulation rates were verified with ^{137}Cs (half-life 30.7 y) via gamma spectroscopy of the 661.6 keV photopeak. Dried, ground sediment samples were placed in sealed, 60-mL containers, taking care to ensure consistent geometry. Each sample was then counted for 24 h using a Canberra germanium detector calibrated following Larsen and Cutshall (1981); activities were decay-corrected to the time of collection and normalized for salt content. ^{137}Cs first appeared in 1954 with the onset of atmospheric weapons testing, and activities peak in 1963 coincident with maximum fallout (Palinkas and Nittrouer, 2006).

The ^{210}Pb-derived rates represent pre-construction conditions in the breakwater-protected area, as they yield a ~100-y average accumulation rate. Short-term, post-construction, deposition rates at the breakwater-protected sites were intended to be calculated via the naturally occurring radionuclides ^{7}Be (half-life 53.3 d) and ^{234}Th (half-life 24.1 d; Sommerfield and Nittrouer, 1999; Sommerfield et al., 1999; Palinkas et al., 2005). ^{7}Be is formed from cosmic ray spallation of nitrogen and oxygen in the atmosphere and is deposited by precipitation and dry deposition onto terrestrial sediments (Olsen et al., 1986); its presence in the nearshore requires that sediments had been on land within the last ~250 d (4-5 half-lives). ^{7}Be has been used in Chesapeake Bay to examine short-term sediment dynamics (Dibb and Rice, 1989a; Dibb and Rice, 1989b), but its use is limited in sandy nearshore environments, because it attaches preferentially to fine-grained particles. ^{234}Th is produced continuously in seawater by the decay of ^{238}U and attaches to particles as they settle through the water column (Aller and Cochran, 1976). ^{7}Be and ^{234}Th activities were determined via gamma spectroscopy of the 477.7 and 63.3 keV photopeaks, following the methods described for ^{137}Cs. Unfortunately, measured activities were near or below the detection limit for many samples, limiting their utility. Thus, for consistency, post-construction deposition rates were calculated by interpreting the depth of breakwater influence from changes in sediment character, observed in grain-size and organic-content profiles, and dividing by the corresponding breakwater age.

Data analysis

SAS 9.2 was used for statistical analysis of data (Table 2.2). Data were tested for a normal distribution; if it was not normal, then a log transformation was performed. Levene's test was utilized to determine equality of variances (Sokal and Rolhf, 1995). The majority of the data fit the assumptions of normality and homogeneity. A paired t-test was conducted for grain size, organic matter, and accumulation rates between adjacent-exposed and breakwater-protected sites, as well as pre- and post-construction rates at the breakwater-protected sites (Sokal and Rolhf, 1995). A one-way ANOVA was completed for each location to determine differences between the adjacent-exposed and breakwater-protected site for grain size and organic matter (see Appendix). Linear regressions were completed for breakwater age versus depth of influence, grain size, and organic content. Linear regressions were also completed for fetch versus grain size and organic content for both adjacent-exposed and breakwater-protected sites, as well as fetch versus depth of influence at breakwater-protected sites (Sokal and Rolhf, 1995).

Table 2.2. Statistical results for sediment characteristics. P-value ≤ 0.05 is significantly different. R^2 value shows how closely the data conforms to a linear relationship.

Site	Factors	Degrees of Freedom	t-value	p-value	r^2-value
Paired T-test					
Adjacent-exposed versus Breakwater-protected	Grain Size	23	-1.21	0.24	
Adjacent-exposed versus Breakwater-protected	Organic Content	23	-1.25	0.22	
Adjacent-exposed versus Breakwater-protected	Accumulation Rates	20	0.79	0.44	

Breakwater-protected	Pre-/Post-construction Sedimentation Rates	21	-1.1	0.28	
Linear Regression					
Breakwater-protected	Depth of Breakwater Influence versus Age of Breakwater	1	4.76	<.0001	0.45
Breakwater-protected Tidal Fresh/ Oligohaline	Depth of Breakwater Influence versus Age of Breakwater	1	0.78	0.48	0.09
Breakwater-protected Mesohaline	Depth of Breakwater Influence versus Age of Breakwater	1	3.94	0.004	0.73
Breakwater-protected Polyhaline	Depth of Breakwater Influence versus Age of Breakwater	1	2.85	0.03	0.59
Breakwater-protected	Grain Size versus Age of Breakwater	1	-2.57	0.02	0.23
Breakwater-protected	Organic Content versus Age of Breakwater	1	-1.12	0.27	0.07
Breakwater-protected	Fetch versus Grain Size	1	1.09	0.29	0.05
Breakwater-protected Tidal Fresh/ Oligohaline	Fetch versus Grain Size	1	2.06	0.04	0.41
Breakwater-protected Mesohaline	Fetch versus Grain Size	1	1.00	0.35	0.09
Breakwater-protected Polyhaline	Fetch versus Grain Size	1	-1.32	0.24	0.21
Breakwater-protected	Fetch versus Organic Content	1	0.77	0.45	0.03
Breakwater-protected	Fetch versus Depth of Influence	1	-1.34	0.19	0.08
Adjacent-exposed	Fetch versus Grain Size	1	0.90	0.38	0.04
Adjacent-exposed	Fetch versus Organic Content	1	-0.30	0.77	0.004

RESULTS

Observations at adjacent-exposed sites

Surficial (0-10 cm) sediments at the adjacent-exposed sites tend to be sandy and low in organic content (Table 2.3). The median diameters of surficial sediment at adjacent-exposed sites ranged from medium sand (1.1 phi, 466.6 µm) to fine silt (6.9 phi, 8.4 µm) and have an average size of 3.0 phi (125.0 µm). Organic content ranged from 0.5 to 20.1%, averaging 2.6%. The maximum value occurred at Sue Creek, in the tidal fresh/oligohaline region of Chesapeake Bay, (20.1%) and is more than twice that of the next highest value (7.9 % at Mason Neck 1, in the oligohaline region of the Potomac River). Sedimentation rates ranged from 0.3 to 2.3 cm/y.

Table 2.3. Sediment characteristics at the adjacent-exposed (ADJ) and breakwater-protected (BW) sites for each location. Average median diameter (grain size) and organic content (mean±SE) refers to averages for surficial (0-10 cm) sediment. Grain-size trend for adjacent-exposed sites refers to that observed in vibracore profiles (see Fig. 3). Grain-size trend for the breakwater-protected sites refers to that observed in vibracore grain-size profiles below the depth of breakwater influence, which reflects historical (i.e., pre-construction) conditions. For many sites, only minimum accumulation rates can be calculated due to uniform-activity ^{210}Pb profiles or downward increases in activity. At the Red Eyed Yacht Club, the vibracore at the adjacent-exposed site was not analyzed for ^{210}Pb and so an accumulation rate was not calculated; the vibracore at the breakwater-protected site was not able to penetrate landscaping fabric emplaced during construction, so the pre-construction rate could not be determined.

Location	Average median diameter, phi (μm)	Grain-size trend (upward)	Average organic content, %	Sediment accumulation rate, cm/y, BW – pre-/post- construction
Tidal fresh				
Elk Neck- ADJ	2.6±0.02 (164.9)	Fining	0.6±0.1	1.2
BW	2.8±0.1 (143.6)	Fining	1.4±0.2	1.1/2.7
Mason Neck1-ADJ	3.0±0.5 (125.0)	No change	7.9±4.2	0.5
BW	4.0±0.4 (62.5)	No change	3.4±0.5	0.6/0.6
Mason Neck2-ADJ	1.7±0.1 (307.8)	No change	0.8±0.1	>1.5
BW	2.9±0.1 (134.0)	Fining	1.7±0.4	1.9/2.0
Hart-Miller Island-ADJ	1.6±0.03 (329.9)	No change	0.6±0.1	>1.6
BW	2.3±0.03 (203.1)	No change	0.4±0.02	3.1/0.9
Sue Creek-ADJ	2.3±0.4 (203.1)	Fining	20.1±3.6	>1.5
BW	1.5±0.1 (353.6)	No Change	0.6±0.2	0.5/0.5
Red Eyed Yacht Club-ADJ	2.7±0.1 (153.9)	No change	1.7±0.3	NA
BW	1.7±0.1 (307.8)	n/a	0.9±0.2	NA/1.1
Mesohaline				
Taylors Island-ADJ	6.9±0.2 (8.4)	No change	3.9±0.1	2.0
BW	5.5±1.1 (22.1)	No change	1.9±0.2	1.4/1.0
Tangier Island-ADJ	4.5±1.0 (44.2)	Fining	7.2±1.9	1.4
BW	3.3±0.2 (101.5)	No change	3.9±1.5	2.1/0.5
Mayo North-ADJ	2.0±0.1 (250.0)	Coarsening	0.7±0.04	0.4
BW	2.8±0.04 (143.6)	Coarsening	1.1±0.04	0.7/0.7
Mayo South-ADJ	2.0±0.1 (250.0)	No change	0.8±0.1	0.9
BW	3.0±0.04 (125.0)	No change	1.1±0.1	>0.5/>0.5
Bishops Head-ADJ	6.8±0.7 (9.0)	Fining	3.3±0.2	0.3
BW	4.5±0.3 (44.2)	Fining	4.1±0.3	1.1/2.0
Hoopers Island-ADJ	4.7±0.3 (38.5)	Fining	2.6±0.5	0.4
BW	3.0±0.03 (125.0)	Fining	2.1±0.8	0.6/1.1
Eastern Neck-ADJ	6.4±0.6 (11.8)	Fining	2.2±0.4	2.3
BW	2.5±0.03 (176.8)	Fining	0.4±01	2.6/4.9
Highland Beach-ADJ	1.1±0.1 (466.5)	No change	0.6±0.04	1.2
BW	2.4±0.03 (189.5)	No change	1.6±0.03	1.7/2.1
Gratitude-ADJ	2.2±0.2 (217.6)	No change	1.0±0.1	1.1
BW	1.7±0.2 (307.8)	Coarsening	1.9±0.7	1.1/1.8
Brannock Bay-ADJ	2.7±0.2 (153.9)	No change	1.3±0.1	0.9
BW	2.6±0.1 (164.9)	No change	1.1±0.1	1.0/1.6
Polyhaline				
Cape Charles Bay Creek-ADJ	2.1±0.04 (233.3)	Fining	1.3±0.3	Erosion
BW	1.9±0.04 (267.9)	No change	0.6±0.08	Erosion/0.8
Cape Charles Public Beach-ADJ	2.3±0.04 (203.1)	No change	0.6±0.01	Erosion

BW	2.1±0.1 (233.3)	No change	0.7±0.2	1.4/1.4
Mobjack Bay-ADJ	2.4±0.1 (189.5)	No change	0.6±0.1	>0.6
BW	2.9±0.1 (134.0)	No change	1.6±0.2	>0.6/4.4
Mobjack Bay5-ADJ	2.4±0.01 (189.5)	No change	0.5±0.3	>1.8
BW	2.5±0.02 (176.8)	No change	1.2±0.04	>1.5/1.2
Mobjack Bay7-ADJ	2.7±0.04 (153.9)	No change	0.9±0.1	>0.8
BW	2.1±0.1 (233.3)	No change	1.2±0.2	>0.8/2.0
Yorktown-ADJ	2.4±0.1 (189.5)	No change	0.7±0.1	>1.9
BW	2.8±0.1 (143.6)	Fining	1.0±0.1	1.8/1.8
Mobjack Bay3-ADJ	2.1±0.02 (233.3)	No change	0.7±0.1	>2.0
BW	2.0±0.1 (250.0)	No change	1.8±0.5	1.9/1.9
Schley-ADJ	2.5±0.03 (176.8)	No change	1.3±0.3	>1.9
BW	2.1±0.03 (233.3)	No change	0.7±0.04	>1.6/>1.6

Regional trends in sedimentation can be discerned by averaging the observed average median diameters and organic-content values, as well as the accumulation rates, by salinity region (Figure 2.2).

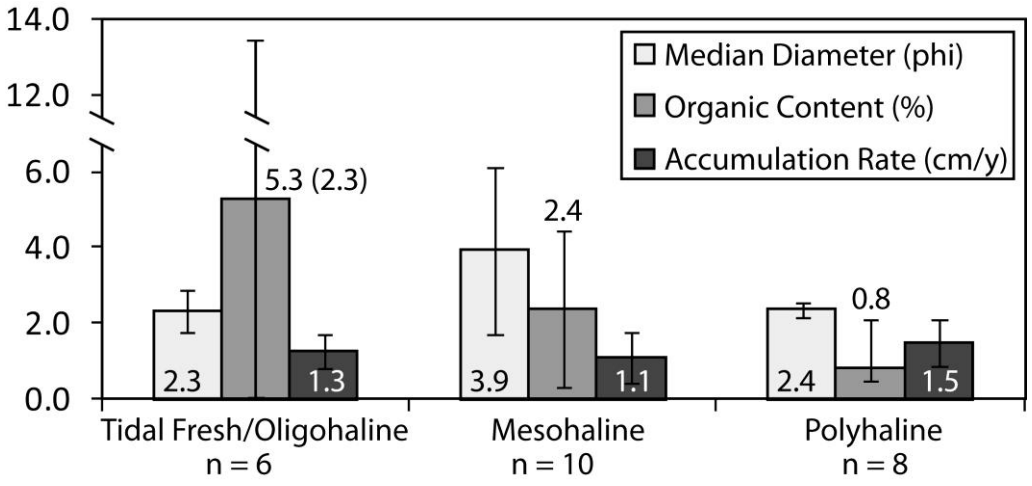

Figure2. 2. Average median diameter (grain size), organic content, and accumulation rates at the adjacent-exposed sites, averaged by salinity region. Error bars represent the standard deviation. The organic content in the tidal fresh/oligohaline region is skewed by observations at Sue Creek, which has an organic content more than twice that observed at any other location. When this value is removed, the average organic content decreases to 2.3%, noted in the parentheses.

The finest sediment is found in the mesohaline (salinity 5-18) region, which is somewhat unexpected. The tidal fresh/oligohaline (salinity 0-5) regions are generally located above the estuarine turbidity maximum (ETM) and thus should be more influenced by muddy fluvial sediment (Hobbs et al., 1992). However, it is likely that waves and currents remove or prevent deposition of finer grains in the nearshore, leaving coarse sand deposits behind (Kerhin et al., 1988). Finer particles may not settle out until they reach deeper water and/or flocculate in the ETM (Sanford et al., 2001). In the mesohaline region, many sites are adjacent to eroding marshes (e.g., Hoopers Island) rather than the more typical sandy shoreline (Hobbs et al., 1992) explaining the presence of finer, more organic sediment in this region. The polyhaline (salinity 18-25) region has the least organic sediment, because sediment supply in this region is dominated by input of ocean sediment (Hobbs et al., 1992) and extensive sand deposits are found along the shorelines. While the character of sediment may vary among the three regions, average accumulation rates are similar – 1.3 cm/y, 1.1 cm/y, and 1.5 cm/y for the tidal fresh/oligohaline, mesohaline, and polyhaline regions, respectively.

Down-core profiles of grain size (median diameter) and organic content typically sort into 3 categories: coarsening upward with a decrease in organic content, fining upward with an increase in organic content, and relatively uniform grain size and organic content (Table 2.3). The first (coarsening upward) is exemplified by Mayo North (Figure 2.3a), where grain size coarsens from 8.7 phi (2.4 μm) at the base of the core to 2.1 phi (233.3 μm) at the top, and organic content decreases from 5.5% to 0.7%. The ^{210}Pb profile indicates steady-state sedimentation and an accumulation rate of 0.4 cm/y. Note that, for these types of cores, the ^{210}Pb activities measured at each depth horizon have

been normalized to the corresponding mud content (see Methods). The coarse-grained material at the top of the core is likely supplied by the adjacent sandy shoreline, while the more organic, finer sediment at the base is likely reflective of relict marsh material. Cores with a fining upward trend are exemplified by Hoopers Island (Figure 2.3b), where grain size fines from 3.5 phi (88.4 μm) at the base of the core to 8.3 phi (3.2 μm) at the top, and organic content increases from 1.2% to 3.6%. The ^{210}Pb profile indicates steady-state sedimentation, under a 15-cm-thick uniform-activity layer, and the accumulation rate is 0.3 cm/y. Note that while there is a strong grain-size trend in this core, the median diameter lies within the mud fraction for most of the core – except for the base, which is below the penetration depth of excess ^{210}Pb. Thus, the decrease in ^{210}Pb activity is likely not due to grain-size changes but rather due to radioactive decay, and activities have not been normalized. These types of cores tend to occur adjacent to eroding marshes, which supply finer and more organic sediment to the nearshore. The third type of profiles are those without obvious down-core changes in either the median diameter or organic content, as shown for Mobjack Bay 5 (Figure 2.3c), suggesting that the source of sediment has not changed significantly over the last ~100 y. Notably, all cores collected in Mobjack Bay, as well as the core at Yorktown, show an increase in ^{210}Pb activity with depth. As grain size and organic content vary little, it is likely that the initial activity of ^{210}Pb has changed, violating the assumptions of the accumulation-rate calculations. Thus, only a minimum accumulation rate can be calculated for these cores, by noting the presence of excess ^{210}Pb at the base of the core and assuming a detection limit of ~100 y (4-5 half-lives). While most adjacent-exposed sites are net depositional, and thus have depth-integrated excess ^{210}Pb inventories above the atmospheric inventory (~25

dpm/cm^2; Kim et al., 2000), the sites near Cape Charles (Bay Creek and Public Beach) have inventories below this value, even when measured activities are normalized to the mud content, indicating erosion. Normalizing the activities (and adjusting the corresponding supported level of ^{210}Pb) before calculating the inventory removes the potential effect of dilution by coarse particles that may not scavenge ^{210}Pb as effectively. Inventories at all other sites are above the atmospheric inventory, supporting the interpretation of net sediment accumulation.

Mayo North is the only site where coarsening upward throughout the core is observed. More typical trends are fining upward (7 sites) and no change (16 sites; see Table 2.3). In the tidal fresh/oligohaline, fining upward is observed at Elk Neck and Sue Creek. In the mesohaline, fining upward is observed at 4 sites (Tangier Island, Bishops Head, Hoopers Island, and Easter Neck) adjacent to eroding marsh shorelines. In the polyhaline, Cape Charles Bay Creek is the only site with a fining upward trend. No change is observed at the other sites, indicating that the source of sediments has remained relatively constant over time.

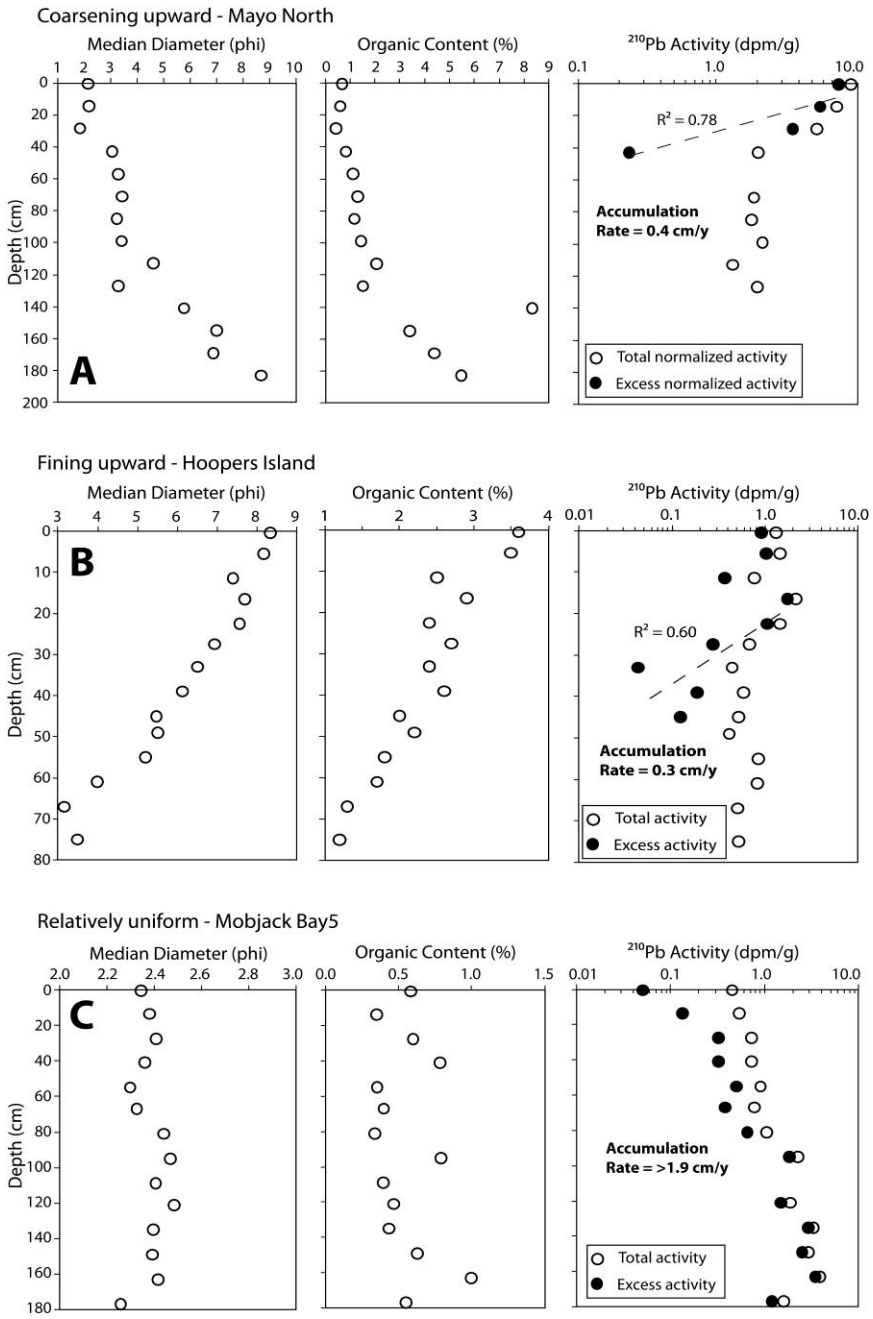

Figure 2.3. Vibracore profiles of grain size (median diameter), organic content, and ^{210}Pb activity at the adjacent-exposed sites at Mayo North (A), Hoopers Island (B), and Mobjack Bay5 (C). Note that scales differ among plots; in particular, the x-axis of the median-diameter plot for Mobjack Bay5 is at a much finer scale than the others due to the uniformity of measurements.

Observations in the breakwater-protected areas

Determining the depth of breakwater influence

Discerning trends in the breakwater-protected areas is more complicated, because historical trends must be separated from those potentially induced by breakwater installation. In order to do this, the depth of breakwater influence (Table 2.1) is interpreted for each site from its grain-size, organic-content, and ^{210}Pb-activity profiles. The procedure for determining this depth at representative sites follows. Further details, as well as the associated down-core profiles, for every site are available in the Appendix. For older (>15 y) breakwaters, post-construction sedimentation rates usually can be determined via ^{210}Pb, if the down-core activity profile shows a change in slope, indicating a change in the sedimentation rate. For example, at Highland Beach (18-y old), a change in slope occurs at ~32 cm (Figure 2.4a) and is interpreted to be caused by breakwater installation. The sedimentation rate calculated for the lower portion of the profile is 2.1 cm/y, corresponding to pre-construction sedimentation. The rate for the upper portion is 1.7 cm/y, corresponding to post-construction sedimentation. This latter rate, multiplied by the breakwater age, yields a depth a 31 cm, supporting the conclusion that the change in slope is related to breakwater installation. There is little obvious change in either the grain size or organic content of post-construction material at this site (i.e., sediment above 32 cm), suggesting that the sediment source (most likely the sandy shoreline) is unchanged. The decrease in sedimentation rate may be due to reduced shoreline erosion, decreasing sediment supply.

^{210}Pb is not as useful for calculating post-construction rates for younger breakwaters, due to its relatively long half-life. In these cases, the post-construction sedimentation rate must be inferred by interpreting the depth of breakwater influence, by assuming that changes in sediment character observed near the top of cores are associated with construction. This depth can then be divided by the breakwater age. There may be some biases due to event layers (e.g. hurricanes) and/or time-scale issues, as short-term sedimentation rates can be much larger than longer-term rates due to inclusion of episodic periods of erosion and/or no deposition (McKee et al., 1983). As an example, profiles of grain size (median diameter), organic content, and water content for the breakwater-protected area at Bishops Head are shown in Figure 2.4b. The grain-size profile displays upward fining that abruptly transitions to coarser sediment between 12 and 23 cm in the vibracore profile, likely reflecting the breakwater influence. While this change does not correspond to an obvious change in the organic-content profile, it is co-located with an abrupt increase in water content. The push-core water-content profile can then be used to obtain a higher-resolution estimate – 22 cm. Dividing this thickness by the breakwater age (11 y) yields the post-construction sedimentation rate of 2.0 cm/y. Note that samples were collected in August 2008; some of this fine, high water-content material may be eroded during winter storms, so the net post-construction layer may be thinner. The post-construction rate can then be compared to the pre-construction rate calculated from the ^{210}Pb profile (1.1 cm/y) to see that, at Bishops Head, the effect of breakwater construction appears to be an increase in sedimentation rate, grain size, and water content of sediments. Note that post-construction changes are not necessarily only

due to natural processes – at Bishops Head, sandy sediment may have been placed to create a pocket beach during construction (see Appendix).

At some locations, the grain-size and organic-content profiles appear nearly uniform or follow historic trends, and the potential impact of the breakwater is unclear. In the case of Schley (Figure 2.4c), there is a slight upward fining that is unlikely to be influenced by breakwater construction as it begins deep in the core. The ^{210}Pb profile has a low-activity layer 25-100-cm deep, in between layers with higher activity. The low-activity layer likely represents an event layer, with lower initial ^{210}Pb activity than the surrounding sediment. It is possible that the low-activity layer is associated with the breakwater installation, and is overlain by post-construction sediment. If this were the case, the post-construction rate would be ~1.4 cm/y, similar to the minimum accumulation rate of 1.6 cm/y calculated from the presence of excess ^{210}Pb at the base of the core. Since both the pre- and post-construction sedimentation rates are difficult to calculate with certainty, for consistency, the minimum rate is used for the pre-construction rate and assumed to be unaltered by breakwater construction. The corresponding depth of breakwater influence would be 29 cm.

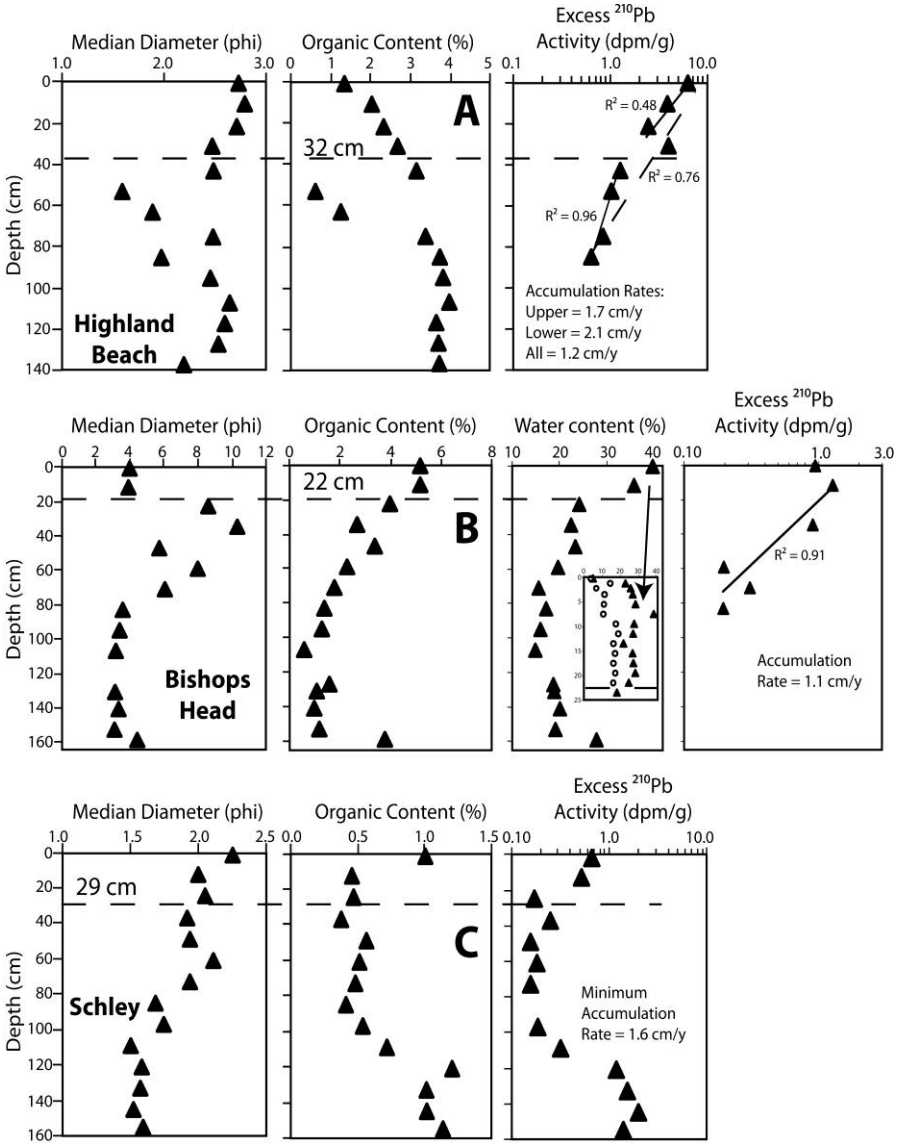

Figure 2.4. Vibracore profiles of grain size (median diameter), organic content, and ^{210}Pb activity at the breakwater-protected sites at Highland Beach (A), Bishops Head (B), and Schley (C). Note that scales differ among plots for visual clarity. The dashed line indicates the interpreted depth of breakwater appearance, which is noted above the line. Note that due to scaling issues (e.g., size of symbols), the line may not appear to correspond with the given depth. The line is intended to show which data points are considered to represent pre- and post-construction conditions.

In summary, pre-construction rates range 0.5-3.1 cm/y; post-construction rates can decrease (e.g., Highland Beach), increase (e.g., Bishops Head), or remain unchanged (e.g., Schley), depending on the local physical setting (Table 2.3). As at the adjacent-exposed site, the breakwater-protected site at Cape Charles Bay Creek has a depth-integrated excess ^{210}Pb inventory below the atmospheric value, indicating net erosion. All other excess inventories at the breakwater-protected sites were above the atmospherically supported inventory.

Spatial and historical trends in sediment character

Once the depth of breakwater influence has been established for each site, historical (down-core) and spatial (surficial sediment) trends can be examined at the breakwater-protected sites and compared to those observed at the adjacent-exposed sites. Historical grain-size trends (Table 2.3) are defined as those occurring below the depth of breakwater influence (i.e., pre-construction sediment), so that observed trends are not confused with those potentially induced by breakwater construction. Historical trends can be grouped in the same manner as for the adjacent-exposed sites – coarsening upward, fining upward, or no change. Overall, the regional trends are similar, with fining upward trends at 2 sites (Elk Neck, Mason Neck2) in the tidal fresh/oligohaline, 3 sites in the mesohaline (Bishops Head, Hoopers Island, Eastern Neck), and 1 site in the polyhaline (Yorktown). Although most adjacent-exposed and breakwater-protected sites at individual locations have similar sediment character and historical trends (e.g., Elk Neck; Figure 2.5a), some may differ. For example, Mason Neck 1 (Figure 2.5b), where the down-core trend of no obvious change is similar, but the adjacent-exposed site has

highly organic and fine sediments in comparison to the coarse, low-organic sediment in the breakwater-protected area (see Appendix). Both the sediment character and historical trends differ at Mason Neck 2 (Figure 2.5c), where the adjacent-exposed site has sandy sediment that is relatively uniform throughout the core in comparison to the breakwater-protected site, which has muddy sediment that fines upward. These differences indicate that observations at the breakwater-protected sites are not necessarily directly comparable to those at the adjacent-exposed sites. Observations at Mason Neck 1 and 2 also highlight the small-scale spatial variability present among study locations. These sites are ~1 km apart and exposed to similar fetch (2.2-2.4 km; see Appendix), but they differ in shoreline sediment source, accounting for the observed differences.

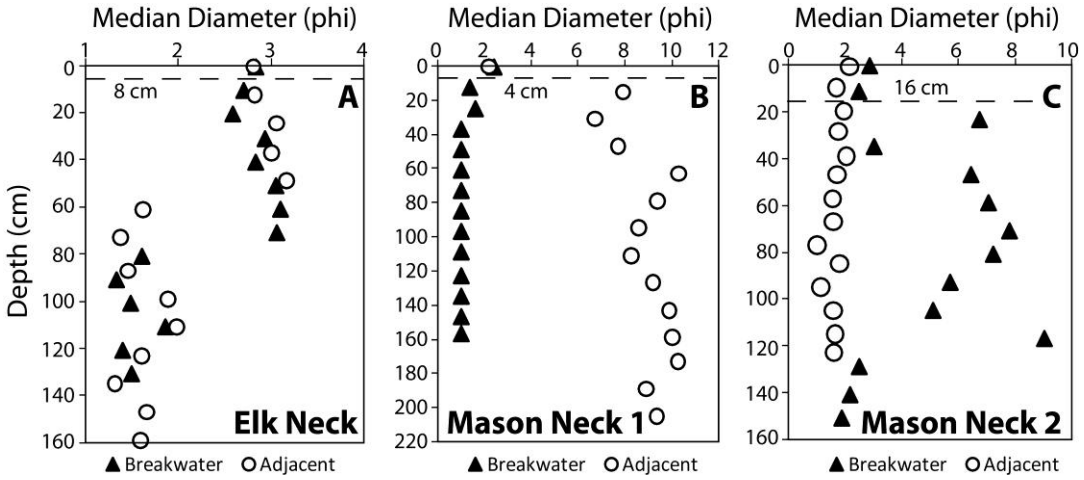

Figure 2.5. Comparison of grain-size profiles observed at the breakwater-protected (closed triangles) versus adjacent-exposed (open circle) sites at (A) Elk Neck, (B) Mason Neck 1, and (C) Mason Neck 2. The dashed line indicates the depth of breakwater influence, which is noted near the line – the historical grain-size trend at the breakwater-protected site is interpreted below this line.

As for the adjacent-exposed sites, surficial-sediment (0-10 cm) characteristics can be examined to determine regional trends (Table 2.3). At most locations, this represents post-construction conditions, except where the depth of breakwater influence is <10 cm. The average median diameters of these sediments ranged from medium sand (1.5 phi, 353.6 µm) to medium silt (5.5 phi, 22.1 µm), averaging 2.7 phi (155.7 µm), and the organic content ranged from 0.4 to 4.1%, averaging 1.5%. Overall regional trends are similar to those observed for the adjacent-exposed sites: sediment in the breakwater-protected areas is coarser and less organic in the tidal fresh/oligohaline and polyhaline regions, and finer and more organic in the mesohaline region (Figure 2.6).

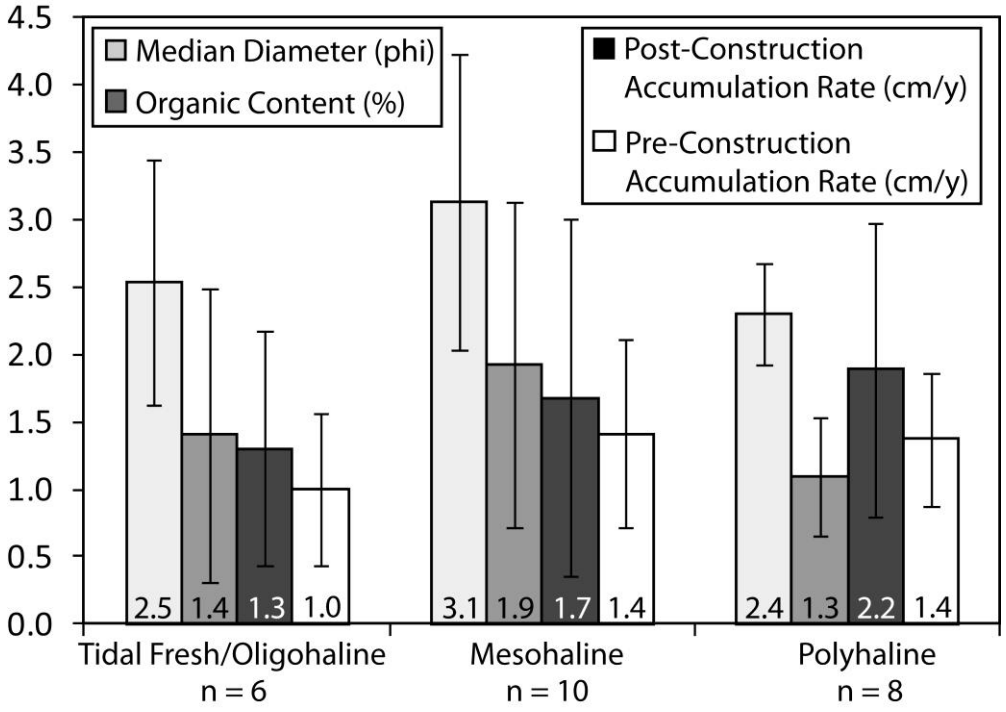

Figure 2.6. Median diameter, organic content, and accumulation rates at the breakwater-protected sites, averaged by salinity region. Error bars represent the standard deviation. As in Figure 2.2, the large standard deviation of observations reflects the site-specific nature of sediment character that is averaged to discern broad regional trends.

Regionally averaged grain size, organic content, or accumulation rates for the adjacent-exposed and breakwater-protected sites are not significant (p=0.24, 0.21, and 0.44, respectively; see Table 2.2) due to the large range of observations. However, in comparison to observations at the adjacent-exposed sites, sediment in the mesohaline region tends to be coarser and less organic in the breakwater-protected areas, on average, probably because breakwaters tend to be constructed adjacent to sandy shorelines for beach protection and/or because sand layers are applied during construction. Regionally averaged post-construction sedimentation rates are either the same as (tidal fresh/oligohaline) or higher than (mesohaline, polyhaline) those observed at the adjacent-exposed sites. Regionally averaged pre-construction sedimentation rates are lower than the post-construction rates. While the differences are not statistically significant (p=0.28), they do suggest that one impact of breakwaters, on a broad spatial scale, is to increase the sedimentation rate in the breakwater-protected area.

DISCUSSION

Breakwater impacts on sedimentation

While the specific sedimentary response to breakwater installation is unique at each site, sampling locations can be categorized according to observed changes in grain size and sedimentation rate. To reduce the number of possible combinations, organic content is not included in this categorization, as organic content is generally directly proportional to grain size – i.e., finer sediments tend to be more organic ($p < .0001$, $r^2 = 0.54$ for surficial-sediment observations; see Table 2.3). There are three categories of grain-size changes attributed to breakwater installation – increase in size (coarsening),

decrease in size (fining), or no change. Similarly, there are three categories of sedimentation-rate changes – increase, decrease, or no change. Thus, there are nine possible combinations (Table 2.4). Note that these categories are defined based on changes observed in push- and/or vibracore profiles at the breakwater-protected site, since observations at the adjacent-exposed and breakwater-protected sites are not necessarily directly comparable, as previously noted.

Table 2.4. Trends in sediment grain size, organic content, and sedimentation rate following breakwater construction at each location, based on changes observed in the push- and/or vibracore at the breakwater-protected site. Locations are categorized into 9 types by grain-size (1 = increase, 2 = decrease, 3 = no change) and sedimentation-rate (a = increase, b = decrease, c = no change) changes. Note that a vibracore was not collected at the Red Eye Yacht Club, so pre-construction sediments were not sampled and thus changes could not be discerned.

Site	Grain size	Organic content	Sedimentation rate	Type
Tidal fresh				
Elk Neck	decrease	Increase	increase	2a
Mason Neck1	increase	no change	no change	1c
Mason Neck2	increase	no change	no change	1c
Hart-Miller Island	decrease	no change	increase	2a
Sue Creek	no change	no change	no change	3c
Red Eyed Yacht Club	NA	NA	NA	NA
Mesohaline				
Taylors Island	decrease	no change	decrease	2b
Tangier Island	no change	Increase	decrease	3b
Mayo North	no change	no change	decrease	3b
Mayo South	no change	no change	no change	3c
Bishops Head	increase	no change	increase	1a
Hoopers Island	increase	Decrease	increase	1a
Eastern Neck	increase	Decrease	increase	1a
Highland Beach	no change	no change	decrease	3b

Gratitude	no change	no change	decrease	3b
Brannock Bay	no change	no change	increase	3a
Polyhaline				
Cape Charles Bay Creek	increase	no change	increase	1a
Cape Charles Public Beach	increase	no change	no change	1c
Mobjack Bay	decrease	decrease	increase	2a
Mobjack Bay5	no change	Increase	decrease	3b
Mobjack Bay7	increase	no change	increase	1a
Yorktown	decrease	no change	no change	2c
Mobjack Bay3	increase	no change	no change	1c
Schley	no change	no change	no change	3c

There is an increase in grain size (coarsening) at 8 of the 24 sampling locations. At 3 of these 8 sites, there is no change in the sedimentation rate; however, the sedimentation rate increases at the other 5. Type 1a cores (increase in grain size, increase in sedimentation rate) are exemplified by Eastern Neck (Appendix; Palinkas et al., 2010), and type 1c cores (increase in grain size, no change in the sedimentation rate) are exemplified by Mason Neck 2 (Figure 2.7a). Interestingly, there are no type 1b cores (increase in grain size, decrease in sedimentation rate). This suggests that post-construction sedimentation at the locations is influenced by trapping of sandy sediment, from shoreline and/or longshore-transport sources, and/or construction technique. Many of these sites (e.g., Hoopers Island, Eastern Neck) likely had a sand layer applied at the time of installation (see Appendix), which would cause an apparent increase in sedimentation rates. Type 2 cores have a decrease in grain size associated with breakwater construction. There are 5 locations with these characteristics – 3 have an increase in sedimentation rate (e.g., Elk Neck; Appendix; Palinkas et al., 2010), 1 has a decrease in sedimentation rate (Taylors Island; Figure 2.7b), and 1 shows no apparent change in sedimentation rate (Yorktown; see Appendix). However, note that Taylors

Island is only 1-y old, so the preservation potential of this fine sediment is unclear, as well potential variability in its thickness. These locations are typically near a source of fine sediment – e.g., Elk Neck, which is located adjacent to the Susquehanna River outflow. The observed fining probably reflects the decrease in hydrodynamic energy typically associated with breakwater construction, which facilitates settling of fine material that would otherwise remain suspended. The third category of cores (type 3) has no obvious change in their grain-size profiles. This is the most prevalent category, with 10 locations. Four of these 10 locations also have no obvious change in their sedimentation rate (e.g., Schley; see Figure 2.4c), another 4 have a decrease in sedimentation rate (e.g., Highland Beach; see Figure 2.4a), and 2 have an increase (e.g., Brannock Bay; Figure 2.7c). The disparity in sedimentation-rate alterations probably reflects variations in changes to the sediment supply induced by breakwaters – some trap sediment from shoreline and/or longshore-transport sources (increasing rate), some reduce shoreline erosion (decreasing rate), some do not alter the sedimentary environment (no change). They latter may result from unchanged sediment source and/or sediment transport patterns, particularly behind breakwaters that are submerged at high tide, that are similar to those that existed before construction.

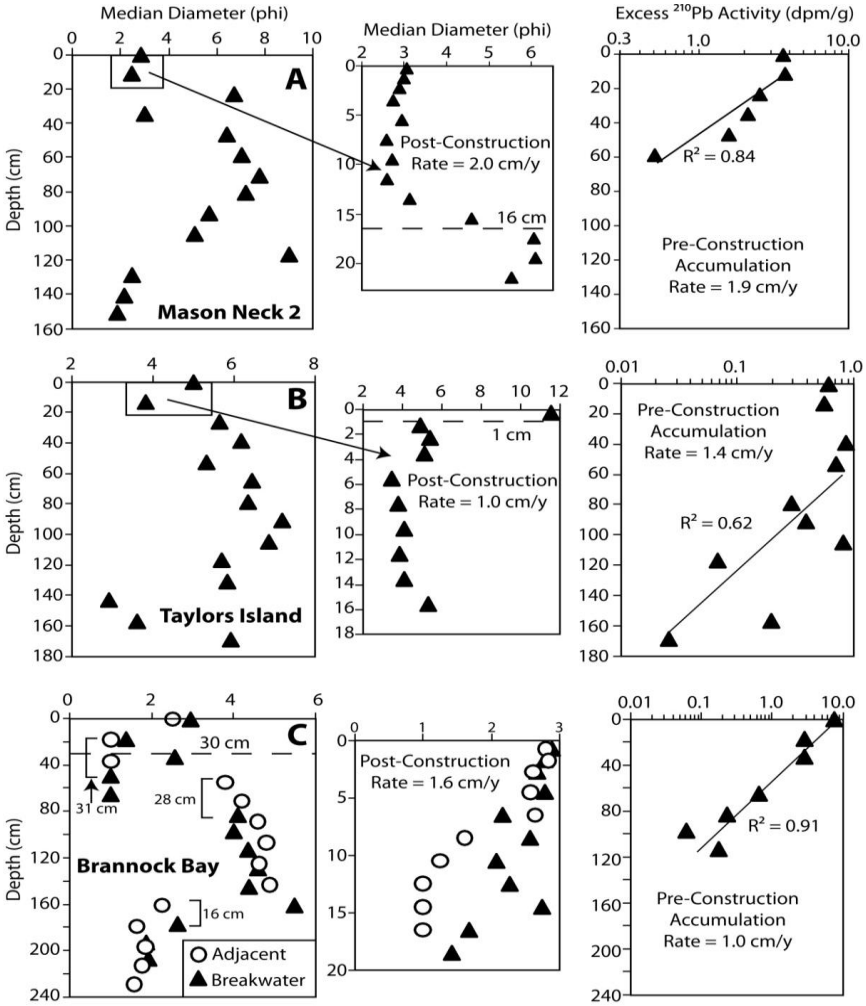

Figure 2.7. Profiles of median diameter and ^{210}Pb activity at the breakwater-protected sites at Mason Neck2 (A), Taylors Island (B), and Brannock Bay (C). Grain-size data at the adjacent-exposed site (open circles) are included for Brannock Bay; comparison of grain-size profiles at both sites reveals distinct layering that is offset. Layers are deeper in the breakwater-protected core due to a thicker surficial layer, reflecting increased sedimentation influenced by breakwater construction. For all locations, the middle panel shows push-core observations, which are less affected by disturbance during sampling and are at a higher resolution than vibracore observations. Also, the dashed line indicates the depth of breakwater influence, which is noted above the line. For Brannock Bay, the depths by which layers are offset are also noted to highlight the observed distinct layers.

It might be tempting to conclude that, because type 3 was the most prevalent, breakwaters have little effect on the sedimentary environment. However, there are two important points to consider. The first is that, as discussed above, breakwaters do induce changes in the sedimentary environment at individual locations. The second is that the locations included in this study are biased toward those with SAV in the vicinity. Thus, because SAV require sufficient light (Kemp et al., 2004), areas with high turbidity are generally excluded from the study. And since high turbidity is typically associated with fine sediment (e.g., Langland and Cronin, 2003), this means that locations likely to be categorized as type 2 cores are under-represented.

Factors that affect sediment properties in the breakwater-protected area

Several factors interact to control sediment properties in the breakwater-protected areas. Two of these can be quantified: breakwater age and fetch, which is an indicator of wave energy. The strongest correlations are observed with breakwater age. As expected, the depth of breakwater influence increases with breakwater age ($p<0.0001$; $r^2 = 0.45$; Figure 2.8a), since sediments have more time to deposit landward of older breakwaters. This is also true when sites are divided by salinity region ($p = 0.004$, $r^2 = 0.73$ and $p = 0.03$, $r^2=0.59$ for the mesohaline and polyhaline regions), except for the tidal fresh/oligohaline region ($p = 0.48$, $r^2 = 0.09$). A weaker correlation is observed between breakwater age and surficial-sediment grain size ($p = 0.02$, $r^2 = 0.23$), with coarser sediment landward of older breakwaters. However, this correlation is driven by observations at Taylors Island, which is young (1 y) and muddy (average median diameter 5.5 phi, 22.1 μm). When removed from the regression, the r^2 value decreases to

0.11. Similarly, breakwater age is not correlated with organic content ($p = 0.27$, $r^2 = 0.07$). Thus, while more sediments have deposited landward of older breakwaters, the character of this material depends on local sediment supply and is not related to breakwater age.

Fetch has been measured for both the adjacent-exposed and breakwater-protected sites and is one way to describe the physical energy of study locations, with a higher fetch implying higher wave energy. The only parameter that is correlated with fetch for the breakwater-protected sites is grain size in the tidal fresh/oligohaline ($p = 0.04$, $r^2 = 0.41$; Figure 2.8b) – grain size decreases (fines) as the fetch increases.

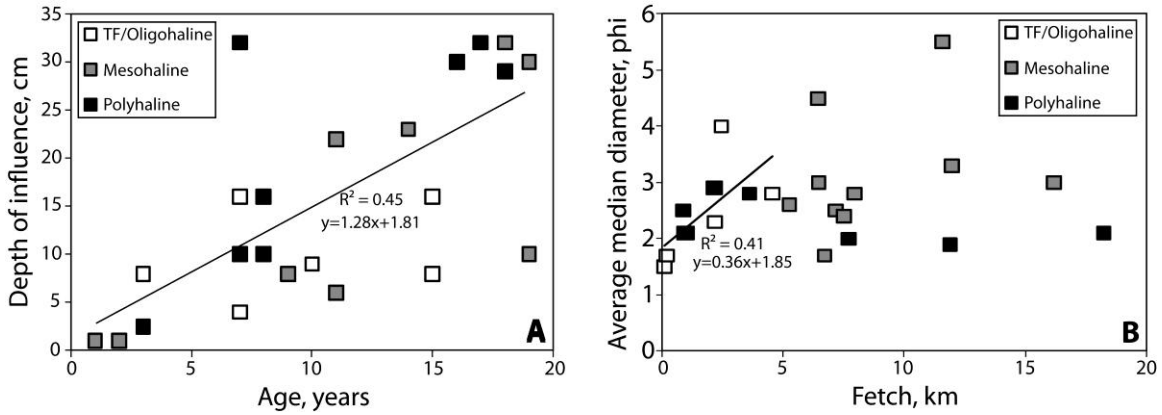

Figure 2.8. Plots of (A) depth of breakwater influence versus breakwater age, and (B) average median diameter versus fetch for the breakwater-protected sites. The lines represent best-fit regressions to the data – using all data points in (A) and only those in the tidal fresh (TF)/oligohaline in (B). R^2 values and equations are given. In both plots, data points are coded by salinity region, as noted in the legend.

These locations are generally near a source of fine sediment –the Susquehanna River for the locations in northern Chesapeake Bay or the Potomac River for Mason Neck 1 and 2. So, the correlation with fetch suggests that this fine sediment is usually kept in

suspension by high wave energy but can deposit when the fetch is reduced by breakwater installation. Also note that the fetch is relatively low (<5 km) at the tidal fresh/oligohaline sites, in contrast to higher fetch values measured in other regions. So, it may be that the relationship with grain size is valid for all low-fetch environments, not just those in the tidal fresh/oligohaline. Indeed, the low-fetch locations in the polyhaline region appear to have the same relationship as for the tidal fresh/oligohaline. In any case, fetch is not correlated with grain size in the mesohaline region ($p = 0.35$, $r^2 = 0.09$) and only weakly so in the polyhaline region ($p = 0.24$, $r^2 = 0.21$). It is also not correlated with organic content ($p = 0.45$) nor the depth of breakwater influence ($p = 0.19$) in any salinity region. Fetch is also not correlated with sediment properties (median diameter, $p = 0.38$; organic content, $p = 0.77$) at the adjacent-exposed sites, indicating that sedimentation is not limited by fetch at these locations, whether or not a breakwater is present. Note that fetch is only one of many processes that affect sediment erosion/deposition. For example, currents are neglected, as is the erodibility of sediments. This discussion presumes that finer (and thus more organic) sediments are easier to erode; however, this is not always the case, especially since several locations are characterized by compacted peat deposits.

Other factors also affect sediment properties in the breakwater-protected area that are difficult to quantify, such as construction technique and shoreline type. As has been discussed previously, there are several sites with thick sand layers (e.g., Eastern Neck, Hoopers Island) that were likely applied at the time of breakwater installation. The sediment properties at these locations would be difficult to predict by considering only natural processes. Also, the type of adjacent shoreline plays a role in supplying sediment

to the breakwater-protected area. An eroding marsh would supply finer and more organic sediment than would a sandy shoreline. All of these factors interact to determine the specific sedimentary response at individual locations.

SUMMARY

Breakwater effects on Chesapeake Bay sedimentation are largely site-specific, varying with physical setting (e.g., sediment supply) and construction technique (e.g., sand-layer application), and overprinted on regional and historical trends. However, some generalizations can be made. If fine sediment from fluvial input or marsh erosion is readily available, the breakwater can facilitate fine-sediment deposition. This fine sediment is generally higher in organic and water content than sandy sediment. However, in places where erosional sand deposits along the shoreline are the dominant source of sediment, breakwaters may trap coarse shoreline sediment, causing an increase in grain size and sedimentation rate. In some locations, this is accentuated by sand-layer application at the time of installation. Some locations show no obvious changes related to breakwater construction, and down-core profiles appear relatively uniform or follow historic trends, indicating that breakwater installation may not always alter the sedimentary environment. However, changes at individual locations may be significant, potentially affecting the long-term suitability of sediments for the original local fauna and flora.

Chapter 3

SAV habitat requirements: sediment grain size and organic content

INTRODUCTION

Submerged aquatic vegetation (SAV) beds are one of the most important ecosystems in the Chesapeake Bay, as they serve as habitat for fish, crabs, waterfowl, and many other organisms (Corona et al., 2000; Lazzari and Stone, 2006; Rybicki and Landwehr, 2007; Ma et al., 2010). SAV beds can also attenuate waves (Fonseca and Cahalan, 1992) and reduce current velocity (Fonseca et al., 1981; Gambi et al., 1990; Peterson et al., 2004), leading to a reduction of sediment resuspension and erosion (Fonseca and Fisher, 1986; Koch, 1999; Gacia and Duarte, 2001; Widdows et al., 2008). However, SAV populations have suffered major declines globally (Waycott et al., 2009; Short et al., 2011), including the Chesapeake Bay (Orth and Moore, 1983; Orth and Moore, 1984; Orth et al., 2008).

Restoration efforts in Chesapeake Bay are attempting to bring SAV back to historical levels but have been met with mixed results (Orth et al., 2002; Shafer and Bergstrom, 2010). Recent improvements in restoration techniques have been made (Ailstock et al., 2010; Busch et al., 2010; Hengst et al., 2010; Koch et al., 2010; Leschen et al., 2010; Moore et al., 2010; Pan et al., 2011). Even so, there is still room for improvement in the site-selection process for large-scale restoration projects.

Light is the main parameter limiting SAV distribution (Kemp et al., 1984), yet SAV do not always grow successfully in areas where this habitat requirement has been met. Parameters other than light may also play a major role in SAV distribution (Koch, 2001). For example, in Florida's Indian River Lagoon, only 50% of the variation in seagrass distribution was attributed to light attenuation, with the rest being influenced by wave action, sediment grain size and toxicity, substrate reflectance, epiphytic growth on shoots, and competition with algae (Steward et al., 2005). Waves limit the upper (shallow-water) distribution depth of the seagrass *Posidonia oceanica* (Infantes, 2009), and sediment characteristics have been shown to play a major role in the restoration of *Zostera marina* in Boston Harbor (Leschen et al., 2010).

Sediment characteristics that may affect SAV growth and distribution include grain size, organic content, and porewater geochemistry (Short, 1987 and Silva et al., 2009). In Boston Harbor, the seagrass *Z. marina* was successfully restored at sites with <35% silt/clay but failed in areas with >57% silt/clay (Leschen et al., 2010). However, Krause-Jensen et al. (2011) determined 13% silt/clay to be a threshold value for *Z. marina* in Danish coastal waters. Thus, these sediment requirements are likely to be species- and site-specific. For example, plants growing in quiescent waters may be more tolerant of fine and organic sediments, as they are not likely to be uprooted (Wicks et al., 2009). Additionally, sediments may become too coarse and hinder recolonization of the substrate, as was observed after dredging caused an increase in tidal wave penetration, and an associated increase in fine-sediment erosion, in Ria de Aveiro, Portugal (Silva et al, 2009).

SAV beds tend to reduce currents and waves and therefore accumulate fine particles (Kleeberg, et al., 2010). As the amount of fine particles in SAV beds increase so does the sediment organic content, since these two characteristics are closely correlated. As with sediment grain size, sediment organic content is also considered limiting for SAV growth and distribution. A threshold of <5% organic content has been suggested for SAV (Barko and Smart, 1983), but this value is likely to be species- and site-specific and may differ between field and laboratory observations. Approximately 20% organic content limited *Myriophyllum spicatum* L. and *Hydrilla verticillata* growth in a greenhouse experiment (Barko and Smart, 1986). In another experiment in mixed cultures with *Vallisneria americana*, *H. verticillata* grew dominantly more in sediments containing 2.3% organic content than sediments containing 0.3% organic content (Ye et al., 2009). However, *V. americana* has been observed growing in sediments ranging from 0.3-44.1% organic content *in situ* (Kreiling et al., 2007; Makkay et al., 2008; Moore et al., 2010). This broad range of values suggests that SAV are rather plastic in their response to sediment characteristics and/or that plants have site-specific responses to local sediments. Sediment habitat requirements for SAV in the Chesapeake Bay have not yet been determined, but healthy SAV beds in this region typically are composed of 6-10% fine (mud) material and have 1.0-5.3% organic content (Batiuk et al., 1992).

The objective of this study was to define the sediment habitat requirements for SAV commonly found in Chesapeake Bay (*Ruppia maritima, Potamogeton perfoliatus, Vallisneria americana,* and *Zannichellia palustris*). To address this objective, sediment characteristics (i.e., organic content and grain size) and SAV distribution were compared at 48 sites in 24 locations in Chesapeake Bay. Additionally, a controlled experiment

specifically evaluated the effect of sediment organic content on growth of these four species.

MATERIALS AND METHODS

Study sites

Breakwaters in the Chesapeake Bay tend to modify the sediments in the breakwater-protected area. In some of these areas the sediments become finer over time, in others they become coarser, and in other places they do not change at all (Chapter 2). This provides a unique opportunity to study SAV in a broad range of sedimentary environments in relative close proximity, such that paired study sites have similar light, salinity, and temperature conditions but have different underlying sediment characteristics. Therefore, aerial photography available at the Virginia Institute of Marine Science (Orth et al., 2009; annual reports 1989-present) was used to identify 24 study locations with breakwaters (Figure 3.1).

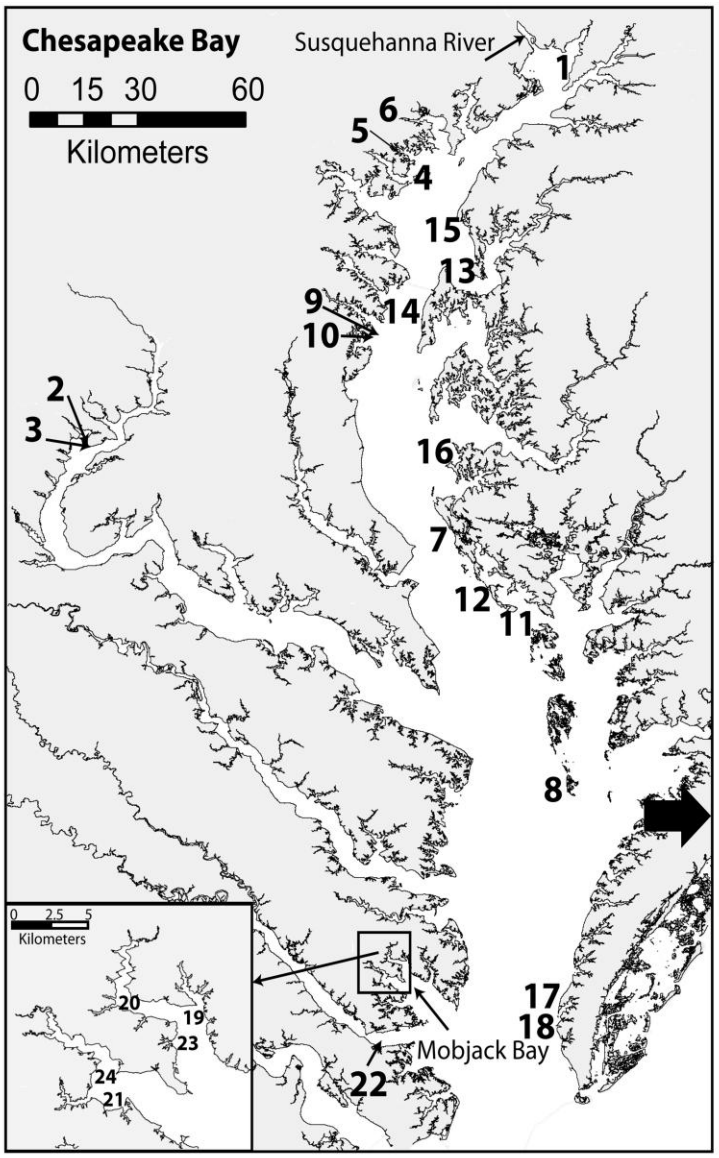

Figure 3.1. Map of study locations in Chesapeake Bay. Numbers correspond to location names in Table 3.1. At this scale, some locations appear to overlap (e.g., Mayo North and South, #9 and 10). Inset shows expanded view of locations in Mobjack Bay. The arrow marks Assateague Island where low organic sediments were collected for the mesocosm study and location #16 is Brannock Bay where highly organic sediments were collected.

Photos were analyzed to determine presence/absence of SAV in the area, as defined by Bay segments (sub-regions in Chesapeake Bay) on the VIMS interactive map (http://web.vims.edu/bio/sav/maps.html), in the last 20 years. If SAV was absent during that timeframe, the location was excluded from the study. Study locations were chosen so

that breakwaters in 4 age groups (<5 y, 6-10 y, 11-15 y, and 16-20 y) were represented in each salinity region of the Chesapeake Bay (tidal fresh/oligohaline (0-5), mesohaline (5-18), and polyhaline (18-25; Table 3.1). Fetch was quantified by measuring the distance to land along 40 vectors radiating from each site using the measuring tool on GoogleEarth and then averaging all distances, including zeros (Koch et al., 2006; Table 3.1).

Table 3.1. Names of study sites and breakwater ages at the time of sampling (ADJ=adjacent-exposed site, BW=breakwater-protected site). Most sediment cores were collected in 2009, except Elk Neck, Brannock Bay, Hoopers Island, and Bishops Head, which were sampled in 2008. Locations are divided by salinity region as defined by the Chesapeake Bay Program (CBP, 2004) and characterized by the values in parentheses. Within each salinity region, locations are listed by ascending age. Top 10 cm sediment averages of organic content (%), median diameter (phi, µm); silt/clay (%), water content (%) and fetch (km) are also given for each site. Values are represented as mean ± SE.

Site # (Fig. 1)	Location	Age (y)	Organic Content (%)	Median Diameter (phi, µm)	Silt/Clay (%)	Water Content (%)	Fetch (km)
	Tidal fresh/oligohaline (0-5)						
1	Elk Neck – ADJ		0.6± 0.1	2.6±0.02 (164.9)	4.5±0.3	12.8± 1.2	4.9± 1.5
	Elk Neck – BW	3	1.4± 0.2	2.8±0.1 (143.6)	17.6±1.1	22.7± 2.5	4.5± 1.0
2	Mason Neck1 - ADJ		7.9± 4.2	3.0±0.5 (125.0)	16.5±2.5	33.8± 6.3	2.4± 0.5
	Mason Neck1 BW	7	3.4± 0.5	4.0±0.4 (62.5)	42.0±2.1	34.9± 3.1	2.4± 0.5
3	Mason Neck2 - ADJ		0.8± 0.1	1.7±0.1 (307.8)	5.5±0.2	16.7± 0.8	2.3± 0.6
	Mason Neck2 - BW	8	1.7± 0.4	2.9±0.1 (134.0)	22.2±0.9	25.6± 2.3	2.2± 0.6
4	Hart-Miller Island - ADJ		0.6± 0.1	1.6±0.03 (329.9)	6.4±0.2	17.7± 0.3	3.0± 1.0
	Hart-Miller Island - BW	10	0.4± 0.02	2.3±0.03 (203.1)	3.9±0.2	19.8± 0.5	2.2± 0.5
5	Sue Creek - ADJ		20.1± 3.6	2.3±0.4 (203.1)	22.8±2.9	55.7± 4.6	0.1± 0.01

	Sue Creek - BW	15	0.6± 0.2	1.5±0.1 (353.6)	7.0±0.5	18.5± 1.4	0.1± 0.1
6	Red Eyed Yacht Club – ADJ		1.7± 0.3	2.7±0.1 (153.9)	12.9±1.3	26.6± 2.3	0.2± 0.1
	Red Eyed Yacht Club – BW	15	0.9± 0.2	1.7±0.1 (307.8)	9.2±0.9	18.6± 0.7	0.2± 0.1
	Mesohaline (5-18)						
7	Taylors Island - ADJ		3.9± 0.1	6.9±0.2 (8.4)	62.3±2.3	32.3± 0.5	7.4± 1.9
	Taylors Island - BW	1	1.9± 0.2	5.5±1.1 (22.1)	95.6±0.3	26.0± 1.3	11.6± 4.5
8	Tangier Island – ADJ		7.2± 1.9	4.5±1.0 (44.2)	55.6±4.8	35.3± 5.0	7.8± 2.0
	Tangier Island - BW	2	3.9± 1.5	3.3±0.2 (101.5)	34.7±1.4	27.1± 3.1	12.0± 3.2
9	Mayo North - ADJ		0.7± 0.04	2.0±0.1 (250.0)	6.0±0.4	18.9± 0.7	8.4± 2.0
	Mayo North - BW	9	1.1± 0.04	2.8±0.04 (143.6)	9.9±1.2	24.5± 0.4	7.9± 2.0
10	Mayo South - ADJ		0.8± 0.1	2.0±0.1 (250.0)	8.5±0.5	19.3± 0.6	5.9± 1.5
	Mayo South - BW	11	1.1± 0.1	3.0±0.04 (125.0)	12.6±0.4	28.2± 4.3	6.5± 1.6
11	Bishops Head - ADJ		3.3± 0.2	6.8±0.7 (9.0)	83.1±3.6	10.8± 0.2	4.3± 1.4
	Bishops Head - BW	11	4.1± 0.3	4.5±0.3 (44.2)	51.3±0.8	25.1± 0.5	6.4± 2.0
12	Hoopers Island - ADJ		2.6± 0.5	4.7±0.3 (38.5)	60.0±1.4	17.0± 6.2	16.2± 4.8
	Hoopers Island - BW	14	2.1± 0.8	3.0±0.03 (125.0)	17.4±0.9	8.6± 3.3	16.2± 4.8
13	Eastern Neck - ADJ		2.2± 0.4	6.4±0.6 (11.8)	70.4±3.8	11.0± 2.1	6.6± 1.5
	Eastern Neck - BW	15	0.4± 0.1	2.5±0.03 (176.8)	2.9±0.1	15.1± 2.2	7.2± 1.5
14	Highland Beach - ADJ		0.6± 0.04	1.1±0.1 (466.5)	4.4±0.2	15.1± 0.3	5.7± 1.6
	Highland Beach - BW	18	1.6± 0.03	2.4±0.03 (189.5)	8.1±0.1	23.8± 0.3	7.5± 2.9
15	Gratitude - ADJ		1.0± 0.1	2.2±0.2 (217.6)	8.7±0.8	14.8± 1.5	6.7± 1.8
	Gratitude - BW	19	1.9± 0.7	1.7±0.2 (307.8)	5.2±0.2	15.0± 0.5	6.7± 1.8
16	Brannock Bay - ADJ		1.3± 0.1	2.5±0.2 (153.9)	4.3±0.2	20.9± 0.8	5.1± 1.6
	Brannock Bay - BW	19	1.1± 0.1	2.6±0.1 (164.9)	5.7±0.2	20.5± 0.7	5.3± 1.6
	Polyhaline (18-25)						
17	Cape Charles Bay Creek - ADJ		1.3± 0.3	2.1±0.04 (233.3)	8.8±0.9	20.2± 1.2	8.8± 2.3
	Cape Charles Bay Creek - BW	3	0.6± 0.08	1.9±0.04 (267.9)	4.2±0.1	18.1± 0.2	11.9± 2.9
18	Cape Charles Public Beach - ADJ		0.6± 0.01	2.3±0.04 (203.1)	3.1±0.1	18.7± 0.3	21.0± 4.5

	Cape Charles Public Beach - BW	7	0.7± 0.2	2.1±0.1 (233.3)	6.5±1.2	17.5± 0.5	18.2± 3.9
19	Mobjack Bay - ADJ		0.6± 0.1	2.4±0.1 (189.5)	7.8±1.2	19.3± 0.2	1.6± 0.6
	Mobjack Bay - BW	7	1.6± 0.2	2.9±0.1 (134.0)	14.0±1.4	24.3± 0.8	2.1± 0.9
20	Mobjack Bay5 – ADJ		0.5± 0.3	2.4±0.01 (189.5)	3.0±0.1	19.9± 0.3	0.9± 0.2
	Mobjack Bay5 - BW	8	1.2± 0.04	2.5±0.02 (176.8)	7.5±0.3	22.8± 0.3	0.9± 0.2
21	Mobjack Bay7 - ADJ		0.9± 0.1	2.7±0.04 (153.9)	5.7±0.1	21.5± 0.2	1.1± 0.2
	Mobjack Bay7 - BW	8	1.2± 0.2	2.1±0.1 (233.3)	9.3±0.4	19.4± 1.0	1.0± 0.2
22	Yorktown - ADJ		0.7± 0.1	2.4±0.1 (189.5)	6.1±0.2	19.0± 0.2	4.8± 1.8
	Yorktown - BW	16	1.0± 0.1	2.8±0.1 (143.6)	10.1±0.3	21.7± 0.5	3.6± 1.6
23	Mobjack Bay3 - ADJ		0.7± 0.1	2.1±0.02 (233.3)	3.9±0.2	19.3± 0.7	1.4± 0.4
	Mobjack Bay3 - BW	17	1.8± 0.5	2.0±0.1 (250.0)	7.7±0.6	25.7± 2.2	7.7± 5.2
24	Schley - ADJ		1.3± 0.3	2.5±0.03 (176.8)	7.0±0.5	25.1± 1.6	0.7± 0.2
	Schley - BW	18	0.7± 0.04	2.1±0.03 (233.3)	4.3±0.1	19.2± 0.2	0.9± 0.2

Sediment collection and analysis

Two push cores (~30-cm long, 5-cm diameter) were collected manually at each study site to capture relatively undisturbed surface sediment. One push core was collected in the protected area landward of the breakwater and one at the same water depth in the adjacent wave-exposed area. Push cores were sectioned into 1-cm increments, except the top 3 cm which were sectioned into 0.5-cm increments, immediately upon returning to the lab for further analysis. For this study, only data for the top 10 cm were used (reported as the mean ± standard error), to determine sediment characteristics of the SAV rhizosphere. Sediments were analyzed for grain size and organic content.

Grain-size distribution was analyzed by wet-sieving samples through a 64-µm mesh to separate the sand and mud fractions. The mud fraction (<64 µm) was placed in a 0.05% sodium metaphosphate solution, placed in an ultrasonic bath, and then analyzed by a SediGraph 5120. Particles >64 µm (i.e., sand and gravel) were placed in a pre-weighed pan, dried for 24 hours and then dry-sieved from 1-4 phi (500-64 µm) in ¼-phi increments (phi = $-\log_2$ (diameter, mm)). The mud and sand data were joined to obtain the complete grain-size distribution for each sample, and the median diameter was calculated using MatLab.

Samples for organic-content analysis were initially dried at 60º C until constant weight was reached (initial weight). Dried sediment was then combusted in a muffle furnace at 450º C for 4 hours cooled and weighed (final weight). The percentage of organic matter was then determined according to Erftemeijer and Koch (2001).

SAV collection and analysis

Maximum SAV biomass in the breakwater-protected and adjacent-exposed area was determined by collecting 10 push cores (15-cm diameter and >10-cm long, so as not to damage the rhizosphere) at each study site during the peak of the growing season (May-July 2009). Cores were placed within the 5 densest patches of SAV in both the breakwater-protected and the adjacent wave-exposed areas. Each core was then sieved (1-mm mesh) in the field, and the plant material retained on the sieve was frozen (-17ºC) until processed. Once thawed, epiphytes were removed by scraping the plants using a paint brush and/or razor blade. All intact (i.e. not broken or grazed) shoots and roots

(reported as mean ± standard error) were measured to the nearest mm with a ruler. "Shoot" length instead of "leaf" length was chosen as SAV morphology differs between species in Chesapeake Bay. SAV with strap-like leaves such as *R. maritima* and *V. americana* clearly have shoots (clusters of leaves). In this case, the longest leaf was measured, as the "shoot length". Other species such as *P. perfoliatus* and *Z. palustris* have a vertical stem with many (often small) leaves. In this case, the entire stem was measured for "shoot length". Above- and below-ground biomass (reported as mean ± standard error) was determined by separating shoots (above-ground) from the roots/rhizomes (below-ground) and drying the plant material from each core at 60º C until constant weight was reached.

Mesocosm experiment

In order to determine the tolerance of *Ruppia maritima, Potamogeton perfoliatus, Vallisneria americana, and Zannichellia palustris* to differing levels of sediment organic content, a "common garden" experiment was conducted. These four species were selected as representative species of different salinity regions (*R. maritima*– mesohaline/polyhaline, *P. perfoliatus*- oligohaline/mesohaline, *V. americana*- tidal fresh/oligohaline, and *Z. palustris*-oligohaline/mesohaline) in the Chesapeake Bay, and because they are commonly used in restoration (except *Z. palustris*, as little is known about this species).

Sediment with a broad range of organic content was obtained by collecting sand (0.6% organic content) from the dunes at Assateague Island and mud (13% organic

content) from a marsh creek near Brannock Bay (Figure 3.1). The sand and marsh sediment were mixed to obtain the 4 different levels of organic content (0.6±0.4%, 5.1±0.8%, 8.5±1.1%, and 13.1±2.5%; Table 3.2) used in the experiment. Mixed sediment was placed into 35 cm x 30 cm trays to a depth of 10 cm and trays were placed in mesocosms (192 cm x 100 cm x 61 cm) in a water-cooled greenhouse (7 m x 22 m). Each mesocosm contained 12 trays, 3 of each organic-content composition, so that total organic content was equal in all mesocosms. The 3 trays of each organic content were randomly assigned a position within each mesocosm. Mesocosms were filled with filtered Choptank River water (salinity 11), except the *V. americana* tank, which was filled with well water (salinity 0). The water depth in each tank was 45 cm. Mesocosms were allowed to "rest" for 3 d in order for suspended sediment to settle and geochemical profiles in the sediment to restore. Temperature sensors (StowAway Tidbit Temperature Loggers by Onsett Computers) were placed in each tank at a depth of 32 cm from the water surface. Average temperature of the water in the tanks was 25.6±2.7ºC.

Table 3.2. Mesocosm sediment characteristics. A representative median diameter for each treatment was calculated using the best-fit line from field data (Figure 3.3a) in phi units, then converted to microns. Representative water content was also calculated using the best-fit line from field data (Figure 3.3b). Values are reported as mean ± SE.

Sediment Characteristic	0.6% organic-content treatment	5% organic-content treatment	8.5% organic-content treatment	13% organic-content treatment
Initial organic content	0.6±0.1	5±0.2	8.5±0.3	13±0.7
Final organic content	0.5±0.03	5.4±0.8	9.3±0.6	10.1±0.8
Representative median diameter (phi, µm)	2.1±0.1 (233.3)	6.7±0.3 (9.6)	10.2±0.3 (0.9)	14.8±0.7 (0.04)
Representative water content	19.0±0.2	27.6±0.5	34.0±0.6	42.7±1.3

Trays were randomly assigned a species of SAV (Figure 3.2). Seeds (obtained from Dr. Steve Ailstock) were germinated in the lab in freshwater (salinity = 0) at 20ºC and allowed to grow for 20 days. Six seedlings of each species were planted in each tray at a depth of 0.5-1 cm, using an unsharpened pencil that had been marked in 0.5 cm increments. For the next 3 d, trays were observed for any seedlings loss due to death or dislodgement; these seedlings, were replaced with new ones. SAV was allowed to grow from 5 June to 20 August 2009. Water was partially exchanged every 2 weeks by draining the tank to 20 cm and then refilling to 45 cm.

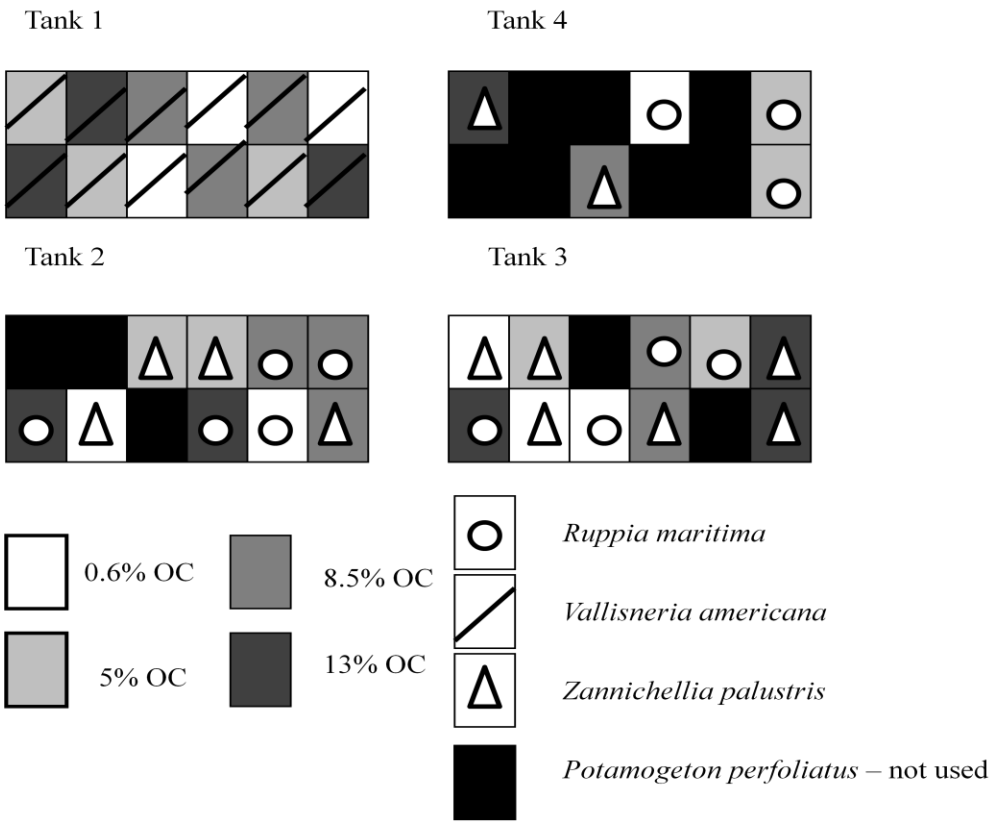

Figure 3.2. Greenhouse mesocosm experiment layout. Mesocosm 1 contained a freshwater species (*Vallisneria americana*) and had salinity 0. Mesocosms 2, 3, and 4 were maintained at a salinity of 11. Distribution of species and organic treatments were random (except *V. americana*), maintaining an equal overall organic concentration within each mesocosm. The patterns and shading refer to the organic content and SAV species in individual trays.

Light was measured daily at the sediment surface and 1 m above water (i.e., the air above the tank) using a photometer (LI-COR Model LI-1400, with spherical quantum sensor LI-193) to determine the percentage of light reaching the plants. During the course of the experiment, algae growing in the mesocosms were removed from the surface of the water and sides of tanks using a net and hand picked off SAV shoots if needed.

At the end of the experiment, SAV was harvested by sieving each tray with a 1-mm mesh sieve, as in the field study. Plant material was placed in bags and processed immediately. As in the field study, root and shoot length were measured on all intact roots and shoots, as well as above- and below-ground biomass. A small sediment sample (~20 g) was also taken from each tray to verify that sediment organic content remained constant during the experiment.

Data analyses

Data analysis was performed using SAS 9.2. Data was tested for normal distribution and Levene's Test was used to determine if variances were equal (Sokal and Rohlf, 1995). If these assumptions were not met then a log transformation was completed.

Field data were analyzed using an analysis of Covariance (ANCOVA) testing the effects of site (adjacent-exposed versus breakwater-protected) and organic content on SAV shoot- and root-length, as well as total biomass. Linear regressions were also conducted for SAV species V. americana shoot- and root-length, and total biomass versus sediment organic content. Linear regressions were also done for organic content versus grain size, water content, and fetch distance (Table 3.3).

Mesocosm data were analyzed with a 2-way ANOVA with tank and organic content as fixed effects. When significant differences existed within the ANOVA, a Tukey test was performed to determine pair-wise differences between organic treatments Table 3.5.

RESULTS

Field results

As expected, the 48 sites (adjacent-exposed and breakwater-protected sites at each of the 24 study locations) within the Chesapeake Bay were variable in grain size (median diameter), organic content, and water content. Overall, the mean sediment grain size was fine sand, and the top 10 cm had an average median diameter of 2.9±0.2 phi (143.6 µm; mean ± SE), average organic content of 2.0±0.4% and average water content of 21.8±1.4%. The variability of observations at individual sites is reflected by the large standard errors of these values. The average median diameter, organic content, and water content for individual sites ranged from 6.9 to 1.1 phi (8.4-466.5 µm), 0.4 to 20.1%, and 8.6 to 55.7%, respectively (Table 3.1). Median diameter and organic content was inversely correlated (r^2=0.54, p<0.0001; Figure 3.3a) with some variation due to large pieces of organic debris (organic content >5% was removed from correlation to account for this) that cause the median diameter to be greater than expected. Organic and water content were also significantly correlated (r^2=0.57, p<0.0001; Figure 3.3b). Since sediment median diameter, organic content, and water content co-vary, and the mesocosm experiment used organic content as the main variable, only organic content will be discussed for the *in situ* SAV results. Relationships between organic content (OC), sediment median diameter (MD) and water content (WC) can be calculated via the following equations:

$$MD = 1.02OC + 1.46, \text{ and} \quad \text{(Eq. 1)}$$

$$WC = 1.89OC + 17.89, \text{ respectively.} \quad \text{(Eq. 2)}$$

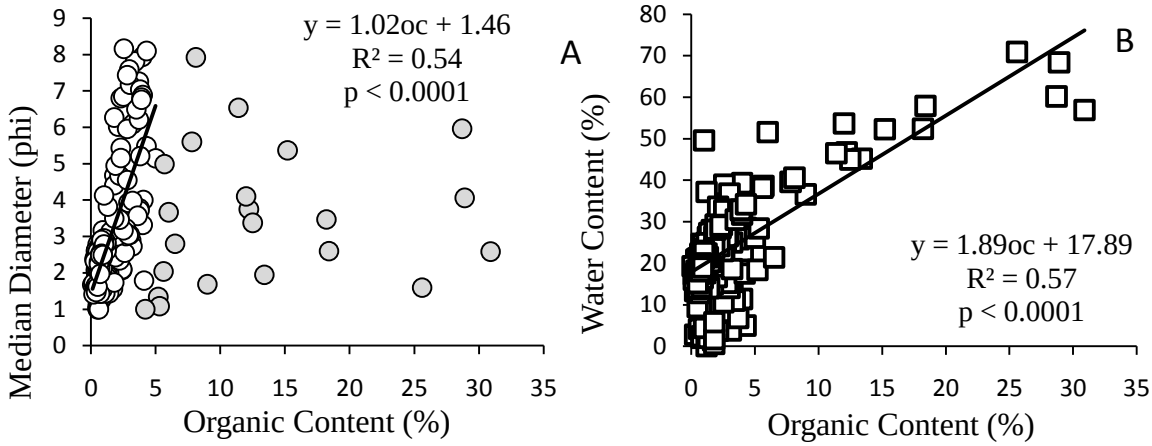

Figure 3.3. Sediment characteristics (grain size, water content) related to sediment organic content at 24 paired sampling sites in Chesapeake Bay, breakwater-protected and adjacent-exposed. Sediment organic content co-varies with grain size (A) and water content (B). Gray circles are not included in best-fit line.

Fetch measured at each site was greatly varied and ranged from 0.1±0.01 to 21.0±4.5 (km; Table 3.1). High fetch sites were characterized by lower organic content whereas low fetch sites had higher organic content (Figure 3.4). However, they were not significantly correlated at either adjacent-exposed ($p = 0.77$) or breakwater-protected ($p = 0.45$) sites.

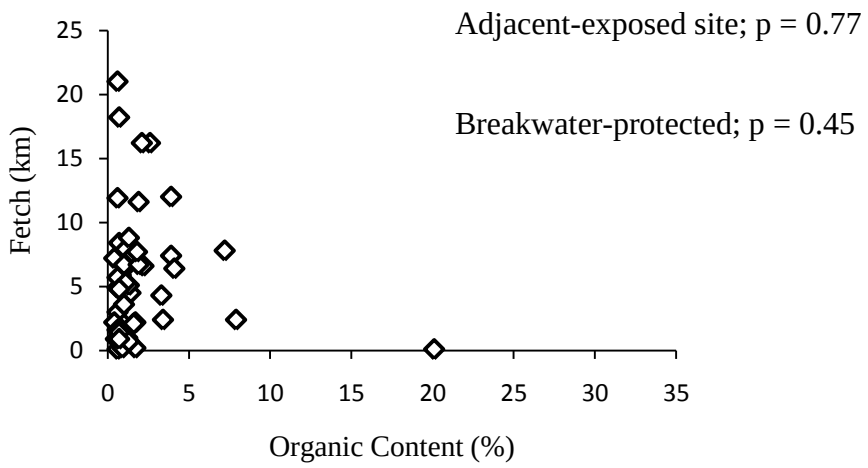

Figure 3.4. Organic content associated with fetch (km), these factors are not correlated. Organic content is based on the average of sediment top 10 cm from a push core. Fetch measured using measuring tool on Google Earth according to Koch et al. (2006).

Ruppia maritima

In situ, R. maritima was observed to grow at both breakwater-protected and adjacent-exposed sites at 10 of the 24 study locations, except for the adjacent-exposed site at Hoopers Island, Bishops Head, and Tangier Island. It was present in sediments varying in organic content from 0.6 to 4.1%, but was absent in sediment with an organic content of 2.6±0.5% (Hoopers Island adjacent-exposed), 3.3±0.2% (Bishops Head adjacent-exposed), and 7.2±1.9% (Tangier Island adjacent-exposed). Note that these 3 sites are characterized by compacted peat – old marsh sediment exposed as a result of marsh erosion and retreat. Shoot and root length for this species were not a function of organic content *in situ* (Figure 3.5a, b), but above-ground, below-ground, and total biomass all increased with organic content (Table 3.4**,** Figure 3.5c). Average *R. maritima* shoot lengths ranged from 3.8±0.1 cm to 22.8±0.7 cm and were longer at the breakwater-

protected sites than at the adjacent-exposed sites (p = 0.92). Average root lengths ranged from 4.5±0.2 cm to 9.1±0.3 cm and were not significantly different between adjacent-exposed and breakwater-protected sites (p = 0.81).

Above-ground and total biomass (Figure 3.5c) for *R. maritima* varied with organic content, but were not significantly different between adjacent-exposed and breakwater-protected sites (above-ground biomass, p = 0.97; below-ground biomass p = 0.80; and total biomass p = 0.91).

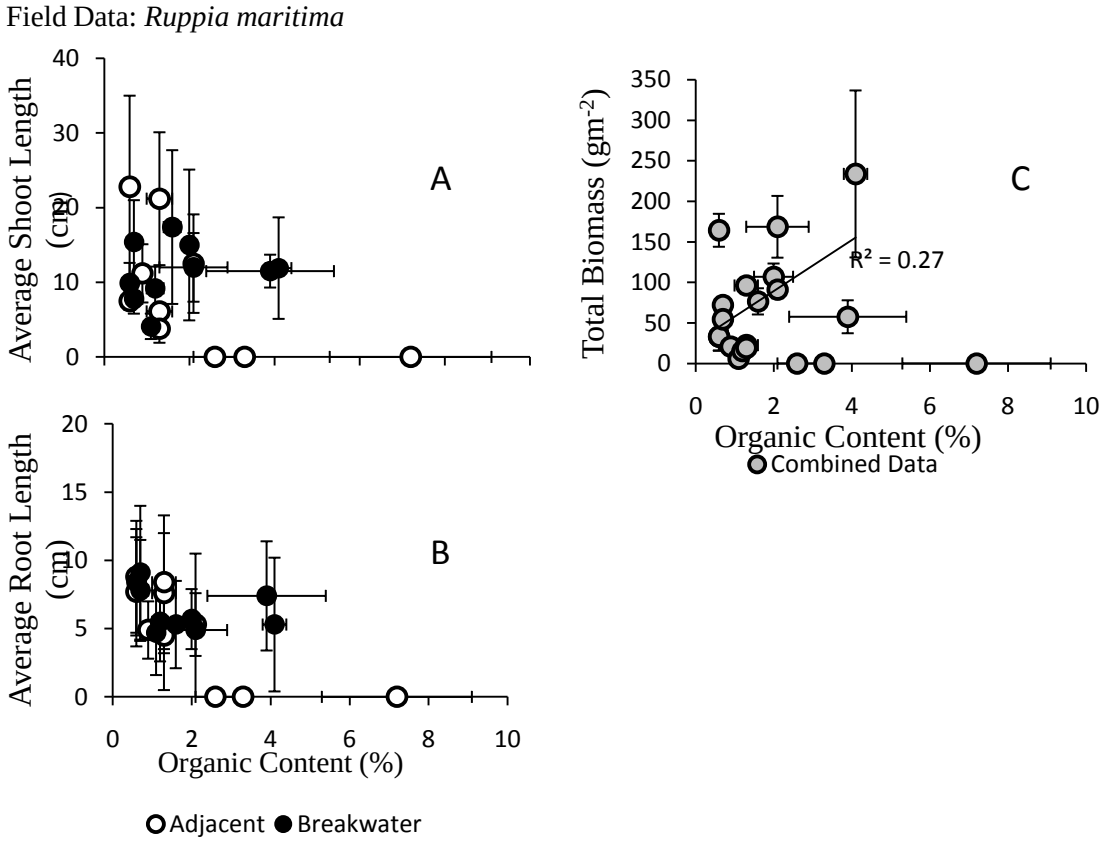

Figure 3.5. A) Average *in situ R. maritima* shoot length. B) Average *in situ R. maritima* root length. C) Average dry weight of total biomass of *in situ R. maritima*. Organic content is based on the average of sediment top 10 cm from a push core. Error bars are standard error.

Vallisneria americana

V. americana was present at both adjacent-exposed and breakwater-protected sites at 5 of the 6 tidal fresh/ oligohaline field locations, with average organic content ranging from 0.4 to 20.1%. It was not observed at the Red Eyed Yacht Club location, which had organic content of 1.7±0.3% at the adjacent-exposed site and 0.9±0.2% at the breakwater-protected site and a monoculture of *Myriophyllum spicatum* at both sites. Elk Neck *V. americana* data are included in the shoot- and root-length data but not the biomass data, as other species of SAV were not separated in the biomass dry-weight measurements. Average shoot lengths ranged from 5.8±0.0 to 44.2±2.7 cm. Shoots were longer at the breakwater-protected sites than the adjacent-exposed sites, although not significantly ($p = 0.39$). Shoot lengths at the adjacent-exposed sites increased in length with increasing organic content ($r^2 = 0.85$; $p = 0.03$), while shoot lengths decreased with increasing organic content at the breakwater-protected sites ($r^2 = 0.65$; $p = 0.20$; Figure 3.6a). Average root lengths were not significantly different between adjacent-exposed and breakwater-protected sites ($p = 0.33$), ranging from 3.3±0.3 to 6.9±0.1 cm, but root lengths increased with increasing organic content, but were not significantly correlated ($r^2 = 0.29$, $p = 0.14$; Figure 3.6b). However, note that this trend is driven by two sites: the adjacent-exposed sites at - Mason Neck 1 and Sue Creek (length and biomass data can be found in Table 3.4).

V. americana above-ground and total biomass was significantly higher ($p = 0.03$, 0.01, respectively) at the adjacent-exposed versus the breakwater-protected sites. Below-ground biomass was not significantly different ($p = 0.64$) between sites. Total biomass decreased with organic content at the breakwater-protected sites ($r^2 = 0.86$; $p = 0.30$), but

increased at the adjacent-exposed sites ($r^2 = 0.47$; $p = 0.25$; Figure 3.6c). Again, this trend was driven by two the two adjacent-exposed sites at Mason Neck 1 and Sue Creek. Below-ground biomass also increased with organic content at the adjacent-exposed sites, however; unlike above-ground biomass it decreased at the highest organic content value (Figure 3.6d). Due to the large amount of above-ground biomass at Sue Creek, the total biomass at Sue Creek was not different from Mason Neck 1, even though Mason Neck 1 had more below-ground biomass. Mason Neck 2 and Hart-Miller Island had significantly less total biomass than Mason Neck 1.

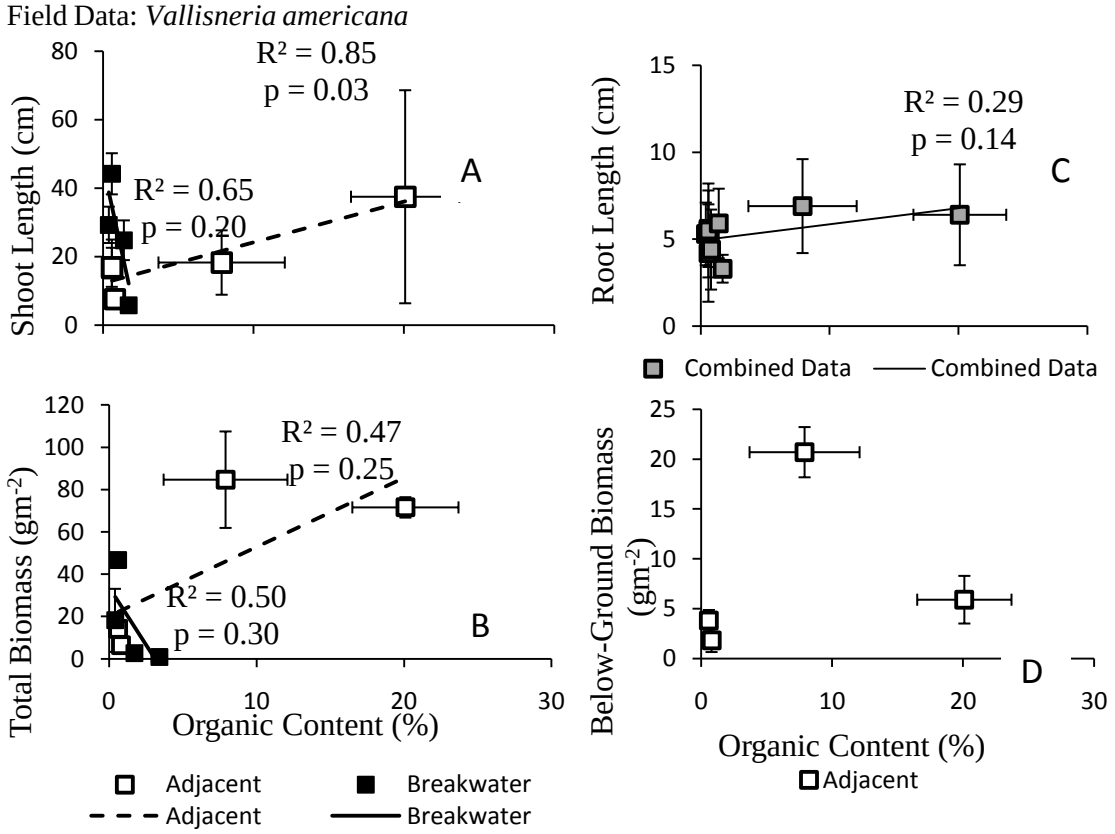

Figure 3.6. (A) Average *in situ V. americana* shoot length. (B) Average dry weight of total biomass of *in situ V. americana*. (C) Average *in situ V. americana* root length. (D) Average dry weight of below-ground biomass of *in situ V. americana*. Organic content is based on the average of sediment top 10 cm from a push core. Error bars are standard error.

Zannichellia palustris

Z. palustris was found at 3 study sites (Eastern Neck breakwater-protected and Hart-Miller Island adjacent-exposed and breakwater-protected). Sediment organic content at these sites ranged from 0.4±0.1 to 0.6±0.1%. Unfortunately, all shoots collected at Hart-Miller Island (either site) were broken and not able to be measured. However intact shoots were collected at the Eastern Neck breakwater-protected site and averaged 6.4±0.1 cm, with the majority (99.4%) being <10 cm long. Average root length at this site was 2.2±0.2 cm (Table 3.4). The small number of samples for biomass data did not allow for statistical analysis.

Table 3.3. (A) *In situ* SAV ANCOVA results. *Log transformation was completed so that data fit assumptions of normal distribution and equal variances. (B) Linear regression results for *V. americana*. ** indicates a significant p-value of < 0.05.

SAV response	Effects	Degree of Freedom	F-value	P-value
A		*Ruppia maritima*		
Shoot Length*	Organic*Location	1	1.65	0.22
	Organic*	1	0.01	0.91
	Location	1	0.01	0.92
Root Length*	Organic*Location	1	0	0.96
	Organic*	1	2.37	0.15
	Location	1	0.06	0.81
Above-ground Biomass*	Organic*Location	1	2.64	0.13
	Organic*	1	0.97	0.34
	Location	1	0	0.97
Below-ground Biomass*	Organic*Location	1	1.34	0.27
	Organic*	1	1.2	0.29
	Location	1	0.07	0.8
Total Biomass*	Organic*Location	1	2.5	0.14

	Organic*	1	1.12	0.31
	Location	1	0.01	0.91
		Vallisneria americana		
Shoot Length	Organic*Location	1	5.46	0.07
	Organic*	1	0.49	0.51
	Location	1	0.85	0.39
Root Length	Organic*Location	1	0.96	0.37
	Organic*	1	1.33	0.29
	Location	1	1.13	0.33
Above-ground Biomass	Organic*Location	1	10.18	0.03**
	Organic*	1		
	Location	1		
Below-ground Biomass	Organic*Location	1	0.28	0.63
	Organic*	1	1.06	0.36
	Location	1	0.25	0.64
Total Biomass*	Organic*Location	1	21.87	0.01**
	Organic*	1		
	Location	1		
V. americana response	Factor	Degree of Freedom	T-value	P-value
B				
Breakwater-protected Shoot Length	Organic	1	-1.93	0.2
Adjacent-exposed Shoot Length	Organic	1	4.07	0.03
Root Length	Organic	1	1.68	0.14
Breakwater-protected Total Biomass	Organic	1	-1.40	0.30
Adjacent-exposed Total Biomass	Organic	1	1.63	0.25

Table 3.4. *In situ* SAV data. Data are organized according to species and increasing organic content within that species. Organic contents are grouped in 1% increments. BW = Breakwater-protected site. ADJ = Adjacent-exposed site. Values are reported in mean ± SE.

Site	Organic Content (%)	Above-Ground Biomass (gm^{-2})	Below-Ground Biomass (gm^{-2})	Total Biomass (gm^{-2})	Ratio of Above-/ Below-Ground Biomass	Shoot Length (cm)	Root Length (cm)
			Ruppia	*maritima*			
Cape Charles Bay Creek - BW	0.6±0.08	19.4±9.7	13.7±7.6	33.1±17.1	1.7±0.5	9.9±0.2	8.4±0.3
Cape Charles Public Beach - ADJ	0.6±0.01	15.9±9.1	17.3±8.7	33.2±17.5	1.4±0.9	7.5±0.1	8.8±0.3
Mobjack Bay - ADJ	0.6±0.1	151.6±18.7	12.7±2.3	164.3±20.3	13.1±4.9	22.8±0.7	7.7±0.3
Cape Charles Public Beach - BW	0.7±0.2	38.1±1.1	34.0±7.8	72.1±8.9	1.2±0.2	7.8±0.2	7.8±0.2
Schley – BW	0.7±0.04	43.3±11.7	11.2±2.3	54.5±13.3	4.1±1.1	15.4±0.4	9.1±0.3
Mobjack Bay7- ADJ	0.9±0.1	17.1±9.1	3.8±1.3	20.9±10.3	4.8±1.5	11.2±0.5	4.9±0.3
Brannock Bay – BW	1.1±0.1	3.4±0.6	2.4±0.5	5.8±0.9	1.6±0.4	4.1±0.1	4.7±0.3
Mobjack Bay7 – BW	1.2±0.2	10.9±1.7	4.4±0.8	15.3±2.3	2.7±0.5	9.2±0.4	5.5±0.3
Cape Charles Bay Creek - ADJ	1.3±0.3	12.6±5.6	10.0±3.3	22.6±8.7	1.1±0.2	6.1±0.1	7.6±0.3
Brannock Bay - ADJ	1.3±0.1	7.3±3.3	11.9±4.9	19.3±8.2	0.6±0.1	3.8±0.1	4.5±0.2
Schley - ADJ	1.3±0.3	86.6±8.6	9.5±0.9	96.2±9.1	9.2±0.9	21.2±0.6	8.4±0.3
Mobjack Bay – BW	1.6±0.2	67.2±13.9	9.4±2.3	76.6±16.2	7.5±0.8	17.4±0.6	5.3±0.3
Mobjack Bay3 – BW	2±0.5	86.2±14.8	20.7±2.0	106.9±16.4	4.1±0.9	15.0±0.6	5.7±0.1
Hoopers Island – BW	2.1±0.8	126.2±33.6	42.4±4.6	168.6±38.1	2.9±0.5	12.0±0.2	4.9±0.3
Mobjack Bay3 – ADJ	2.1±0.1	71.0±10.6	20.0±1.1	91.0±10.6	3.6±0.5	12.5±0.4	5.3±0.1
Hoopers Island – ADJ	2.6±0.5	0±0	0±0	0±0	0±0	0±0	0±0
Bishops Head – ADJ	3.3±0.2	0±0	0±0	0±0	0±0	0±0	0±0
Tangier Island – BW	3.9±1.5	36.5±10.7	21.1±0	57.6±20.3	3.8±2.2	11.5±0.2	7.4±0.3
Bishops Head – BW	4.1±0.3	181.2±91.8	52.6±12.4	233.8±103.0	2.8±1.7	11.9±0.3	5.3±0.2
Tangier Island –	7.2±1.9	0±0	0±0	0±0	0±0	0±0	0±0

ADJ							
			Vallisneria	*americana*			
Hart-Miller Island – BW	0.4±0.0	15.6±13.9	3.9±0.7	18.2±14.9	5.0±4.6	29.3±3.8	5.3±0.3
Hart-Miller Island – ADJ	0.6±0.1	10.3±3.6	3.8±1.1	14.1±4.1	3.1±1.0	16.7±2.1	5.6±0.2
Elk Neck – ADJ	0.6±0.1	n/a	n/a	n/a	n/a	16.9±1.0	5.5±0.2
Sue Creek – BW	0.6±0.2	45.7±0.0	1.0±0.0	46.7±0.0	45.7±0.0	44.2±2.7	4.2±1.2
Mason Neck2 – ADJ	0.8±0.1	4.6±2.7	1.8±1.2	6.4±3.8	2.8±0.3	7.6±1.1	4.4±0.5
Elk Neck – BW	1.4±0.2	n/a	n/a	n/a	n/a	24.8±1.8	5.9±0.2
Mason Neck2 – BW	1.7±0.4	1.4±0.7	1.4±1.1	2.7±1.8	1.6±0.7	5.8±0.0	3.3±0.3
Mason Neck1 – BW	3.4±0.5	0.9±0.6	0.0±0.0	0.9±0.6	0.0±0.0	n/a	n/a
Mason Neck1 – ADJ	7.9±4.2	64.0±22.7	20.7±2.5	84.7±22.8	3.2±1.2	18.3±1.1	6.9±0.1
Sue Creek – ADJ	20.1±3.6	65.7±7.2	5.9±2.4	71.6±4.8	13.8±6.7	37.5±2.6	6.4±0.3
			Zannichellia	*Palustris*			
Eastern Neck – BW	0.4±0.1	4.8±1.3	2.1±0.5	6.9±1.8	2.2±0.1	6.4±0.1	2.2±0.2
Hart-Miller Island – BW	0.4±0.0	2.2±1.3	0.0±0.0	2.2±1.3	n/a	n/a	n/a
Hart-Miller Island – ADJ	0.6±0.1	0.2±0.0	0.3±0.0	0.5±0.0	0.7±0.0	n/a	n/a

Mesocosm results

Ruppia maritima and *Vallisneria americana* did rather well in the mesocosm, with all but one of the treatments surviving until collection. *Zannichellia palustris* had 8 of 12 trays surviving for analysis. More than half of the *Potamogeton perfoliatus* replicates did not survive: therefore this species was not analyzed further. All mesocosms received >50% of surface light. SAV grown in the mesocosms showed a bell-shaped curve of biomass as a function of organic content, suggesting that they have an optimum organic content (Figure 3.7). For *R. maritima* and *V. americana*, this optimum appears to

be ~5%, while for *Z. palustris* it is ~8%. The higher value for *Z. palustris* is due to more resource allocation to root biomass. It is also interesting to note that at higher organic content (>8%), *V. americana* biomass was significantly reduced but *R. maritima* continued to produce biomass.

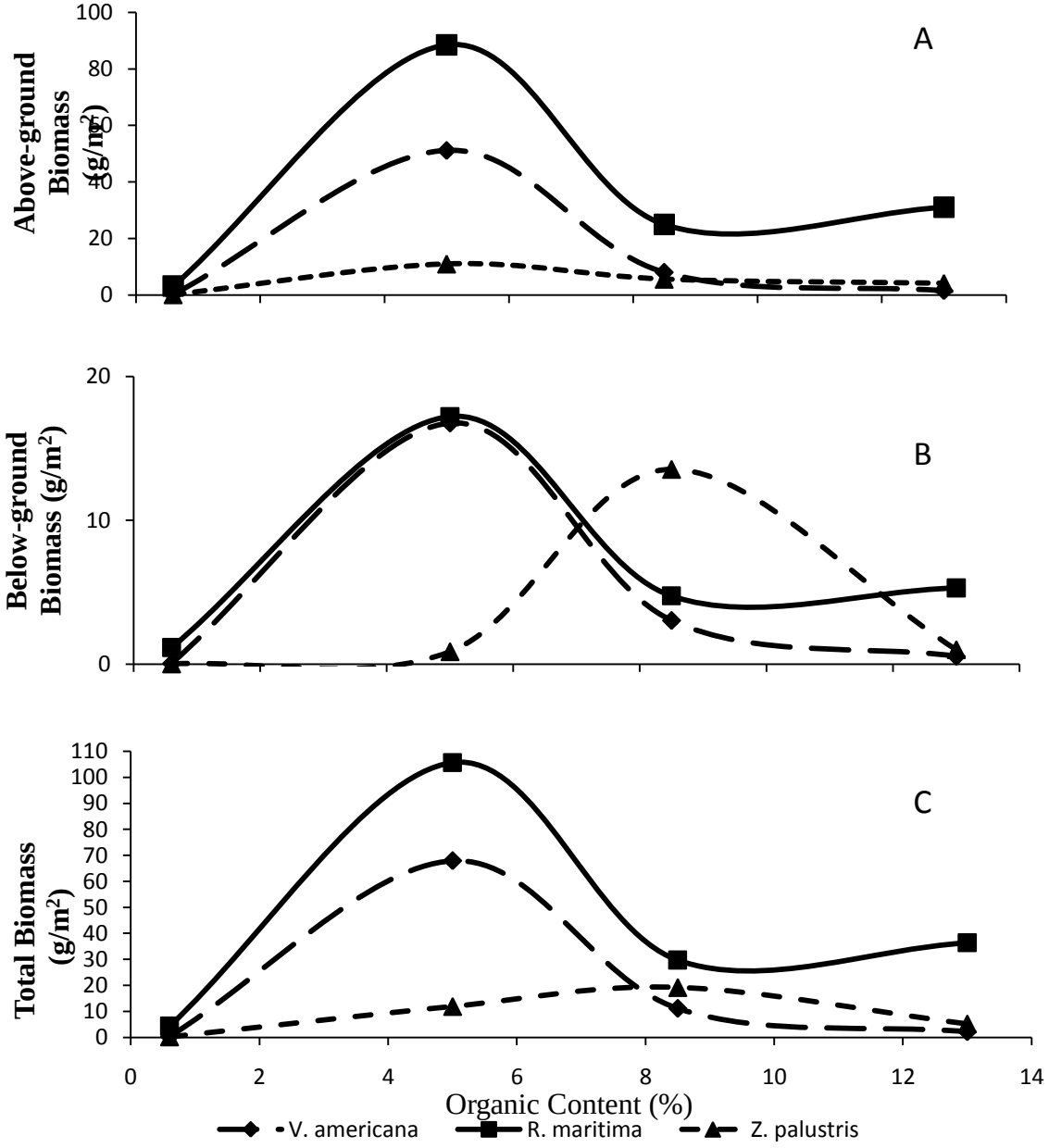

Figure 3.7. Mean dry weight of above-ground (A), below-ground (B), and total biomass (C) for 3 species grown in 4 organic-content treatments in a controlled mesocosm study.

Ruppia maritima

R. maritima shoots were longest, 25.4±1.0 cm (mean ± SE, $p < 0.0001$, Figure 3.8a, 3.9a) in the 5% organic-content treatment. Shoots for this species were shortest (11.7±0.7 cm) in the lowest organic-content treatment (0.6%), and had intermediate lengths in the higher organic-content treatments: 18.7±1.1 cm at 8.5% organic content and 21.3±0.9 cm at 13% organic content. Organic content also influenced reproductive abilities of this species as only 4.9% of the shoots were reproductive at the 0.6% organic content level, but reproductive shoots in the other organic-content treatments ranged from 10.9 to 15.9%.

R. maritima roots (Figure 3.8b, 3.9b) by the different levels of organic content, with mean root lengths ranging from 5.8±0.2 cm, in the 13% organic-content treatment, to 7.2±0.3 cm, in the 8.5% treatment. Shoot- and root-length response was linear (Figure 3.9) for *R. maritima* in the mesocosms, but biomass response was not (Figure 3.7). Total biomass was significantly higher ($p = 0.03$) in the 5% organic treatment, as was above-ground ($p = 0.04$) and below-ground biomass ($p = 0.01$). The 5% treatment had ~3 times greater biomass than the 13% organic-content treatment, which had the second highest value (ANOVA results can be found in Table 3.5 and length and biomass data can be found in Table 3.6).

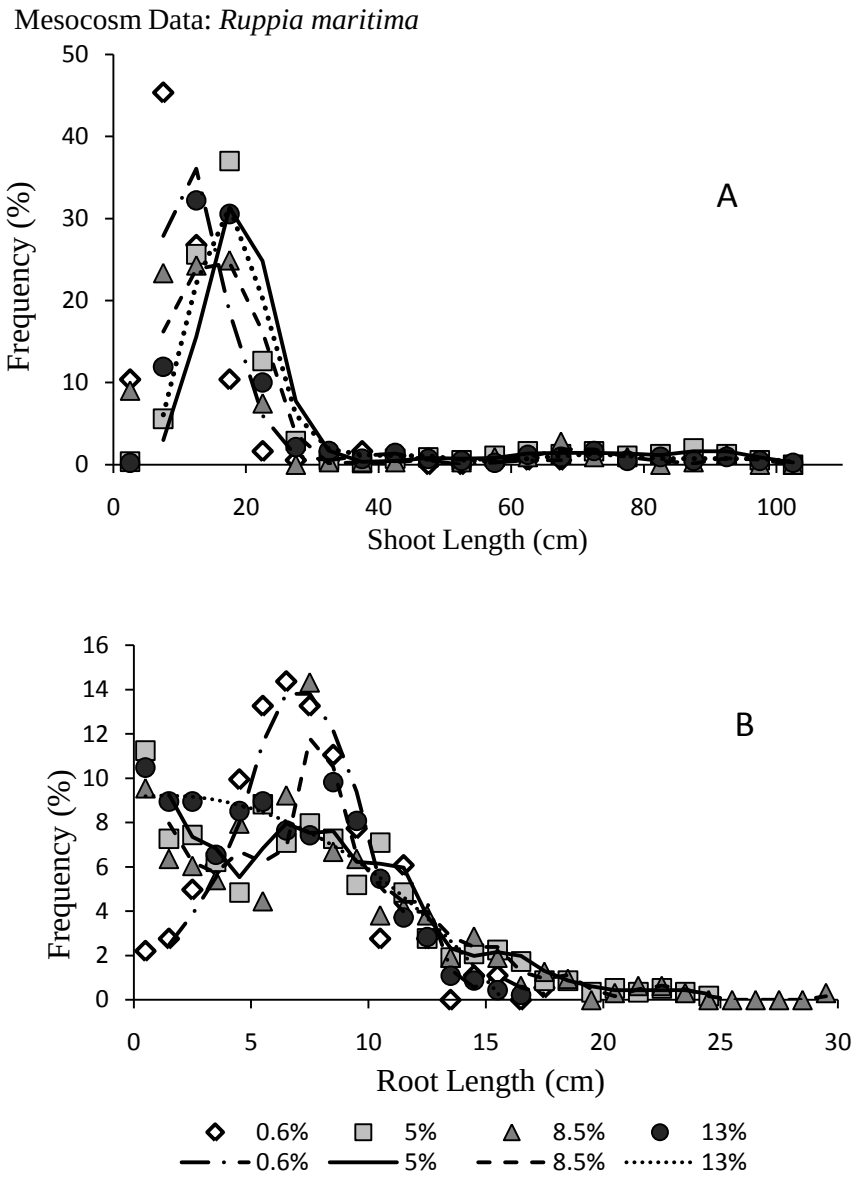

Figure 3.8. Percent frequency of *R. maritima* shoot lengths (A) and root lengths (B) in 4 organic-content treatments in a controlled mesocosm study.

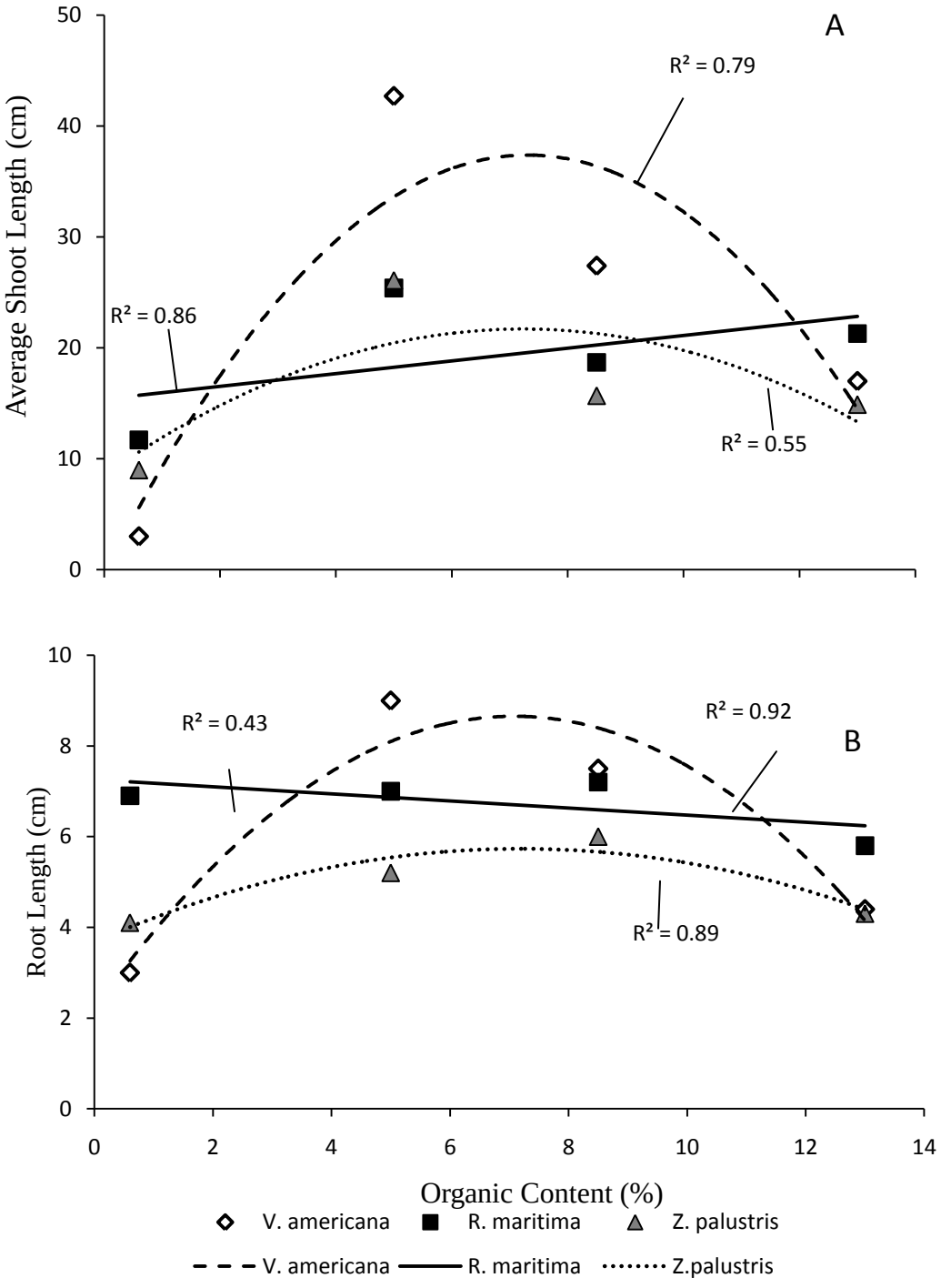

Figure 3.9. Average shoot (A) and root (B) length of *R. maritima*, *V. americana*, and *Z. palustris* in 4 organic-content treatments in a controlled mesocosm experiment.

Vallisneria americana

V. americana shoots were the longest (42.7±3.9 cm, $p < 0.0001$) in the 5% organic-content treatment and significantly shorter ($p < 0.0001$) in the 0.6% (3.0±0.2 cm, Figure 3.9a, 3.10a). Significant differences of shoot length was not observed between the 8.5% and 13% organic content treatments (Figure 3.9a, Table 3.5).

Roots for this species were significantly shorter (3.0±0.4 cm, $p < 0.0001$) in the 0.6% organic-content treatment and ranged from 4.4±0.4 cm (13% organic content) to 9.0±0.3 cm (5% organic content) in the other treatments (Figure 3.9b, 3.10b). Significant differences were observed between all treatments, except 0.6% and 13% organic content.

V. americana had significantly more above-ground biomass in the 5% organic-content treatment (51.2±3.4 gm^{-2}, $p < 0.0001$) than at the other treatments. This was ~6 times greater than the next highest observed above-ground biomass, (11.1±14.1 gm^{-2}) in the 8.5% organic-content treatment. Below-ground biomass in the 5% organic-content treatment (16.8±5.8 gm^{-2}, $p = 0.002$) was >5 times higher than in the other organic-content treatments. Total biomass in the 5% treatment (67.9±5.1 gm^{-2}; $p < 0.0001$) was >6 times higher than the other treatments (length and biomass data can be found in Table 3.4).

Mesocosm Data: *Vallisneria americana*

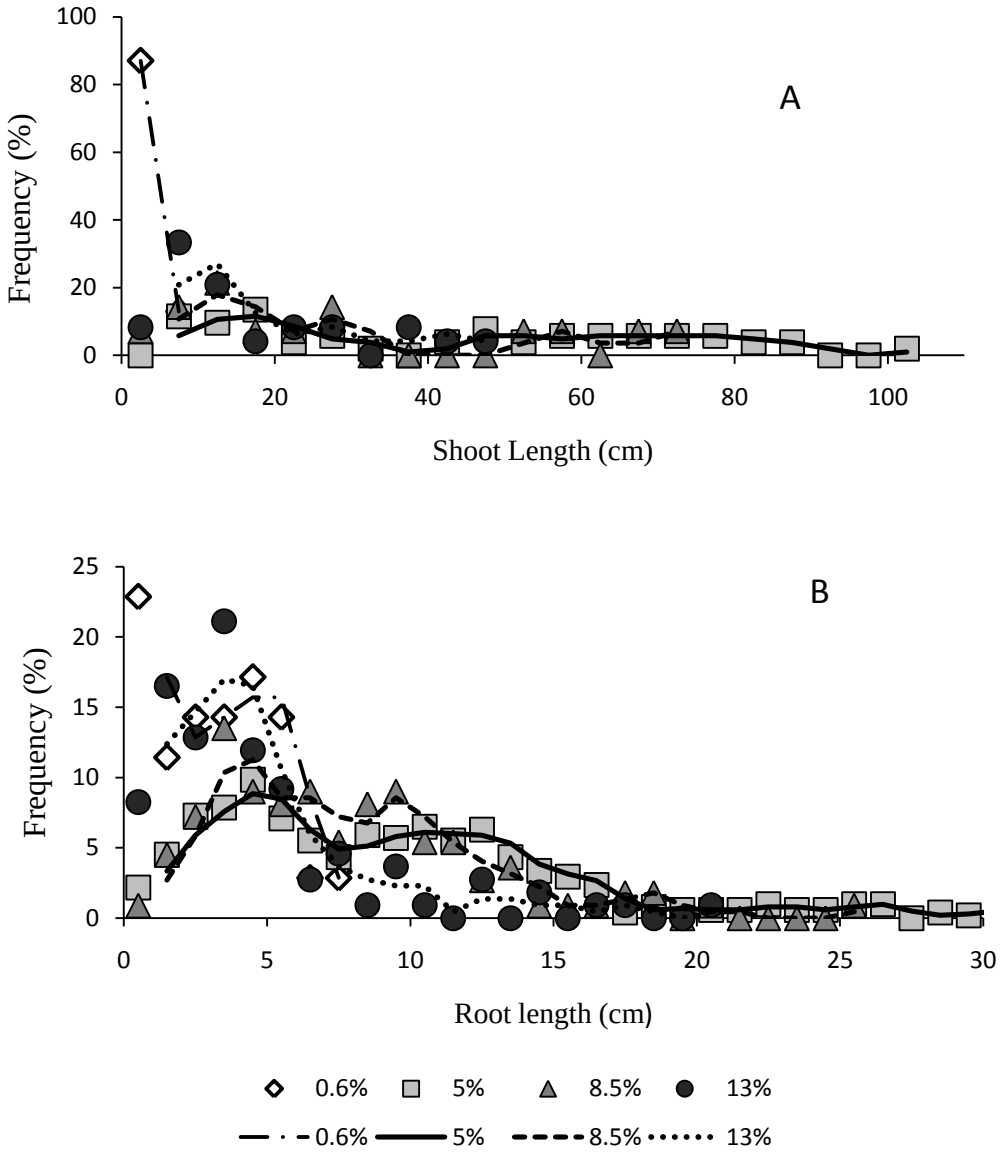

Figure 3.10. Percent frequency of *V. americana* shoot lengths (A) and root lengths (B) in 4 organic-content treatments in a controlled mesocosm study.

Zannichellia palustris

Z. palustris had significantly longer shoots ($p < 0.0001$; 26.1±1.3 cm) in the 5% organic-content treatment, which was the only treatment that was different from the others. Average shoot lengths ranged from 9.0±1.0 cm (0.6% organic content treatment) to 15.7±0.8 cm (8.5% organic content treatment; Figure 3.9a, 3.11a). Roots of this species were longest in the 8.5% organic-content treatment (6.0±0.4 cm; $p = 0.001$) different from other treatments. Root lengths ranged from 4.1±0.4 (0.6% organic content) to 5.2±0.3 cm (5% organic content; Figure 3.9b, 3.11b).

Above-ground biomass of *Z. palustris* was highest, ($p = 0.01$) in the 5% organic-content treatment (11.0±13.6 gm^{-2}). Below-ground biomass was highest in the 8.5% treatment (13.6±0 gm^{-2}, $p = 0.0004$). Below-ground biomass in this treatment was the only one with a significant difference from the others and was at least ~13 times greater than the below-ground biomass measured in the other treatments. Total biomass at 5% organic content consisted of dominantly above-ground biomass, whereas total biomass at 8.5% organic content was dominated by below-ground biomass. Total biomass at the 8.5% organic content treatment was significantly greater than the 0.6% and 13% treatments and the 5% organic content treatment was significantly greater than the 0.6% ($p = 0.004$). Reproductive growth did not seem to be influenced by organic content as all treatments contained plants with seeds (length and biomass data can be found in Table 3.4).

Mesocosm Data: *Zannichellia Palustris*

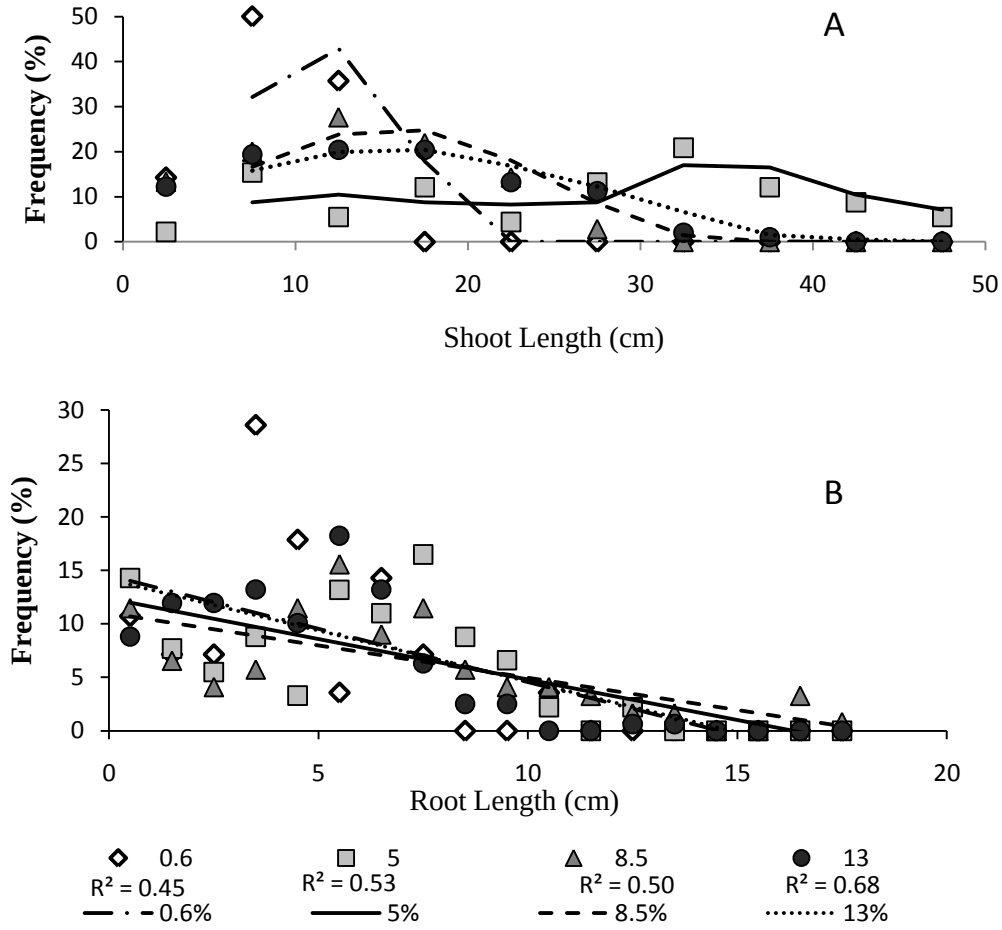

Figure 3.11. Percent frequency of *Z. palustris* shoot lengths (A) and root lengths (B) in 4 organic-content treatments in a controlled mesocosm study.

Table 3.5. Mesocosm SAV 2-Way ANOVA results for *R. maritima* and *Z. palustris*, 1-Way ANOVA results for *V. americana*. *Log transformation was completed so that data fit assumptions of normal distribution and equal variances.

SAV response	Effects	Degree of Freedom	F-value	P-value
	Ruppia	*maritima*		
Shoot Length	Tank	2	36.17	< 0.0001
	Organic	3	17.65	< 0.0001
	Tank*Organic	3	5.39	0.001
Root Length*	Tank	2	15.53	< 0.0001
	Organic	3	14.75	< 0.0001
	Tank*Organic	3	2.09	0.10
Above-ground Biomass*	Tank	2	1.56	0.39
	Organic	3	24.25	0.04
	Tank*Organic	3	4.15	0.20
Below-ground Biomass*	Tank	2	5.53	0.15
	Organic	3	131.60	0.01
	Tank*Organic	3	33.35	0.03
Total Biomass*	Organic*Location	2	1.78	0.36
	Organic*	3	31.03	0.03
	Location	3	5.76	0.15
	Vallisneria	*americana*		
Shoot Length	Organic	3	38.9	< 0.0001
Root Length	Organic	3	31.18	< 0.0001
Above-ground Biomass	Organic	3	91.53	< 0.0001
Below-ground Biomass	Organic	3	15.38	0.002
Total Biomass	Organic	3	80.65	< 0.0001
	Zannichellia	*palustris*		
Shoot Length	Tank	1	7.63	0.01
	Organic	3	27.59	< 0.0001
	Tank*Organic	1	0.04	0.83
Root Length	Tank	1	10.15	0.002
	Organic	3	5.44	0.001
	Tank*Organic	1	0.16	0.69
Above-ground Biomass	Tank	1	12.83	0.04

	Organic	3	46.17	0.01
	Tank*Organic	1	69.72	0.004
Below-ground Biomass	Tank	1	177.01	0.001
	Organic	3	267.66	0.0004
	Tank*Organic	1	4.30	0.13
Total Biomass	Tank	1	0.27	0.64
	Organic	3	58.87	0.004
	Tank*Organic	1	46.60	0.06

Table 3.6. Mesocosm SAV data. Note optimal growth at 5% organic content for *R. maritima* and *V. americana* and 8% for *Z. palustris*. Data is grouped by species with increasing organic content for each. Values are reported as mean ± SE.

Treatment (% Organic Matter and Species)	Above-Ground Biomass (gm-2)	Below-Ground Biomass (gm-2)	Total Biomass (gm-2)	Ratio Above- / Below-Ground Biomass	Shoot Length (cm)	Root Length (cm)
0.6% Ruppia (n=3)	3.2±1.5	1.2±0.7	4.3±2.3	3.0±0.6	11.7±0.7 (n=183)	6.9±0.2 (181)
5% Ruppia (n=2)	88.5±15.3	17.2±4.4	105.7±19.7	5.2±0.4	25.4±1.0 (n=554)	7.0±0.2 (578)
8.5% Ruppia (n=2)	25.0±27.2	4.8±4.3	29.7±31.5	4.6±1.7	18.7±1.1 (n=321)	7.2±0.3 (314)
13.1% Ruppia (n=3)	31.1±0.9	5.3±1.1	36.4±1.6	6.1±1.3	21.3±0.9 (n=419)	5.8±0.2 (458)
0.6% Vallisneria (n=3)	0.24±0.12	0.05±0.1	0.29±0.11	5.7±4.5	3.0±0.2 (n=54)	3.0±0.4 (35)
5% Vallisneria (n=3)	51.2±3.4	16.8±5.8	67.9±5.1	3.3±1.1	42.7±3.9 (n=52)	9.0±0.3 (508)
8.5% Vallisneria (n=2)	8.1±10.1	3.0±4.0	11.1±14.1	3.3±0.9	27.4±24.1 (n=14)	7.5±1.0 (111)
13.1% Vallisneria (n=3)	1.6±1.9	0.6±0.8	2.1±2.7	3.6±1.0	17.0±2.6 (n=24)	4.4±0.4 (109
0.6% Zanichellia (n=3)	0.2±0.1	0.03±0.03	0.2±0.1	10.3±9.9	9.0±1.0 (n=14)	4.1±0.4 (28)

5% Zanichellia (n=2)	11.0±13.6	0.9±1.1	11.9±14.7	13.1±1.1	26.1±1.3 (n=91)	5.2±0.3 (91)
8.5% Zanichellia (n=1)	5.7	13.6	19.2	0.4	15.7±0.8 (n=105)	6.0±0.4 (122)
13.1% Zanichellia (n=2)	4.2±1.8	1.0±0.06	5.2±2.4	4.3±0.7	14.9±0.8 (n=98)	4.3±0.2 (159)

Mesocosm initial and final organic content did show some fluctuation as see in Table 3.2. Increases in treatments are likely due to suspension of sediment from the higher organic treatments that settled onto other trays or algal growth on sediment surface. Grain size and water content were calculated from best-fit lines from Figure 3.3.

DISCUSSION

SAV in the Chesapeake Bay is exposed to a broad range of sediment characteristics that are highly variable. Some species may be more suitable to some sediment than to others. Mesocosm and field results in this study did not always agree but in doing so provided insight into other possible important parameters that also need to be considered when evaluating SAV habitat requirements. SAV grown in the mesocosms appeared to have well defined sediment organic content requirements where growth was optimal: 5% organic content for *R. maritima* and *V. americana* and 8.5% for *Z. palustris*. In the field, however, other environmental factors, such as currents, waves, sediment compaction, grazing and interspecific competition are likely to also influence SAV development and growth (Koch, 2001).

Ruppia maritima

R. maritima shoot lengths showed no significant differences between the organic-content treatments in the mesocosm experiment but shoot lengths were highly variable between sites of the same organic content *in situ*. For example, at the Mobjack Bay adjacent-exposed site (0.6±0.1% organic content) mean shoot length was 22.8±0.7 cm, however at the Cape Charles Public Beach adjacent-exposed site which also had 0.6±0.01% organic content, mean shoot length was only 7.5±0.1 cm. It appears that shoot length for this species is not only a function of sediment organic content but also wave exposure. The fetch at Mobjack Bay adjacent-exposed site was much smaller (1.6±0.6 km) than at the Cape Charles Public Beach adjacent-exposed site (21.0±4.5 km) thereby allowing shoots to grow longer where wave action was lowest. *R. maritima* shoots were also longer at the breakwater-protected sites (i.e., fetch near zero) than at the adjacent-exposed sites, supporting the idea that shoot length is closely related to wave energy (See Table 3.1 for fetch values.)

High sediment compaction (Wicks et al., 2009) and silt/clay content (Leschen et al., 2010) have been previously suggested as limiting to the seagrass *Z. marina*. The same appears to be true for *R. maritima*. Although this species grew in sediments with organic content up to 13% in the mesocosms and 4.1% *in situ*, it was absent at 3 sites with 2.6% (Hoopers Island adjacent-exposed), 3.3% (Bishops Head adjacent-exposed) and 7.2% (Tangier Island adjacent-exposed) organic content. Water content at the Bishops Head adjacent-exposed site was low (10.8±0.2%), suggesting that this sediment is compacted, whereas the Tangier Island adjacent-exposed site had higher water content (35.3±5.0%) suggesting that it is rather “fluffy”. Both of these sediment types have been shown to be

limiting to the growth of *Z. marina* (Wicks et al., 2009). Additionally, all 3 sites had sediments containing >55% silt/clay, much higher than the 35% silt/clay threshold suggested by Leschen et al. (2010). Within the present study, 8 of the 48 sites had sediment with >35% silt/clay, and only 2 (Bishops Head breakwater-protected and Mason Neck 1 breakwater-protected) of these 8 supported SAV growth (*R. maritima, V. americana, H. verticillata, N. gracillima,* and *M. spicatum*).

As with shoots in the mesocosm, rhizomes and roots of *R. maritima* also showed a clear preference for sediments with 5% organic content as shown by the bell-shaped biomass curve in Figure 3.6b. In the mesocosm, root length decreased linearly with organic content, so the higher root biomass at 5% was probably not due to root length but rather an increase in the number of roots or their thickness (Ye et al., 2009). The longer (but not statistically significant) root length (10-20 cm) at the lowest organic content is a nutrient acquisition strategy commonly observed in other plants (Sagova-Mareckova, 2009). Average *in situ* roots were <10 cm at all sites colonized by *R. maritima* suggesting sufficient nutrient availability.

R. maritima growing in the low organic-content treatment (0.6%) produced very few reproductive shoots in the mesocosm (4.9%). This was supported in the field data as *R. maritima* growing at sites with <1% organic content had a small percentage of reproductive shoots (<2.3%; usually 0%), with the exception of the Mobjack Bay adjacent-exposed site where sediment was 0.6% but 26.3% of the shoots were reproductive. The low number of reproductive shoots in sediments with low organic content is somewhat surprising as *R. maritima* is considered a primary colonizer (Rosenzweig, 1994). If seeds germinate in sediments with low organic content as

commonly found in unvegetated areas colonized by primary species, the plants will produce few or no seeds unless they immediately start accumulating fine and organic particles.

Vallisneria americana

Sediments may be particularly important for *V. americana*, since this species is capable of using sediment CO_2 for photosynthesis, especially when CO_2 concentrations in the water column are low (Winkel and Borum, 2009). Low concentrations of CO_2 in the water column occurs when dense canopies develop, slowing water movement and removing CO_2 from the water. As a result, the flux of CO_2 to the leaf surface is reduced. This may explain the stunted growth of *V. americana* in 0.6% organic content in the mesocosm: water was stagnant, limiting CO_2 acquisition from the water column, and the low organic content did not supply sufficient CO_2 in the sediment. In the field, plants growing in sediments with <1% organic content were not stunted, probably because water flow allowed for sufficient resource acquisition through the shoots.

It is well known that water motion by currents and/or waves is important for *V. americana* (Nishihara and Ackerman, 2006), as maximum biomass tends to occur when fetch >2 km (Kreiling et al., 2007). The low to medium fetch (<4.9 km) *V. americana* experienced at adjacent-exposed sites in Chesapeake Bay apparently provided ideal conditions for growth but the breakwaters reduced the fetch to near zero. As a result, biomass in breakwater-protected areas was lower than in the adjacent-exposed areas. The additional organic content at breakwater-protected sites seemed to induce an additional

stress (negative trends in Figure 3.5a and 3.5c). Microbial breakdown of organic content in freshwater sediments produces methane Capone and Kiene, 1988) which can infiltrate into SAV roots and the lacunar network causing stress or damage to the plant (Heilman and Carlton, 2001). SAV respond by oxidizing the methane into usable CO_2 (Heilman and Carlton, 2001) but this process seems to need actively photosynthesizing leaves and not diffusion-limited leaves (Sand-Jensen et al., 1982; Smith et al., 1984; Caffrey and Kemp, 1991) as found in the mesocosms and breakwater-protected areas. This stress was also observed when organic content exceeded 5% under stagnant conditions in the mesocosm. In contrast, when *V. americana* was exposed to some wave action at the adjacent-exposed sites, the fetch limitation was removed and the plants were able to take advantage of the extra nutrients and CO_2 provided by the organic content in the sediments, up to 20%.

These findings suggest that the habitat requirement for organic content for *V. americana* is strongly tied to local hydrodynamics, Although *V. americana* reached its maximum biomass at 5% organic content in the mesocosm, this may not be the ideal organic content for this species *in situ*. If sufficient water flow exists, *V. americana* can grow in sediments with rather high organic content, as high as 20% or possibly even more. If strong currents and/or waves are required for successful colonization of sediments with high organic content, and leaf length increases with organic content, how do the plants remain anchored? Longer leaves imply higher leaf area as *V. americana* leaf width does not change as much as leaf length and higher leaf area leads to increasing drag exerted on the plants (Schanz and Asmus, 2003). The question that remains is "how does *V. americana* stay anchored in the sediment when its leaves become longer with

increasing organic content?" Perhaps the answer lies in the constant above- to below-ground biomass ratios at medium to high organic contents. As leaves become longer and dislodgement potential increases, roots also become longer increasing the anchoring capacity. It appears the *V. americana* has better adapted to grow in sediments with high organic content than *Z. marina*. In *Z. marina*, leaves become longer as organic content increases but roots increase at a lower rate leading to their dislodgement in high wave environments (Wicks et al., 2009).

The need for water flow for *V. americana* may be related to the amount of fine material (silt + clay) in the sediment. It appears that *V. americana* can grow in sediments of higher organic content as long as the percent of fine material does not get too high (*in situ* data suggests ≤42.0% silt/clay); conditions found when fetch is medium. Sue Creek adjacent-exposed site (22.8% silt/clay; 0.1±0.01 km fetch) shoreline was forested, providing leaves and twigs that had entered the water providing organic material that was not associated with fine particles. In this instance organic content was high, providing plentiful nutrients while sediment grain size stayed within a desirable level (<42%).

Zannichellia palustris

Z. palustris produced prolific seeds even at the lowest organic content tested. Therefore, this species may be a better primary colonizer and may lead to higher success rates in restoration of SAV habitats with low organic content sediments. Although its growing season is rather short (February through June), it may trap sufficient organic matter to promote the rapid growth of other species such as *R. maritima*.

Small sample sizes of *Z. palustris* from the field make comparisons between laboratory and field response difficult. The lack of field samples could be due to the natural seasonal early die-off and not related to sediment characteristics. *Z. palustris* grown in the mesocosm had an ideal organic content of 5% for shoot and 8% for root growth. *Z. palustris* can therefore potentially colonize sediment habitats with >5% organic content and have very quiescent waters that are not colonized by other species with lower sediment organic content and/or water flow requirements.

Determining site suitability is a crucial part of restoration. Previously it was thought that organic content >5% was detrimental to SAV success (Barko and Smart, 1983). This value seems to be too conservative as mesocosm and field data show that SAV can indeed survive in sediments greater than this. Our study shows that: 1) sediment organic content optima for SAV is species-specific; 2) sediment organic content requirements depend on other parameters such as water flow/fetch and silt+clay amounts; and 3) sediment organic content affects not only SAV morphology but also its ability to reproduce. Even though the environmental factors that influence SAV are numerous, this study has defined more specific sediment requirements for 3 species in the Chesapeake Bay aiding in improvements of site selection and increased success in restoration efforts.

SUMMARY

Determining sediment requirements for species of SAV in the Chesapeake Bay is of utmost importance for the successful restoration of populations. This study successfully outlined some of these requirements for *R. maritima, V. americana,* and *Z. palustris* according to sediment organic content. *R. maritima* requires sediment organic content >1%, sheltered conditions and non-compacted sediments. *V. americana* has no organic content requirements but grows best in sediment with high organic content (~20%), as long as fetch and sediment silt/clay percent are not limiting. Water flow is of the essence for this species and should be one of its habitat requirements. *Z. palustris* appears to have no water flow or organic content requirement although growth was best in sediments with ~8% organic content, producing seeds at all organic-content levels. When making decisions for suitable habitat for restoration attempts of these 3 species these parameters will be important to take into account for increased success of restoration projects.

Chapter 4

The growth of submersed aquatic vegetation (SAV) in breakwater-protected areas of Chesapeake Bay, USA.

INTRODUCTION

The acceleration of sea-level rise (SLR) has increased coastal erosion (Titus et al., 1991), leading to the retreat of 70% of the world's beaches (Bird, 1993). In the USA, the areas experiencing highest relative SLR and extensive shoreline erosion are the marshes along the Mississippi River delta as well as the Chesapeake Bay (Titus and Richman, 2001). In the last 40 years, relative SLR in Chesapeake Bay has been 2.5-3.6 mm/y (Hicks et al., 1983; Kearney et al., 2002). Approximately one-third of Chesapeake Bay's 18,800 km of shoreline is classified as eroding, with rates up to 20-40 cm/y depending on local wave characteristics, fetch, and sediment composition (Wray et al., 1995). As a result, shorelines are being hardened at an alarming rate in the Chesapeake Bay and worldwide. For example, over 24% of the Chesapeake Bay shoreline, 50% of the Italian coast and more than 70% of Barnegat Bay, NJ and San Diego, CA shorelines are already hardened (Lathrop, et al., 1997; Berman et al., 2000; Davis et al., 2002; Bacchiocchi and Airoldi, 2003).

The impact of shoreline hardening structures like rip-rap, groins, and breakwaters on physical and geological processes is relatively well known (Neelamani and Sandhya, 2004; Nordstrom et al., 2009). Unfortunately, the impact of shoreline hardening

structures on plants and animals is much less clear (French, 1997; Loreau et al., 2002; Airoldi et al., 2005; Martin et al., 2005; Moschella et al., 2005; Birben et al., 2007; Gislason et al., 2009; Martins et al., 2009). In general, the introduction of rocky substrate, such as the material used in many coastal structures, alters the benthic habitat and fragments the coast (Moschella et al., 2005). Species diversity also shifts as rocky substrate replaces the soft bottom habitat (Loreau et al., 2002). Structures that trap fine particles lead to the creation of a muddy habitat typically characterized by burrowing, deposit-feeding organisms, while sandy sediments tend to have mobile, suspension-feeding organisms (Martins et al., 2009).

The effects of breakwaters on the ecosystem depend on many factors (Birben et al., 2007) and are typically site-specific (Airoldi et al., 2005). Breakwaters tend to cause decreasing sediment grain size, increasing sediment organic content, and changing redox conditions landward of the structure (Martins et al., 2009). The exchange of sediment and biota between nearshore and deeper water is disrupted (Martins et al., 2009), as is the sediment supply to natural coastal defenses such as dunes, beaches and marshes (French, 1997). Breakwaters also tend to trap sediment landward of the structure, increasing sediment accumulation rates (Birben et al., 2007). Even so, breakwaters are viewed as an alternative to direct hardening of the shoreline (rip rap, bulkhead) for the protection of relatively exposed shorelines (Hardaway and Gunn, 2010). Just as for other coastal structures, not much is known about the impact of breakwaters on the biota. An evaluation of the effect of 20 breakwaters on SAV within the Chesapeake Bay, using aerial photography, determined that SAV coverage in the area surrounding the breakwater (i.e., in the breakwater-protected and as well as the adjacent-exposed areas)

was influenced by regional processes rather than the existence of the breakwater (Karrh, 2000). Of the 20 breakwaters, 8 had small increases in SAV coverage, which was attributed to reduced wave action by the breakwater. In 5 breakwater locations, a minor decrease in SAV was observed. The overall conclusion of the study was that breakwaters have no effect on SAV presence; however, actual SAV density, species composition, or biomass were not measured (Karrh, 2000). In a modeling study, SAV growth potential was predicted to increase by 0.3% (2.5 shoots m^{-2} d^{-1}) when breakwaters attenuate waves and reduce sediment resuspension, resulting in less turbid water (Smith et al., 2009) suggesting that breakwaters can be used for SAV habitat enhancement or creation.

SAV, one of the most important ecosystems in estuaries worldwide for their provision of many ecosystem services, can only colonize areas where certain habitat requirements have been met. For example, sufficient light has to reach the plants, therefore SAV growth is limited to shallow waters (Dennison et al., 1993). Excessively shallow waters where plants are exposed to the air during low tide are also detrimental (Duarte, 1991; Koch and Beer, 1996). SAV also needs carbon and nutrients to grow and, therefore, needs water flow that allows sufficiently high fluxes to the leaf surface (Koch, 1994; Jones et al., 2000). However, excessive water flow or wave exposure may lead to plants being uprooted (James et al., 2008; Wicks et al. 2009). Sediments were also suggested to limit SAV growth (Barko and Smart, 1983; Wicks et al., 2009) but Barth et al. (Chapter 3) have shown that SAV can grow in a wide range of sediments (organic content from 0 to 20%). Since breakwaters modify sediment characteristics (Martins et al., 2009) and water flow (Stamos and Hajj, 2001), it is likely that breakwaters will affect SAV. In this study, we test the general hypothesis that breakwaters initially enhance

SAV distribution but later hinder their growth due to changes in sediment characteristics in the breakwater-protected area.

MATERIALS AND METHODS

Study sites

Aerial photos taken annually since 1989 to monitor SAV distribution in the Chesapeake Bay were used to select the study sites. The criteria for site selection were the presence of a breakwater as well as the presence of SAV in the general area of the breakwater (i.e. in the Bay segment containing the breakwater) in the last 20 yrs. The selected breakwaters are segmented, emergent rock mounds in shallow areas (1 to 2 m water depth). Of the 24 selected sites, 17 had SAV in the breakwater-protected area (Table 4.1; Figure 4.1). These sites were used to evaluate the effect of breakwaters on SAV distribution over time.

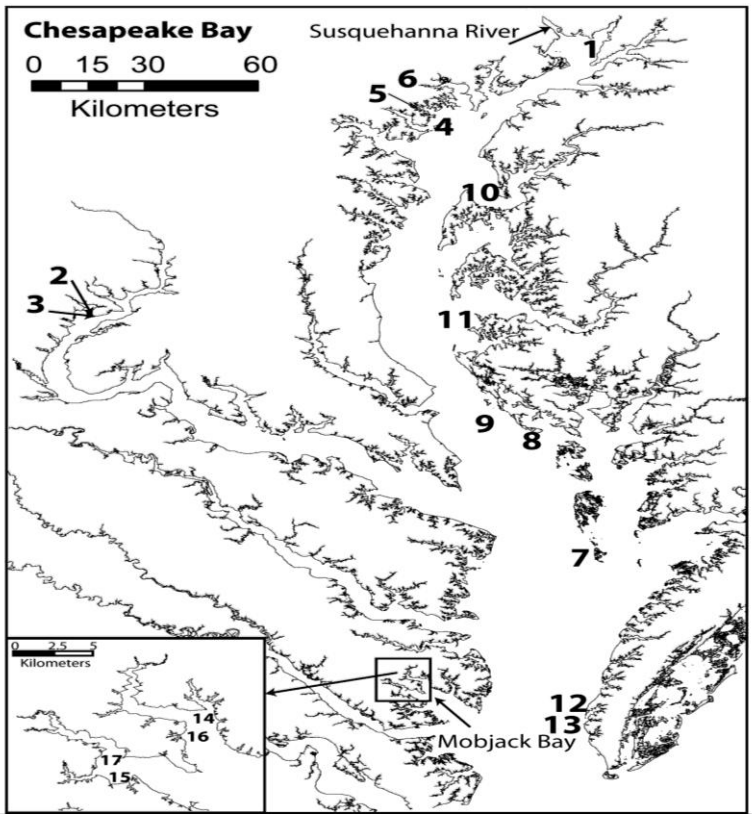

Figure 4.1. Map of the Chesapeake Bay with breakwater study sites, site numbers correspond to site names in Table 4.1.

Table 4.1. Study locations and breakwater ages at the time of sediment sampling. Most sediment cores were collected in 2009, except Elk Neck, Brannock Bay, Hoopers Island, and Bishops Head, which were sampled in 2008. SAV samples were collected from May-July 2009. Locations are divided by salinity region as defined by the Chesapeake Bay Program (CBP, 2004) and characterized by the values in parentheses. Within each salinity region, locations are listed by ascending age.

Site # (Fig. 4.1)	Location	Age (y)
	Tidal fresh/oligohaline (0-5)	
1	Elk Neck	3
2	Mason Neck1	7
3	Mason Neck2	8
4	Hart-Miller Island	10
5	Sue Creek	15
6	Red Eyed Yacht Club	15
	Mesohaline (5-18)	
7	Tangier Island	2
8	Bishops Head	11
9	Hoopers Island	14
10	Eastern Neck	15
11	Brannock Bay	19
	Polyhaline (18-25)	
12	Cape Charles Bay Creek	3
13	Cape Charles Public Beach	7
14	Mobjack Bay	7
15	Mobjack Bay7	8
16	Mobjack Bay3	17
17	Schley	18

Past SAV distribution

In order to quantify changes in SAV distribution in the breakwater-protected area over time, aerial photos for each of the 17 sites were selected for at least 3 years pre-construction until present (2010). Aerial photos were georeferenced using ArcMap 9.3

(ESRI) and the area protected by the breakwater was quantified. For simplicity, this area was defined as the area between the rock mounds and the shoreline and between the edges of the outer most rock segments (Figure 4.2). Subsequently, a rectangle of similar area was created adjacent to the structure in order to compare SAV distribution in the breakwater-protected and a nearby unprotected area. The width of the rectangle was equal to the distance of the breakwaters to the shore, and the length of the rectangle was the distance along the shore needed to obtain the same area as the breakwater-protected area (Figure 4.2). The areas covered by SAV in the breakwater-protected and in the adjacent-exposed rectangle were determined for each photograph (3 years prior to breakwater construction to 2010) for each study site. In order to separate breakwater effects on SAV distribution from inter-annual fluctuations in regional SAV distribution, the breakwater-specific time series of SAV distribution were then compared with the SAV time series for the segment of the Chesapeake Bay in which the breakwater was located.

A sub-sample of 5 sites was selected to describe temporal patterns in SAV distribution. Three of the selected sites are located in two tidal fresh/oligohaline (0 to 5 salinity) segments of the Bay: Elk Neck in the northern portion of the Bay and Mason Neck 1 and 2 in the upstream portion of the Potomac River (Figure 4.1). The remaining two sites were located in the mesohaline (5 to 18 salinity) area of Chesapeake Bay: Bishops Head and Hoopers Island on the eastern shore of the Bay (Figure 4.1). The Elk Neck (ELK) breakwater (Table 4.2) was constructed in 2005 in order to protect a summer camp in a low-lying area surrounded by bluffs up to 30 m tall (Figure 4.2). It is located in the upper portion of Chesapeake Bay, near the mouth of the Susquehanna River, which

drains 71,188 km^2 in 3 states. It is the major source of fine sediment and fresh water in the Bay (Hobbs et al., 1992). The two breakwaters at Mason Neck (MN; Table 4.2) were constructed in 2002 to protect a small, ~ 1 m tall (MN1) and a large, ~ 6 m tall (MN2) eroding bluff (Figure 4.2) in the upper portion of the Potomac River, which drains 38,000 km^2 The Bishops Head (BH) breakwater (Table 4.2) was built in 1997 to protect a building on this low-lying point colonized mainly by salt marshes (Figure 4.2). And the Hoopers Island (HI) breakwater (Table 4.2) was constructed in 1991 to protect the road from Upper Hoopers to Lower Hoopers Island (Figure 4.2). These islands are mostly colonized by marshes with some pine forests. The HI breakwater is the oldest and most exposed breakwater in this study.

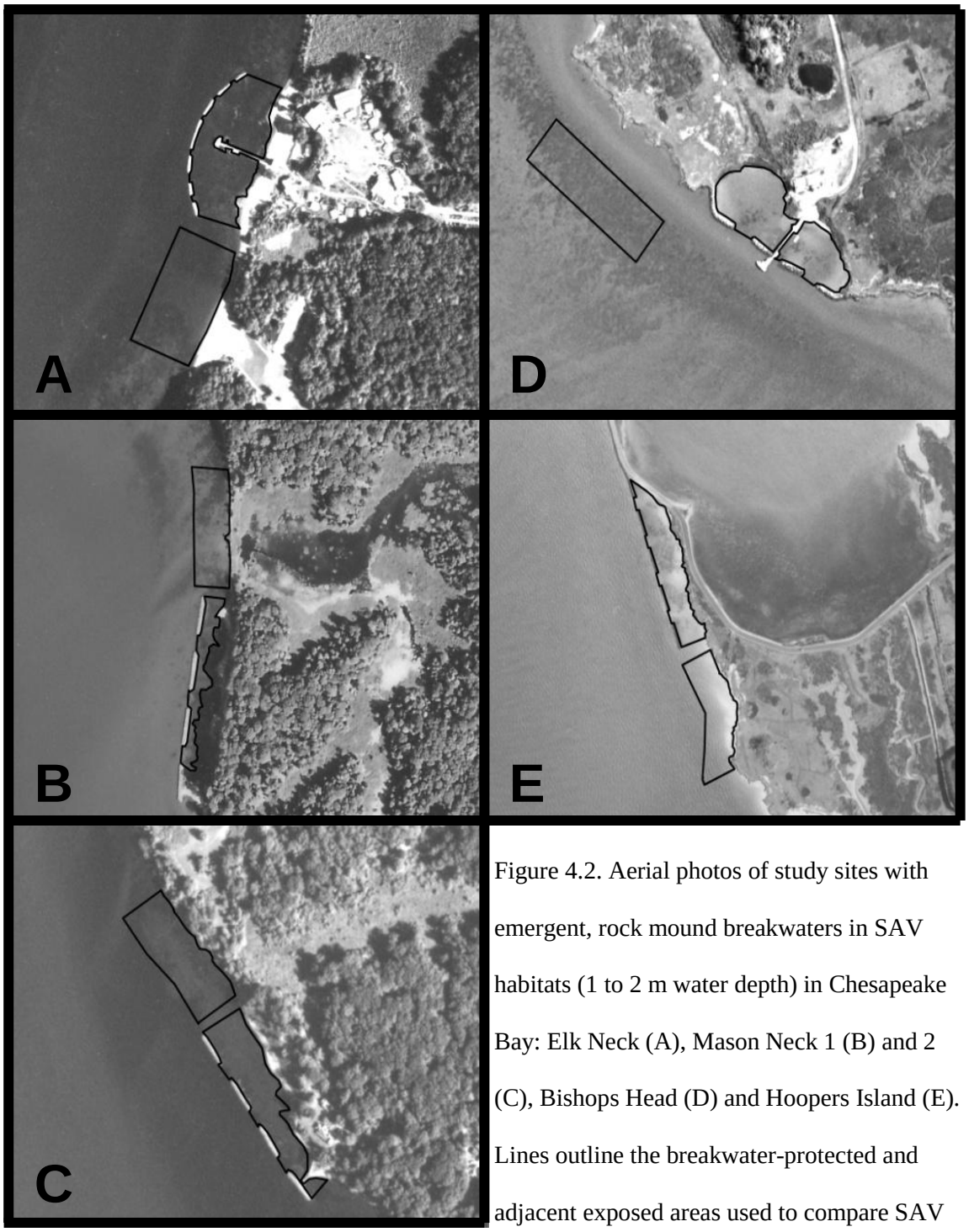

Figure 4.2. Aerial photos of study sites with emergent, rock mound breakwaters in SAV habitats (1 to 2 m water depth) in Chesapeake Bay: Elk Neck (A), Mason Neck 1 (B) and 2 (C), Bishops Head (D) and Hoopers Island (E). Lines outline the breakwater-protected and adjacent exposed areas used to compare SAV distribution under the influence of breakwaters and exposed to waves. Note that waves in SAV habitats in Chesapeake Bay usually have a 3s period and significant wave heights between 0.1 and 0.4 m (Chen et al. 2007).

Table 4.2. Characteristics of the breakwaters studied. All breakwaters were segmented, emergent rubble mounds in shallow areas (1 to 2 m water depth) characterized by 3 second waves with significant wave heights between 0.1 and 0.4 cm. SE indicated standard error of the mean.

	Elk Neck	**Mason Neck 1**	**Mason Neck 2**	**Bishops Head**	**Hoopers Island**
Latitude Longitude	39º29'46.5"N 75º59'20.2"W	38º37'17.4"N 77º12'18.8"W	38º37'45.6"N 77º12'38.7"W	38º13'14.7"N 76º2'19.2"W	38º17'29.8"N 76º12'9.7"W
Year built	2005	2002	2002	1997	1991
Type	Detached, semi-circular	Detached, straight	Detached, straight	Attached, curved end segments	Attached, straight
Distance from shore (m), ± SE	100±21	36±2	42±10	50±14	46±13
Total length (m)	253.9	233.8	264.1	188.1	363.5
Segment length, width of openings (m), ± SE	31±11 10±3	49±2 20±1	41±1 22±1	34±9 16±6	49±2 25±1
Fetch (km), ± SE	4.5 ± 1.0	2.4 ± 0.5	2.2 ± 0.6	6.4 ± 2.0	16.2 ± 4.8
Shoreline characteristics	Sandy Beach	Small bluff	High bluff	Marsh, pocket beach	Marsh
Average median grain size (phi) in top 10 cm, breakwater-protected ± SE	2.8 ± 0.1 fine sand	4.0 ± 0.4 very fine sand	2.9 ± 0.1 fine sand	4.5 ± 0.3 very fine sand	3.0 ± 0.1 fine sand
Silt+Clay (%), Breakwater-protected ± SE	17.6 ± 1.1	42.0 ± 2.1	22.2 ± 0.9	51.3 ± 0.8	17.4 ± 0.9
Average organic content (%) in top 10 cm, breakwater-protected, ± SE	1.4 ± 0.2	3.4 ± 0.5	1.7 ± 0.4	4.1 ± 0.3	2.1 ± 2.0
Trends since construction of breakwater	↓ grain size ↑ org. content ↑ sedim. rate	↑ grain size = org. content = sedim. rate	↑ grain size = org. content = sedim. rate	↑ grain size = org. content ↑ sedim. Rate	↑ grain size ↓ org. content ↑ sedim. Rate
SAV species present	*Myriophyllum spicatum, Vallisneria americana, Hydrilla verticillata*	*Myriophyllum spicatum, Vallisneria americana*	*Myriophyllum spicatum, Vallisneria americana*	*Ruppia maritima*	*Ruppia maritima*
Sampling Date	21 May 2009	16 June 2009	16 June 2009	29 May 2009	20 May 2009

Present SAV characteristics

SAV in the breakwater-protected and adjacent-exposed area was assessed by collecting 10 push cores (15-cm diameter and 20-cm long, enough to capture the entire root length) at each study site during the growing season (May-July 2009). Cores were placed within the 5 densest patches of SAV in both the breakwater-protected and the adjacent wave-exposed areas. Each core was then sieved (1-mm mesh) in the field, and the plant material retained on the sieve was frozen (-17 ºC) until processed. Once thawed, epiphytes were removed by scraping the plants with a paint brush and/or razor blade. Above- and below-ground biomass were determined by separating shoots (above-ground) from the roots/rhizomes (below-ground) and drying the plant material from each core at 60 ºC until constant weight was reached.

Sediment collection

Two vibracores (7-cm diameter, 3 m long) were collected at each study site using a backpack vibrator (cement mixer-backpack model 402BP) with a 6 cm x 6 cm x 19 cm head weighing 80 kg. One vibracore was collected in the protected area landward of the breakwater and one at the same water depth in the adjacent wave-exposed area. A companion push core (~30-cm long, 5-cm diameter) was taken manually at the site of each vibracore to capture relatively undisturbed surface sediment. The vibracores were returned to the laboratory and frozen (-13ºC) in a vertical position until further analysis. Push cores were sectioned immediately upon returning to the lab. Frozen vibracores were cut in half lengthwise and sectioned into 1- and 2-cm increments. Sediments were analyzed for grain size and organic content.

Grain size was analyzed by wet-sieving samples through a 64-μm mesh to separate the sand and mud fractions. The mud fraction was placed in a 0.05% sodium metaphosphate solution, placed in an ultrasonic bath, and then analyzed by a SediGraph 5120. Particles >64 μm (i.e., sand and gravel) were placed in a pre-weighed pan, dried for 24 hours and then dry-sieved from 1-4 phi (500-64 μm) in ¼-phi increments (phi = $-\log_2$ (diameter, mm)). The mud and sand data were joined to obtain the complete grain-size distribution for each sample, and the median diameter was calculated using MatLab.

Samples for organic-content analysis were initially dried at 60 ºC until constant weight was reached (initial weight). Dried sediment was then combusted in a muffle furnace at 450º C for 4 hrs cooled and weighed (final weight). The percentage of organic content was then determined according to Erftemeijer and Koch (2001):

$$\% \text{ organic content} = \frac{\text{initial weight} - \text{final weight}}{\text{initial weight}} \times 100 \qquad \text{Eq. 1}$$

Fetch

Fetch distance was quantified by measuring the distance to land along 40 vectors radiating from each study site using the measuring tool on GoogleEarth and then averaging all distances, including zeros (Koch et al., 2006).

Data Analysis

SAS 9.2 was used for statistical analysis of data (Table 4.3). Data were tested for a normal distribution; if it was not normal, then a log transformation was performed. Levene's test was utilized to determine equality of variances (Sokal and Rolhf, 1995). The majority of the data fit the assumptions of normality and homogeneity. A paired t-

test was conducted for SAV above- and below-ground biomass between adjacent-exposed and breakwater-protected sites (Sokal and Rolhf, 1995). A one-way ANOVA was completed for Type I and Type II breakwaters to determine differences between the adjacent-exposed and breakwater-protected site for sediment grain size and organic matter, as well as SAV above- and below-ground biomass (Sokal and Rolhf, 1995).

RESULTS

SAV Percent Cover

SAV colonization in the breakwater-protected areas fell into two categories: Type I) Initial SAV expansion followed by a decline (Elk Neck, Mason Neck 1 and 2,) and Type II) slow initial colonization followed by persistent SAV over time (Bishops Head, Hoopers Island). The three Type I breakwaters that best represent the type of SAV colonization were relatively new (< 10 years) and were located in the oligohaline area of either Chesapeake Bay (Elk Neck) or the Potomac River (Mason Neck 1 and 2). SAV distribution in the Elk Neck region was relatively stable at the time of breakwater construction, although no SAV had been present for at least 3 years at the construction site. In the first year following construction, SAV distribution in the breakwater-protected area increased from non-existent to more than 90% cover. It also appeared in the adjacent-exposed area at lower (not significantly different; $p = 0.28$) quantities (Figure 4.3a). In the breakwater-protected area, SAV cover remained high for 2 years, declining in the 3rd year to ~30% cover and slightly recovering (~60% cover) in the following year. This drastic decline was a breakwater effect as the regional trend continued upward

during that time (Figure 4.3). SAV in the adjacent control area followed the regional trend, expanding to ~60% cover and remaining at that level (Figure 4.3a).

The general Mason Neck region also had a relatively stable SAV distribution at the time of breakwater construction although, as with Elk Neck, the construction site was unvegetated. Two to three years following construction, regional conditions must have been favorable as SAV distribution in the general area increased. It was during this time that SAV also colonized the breakwater-protected areas of Mason Neck 1 and 2 (Figure 4.3b and 4.3c). The adjacent-exposed area remained unvegetated for an additional 2 to 3 years when SAV also appeared. Once SAV became established at a site, it rapidly achieved 80 to 90% cover in the breakwater-protected area and 60 to 70% cover in the adjacent area in a matter of 3 years. As observed at Elk Neck, this rapid expansion was followed by a decline of SAV distribution in the breakwater-protected area at Mason Neck 1 and 2 but not in the adjacent-exposed area (Figure 4.3b, 4.3c). This decline was more severe in Mason Neck 2 (<10% cover) than in Mason Neck 1 (~50% cover).

The two Type II breakwaters where SAV persisted over time were the oldest breakwaters in this study and were located in the polyhaline area of Chesapeake Bay. Construction of the breakwater at Bishops Head occurred during a time when SAV distribution in the area was declining. Two years after construction this trend was reversed and, for the next 4 years, SAV expanded in the general area, as well as in the breakwater-protected and adjacent-exposed sites (Figure 4.3d). While the adjacent-exposed site was 100% covered with SAV (mainly *Ruppia maritima*), the breakwater-protected site only had 70 to 90% cover of the same species. Six years after construction, SAV distribution in the region as well as in the breakwater-protected area declined.

Although the regional trend continued downward, SAV in the breakwater-protected and adjacent-exposed areas rebounded after 2 years. While the SAV distribution in the adjacent area remained high (100% cover), the SAV in the breakwater-protected area followed the regional trend and declined, followed by a slight recovery. Currently, SAV distribution in the breakwater-protected area is not as high (~50%) as in the past (up to 90%), but 14 years after the breakwater was constructed, SAV is still present (Figure 4.3d).

Construction of the breakwater at Hoopers Island occurred at a time when SAV (mainly *Ruppia maritima*) distribution in the area had declined and was absent from the breakwater-protected site. Four years after construction, SAV in the general area began to recover but SAV was still absent from the breakwater-protected and adjacent-exposed areas. It took an additional 2 years for SAV to become established behind the breakwater, but the adjacent area remained unvegetated (Figure 4.3e). The breakwater-protected area has followed regional fluctuations in SAV distribution but remained vegetated at relatively sparse levels (<50%) over the last 9 years (Figure 4.3e).

Table 4.3. Statistical analysis results using SAS 9.2. P-value > 0.05 is significant. BW = breakwater-protected site, ADJ = Adjacent-exposed site.

Statistical Test	Factors	Degree of Freedom	T-value or F-value	P-Value
Paired T-test	Above-ground biomass BW versus ADJ	11	-0.78	0.45
Paired T-test	Below-ground biomass BW versus ADJ	9	-1.01	0.34
ANOVA	Above-ground biomass Type I versus Type II	1	8.51	0.01
ANOVA	Below-ground biomass Type I versus Type II	1	36.88	< 0.0001
ANOVA	Type I BW versus ADJ Grain Size	1	26.18	< 0.0001
ANOVA	Type I BW versus ADJ Organic Content	1	8.96	0.004
ANOVA	Type II BW versus ADJ Grain Size	1	25.87	< 0.0001
ANOVA	Type I BW versus ADJ Organic Content	1	0.60	0.44

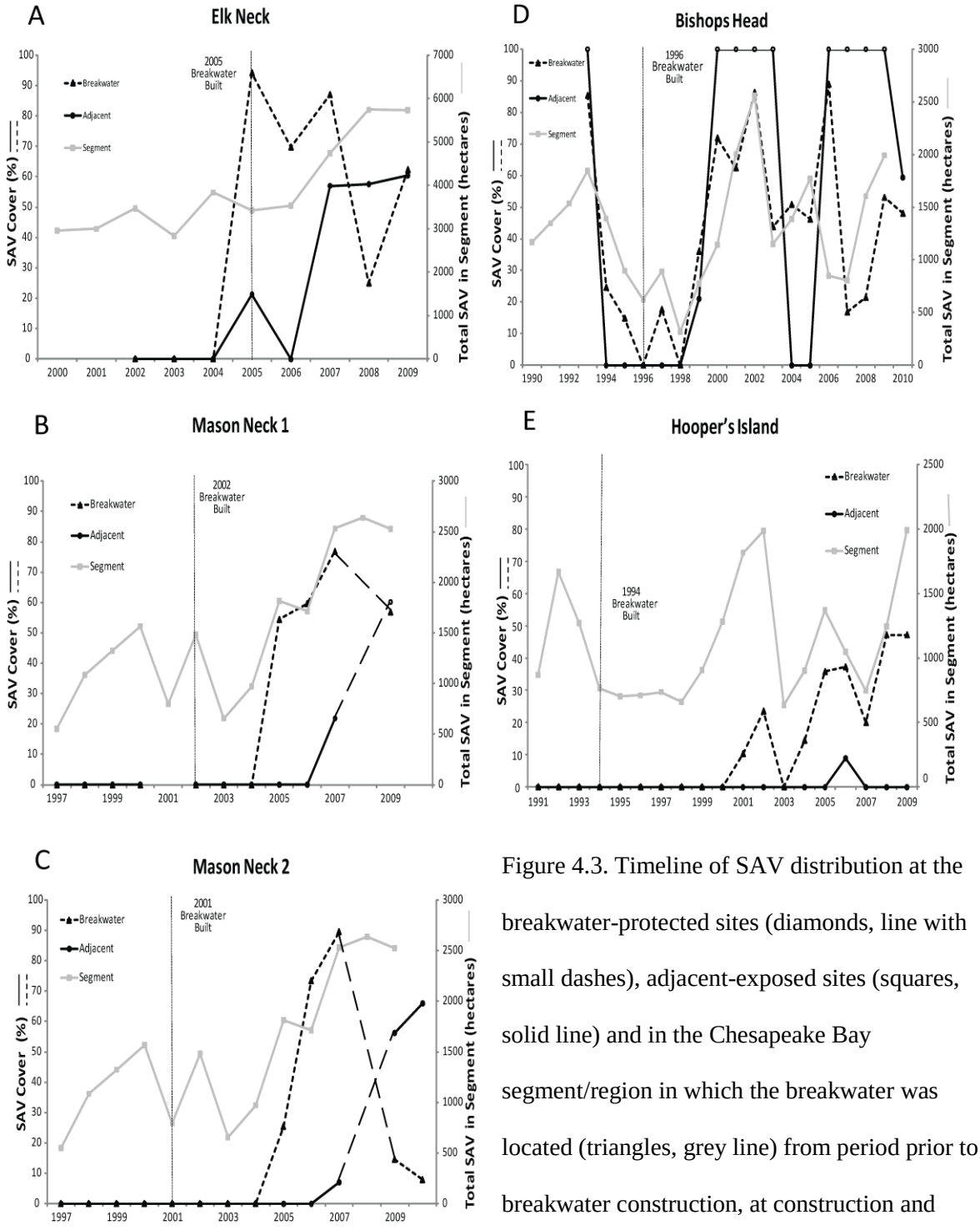

Figure 4.3. Timeline of SAV distribution at the breakwater-protected sites (diamonds, line with small dashes), adjacent-exposed sites (squares, solid line) and in the Chesapeake Bay segment/region in which the breakwater was located (triangles, grey line) from period prior to breakwater construction, at construction and following construction. The vertical dotted line indicates the year of breakwater construction. Lines with long dashes (Mason Neck 1 and 2) connect points between which data are missing. Elk Neck (A), Mason Neck 1 (B) and 2 (C), Bishops Head (D) and Hoopers Island (E).

In summary, in Type I and Type II SAV colonization patterns, the initial establishment of SAV differs but once established, SAV persists over time although at a lover percent cover (<60%) than possible in nature (100%). Additionally, the SAV cover in the breakwater-protected areas did not show a clear pattern with age of the structure, but SAV biomass in the breakwater-protected area fell into one of three categories: increase over time, decrease over time and remain the same.

SAV biomass and sediment characteristics

In general, above-ground biomass in the breakwater-protected areas was not significantly different from adjacent-exposed sites when all 17 sites are combined ($p = 0.45$), neither was below-ground biomass ($p = 0.34$). However, differences can be seen between breakwater-protected sites and adjacent-exposed at individual locations (see Appendix). In the case of Type I and II breakwaters, breakwaters with SAV that persistent over time (Type II; colonized by *R. maritima* in the mesohaline area) had higher above-ground biomass ($p = 0.01$; Figure 4.4a) and higher ($p < 0.0001$) below-ground biomass than Type I breakwaters.

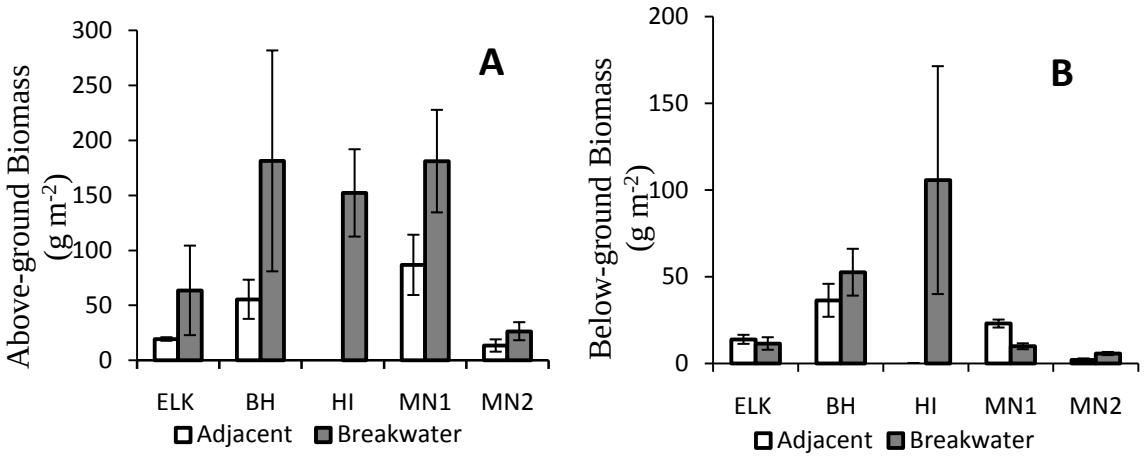

Figure 4.4. (A) SAV above-ground and (B) below-ground biomass in breakwater-protected areas and adjacent-exposed areas. Breakwaters are listed in ascending age order: Elk Neck (ELK), 4 yrs old; Mason Neck 1 (MN1), 7 yrs old; Mason neck 2 (MN2), 8 yrs old; Bishops Head (BH), 11 yrs old and Hoopers Island (HI), 14 yrs old. Vertical bars represent SE.

Differences between SAV biomass at the breakwater-protected and adjacent-exposed area is an indication of the breakwater effect. When plotting this difference against the age of the breakwaters (Figure 4.5), three clear categories emerge: 1) no breakwater effect; 2) a positive effect of the breakwater on SAV biomass and 3) a negative effect of the breakwater on SAV biomass. Note that this pattern is unique for biomass and did not show when SAV cover (%) was plotted against breakwater age.

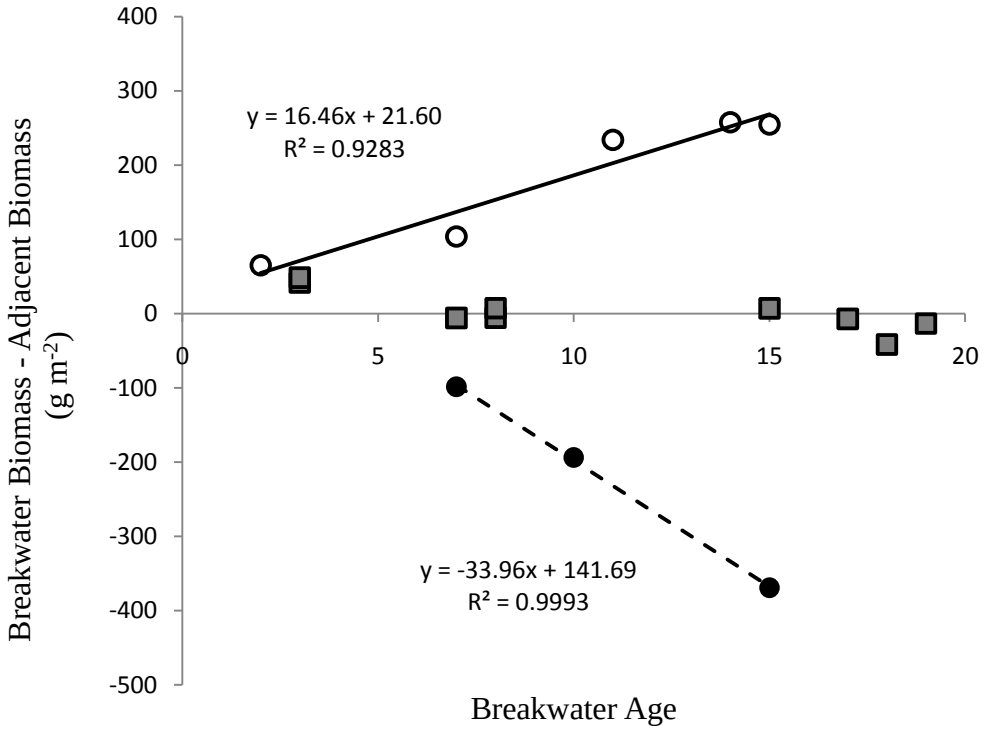

Figure 4.5. The difference in SAV biomass between breakwater-protected and adjacent-exposed areas (i.e. breakwater effect on SAV biomass) as a function of breakwater age clearly shows three patterns: 1) increase in SAV biomass over time (open circles), 2) no change in SAV biomass (0 ± 50 g m^{-2}; grey squares) and 3) decline of SAV biomass over time (black circles).

The sites that benefited from the breakwater were those exposed to high fetch (> 10 km; Cape Charles Public Beach, Hoopers Island, Tangier; Figure 4.6) or had sand being deposited as part of the construction process (Bishops Head and Sue Creek). In contrast, sites that showed breakwaters to be detrimental to SAV were all located in areas with small fetch (< 3 km), had a decrease in grain size and an increase in sedimentation rate (chapter 2; Hart-Miller Island; Mobjack Bay and Red Eye Yacht Club).

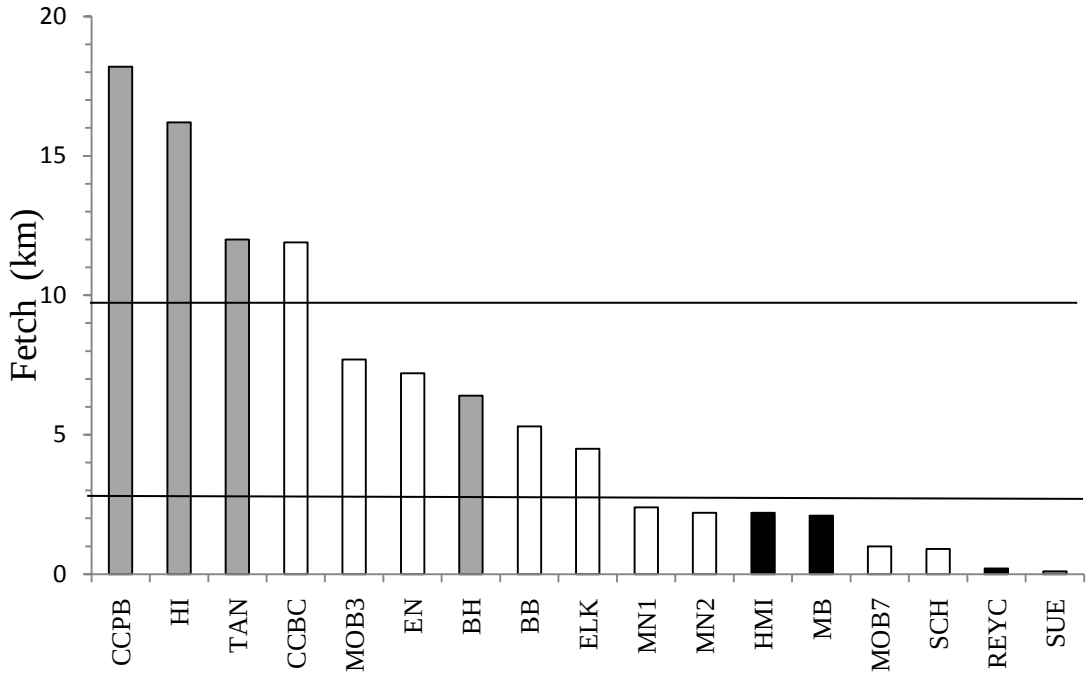

Figure 4.6. Fetch of the study sites colonized by SAV. Horizontal lines show limits of small fetch (< 3 km), medium fetch (3 to 10 km) and high fetch (> 10 km). Grey bars represent sites where SAV biomass tended to increase in breakwater-protected areas over time; white bars where SAV biomass was unaltered by the presence of the breakwater and black bars represent sites where SAV biomass tended to decrease in breakwater-protected areas over time. Note that at Hoopers Island (HI), Bishops Head (BH) and Sue Creek (SUE; grey bar) a layer of sand was added at time of construction.

At the five sites that best describe the initial pattern of colonization of SAV in breakwater-protected area, sediments in the top 10 cm (where most of the roots are found) of Type I breakwaters (SAV expanding and then declining over time) were significantly finer ($p<0.0001$) and contained significantly more organic matter ($p=0.004$)

in the breakwater-protected than in the adjacent-exposed areas (Figure 4.7a, 4.7b). In contrast, sediment in the top 10 cm of Type II breakwaters (persistent SAV over time) was significantly coarser ($p < 0.0001$) in the breakwater-protected than in the adjacent-exposed site (Figure 4.7a) and sediment organic content showed no clear pattern ($p = 0.44$; Figure 4.7b), although it reached relatively high levels ($4.1 \pm 0.8\%$) at the Bishops Head breakwater-protected site.

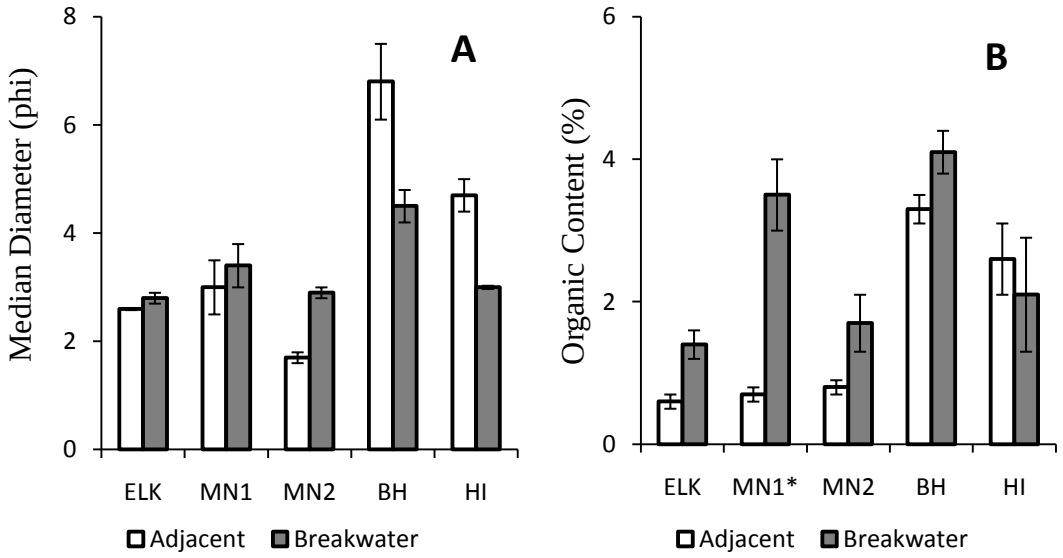

Figure 4.7. Sediment grain size (top) and organic content (bottom) in the top 10 cm (*top 4 cm for MN1) in breakwater-protected areas and adjacent exposed areas. Breakwaters are listed in ascending order of age: Elk Neck (ELK), built in 2005; Mason Neck 1 (MN1), built in 2002; Mason neck 2 (MN2), built in 2001; Bishops Head (BH), built in 1997 and Hoopers Island (HI), built in 1991. Vertical bars represent SE.

DISCUSSION

SAV are rooted aquatic plants that require both water-column and sediment characteristics to be suitable for their growth (Koch 2001). If light criteria are not met, SAV will be absent or sparse in the region, including breakwater-protected areas. As suggested by Karrh (2000), light availability in the breakwater-protected area seems to be a function of regional, rather than local, processes and events, as seen by the similar trends in SAV distribution in breakwater-protected areas and the segment/region where the breakwater is located during periods of SAV expansion and maintenance. In contrast, sediment characteristics in breakwater-protected areas are affected by regional and local sediment sources as well as breakwater particle trapping effects. At all studied breakwaters in two oligohaline areas of the Bay (upper Chesapeake Bay and Potomac River), sediments in the breakwater-protected area have become finer and at Elk Neck, also more organic (not always at a statistically significant level) than the sediment in the adjacent-exposed area (Chapter 2). In contrast, at the studied mesohaline sites, sediments in the breakwater-protected area became coarser, not as a result of natural processes, but as a result of the construction method (sand deposition prior to the construction of the breakwater at Hoopers Island) and the creation of a pocket beach (sand deposition on top of the eroding marsh shoreline to create a beach at Bishops Head). Independent of how the sediments reached their present composition, they may be contributing to the current pattern of SAV distribution observed in the breakwater-protected area.

Initial colonization of SAV in breakwater-protected areas appears to be related to sediment characteristics. Sediments in the Type I breakwaters which showed an initial SAV expansion followed by a decline (Elk Neck, Mason Neck 1 and 2) have become

finer and more organic in the recent past. It appears that the construction of a breakwater in an area with no or sparse SAV (A in Figure 4.8) led to the trapping of SAV propagules and/or seeds present in the region (one of the site selection criteria) which were able to become established in the quiescent waters and benefitted from the sediment organic matter also trapped by the breakwater. This led to the rapid growth of SAV (B in Figure 4.8) creating dense SAV beds (100% cover) with high biomass (C in Figure 4.8). These dense beds become stressed leading to their decline (D in Figure 4.8). This decline took between 3 and 8 years at our study sites.

The causes of stress leading to the abrupt loss of SAV in breakwater-protected areas after 3 to 8 years may be 1) high sediment organic content, 2) lack of water flow in the vegetation and/or 3) shallow water depth in the breakwater-protected area. The shortest time for the decline to take place was 3 years since construction of the breakwater at Elk Neck, a period during which sediment organic content increased from ~0.5 to ~2.5% (see Appendix). Although Barko and Smart (1983) suggested that 5% is the maximum threshold for SAV distribution, Barth et al. (Chapter 3) demonstrated that although SAV may have optimal organic contents for growth under stagnant conditions, *V. americana* can grow over a broad range of sediment organic contents (0 to 20%) as long as sufficient water flows through the vegetation. Therefore, even the highest sediment organic content in Type I breakwaters (4% at Mason Neck 1) is unlikely to be the cause for the decline in SAV distribution in oligohaline and mesohaline areas of Chesapeake Bay. Instead, water flow may be an important requirement for SAV distribution, especially when extremely dense beds develop shoreward of the breakwaters. Breakwaters trap organic particles which fertilize the sediment and lead to

higher SAV biomass in breakwater-protected than adjacent-exposed areas. But breakwaters attenuate waves and the vegetation reduces currents and waves even further, leading to leaf boundary layer limitations (Koch, 1994; Chapter 3) and the loss of SAV. This is evident at the Mason Neck breakwaters where the decline recently occurred. At these sites, *V. americana* above-ground biomass is less abundant than in the adjacent exposed areas. Once the canopy has become less dense and water can flow once again, the SAV may become re-established at a lower density which fluctuates inter-annually with regional water quality conditions (E in Figure 4.8). It appears that an oligohaline SAV bed with 50 to 60% cover in the breakwater-protected area can be quite productive as seen in the higher above-ground biomass than in the adjacent-exposed sites. This pattern is likely the result of higher sediment organic content and shelter from waves in breakwater-protected areas. In polyhaline areas, this pattern may not hold as the dominant species, *Zostera marina*, is less tolerant to fine and organic sediments (Wicks et al., 2009).

Both initial colonization processes (Type I and II) appear to lead to steady state levels of SAV distribution that is lower (< 60%) than what can be found in nature as well as in the initial colonization of Type I breakwaters (100% cover). This suggests that some stress may still be limiting SAV expansion. This could be a result of warmer temperatures in the breakwater-protected area (personal observation), reduced water flow, or perhaps herbivory of plants and seeds by organisms that use the breakwaters as habitat. SAV distribution/density also fluctuates annually with regional trends suggesting that this parameter may also depend on light availability. In contrast, SAV biomass appears to be a better indicator of local conditions. For example, the decline in biomass

difference between breakwater-protected and adjacent-exposed areas over time (i.e. breakwater effect) seems to be associated to small fetch sites where fine sediments tend to settle in the breakwater-protected area at a high sedimentation rate. The opposite trend is observed when breakwaters are in high fetch areas (> 10 km) which are usually characterized by sandy sediments or if sand is added to the site as part of the construction process. In high fetch areas, breakwaters allow SAV to grow longer leaves/shoots which then lead to the higher SAV biomass in breakwater protected than adjacent exposed areas.

Breakwater-protected areas can only support SAV if the water column is deep enough to avoid regular desiccation during low tides. Therefore, if sediment accumulation in breakwater-protected areas is high, the area may become too shallow to support SAV growth. In that case, the breakwater-protected area will become intertidal and colonized by marsh vegetation. This seems to be the cause of loss of SAV at Mason Neck 2 as evident by the appearance of marsh plants in the shallowest areas. The breakwater at this site protects a high sand bluff but it continues to erode at high tide and/or due to drainage of the bluff. The sediment eroded is accumulating in the breakwater-protected area as the structure likely interrupts longshore transport and/or limits offshore transport. Therefore, over time, this site is likely to become a marsh and could even be colonized by terrestrial vegetation, unless bluff erosion ceases.

The mesohaline breakwaters at Bishops Head and Hoopers Island are relatively old (> 10 years) and, once vegetated, remained vegetated at approximately the same levels as the oligohaline “initial increase followed by subsequent decline” breakwaters. Inter-annual variability in SAV distribution in the polyhaline breakwater-protected areas

is driven by regional water quality trends as seen by the similar trends in variability in the region/segment and at the breakwater site and previously suggested by Karrh (2000). Sediment composition is also quite important in this area as when marshes erode and retreat, compacted marsh peat is exposed in the subtidal and becomes the substrate for SAV in breakwater-protected areas. Unfortunately this sediment is unsuitable for the colonization of SAV such as *R. maritima* and *Z. marina* (Wicks et al., 2009) as seen in the adjacent-exposed area at Hoopers Island. The addition of sand as the base for the breakwater at Hoopers Island and for the creation of a beach at Bishops Head has lead to suitable conditions for the colonization of *R. maritima*. The initial growth of the population at Bishops Head may have been faster as a layer of non-compacted highly organic sediment overlays the compacted peat (see Appendix). The mixture of this sediment with the sand created ideal growth conditions. At Hoopers Island, initial growth was slower, possibly a result of the lack of *R. maritima* seed production at very low organic content (<1%; Chapter 3). If few or no seeds were produced locally, the area depended on trapping of seeds for re-establishment of SAV on an annual basis. This may no longer be the case as sediment organic content is now 2.1% and the SAV population has sustained ~50% cover for at least 2 years in the row.

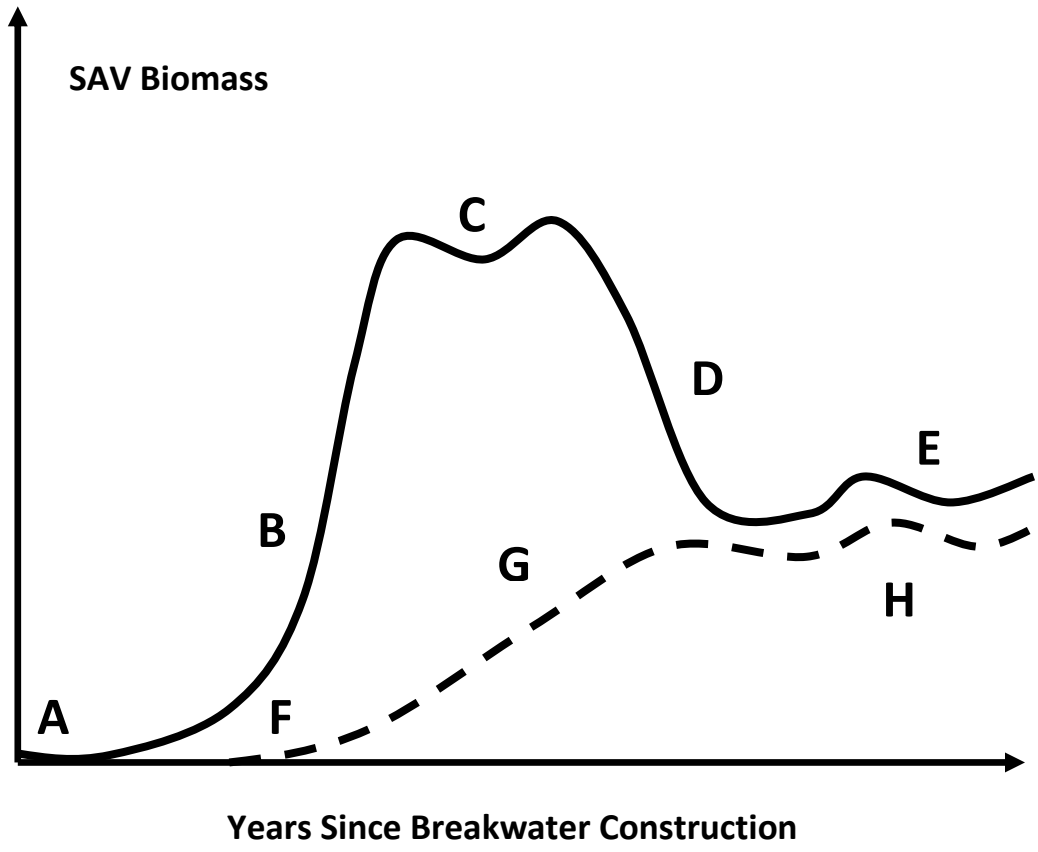

Figure 4.8. Timelines of SAV biomass in breakwater-protected areas: grow and crash type (solid line) and persist over time type (dashed line). An area with little or no SAV (A) may experience rapid SAV colonization (B) following breakwater construction, a result of organic matter enrichment of the sediment. The population then reaches its maximum biomass (C) but collapses (D) due to water flow, sediment characteristics and/or particle trapping. The SAV population may remain in the area but at a lower biomass (E) than the initial peak. Alternatively, an unvegetated area (F) may be slowly colonized by SAV (G) and reach a peak that is sustainable over time (H). In both cases (E and H), SAV fluctuates with regional water quality trends over time (see Discussion for details).

SUMMARY

Breakwater-protected sites can be slowly colonized by SAV over time or initially support dense SAV canopies for only a limited amount of time (2 to 3 years) after which somewhat sparse (~50% cover) SAV canopies can be sustained as long as regional and local habitat requirements are met: 1) water quality needs to be such that sufficient light reaches the plants in the region; 2) water depth also needs to be appropriate for the growth of submersed vegetation, i.e. the plants need to remain submersed even during low tide; 3) sufficient water flow exists in the canopy of oligohaline species to minimize carbon limitation and the exclusion of water flow loving species such as *V. americana*; and 4) the sediment needs to meet SAV habitat requirements, especially in the mesohaline region where compacted marsh peat limits the distribution of *R. maritima* and *Z. marina*. Even if the SAV populations in breakwater-protected areas are relatively sparse, their biomass can be higher than in adjacent-exposed sites especially when fetch is high and the sediment is naturally sandy or a layer of sand is deposited at the site during the construction process. Actually, given the right conditions (reduced fetch and sand), SAV biomass tends to increase with the age of the breakwater suggesting that positive feedback loops develop in breakwater-protected areas just as in other natural environments. Some of the above described SAV requirements can be achieved as part of the engineering project. For example, the deposition of a sand layer in the breakwater-protected area benefited breakwaters in areas where marsh erosion exposed compacted peat in the sub-tidal or where fetch was small. This sand layer should be at least 2 cm in depth (Wicks et al. 2009) to allow for seasonal sediment erosion (Palinkas et al., 2010). Engineering could also address the excessive sediment input into the breakwater-

protected area when this structure is protecting high bluffs. It would allow the breakwater-protected area to remain a SAV habitat and not turn into a marsh. We conclude that breakwaters can sustain patchy SAV populations with high biomass if basic conditions are met. Engineers, biologists and oceanographers are encouraged to work together to design breakwaters that best meet these requirements and create conditions that can support dense SAV beds in the long term.

Chapter 5

Summary

Rising sea level within the Chesapeake Bay has led to an increase in shoreline erosion and a subsequent rise in construction of coastal protection structures (Titus and Richman, 2001) such as breakwaters. This study examined the impact of breakwaters of various ages (1-19 y) in 3 salinity regions of the Chesapeake Bay on sediment characteristics and submerged aquatic vegetation (SAV). Grain size, organic content, and sedimentation rates were quantified, SAV shoot and root length were measured, and above- and below-ground biomass, as well as total biomass, were quantified at adjacent-exposed and breakwater-protected sites in 24 locations in the Chesapeake Bay. A controlled mesocosm experiment was also conducted to evaluate SAV response (biomass, shoot and root length) to 4 levels of sediment organic content for 3 SAV species found in the Chesapeake Bay (*Ruppia maritima, Vallisneria americana* and *Zannichellia palustris*), 2 of which are commonly used for restoration.

The results of this study were used to make coastal management recommendations as well as to define habitat requirements of SAV species within the Chesapeake Bay. The general hypothesis of this study stated that for a short period (few years) following construction, breakwaters enhance SAV distribution, but hinder their growth at a later time due to changes in sediment characteristics in the breakwater-protected area. This hypothesis was only partially supported as SAV distribution was not always initially enhanced. Instead, in some cases, SAV slowly appeared years after construction or the breakwater-protected area remained barren over time. Therefore, the

effect of breakwaters on SAV is site- and species-specific. Sediment requirements are species-specific and breakwater impacts on local environments are site-specific; however, thorough investigation of sediments at these sites allows for better evaluation on impacts of breakwater construction, and whether it will be detrimental or beneficial to surrounding SAV.

MANAGEMENT RECOMMENDATIONS

In general, it seems that SAV populations can be sustained over time in the breakwater-protected area, if certain habitat requirements are met: 1) water quality in the region needs to be such that sufficient light reaches the plants; 2) water depth must be appropriate for the growth of SAV, so plants can remain submersed even during low tide; 3) sufficient water flow exists in the SAV canopies to minimize carbon limitations; 4) the sediment needs to meet SAV habitat requirements. Here, we present guidance on how to achieve secondary ecological benefits (e.g. SAV habitat) in conjunctions with the primary breakwater purpose of protecting the shoreline from erosion, in a variety of shoreline sedimentary environments (Figure 5.1).

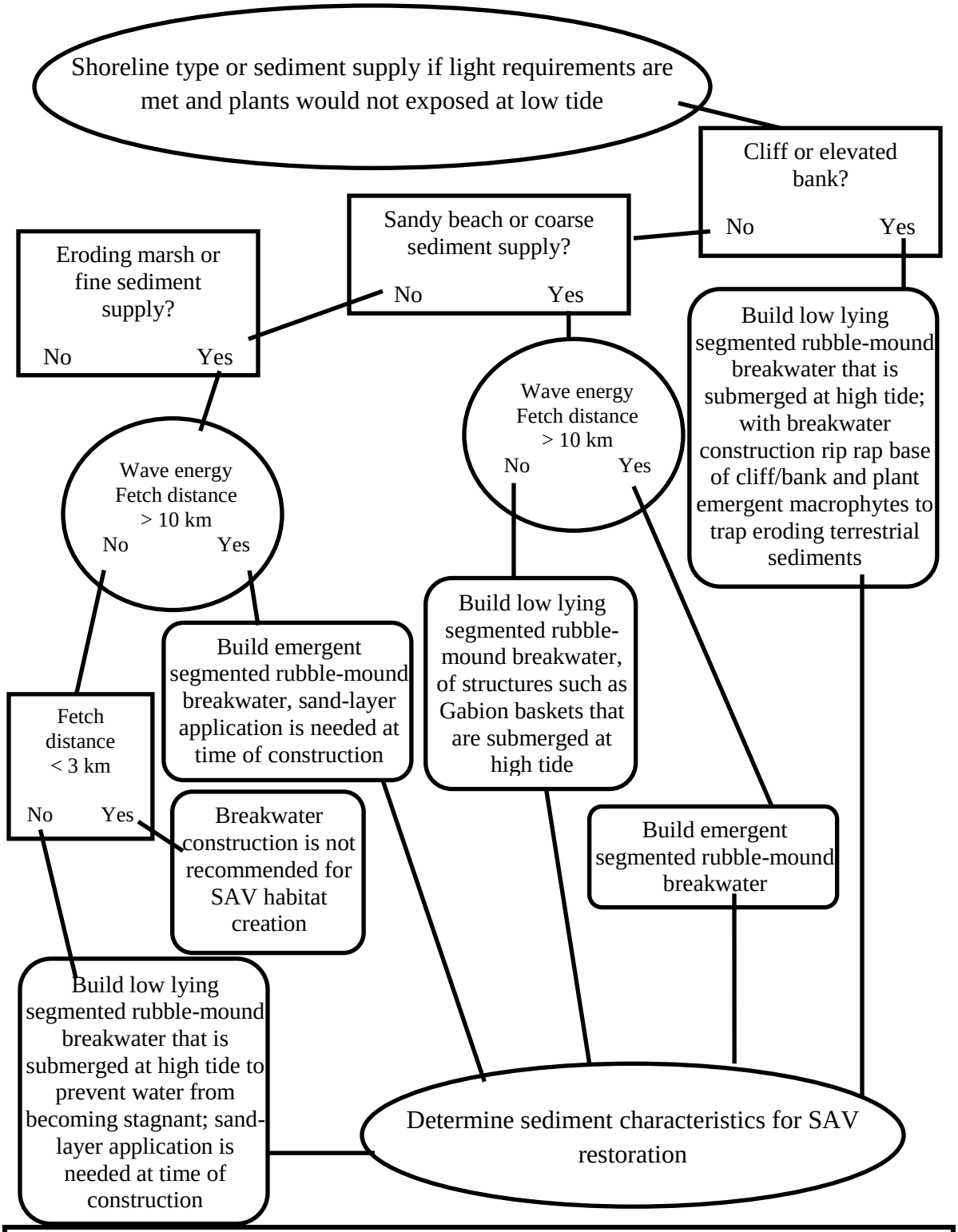

Figure 5.1 Recommendations for achieving secondary SAV habitat benefits in connection with breakwater construction within different salinity regions of the Chesapeake Bay.

If a shoreline characterized by marsh or a fine-sediment supply (e.g. river, eroding marsh) is nearby, the breakwater will facilitate fine-sediment deposition. Fine sediment is generally higher in organic and water content than sandy sediment. This increase in fine sediment can violate the SAV light or sediment requirements. In this case a sand-layer application in conjunctions with breakwater construction would be necessary to meet SAV sediment requirements, such as was seen at Hoopers Island. Fetch distance should also be measured (see Appendix) for the site of breakwater construction. If the fetch distance is < 3 km construction of the breakwater should not take place. If the fetch distance is from 3 to 10 km then a low-lying segmented rubble-mound breakwater that is submerged at high tide is recommended. This will facilitate greater exchange of water and sediments landward of the structure and will prevent water from becoming stagnant. If fetch distance is > 10 km then an emergent, segmented rubble-mound breakwater is recommended.

In contrast, if the shoreline is a sandy beach or when sand is the dominant sediment source, breakwaters can trap these coarser particles. In this case, breakwaters are beneficial for SAV establishment, especially if wave energy is high (fetch distance > 10 km) as plants will be sheltered landward of the structure. If the desired breakwater site has a fetch distance of > 10 km then an emergent, segmented rubble-mound breakwater is recommended. If fetch is < 10 km the breakwater can be emergent or a submerged segmented rubble-mound breakwater, as to keep water from becoming stagnant but flushing sediment from behind the structure is not crucial to SAV success when the dominant sediment source is sand as any fine, organic particles that the breakwater can trap will provide nutrients to the plants.

If a breakwater must be constructed along shorelines characterized by cliffs or elevated banks a low-lying segmented rubble-mound breakwater that is submerged at high tide is recommended. However, with breakwater construction rip rap must also be installed at the base of cliff/bank and emergent macrophytes must be planted to trap eroding terrestrial sediments. Otherwise, as the cliff erodes, sediment is trapped landward of the structure, filling in the breakwater-protected area and allowing beach or marsh establishment, which violates the water-depth requirement for SAV.

Once the breakwater is constructed sediment characteristics need to be evaluated to improve the success of SAV restoration in the area (Figure 5.2). In this study, habitat requirements were defined for 3 species of SAV in the Chesapeake Bay, and observations recorded for 5 others (2 of which are invasive; Table 5.1).

Table 5.1: Habitat characteristics of the 8 SAV species observed at study locations in the Chesapeake Bay, as well as characteristics of locations where SAV were absent.

Species	# of sites present (total 48)	Region	Sediment Median Diameter (phi) (µm)	Sediment Silt/clay (%)	Sediment Organic Content (%)	Water Content (%)	Fetch (km)
R. maritima	17	Mesohaline/ Polyhaline	1.9-4.5 (267.9-44.2)	3.1-51.3	0.6-4.1 0.6-13 in mesocosm	8.6-27.1	0.7-21.0
Z. palustris	3	Oligohaline/ Mesohaline	1.6-2.5 (329.9-176.8)	2.9-6.4	0.4-0.6 0.6-13 in mesocosm	15.1-19.8	2.2-7.2
V. americana	10	Tidal Fresh/ Oligohaline	1.5-4.0 (353.6-62.5)	3.9-42.0	0.4-20.1	12.8-55.7	0.1-4.9
P. perfoliatus	2	Oligohaline/ Mesohaline	1.6-2.3 (329.9-203.1)	3.9-6.4	0.4-0.6	17.7-19.8	2.2-3.0
H. verticillata	6	Tidal Fresh/ Oligohaline	1.7-4.0 (307.8-62.5)	4.5-42.0	0.6-7.9	12.8-34.9	2.2-4.9
M. spicatum	8	Tidal Fresh/ Oligohaline	1.5-2.9 (353.6-134.0)	4.5-22.8	0.6-20.1	12.8-55.7	0.1-4.9
N. gracillima	3	Tidal Fresh	1.7-4.0 (307.8-62.5)	5.5-42.0	0.8-7.9	16.7-34.9	2.2-2.4
Z. marina	8	Mesohaline/ Polyhaline	1.9-3.3 (267.9-101.5)	3.1-34.7	0.6-3.9	8.6-27.1	1.4-21.0
No SAV	14	Mesohaline/ Polyhaline	1.1-6.9 (466.5-8.4)	3.0-95.6	0.5-3.9	14.8-32.3	0.9-11.6

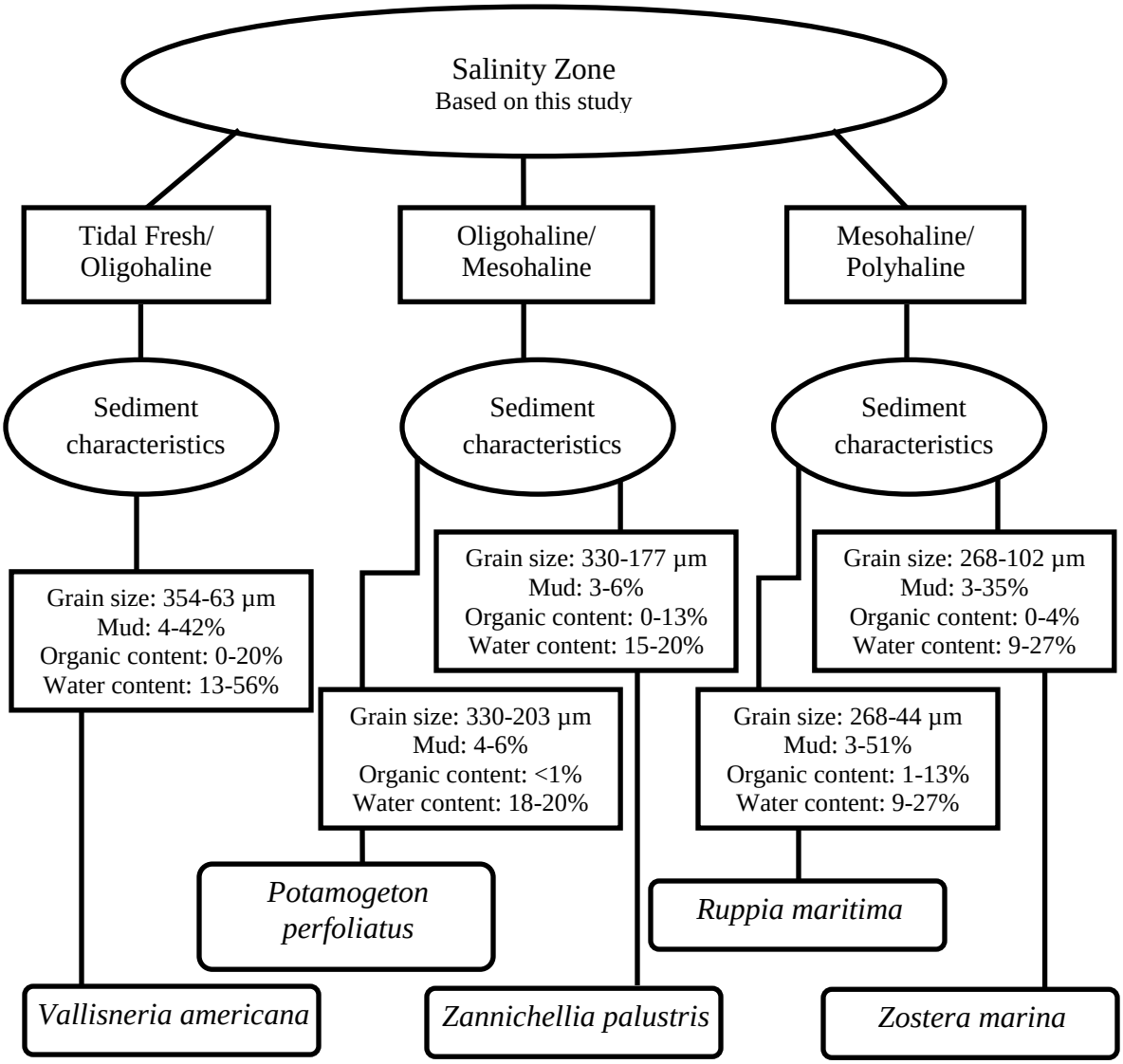

Figure 5.2. Sediment requirements for SAV species located within different salinity regions of the Chesapeake Bay.

Sediments >1% organic content that are sheltered and non-compacted would be more successfully colonized by *R. maritima*. *V. americana,* which has no organic content requirement, can be planted in the oligohaline region in sediments with high organic content (~20%), as long as water is not stagnant and the sediment silt/clay composition is < 42%. *Z. palustris* appeared to have no organic content requirement, although growth was best in ~8% organic content, and it produced seeds at all organic-content levels. Even though the growing season for this species is short (Feb-June), it may be successfully used as a colonizing species, as it produced seeds even at low organic levels and may trap sufficient organic matter to promote the growth of other species.

Other species such as *Z. marina, P. perfoliatus, H. verticillata, M. spicatum,* and *N. gracillima* were collected *in situ*. Data collected for habitat requirements can be found in Table 5.1. Due to small sample sizes conclusions are difficult to make on some species. *M. spicatum* and *H. verticillata* are invasive and therefore are not used in restoration efforts. They can however colonize sediments of higher organic content. They are canopy-forming, which reduces light penetration into the water column and traps large amounts of fine particles within beds (Newbolt et al., 2008). This makes competing with these species difficult, as Chesapeake Bay SAV is mainly limited by light and fine-grained sediments (Kemp et al., 1984; Koch, 2001).

CONCLUSIONS

Ecological engineering projects are receiving increased attention worldwide, particularly in the Netherlands, where they have embraced the concept of adapting and working with nature (Inman 2010). Here in the U.S., the U.S. Army Corps of Engineers has also begun to place more emphasis on ecological engineering projects, using the term "building with nature." The data presented here have shown that it should be possible to design and build coastal protection structures that not only reduce shoreline erosion but have secondary ecological benefits. We have shown that consideration of sources and types of sediment supply are key to successful establishment of SAV in breakwater-protected areas of Chesapeake Bay. Engineers and scientists are encouraged to continue to work together to design breakwaters that meet these habitat requirements and create conditions that can support dense SAV beds in the long term, thus furthering success in establishing SAV to historical levels and ultimately restoring the Chesapeake Bay to a healthier state.

APPENDIX

Information about each of the 24 study locations are presented in this appendix. Locations are divided by salinity region as defined by the Chesapeake Bay Program (CBP, 2004), within each salinity region, locations are listed by ascending age.

Tidal Fresh/ Oligohaline

Mesohaline

Polyhaline

Data analysis

SAS 9.2 was used for statistical analysis of data (Table Appendix1). Data were tested for a normal distribution; if it was not normal, then a log transformation was performed. Levene's test was utilized to determine equality of variances (Sokal and Rolhf, 1995). The majority of the data fit the assumptions of normality and homogeneity. A paired t-test was conducted for sediment characteristics and SAV characteristics between adjacent-exposed and breakwater-protected sites (Sokal and Rolhf, 1995). A one-way ANOVA was then completed for individual sites, comparing sediment grain size and organic matter, as well as SAV shoot- and root- length and total biomass between adjacent-exposed and breakwater-protected sites (Sokal and Rolhf, 1995).

Table Appendix1. Results of sediment and SAV data statistical analysis. P-value > 0.05 is significant. ('*' = log transformation was needed)

Site	Factors	Degrees of Freedom	t-value	p-value
Paired T-test				
Adjacent-exposed versus Breakwater-protected	Grain Size	23	-1.21	0.24
Adjacent-exposed versus Breakwater-protected	Organic Content	23	-1.25	0.22
Adjacent-exposed versus Breakwater-protected	Shoot Length	18	1.37	0.19
Adjacent-exposed versus Breakwater-protected	Root Length	18	-1.17	0.26
Adjacent-exposed versus Breakwater-protected	Total Biomass	17	0.87	0.39
Site	**Factors**	**Degrees of Freedom**	**f-value**	**p-value**
1-Way ANOVA				
ELK	Grain Size	1	24.47	0.0003
	Organic Content	1	9.27	0.01
	Shoot Length (*V. americana*)	1	14.33	0.001
	Root Length (*V. americana*)	1	1.49	0.22
	Total Biomass*	1	1.37	0.28
MN1	Grain Size*	1	4.27	0.06
	Organic Content*	1	0.14	0.72
	Total Biomass	1	963	0.03
MN2	Grain Size	1	82.93	< 0.0001
	Organic Content	1	5.73	0.03
	Root Length* (*V. americana*)	1	0.32	0.57
	Total Biomass	1	2.38	0.16
HMI	Grain Size	1	250.86	< 0.0001
	Organic Content	1	8.45	0.01
	Shoot Length (*P. perfoliatus*)	1	2.31	0.13
	Root Length* (*P. perfoliatus)*	1	1.61	0.20
	Total Biomass*	1	0.06	0.81
SUE	Grain Size	1	7.77	0.02
	Organic Content*	1	127.13	< 0.0001
	Shoot Length (*M. spicatum*)	1	5.51	0.02
	Root Length (*M. spicatum*)	1	0.99	0.32

	Shoot Length* (*V. americana*)	1	2.99	0.10
	Root Length* (*V. americana*)	1	5.59	0.02
	Total Biomass	1	0.61	0.46
REYC	Grain Size	1	96.79	< 0.0001
	Organic Content	1	6.47	0.03
	Shoot Length* (*M. spicatum*)	1	7.67	0.01
	Root Length (*M. spicatum*)	1	3.08	0.08
	Total Biomass	1	6.35	0.04
TAY	Grain Size*	1	3.85	0.07
	Organic Content	1	80.71	< 0.0001
TAN	Grain Size	1	1.46	0.25
	Organic Content	1	1.95	0.19
	No SAV in adjacent-exposed			
MayN	Grain Size	1	141.24	< 0.0001
	Organic Content	1	68.27	< 0.0001
MayS	Grain Size	1	44.54	< 0.0001
	Organic Content	1	8.58	0.01
BH	Grain Size	1	9.66	0.01
	Organic Content	1	5.01	0.04
	Shoot Length*	1	11.50	0.001
	Root Length*	1	3.31	0.07
	Total Biomass*	1	2.17	0.17
HI	Grain Size	1	29.44	0.0002
	Organic Content*	1	1.57	0.24
	No SAV in adjacent-exposed			
EN	Grain Size	1	34.14	0.0001
	Organic Content	1	36.59	< 0.0001
	No SAV in adjacent-exposed			
HB	Grain Size	1	927.02	< 0.0001
	Organic Content	1	388.8	< 0.0001
G	Grain Size	1	4.36	0.06
	Organic Content*	1	1.11	0.31
BB	Grain Size	1	0.73	0.41
	Organic Content	1	1.23	0.29
	Shoot Length	1	3.01	0.08
	Root Length	1	0.28	0.59
	Total Biomass*	1	5.27	0.05
CCBC	Grain Size	1	18.70	0.001
	Organic Content	1	5.38	0.04
	Shoot Length* (*R. maritima*)	1	411.76	< 0.0001
	Root Length (*R. maritima*)	1	3.72	0.05
	Shoot Length* (*Z. marina*)	1	53.76	< 0.0001
	Root Length (*Z. marina*)	1	7.23	0.01
	Total Biomass	1	9.00	0.01

CCPB	Grain Size	1	5.99	0.03
	Organic Content	1	1.43	0.26
	Shoot Length* (*R. maritima*)	1	0.86	0.36
	Root Length (*R. maritima*)	1	7.97	0.01
	Shoot Length* (*Z. marina*)	1	1.28	0.26
	Root Length* (*Z. marina*)	1	24.89	< 0.0001
	Total Biomass	1	0.00	1.00
MB	Grain Size	1	46.44	< 0.0001
	Organic Content*	1	30.75	0.0001
	Shoot Length*	1	44.36	< 0.0001
	Root Length	1	39.42	< 0.0001
	Total Biomass*	1	10.85	0.01
MOB5	Grain Size	1	20.71	0.001
	Organic Content	1	145.20	< 0.0001
MOB7	Grain Size	1	25.47	0.0003
	Organic Content*	1	3.19	0.10
	Shoot Length*	1	10.11	0.002
	Root Length*	1	0.33	0.57
	Total Biomass*	1	0.00	0.99
YT	Grain Size	1	21.89	0.001
	Organic Content	1	14.69	0.002
MOB3	Grain Size	1	3.60	0.08
	Organic Content	1	5.88	0.03
	Shoot Length*	1	13.34	0.0003
	Root Length	1	5.31	0.02
	Total Biomass	1	0.66	0.44
SCH	Grain Size	1	92.31	< 0.0001
	Organic Content*	1	7.04	0.02
	Shoot Length*	1	62.43	< 0.0001
	Root Length*	1	62.43	< 0.0001
	Total Biomass	1	6.69	0.03

Elk Neck

Description: This semi-circular, segmented, rock-mound breakwater has 7 segments. The total breakwater length is 253.9 m, with segment lengths 31±11 m (mean ± SD) and gap lengths 10±3 m. Average distance from shore is 100±21 m. This breakwater protects a boat pier and swimming area/ sandy beach for a summer camp. The adjacent-exposed area shoreline is a sandy beach.

Year of Construction: 2005 **Age at Sampling:** 3 years

Salinity Regime: Tidal fresh

Fetch: Adjacent: 4.9±1.5 km

Breakwater: 4.5±1.0 km

Sampling Coordinates:

Elk A vbc	39º29'40.3"N	75º59'22.5"W
Elk A pc	39º29'40.3"N	75º59'22.5"W
Elk B vbc	39º29'45.1"N	75º59'20.4"W
Elk B pc	39º29'45.1"N	75º59'20.4"W
SAV A1	39º29'42.5"N	75º59'22.2"W
SAV A2	39º29'41.8"N	75º59'22.6"W
SAV A3	39º29'40.8"N	75º59'23.4"W
SAV A4	39º29'38.9"N	75º59'25.3"W
SAV A5	39º29'37.5"N	75º59'26.5"W
SAV B1	39º29'46.5"N	75º59'20.2"W
SAV B2	39º29'47.4"N	75º59'22.3"W
SAV B3	39º29'46.0"N	75º59'22.3"W
SAV B4	39º29'44.7"N	75º59'22.4"W
SAV B5	39º29'42.8"N	75º59'22.0"W

Table ELK1. Latitude and longitude of vibracores (vbc), pushcores (pc), and SAV cores taken at the adjacent-exposed ("A") and breakwater-protected ("B") sites at Elk Neck.

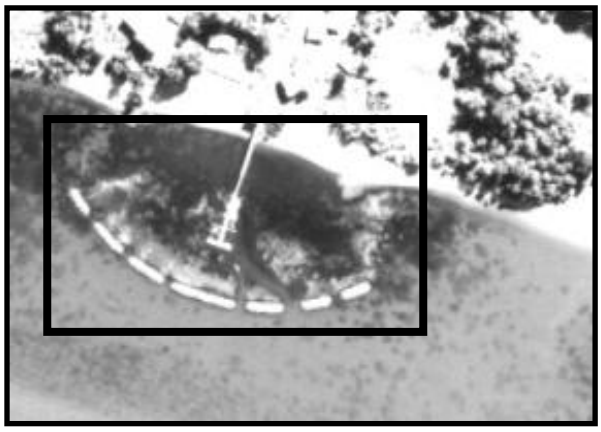

Figure ELK1. Aerial photo of the breakwater at Elk Neck, MD

Sediment Data:

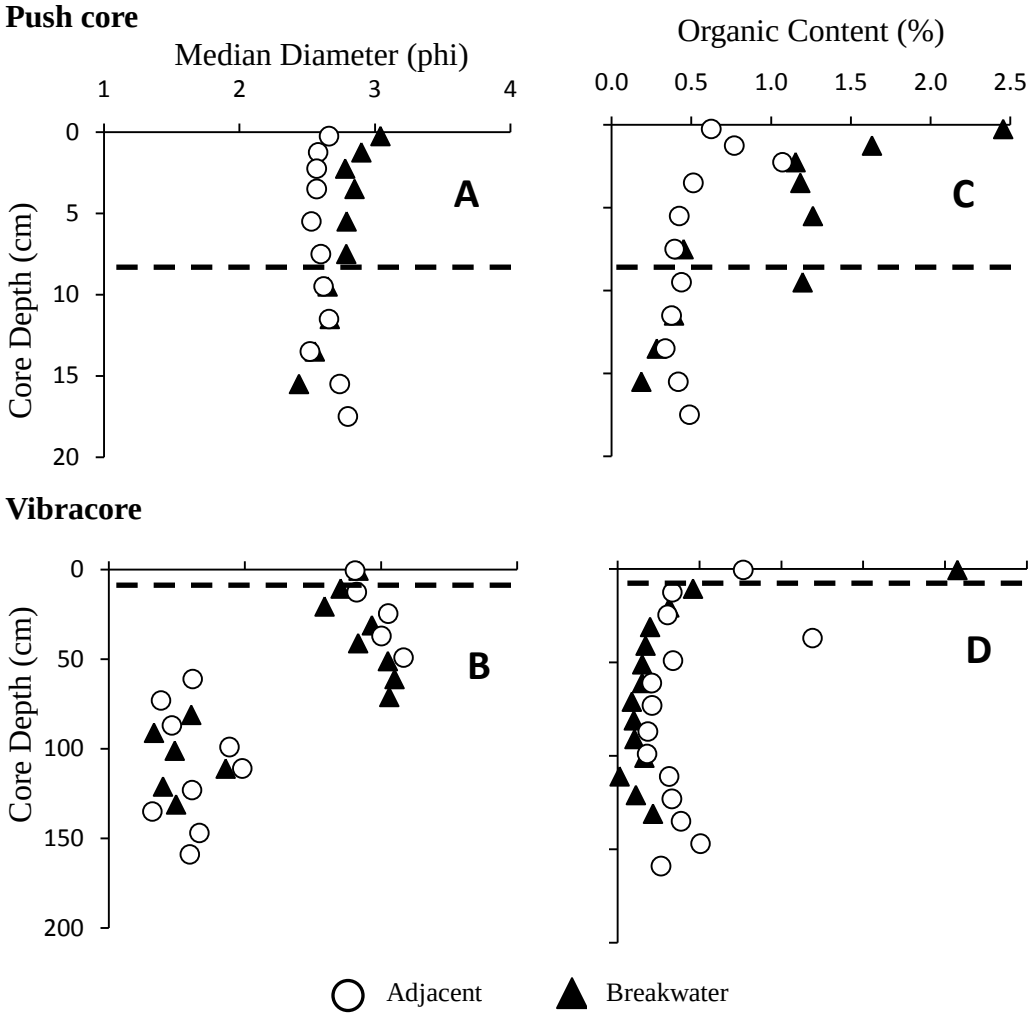

Figure ELK2. Sediment grain size (median diameter) collected with a push core (A) or vibracore (B) at the adjacent-exposed (open circles) and breakwater-protected (closed triangles) sites. The dashed line represents the interpreted depth of breakwater appearance. Sediment organic content collected with a push core (C) or vibracore (D) at the adjacent-exposed and breakwater-protected sites.

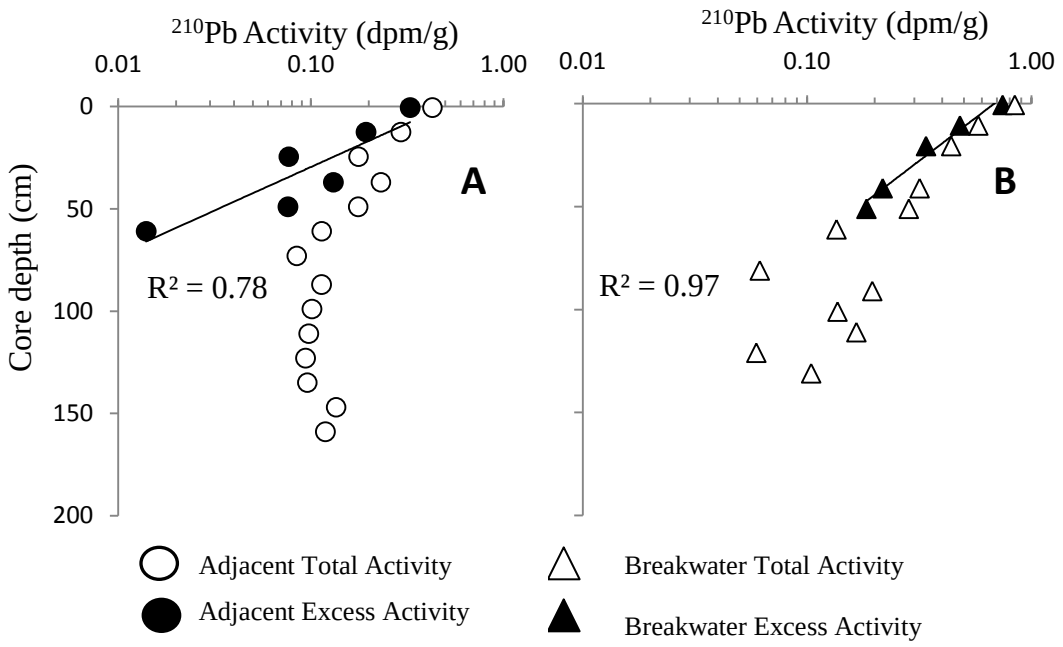

Figure ELK3. ^{210}Pb profiles at the adjacent-exposed (A) and breakwater-protected (B) sites. The calculated sediment accumulation rate at both sites is 1.1 cm/y.

Summary of sediment data:

The average median diameter of surficial (0-10 cm) sediments at the adjacent-exposed site is 2.6±0.02 (164.9 μm), and the average organic content is 0.6±0.1%. At the breakwater-protected site, the average median diameter is 2.8±0.1 (143.6 μm) and average organic content is 1.4±0.2%. The adjacent-exposed site was statistically coarser ($p = 0.0003$) and less organic ($p = 0.01$).

Both cores at Elk Neck display steady-state sedimentation and an accumulation rate of ~1 cm/y. This is expected, because this breakwater was constructed only 3 years prior to sampling – a short time relative to the half-life of ^{210}Pb (22.3 y). Clues as to how much and what type of sediment deposited post-construction can be found in the grain-

size data. Median diameter decreases (increasing phi units) from 1.5 to 3.0 phi (363.5 to 129.4 µm) at ~80 cm behind the breakwater, and from 1.5 to 3.1 phi (361.0 to 120.7 µm) at ~60 cm adjacent to it. Also, sediment fines upward behind the breakwater at ~20 cm, which is the expected trend in response to reduced physical energy; this trend is absent adjacent to the breakwater. A higher-resolution of the depth of breakwater influence can be obtained by examining the push-core grain-size profiles. In these profiles, median diameters observed in cores in the adjacent-exposed and breakwater-protected areas deviate at 8 cm, yielding a post-construction sedimentation rate of 2.7 cm/y. Thus, sediment is finer and more organic in the breakwater-protected area, and the sedimentation rate has increased. These changes may ultimately prove detrimental to SAV, outweighing the apparent initial benefit of the breakwater in alleviating potential wave limitation.

SAV Data:

Table ELK2. Characteristics of SAV species *Vallisneria americana, Hydrilla verticillata*, and both species combined growing at the adjacent-exposed and breakwater-protected sites, values are reported as mean ±SE.

Location	Species	Shoot Length (cm)	Root Length (cm)	Above-ground Biomass (g m^{-2})	Below-ground Biomass (g m^{-2})	Total Biomass (g m^{-2})	Ratio Above-/ Below-ground Biomass
Adjacent-exposed	*Vallisneria americnana*	16.9± 1.0	5.5± 0.2				
Breakwater-protected	*Vallisneria americnana*	24.8± 1.8	5.9± 0.2				
Adjacent-exposed	*Hydrilla verticillata*	14.8± 2.2	5.1± 0.9				
Breakwater-protected	*Hydrilla verticillata*	18.7± 3.6	5.1± 0.6				
Adjacent-exposed	All Species			19.3± 1.6	13.9± 2.6	33.2± 3.6	1.6± 0.3
Breakwater-protected	All Species			63.5± 40.8	11.5± 3.6	75.0± 38.7	15.5± 12.6

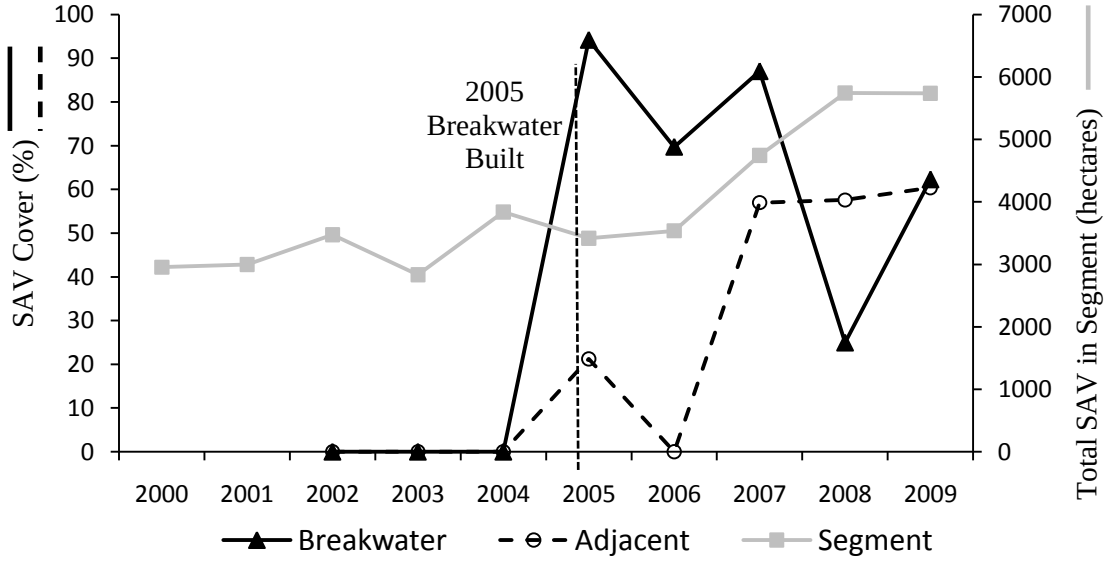

Figure ELK4. SAV % cover plotted against the total SAV in the bay segment as determined by VIMS aerial photography from 5 years prior to breakwater installation to present day.

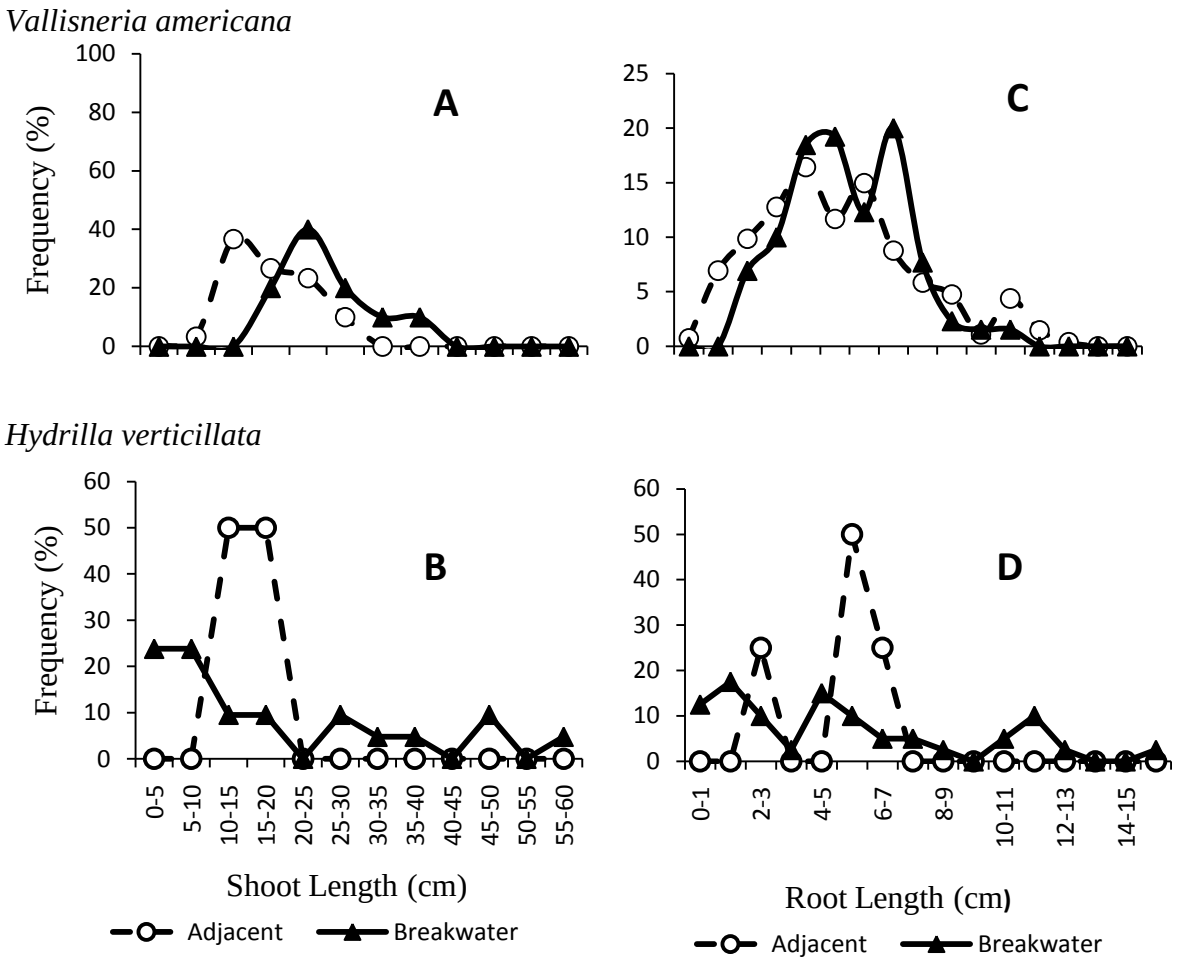

Figure ELK5. (A) Shoot- and (C) root-length frequency plots for *Vallisneria americana* and (B) shoot- and (D) root-length frequency plots for *Hydrilla verticillata* at the adjacent-exposed (open circles) and breakwater-protected (closed triangle) sites.

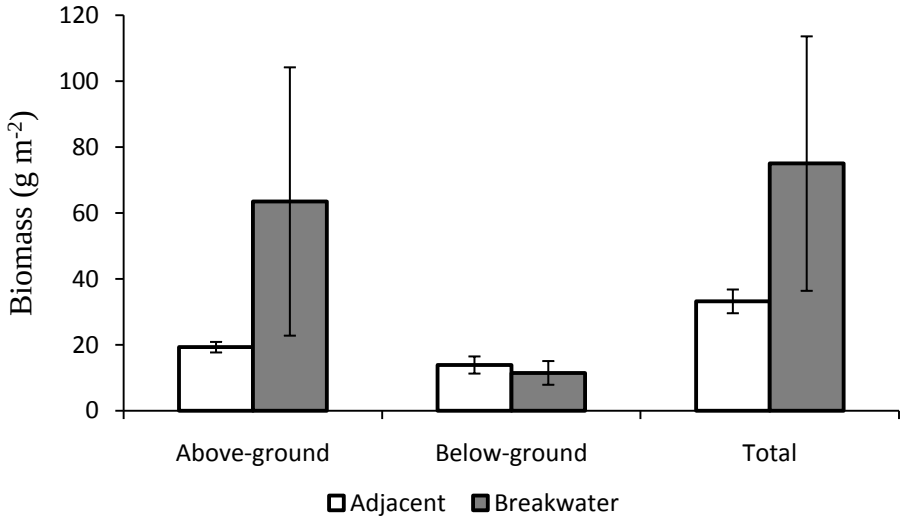

Figure ELK6. Biomass of the all species of SAV at the adjacent-exposed (open bars) and breakwater-protected (closed bars) sites.

Summary of SAV data:

SAV abundance in the segment containing the Elk Neck site generally increased from 2000 to 2009. At the Elk Neck site SAV also increased both in the adjacent site and the breakwater site until the breakwater was built. There was a sharp drop in SAV in the year following, potentially due to the environmental impacts of construction. Then the area behind the breakwater appears to decrease in the years following, while the area adjacent sees an increase in SAV coverage, mirroring the segment totals (Figure ELK4). *Myriophyllum spicatum* and *Hydrilla verticillata* are invasive species that are able to tolerate high organic sediments as well as stagnant water (Newbolt et al., 2008).

Sediments of high organic content (~20%) are also able to support growth of *Vallisneria americana* as long as water is not stagnant (Chapter 3). After SAV had 100% coverage populations declined in the breakwater-protected area allowing for stagnant conditions to be alleviated. Even though percent cover of the area was reduced biomass remained greater ($p = 0.28$) in the breakwater-protected site than the adjacent-exposed site (Figure ELK6). *V. americana* shoot lengths were longer ($p = 0.001$) in the breakwater-protected site than the adjacent-exposed, however roots were of similar length ($p = 0.22$; Figure ELK5; Table ELK2). *H. verticillata* sample sizes were too small for statistical analysis; however, collected shoots were longer in the breakwater-protected site and roots showed no difference.

Mason Neck 1

Description: This linear, segmented, rock-mound breakwater has 4 segments parallel to the shoreline. The total breakwater length is 233.8 m, with segment lengths 49±2 m (mean ± SD) and gap lengths 20±1 m. Average distance from shore is 36±2 m. This breakwater protects an eroding sand cliff. The adjacent-exposed shoreline was marsh that had been hardened with rip rap.

Year of Construction: 2002 **Age at Sampling:** 7 years

Salinity Regime: Tidal Fresh

Fetch: Adjacent: 2.4±0.5 km

Breakwater: 2.4±0.5 km

Sampling Coordinates:

MN1 A vbc	38º37'52.5"N	77º12'44.2"W
MN1 A pc	38º37'52.5"N	77º12'44.2"W
MN1 B vbc	38º37'47.2"N	77º12'40.0"W
MN1 B pc	38º37'47.2"N	77º12'40.0"W
SAV A1	38º37'52.5"N	77º12'44.3"W
SAV A2	38º37'52.7"N	77º12'44.2"W
SAV A3	38º37'53.8"N	77º12'45.0"W
SAV A4	38º37'54.1"N	77º12'44.9"W
SAV A5	38º37'54.2"N	77º12'45.0"W
SAV B1	38º37'45.6"N	77º12'38.7"W
SAV B2	38º37'46.5"N	77º12'39.6"W
SAV B3	38º37'47.5"N	77º12'40.3"W
SAV B4	38º37'49.1"N	77º12'41.7"W
SAV B5	38º37'50.7"N	77º12'43.2"W

Table MN1.1. Latitude and longitude of vibracores (vbc), pushcores (pc), and SAV cores taken in the adjacent-exposed ("A") and breakwater-protected ("B") sites at Mason Neck 1.

Figure MN1.1. Aerial photograph of the breakwater at Mason Neck north, VA.

Sediment Data:

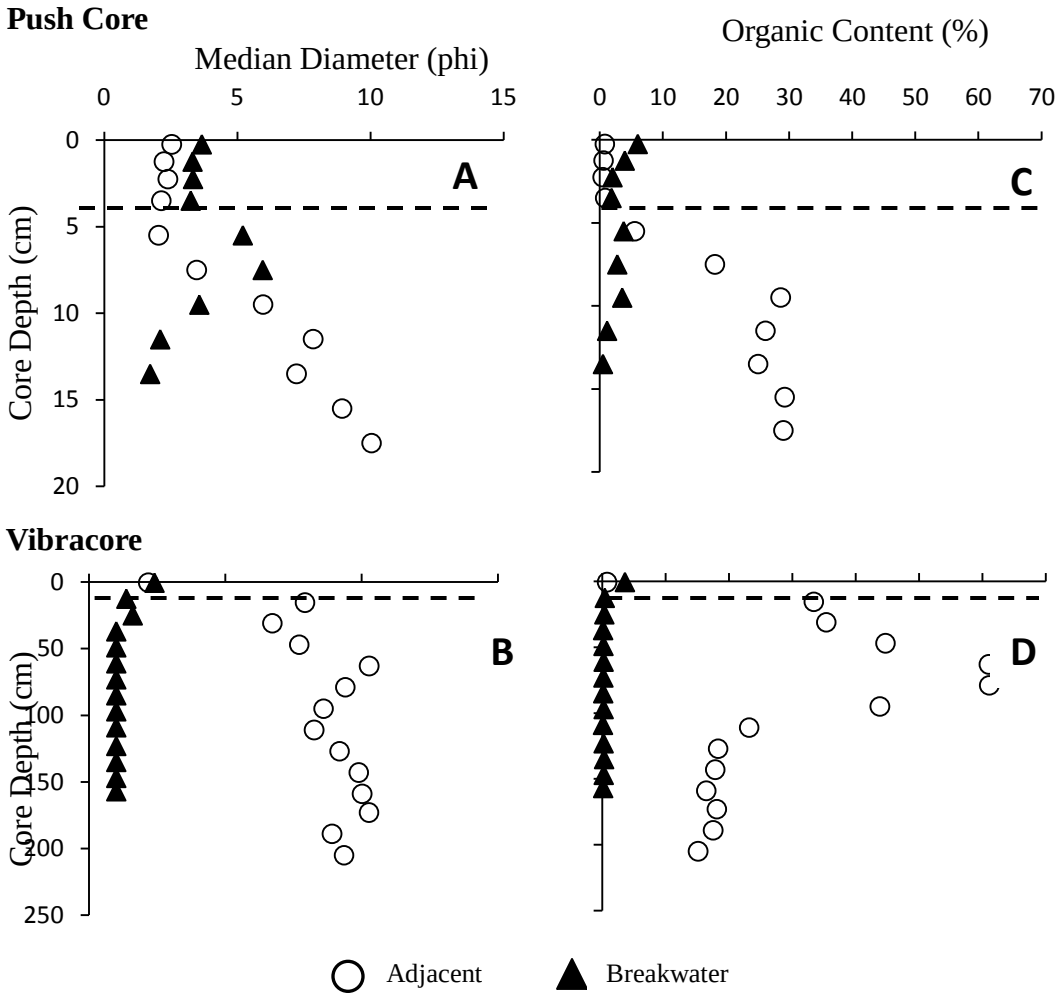

Figure MN1.2. Sediment grain size (median diameter) collected with a push core (A) or vibracore (B) at the adjacent-exposed (open circles) and breakwater-protected (closed triangles) sites. The dashed line represents the interpreted depth of breakwater appearance (4 cm). Sediment organic content collected with a push core (C) or vibracore (D) at the adjacent-exposed and breakwater-protected sites.

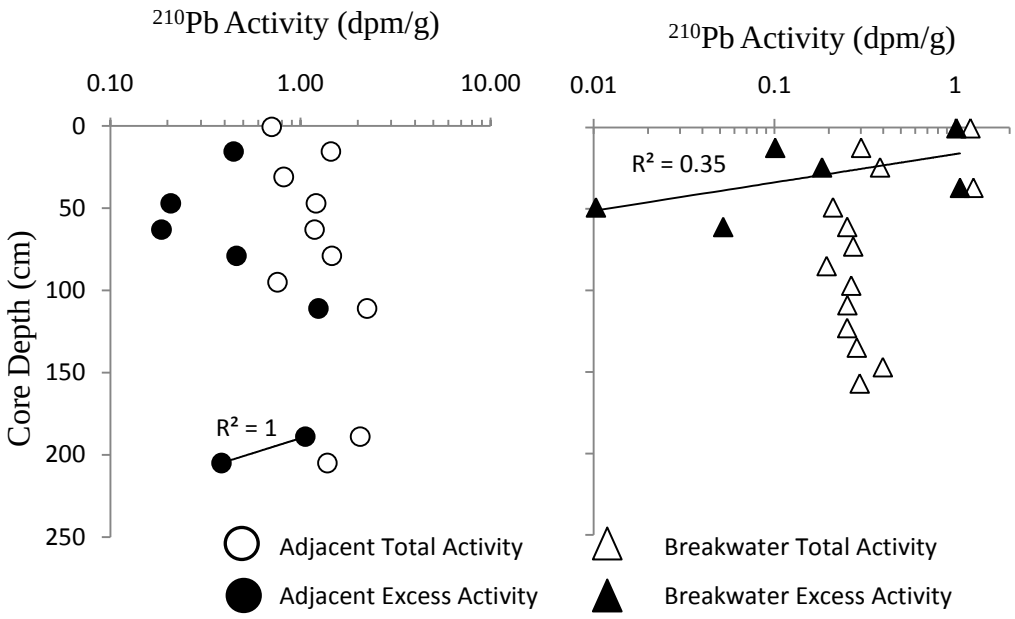

Figure MN1.3. ^{210}Pb profiles at the adjacent-exposed (A) and breakwater-protected (B) sites. The calculated sediment accumulation rate is 0.5 cm/y at the adjacent-exposed site and 0.6 cm/y at the breakwater-protected site, representing the pre-construction sedimentation rate. The x-axis scale differs between plots for visual clarity.

Summary of sediment data:

Surficial (upper 10 cm) sediment at the adjacent-exposed site has an average diameter of 3.0±0.5 phi (125.0 µm) and average organic content of 7.9±4.2%. Push-core profiles at this site have a ~5-cm thick layer with relatively coarse, low organic sediment overlying finer and more organic sediment that dominates the rest of the profile. The breakwater-protected site has finer sediments ($p = 0.06$), with an average median diameter of 4.0±0.4 phi (62.5 µm), that are more organic ($p = 0.72$; average organic content 3.4±0.5%). Sediment at this site is coarser in the upper 4 cm than in the rest of the profile, likely due to the influence of the breakwater.

At the adjacent-exposed site, the ^{210}Pb profile has variable activity for most of the profile. It appears that activities begin to logarithmically decrease at the base of the core, but data points are few. So, while a best-fit regression line can be fit to the profile, resulting in a calculated sediment accumulation rate of 0.5 cm/y, it should be used with caution. At the breakwater-protected site, sedimentation is more steady-state and the calculated (pre-construction) accumulation rate is 0.6 cm/y. The close correspondence of the sediment accumulation rate at the adjacent-exposed and breakwater-protected sites indicates that the rate for the adjacent-exposed site is likely at least of the correct order of magnitude. The post-construction sedimentation rate is 0.6 cm/y, calculating by dividing the depth of breakwater influence (4 cm) by the breakwater age (7 y).

SAV Data:

Table MN1.2. Characteristics of SAV species *Najas gracillima, Hydrilla verticillata, Vallisneria americana, and Myriophyllum spicatum* growing at the adjacent-exposed and breakwater-protected sites, values are reported as mean ±SE.

Location	Species	Shoot Length (cm)	Root Length (cm)	Above-ground Biomass (g m^{-2})	Below-ground Biomass (g m^{-2})	Total Biomass (g m^{-2})	Ratio Above-/ Below-ground Biomass
Adjacent-exposed	*Najas gracillima*	n/a	n/a	0	0	0	0
Breakwater-protected	*Najas gracillima*	19.4± 1.3	5.0± 0.5	14.1± 3.4	0.8± 0.4	14.9± 3.6	32.2± 19.7
Adjacent-exposed	*Hydrilla verticillata*	11.9± 5.3	7.0± 1.2	3.2	3.9	7.1	0.8
Breakwater-protected	*Hydrilla verticillata*	20.9± 1.2	7.5± 0.2	145.9± 31.5	9.2± 1.8	155.1± 31.8	17.3± 3.4
Adjacent-exposed	*Vallisneria americana*	18.3± 1.1	6.9± 0.1	64.0± 22.7	20.7± 2.5	84.7± 22.8	3.2± 1.2
Breakwater-protected	*Vallisneria americana*	n/a	n/a	0.9± 0.6	0	0.9± 0.6	n/a
Adjacent-exposed	*Myriophyllum spicatum*	83.8	11.2± 0.6	43.6± 37.6	24.4	49.7± 43.7	6.4
Breakwater-protected	*Myriophyllum spicatum*	56.3	n/a	34.1± 17.4	0	34.1± 17.4	n/a

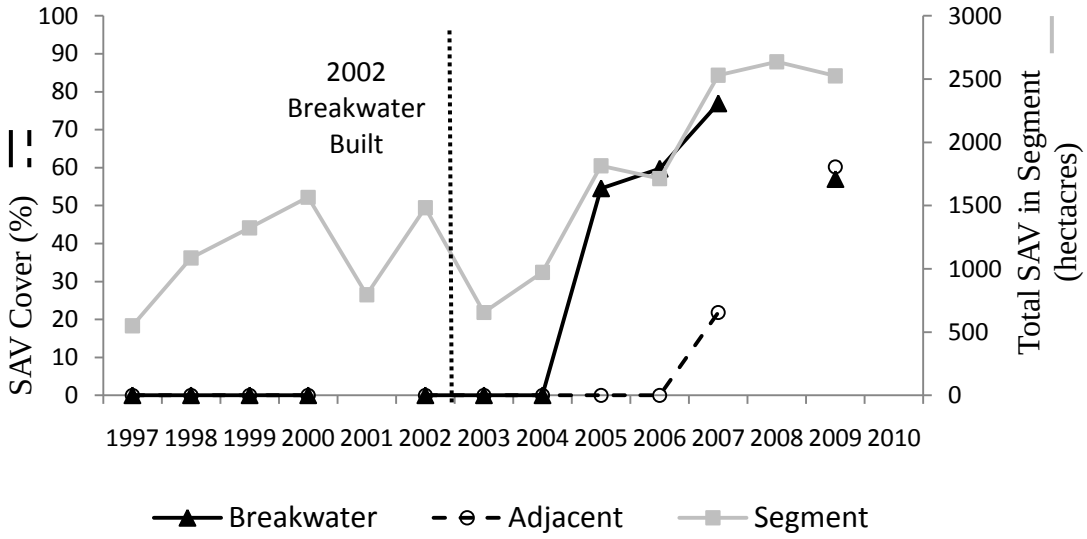

Figure MN1.4. SAV % cover plotted against the total SAV in the bay segment as determined by VIMS aerial photography from 5 years prior to breakwater installation to present day.

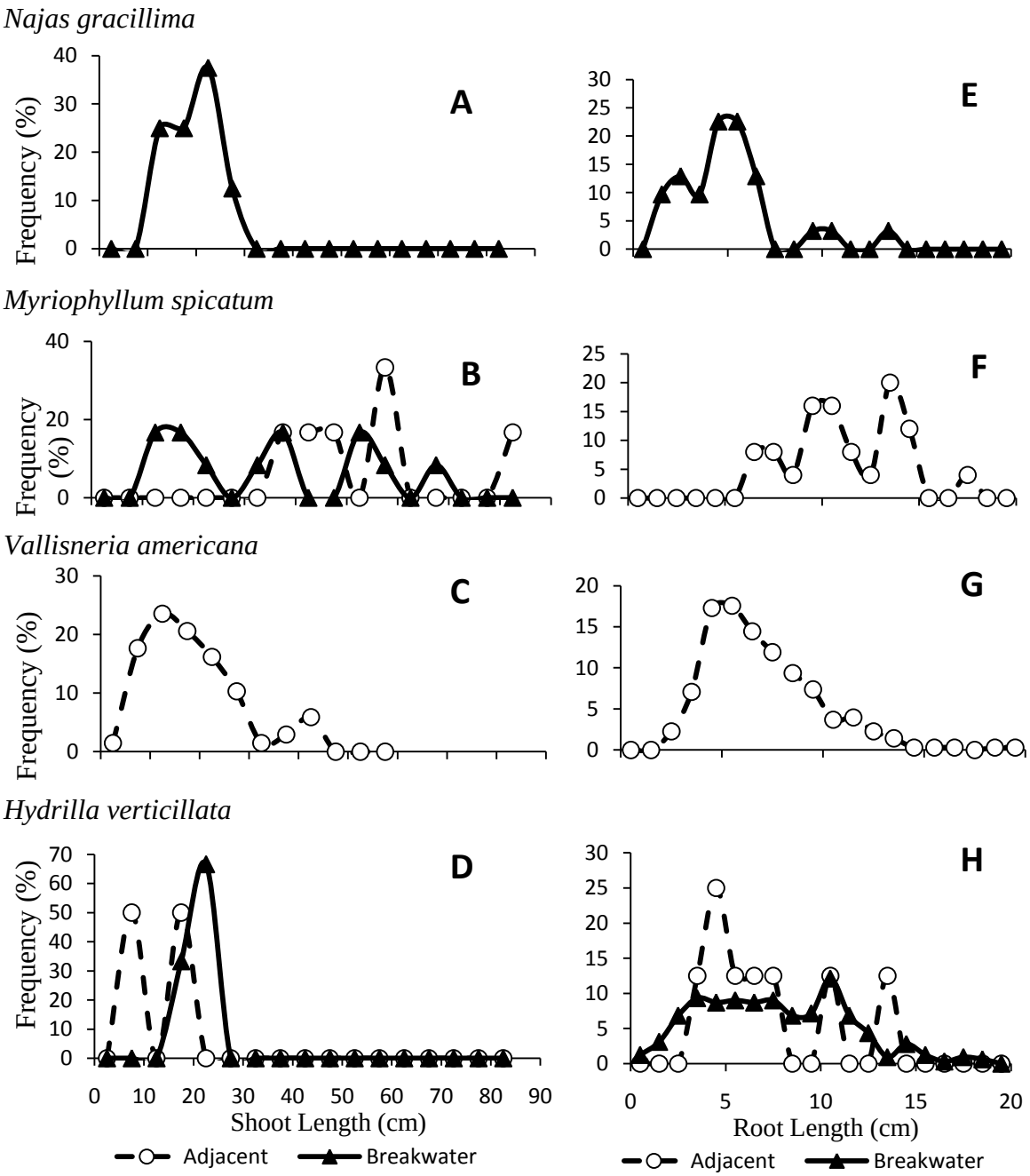

Figure MN2.5. (A) Shoot- and (E) root-length frequency plots for *Najas gracillima*, (B) shoot- and (F) root-length frequency plots for *Myriophyllum spicatum*, (C) shoot- and (G) root-length frequency plots for *Vallisneria americana*, and (D) shoot- and (H) root-length frequency plots for *Hydrilla verticillata* at the adjacent-exposed (open circles) and breakwater-protected (closed triangle) sites.

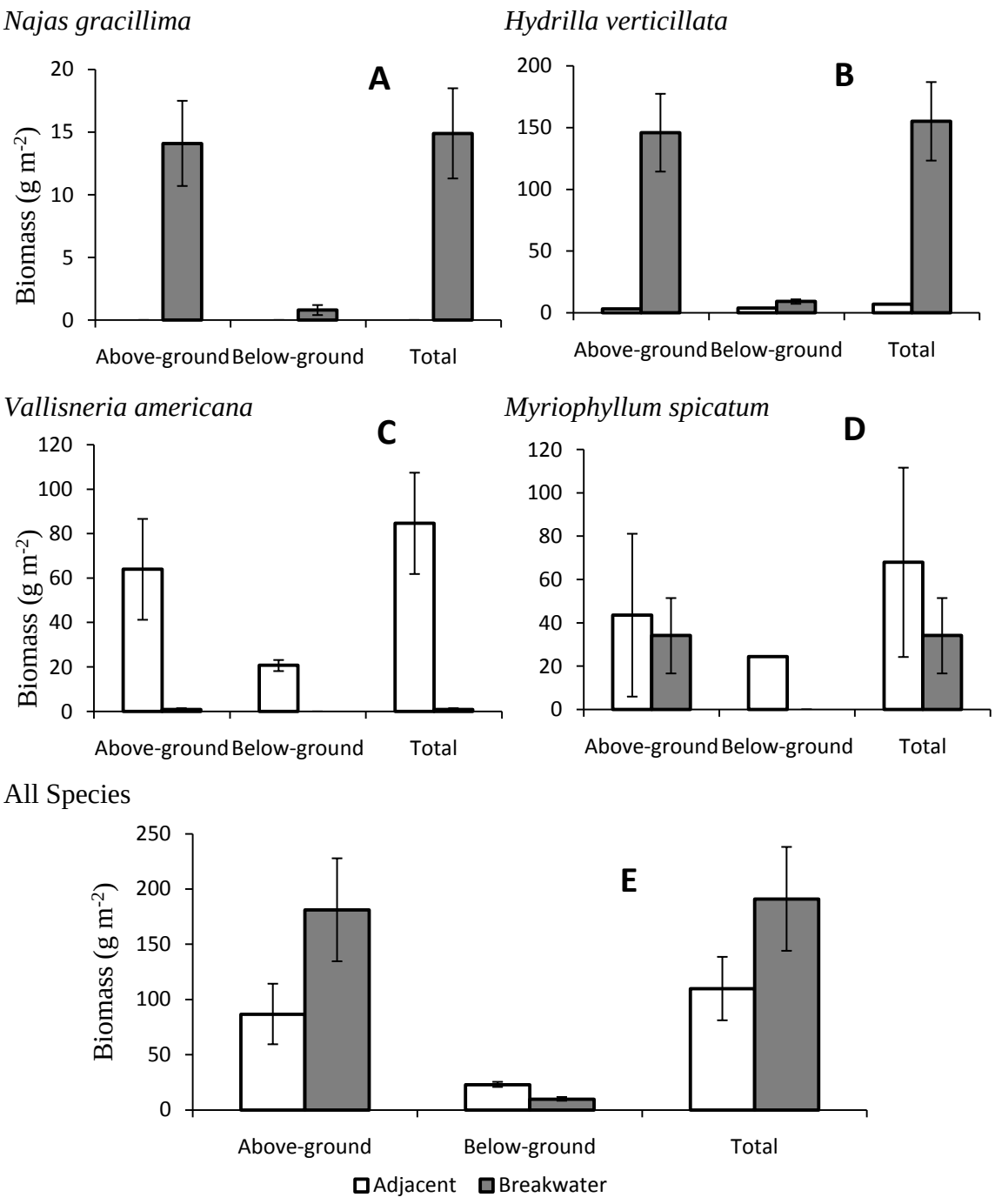

Figure MN1.6. Biomass of the SAV (A) *Najas gracillima,* (B) *Hydrilla verticillata,* (C) *Vallisneria americana,* (D) *Myriophyllum spicatum,* and (E) all species of SAV at the adjacent-exposed (open bars) and breakwater-protected (closed bars) sites.

Summary of SAV data:

SAV abundance in the segment containing the Mason Neck 1 site generally increased over the observation period. At Mason Neck 1 SAV also increased both in the adjacent site and the breakwater site starting 2 years after the breakwater was built. This effect was initially greater in the breakwater site than the adjacent site, though by 2010 the breakwater and adjacent sites are roughly equal.

Total biomass was greater at the breakwater-protected site ($p = 0.98$) than at the adjacent-exposed site. This however was the opposite for the species *Vallisneria americana* which had higher total biomass at the adjacent-exposed ($p = 0.03$) than the breakwater-protected site. It is hypothesized that these plants need water flow to reduce diffusion limitations of the leaves. It is only with reduced % cover in the area influenced by the breakwater that this problem of stagnant water can be alleviated. Sample sizes did not allow for statistical analysis of shoot- and root-length.

Mason Neck 2

Description: This linear, segmented, rock-mound breakwater has 4 segments parallel to the shoreline. The total breakwater length is 264.1 m, with segment lengths 41±1 m (mean ± SD) and gap lengths 22±1 m. Average distance from shore is 42±10 m. This breakwater protects an eroding sand cliff. The adjacent-exposed shoreline was hardened with rip rap.

Year of Construction: 2001 **Age at Sampling:** 8 years

Salinity Regime: Tidal Fresh

Fetch: Adjacent: 2.3±0.6 km

Breakwater: 2.2±0.6 km

Sampling Coordinates:

MN2 A vbc	38º37'24.2"N	77º12'18.7"W
MN2 A pc	38º37'24.2"N	77º12'18.7"W
MN2 B vbc	38º37'19.5"N	77º12'18.9"W
MN2 B pc	38º37'19.5"N	77º12'18.9"W
SAV A1	38º37'23.1"N	77º12'17.7"W
SAV A2	38º37'23.5"N	77º12'18.4"W
SAV A3	38º37'23.8"N	77º12'18.4"W
SAV A4	38º37'24.1"N	77º12'18.0"W
SAV A5	38º37'25.3"N	77º12'18.0"W
SAV B1	38º37'17.4"N	77º12'18.8"W
SAV B2	38º37'16.1"N	77º12'18.9"W
SAV B3	38º37'16.7"N	77º12'19.2"W
SAV B4	38º37'19.9"N	77º12'19.1"W
SAV B5	38º37'21.0"N	77º12'18.6"W

Table MN2.1. Latitude and longitude of vibracores (vbc), pushcores (pc), and SAV cores taken in the adjacent-exposed ("A") and breakwater-protected ("B") sites at Mason Neck 2.

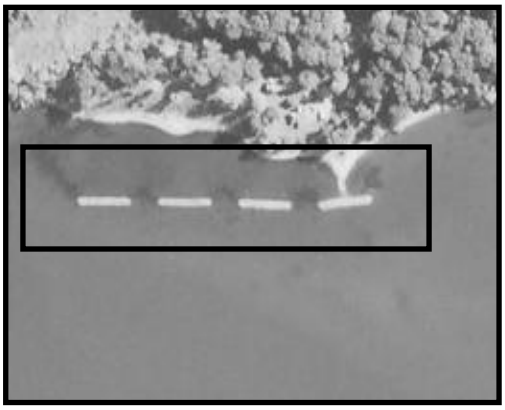

Figure MN2.1. Aerial photo of the breakwater at Mason Neck, VA.

Sediment Data:

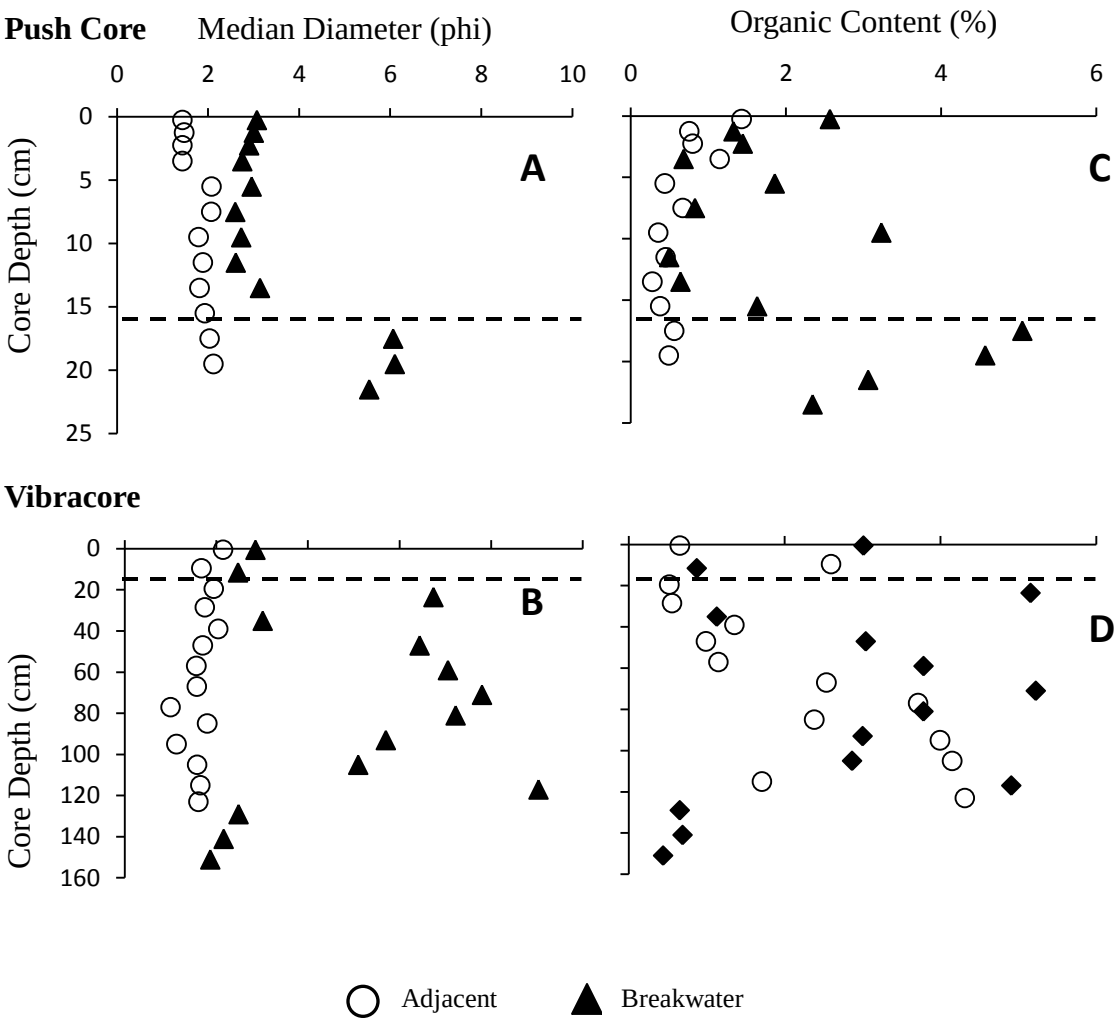

Figure MN2.2. Sediment grain size (median diameter) collected with a push core (A) or vibracore (B) at the adjacent-exposed (open circles) and breakwater-protected (closed triangles) sites. The dashed line represents the interpreted depth of breakwater appearance (16 cm). Sediment organic content collected with a push core (C) or vibracore (D) at the adjacent-exposed and breakwater-protected sites.

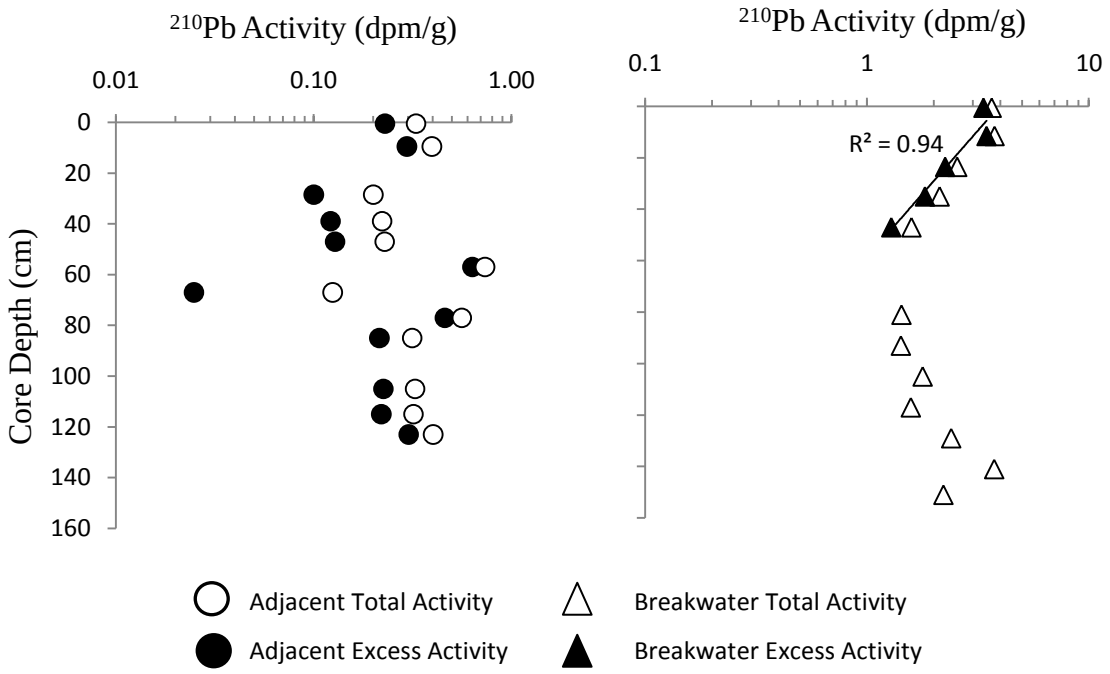

Figure MN2.3. ^{210}Pb profiles at the adjacent-exposed (A) and breakwater-protected (B) sites. At the adjacent-exposed site, down-core activities are variable and only a minimum accumulation rate of >1.2 cm/y can be calculated. ^{210}Pb activities at the breakwater-protected site decrease logarithmically with depth, after normalization to the mud content. The accumulation rate is 1.9 cm/y, representing pre-construction sedimentation.

Summary of sediment data

Surficial (top 10 cm) sediment at the adjacent-exposed site was sandy (average median diameter of surficial sediment 1.7±0.1 phi, 307.8 µm) and low in organic content (0.8±0.1%). Surficial sediment in the breakwater-protected area was also sandy (average median diameter 2.9±0.1 phi, 134.0 µm) but finer ($p < 0.0001$) than that at the adjacent-exposed site, and more organic (1.7±0.4%; $p = 0.03$).

^{210}Pb activities at the adjacent-exposed site are variable with depth, and only a minimum accumulation rate (>1.2 cm/y) can be calculated for this site. Activities at the breakwater-protected site decrease logarithmically with depth, after normalization to the mud content. The pre-construction accumulation rate calculated from the slope of the best-fit regression line is 1.9 cm/y.

In the push-core grain-size profile, there is an abrupt shift toward coarser and less organic sediment above 16 cm, which is the interpreted depth of breakwater influence. Dividing this depth by the breakwater age (8 y) results in a post-construction sedimentation rate of 2.0 cm/y. Thus, the effect of the breakwater at this location appears to be an increase in grain size, decrease in organic content, and no change in sedimentation rate.

SAV Data:

Table MN2.2. Characteristics of SAV species *Najas gracillima, Hydrilla verticillata,* and *Vallisneria americana* and growing at the adjacent-exposed and breakwater-protected sites, values are reported as mean ±SE.

Location	Species	Shoot Length (cm)	Root Length (cm)	Above-ground Biomass ($g\ m^{-2}$)	Below-ground Biomass ($g\ m^{-2}$)	Total Biomass ($g\ m^{-2}$)	Ratio Above-/ Below-ground Biomass
Adjacent-exposed	*Najas gracillima*	n/a	n/a	0.8	0.3	1.1	n/a
Breakwater-protected	*Najas gracillima*	7.5± 0.6	5.2± 0.3	17.2± 9.1	3.2± 1.1	20.4± 10.2	4.8± 1.0
Adjacent-exposed	*Hydrilla verticillata*	19.3± 3.3	4.0± 0.3	18.9± 7.6	2.0± 1.6	20.9± 8.7	29.4± 22.8
Breakwater-protected	*Hydrilla verticillata*	n/a	n/a	19.4± 8.6	3.6± 1.1	23.0± 9.4	4.8± 1.5
Adjacent-exposed	*Vallisneria americana*	7.6± 1.1	4.4± 0.5	4.6± 2.7	1.8± 1.2	6.4± 3.8	2.8± 0.3
Breakwater-protected	*Vallisneria americana*	5.8	3.3± 0.3	1.4± 0.7	1.4± 1.1	2.7± 1.8	1.6± 0.7

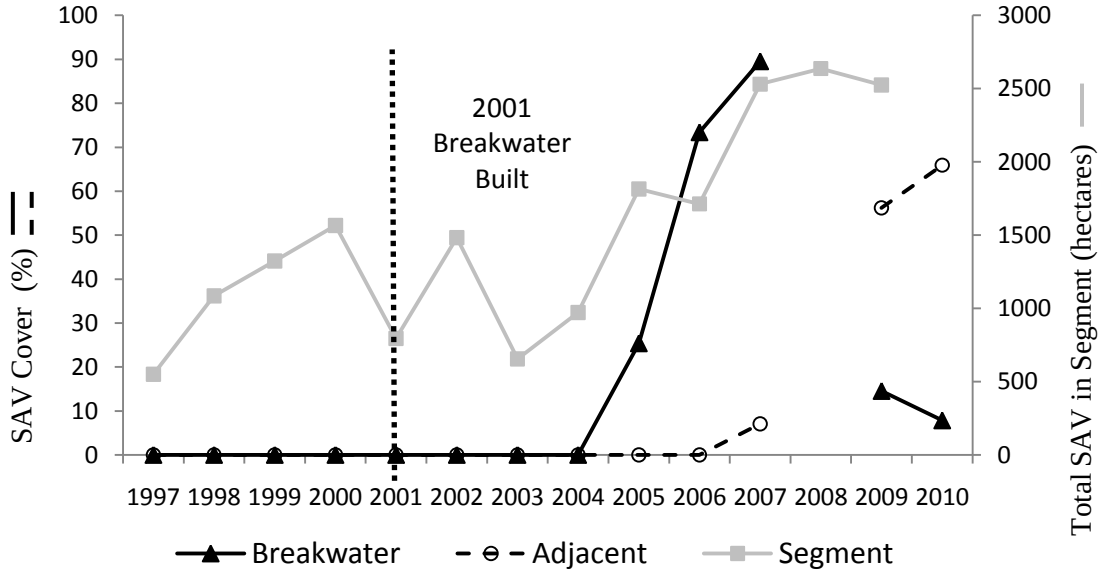

Figure MN2.4. SAV % cover plotted against the total SAV in the bay segment as determined by VIMS aerial photography from 5 years prior to breakwater installation to present day. Aerial photos were not taken in 2008.

Najas gracillima

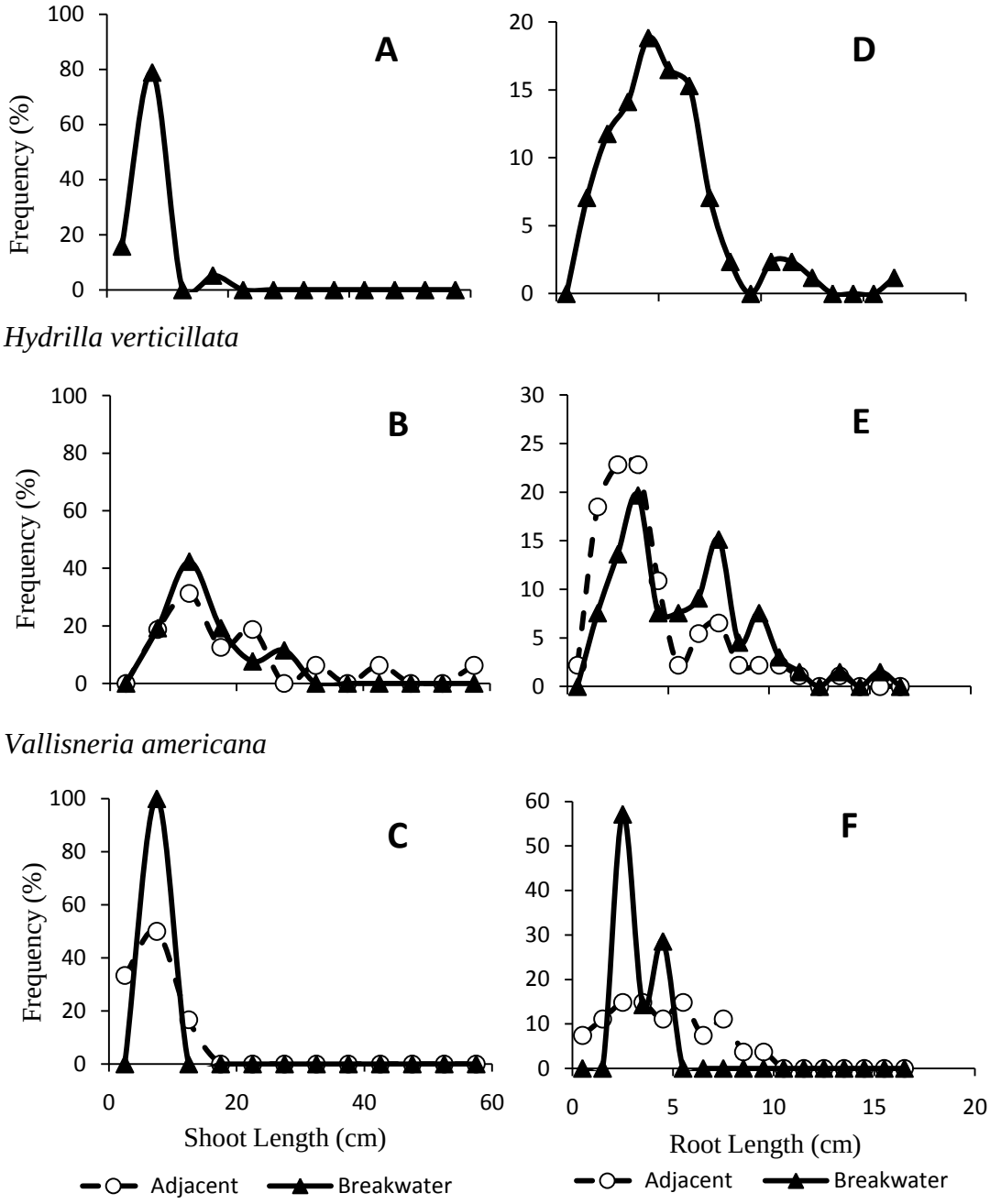

Hydrilla verticillata

Vallisneria americana

Figure MN2.5. (A) Shoot- and (D) root-length frequency plots for *Najas gracillima* and (B) shoot- and (E) root-length frequency plots for *Hydrilla verticillata* and (C) Shoot- and (F) root-length frequency plots for *Vallisneria americana* at the adjacent-exposed (open circles) and breakwater-protected (closed triangle) sites.

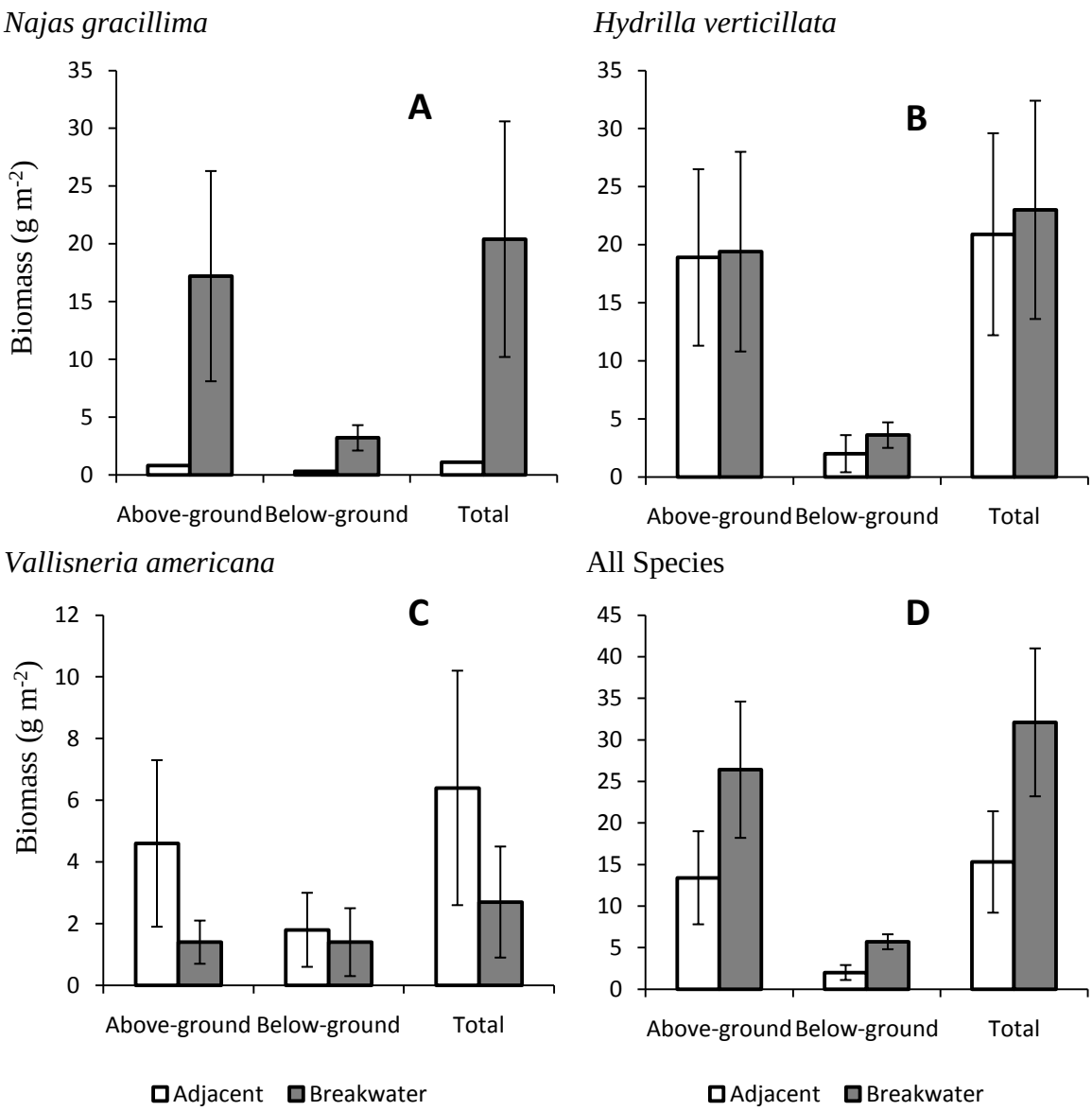

Figure MN2.6. Biomass of the SAV (A) *Najas gracillima*, (B) *Hydrilla verticillata*, (C) *Vallisneria americana*, and (D) all species of SAV at the adjacent-exposed (open bars) and breakwater-protected (closed bars) sites.

Summary of SAV data:

SAV abundance in the segment containing the Mason Neck 2 site generally increased over the observation period. At Mason Neck 2 SAV also increased both in the adjacent site and the breakwater site starting 3 years after the breakwater was built. Both the breakwater and adjacent sites mirror the segment totals until 2009 when the protected area sees a sharp drop in SAV coverage, while the adjacent unprotected area continues to increase.

Even though % cover decreases in 2009, the SAV at the breakwater-protected site was still productive as total biomass was greater, although not significantly ($p = 0.16$), at the breakwater-protected site than at the adjacent-exposed site. However according to Figure MN2.6c this appears to be the opposite for the species *Vallisneria americana* which had higher total biomass at the adjacent-exposed than the breakwater-protected site. It is hypothesized that these plants need water flow to reduce diffusion limitations of the leaves. It is only with reduced % cover in the area influenced by the breakwater that this problem of stagnant water can be alleviated. Sample sizes did not allow for statistical analysis of shoot length, however root lengths were not statistically different between adjacent-exposed and breakwater-protected sites ($p = 0.57$).

Hart-Miller Island

Description: This linear, segmented, rock-mound breakwater has 15 segments parallel to the shoreline. The total breakwater length is 902.7 m, with segment lengths 30±1 m (mean ± SD) and gap lengths 29±1 m. Average distance from shore is 37±8 m. This breakwater protects a sandy beach on an engineered island constructed of dredge material. The adjacent-exposed shoreline was forested.

Year of Construction: 1999 **Age at Sampling:** 10 years

Salinity Regime: Oligohaline

Fetch: Adjacent: 3.0±1.0 km

Breakwater: 2.2±0.5 km

Sampling Coordinates:

HMI A vbc	39º15'07.5"N	76º22'38.8"W
HMI A pc	39º15'07.5"N	76º22'38.8"W
HMI A pc	39º15'07.5"N	76º22'38.8"W
HMI B vbc	39º15'13.7"N	76º22'17.1"W
HMI B pc	39º15'13.7"N	76º22'17.1"W
SAV A1	39º15'08.5"N	76º22'30.8"W
SAV A2	39º15'08.5"N	76º22'31.8"W
SAV A3	39º15'08.5"N	76º22'33.0"W
SAV A4	39º15'08.5"N	76º22'35.2"W
SAV A5	39º15'07.8"N	76º22'37.6"W
SAV B1	39º15'23.2"N	76º21'59.2"W
SAV B2	39º15'21.6"N	76º22'04.0"W
SAV B3	39º15'21.3"N	76º22'05.0"W
SAV B4	39º15'13.5"N	76º22'17.4"W
SAV B5	39º15'10.0"N	76º22'25.7"W

Table HMI1. Latitude and longitude of vibracores (vbc), pushcores (pc), and SAV cores taken in the adjacent-exposed ("A") and breakwater-protected ("B") sites at Hart-Miller Island.

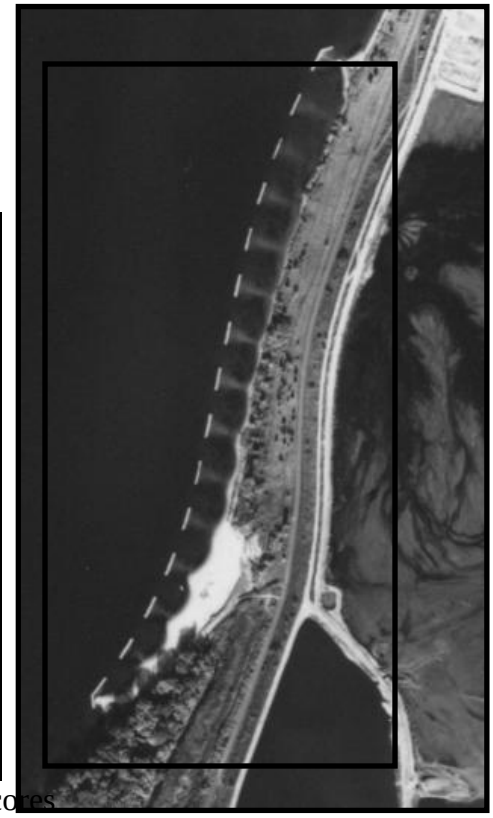

Figure HMI1. Aerial photo of the breakwater at Hart-Miller Island, MD.

Sediment Data:

Push Core

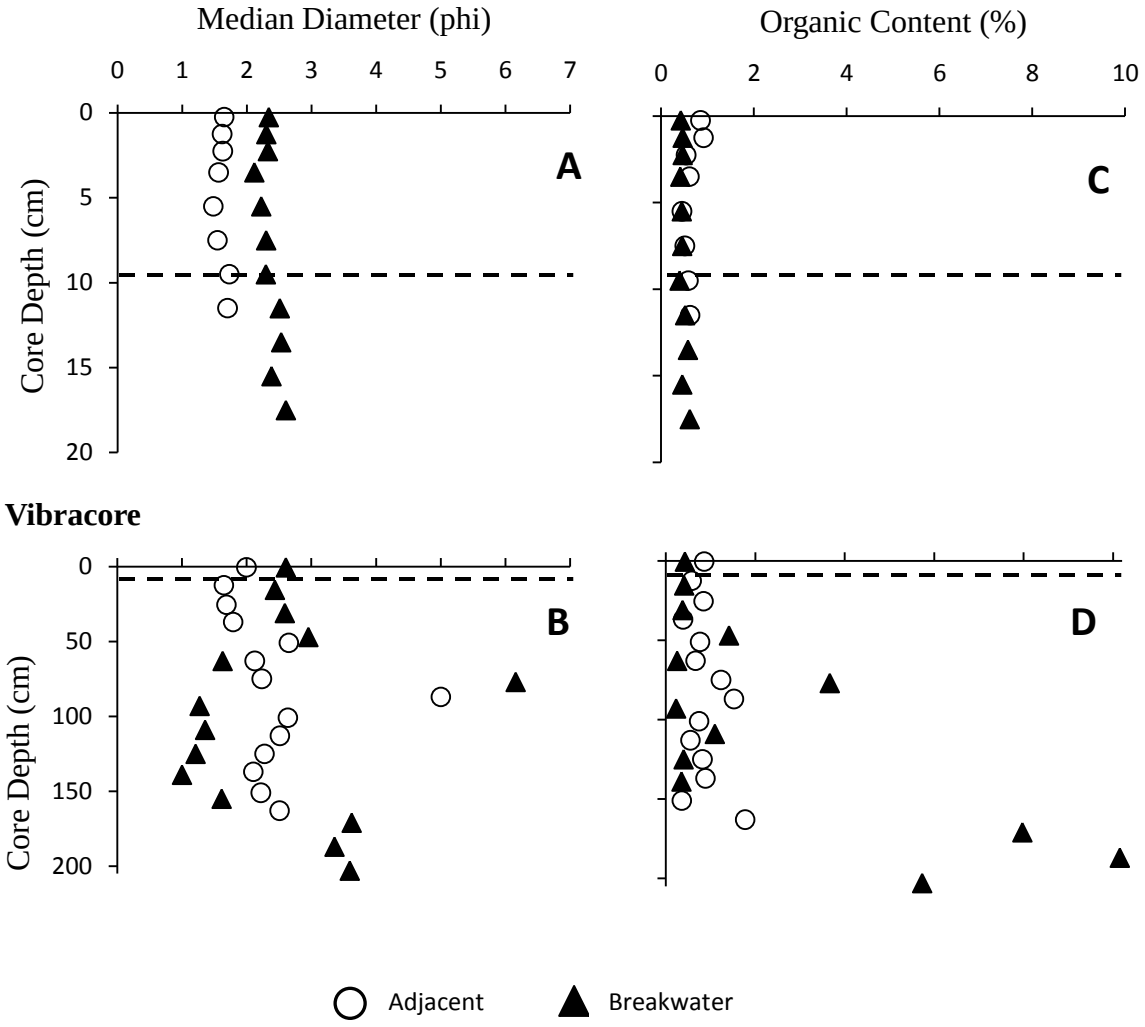

Figure HMI2. Sediment grain size (median diameter) collected with a push core (A) or vibracore (B) at the adjacent-exposed (open circles) and breakwater-protected (closed triangles) sites. Sediment organic content collected with a push core (C) or vibracore (D) at the adjacent-exposed and breakwater-protected sites. The dashed line represents the interpreted depth of breakwater appearance; it is absent in the push-core profiles as the entire profile represents post-construction sedimentation.

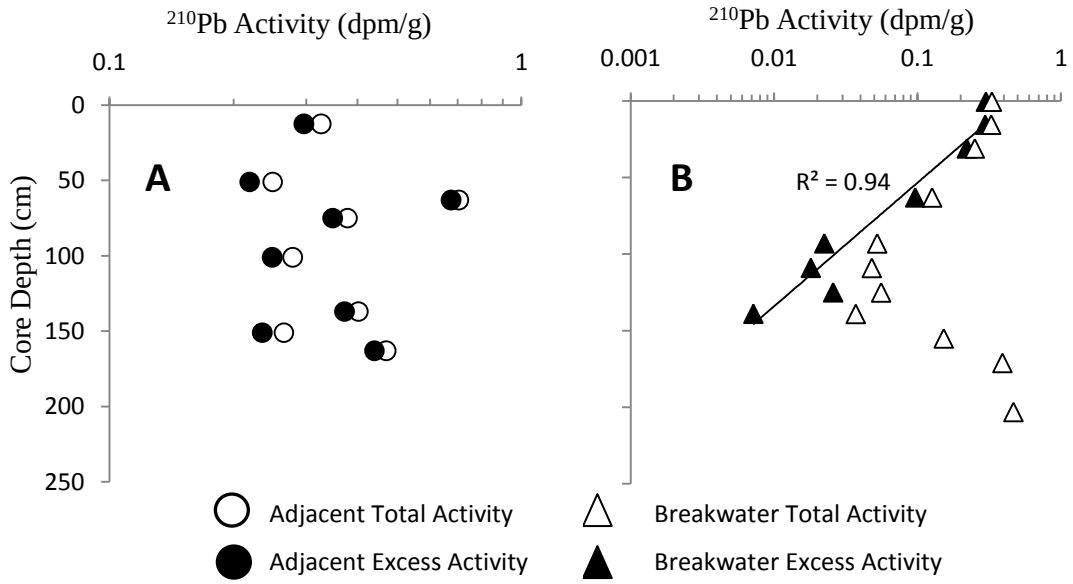

Figure HMI3. ^{210}Pb profiles at the adjacent-exposed (A) and breakwater-protected (B) sites. The calculated sediment accumulation rate is >1.6 cm/y at the adjacent-exposed site and 0.9 cm/y at the breakwater-protected site. The accumulation rate for the adjacent-exposed site is a minimum estimate, due to variable activity with depth. Note that the latter represents the pre-construction sedimentation rate. Also note that the x-axis scale differs between plots for visual clarity.

Summary of sediment data:

Surficial (upper 10 cm) sediment at the adjacent-exposed site has an average median diameter of 1.6±0.03 phi (329.9 µm) and average organic content of 0.6±0.1%. At the breakwater-protected site, surficial sediment is finer ($p < 0.0001$), with an average median diameter of 2.3±0.03 phi (203.1 µm), with similar average organic content (0.4±0.02%; $p = 0.01$). The depth of breakwater influence is inferred from an apparent decrease in vibracore sediments at 31 cm.

Sediment accumulation at the adjacent-exposed site likely occurs in pulses, evidenced by the non-steady-state nature of the ^{210}Pb profile. The calculated accumulation rate is a minimum estimate, determined by noting the presence of excess ^{210}Pb activity (sediment <100 y old) at the base of the core. In contrast, sedimentation at the breakwater-protected site is more constant and activities decrease logarithmically with depth. The pre-construction rate, calculated from the best-fit trendline, is 0.9 cm/y. The post-construction rate is 3.1 cm/y, calculated by dividing the depth of influence (31 cm) by the breakwater age (10 y).

SAV Data:

Table HMI2. Characteristics of SAV *Potamogeton perfoliatus, Vallisneria americana, Myriophyllum spicatum,* and *Zannichellia palustris* growing at the adjacent-exposed and breakwater-protected sites, values are reported as mean ±SE.

Location	Species	Shoot Length (cm)	Root Length (cm)	Above-ground Biomass (g m^{-2})	Below-ground Biomass (g m^{-2})	Total Biomass (g m^{-2})	Ratio Above-/ Below-ground Biomass
Adjacent-exposed	*Potamogeton perfoliatus*	77.2± 1.7	6.4± 0.2	1627.3± 173.3	23.6± 4.2	1650.9± 172.0	82.8± 23.3
Breakwater-protected	*Potamogeton perfoliatus*	67.3± 2.9	6.0± 0.1	999.5± 36.5	15.2± 3.3	1014.7± 35.5	77.5± 13.9
Adjacent-exposed	*Vallisneria americana*	16.7± 2.1	5.6± 0.2	10.3± 3.6	3.8± 1.1	14.1± 4.1	3.1± 1.0
Breakwater-protected	*Vallisneria americana*	29.3± 3.8	5.3± 0.3	15.6± 13.9	3.9± 0.7	18.2± 14.9	5.0± 4.6
Adjacent-exposed	*Myriophyllum spicatum*	n/a	3.3± 0.7	1.3± 0.4	0.03± 0.03	1.3± 0.4	15.0
Breakwater-protected	*Myriophyllum spicatum*	13.5	4.7± 0.4	17.1± 0.8	0.7	17.4± 1.2	26.8
Adjacent-exposed	*Zannichellia palustris*	n/a	n/a	0.2± 0.1	0.28	0.4± 0.2	1.0
Breakwater-protected	*Zannichellia palustris*	n/a	n/a	2.2± 1.3	0	2.2± 1.3	0

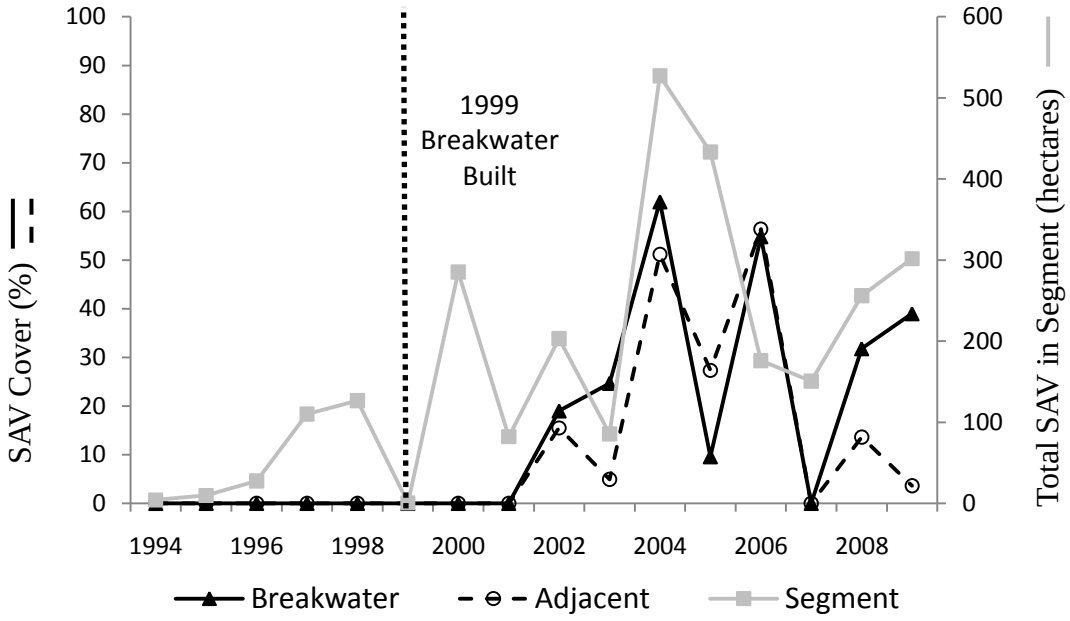

Figure HMI4. SAV % cover plotted against the total SAV in the bay segment as determined by VIMS aerial photography from 5 years prior to breakwater installation to present day.

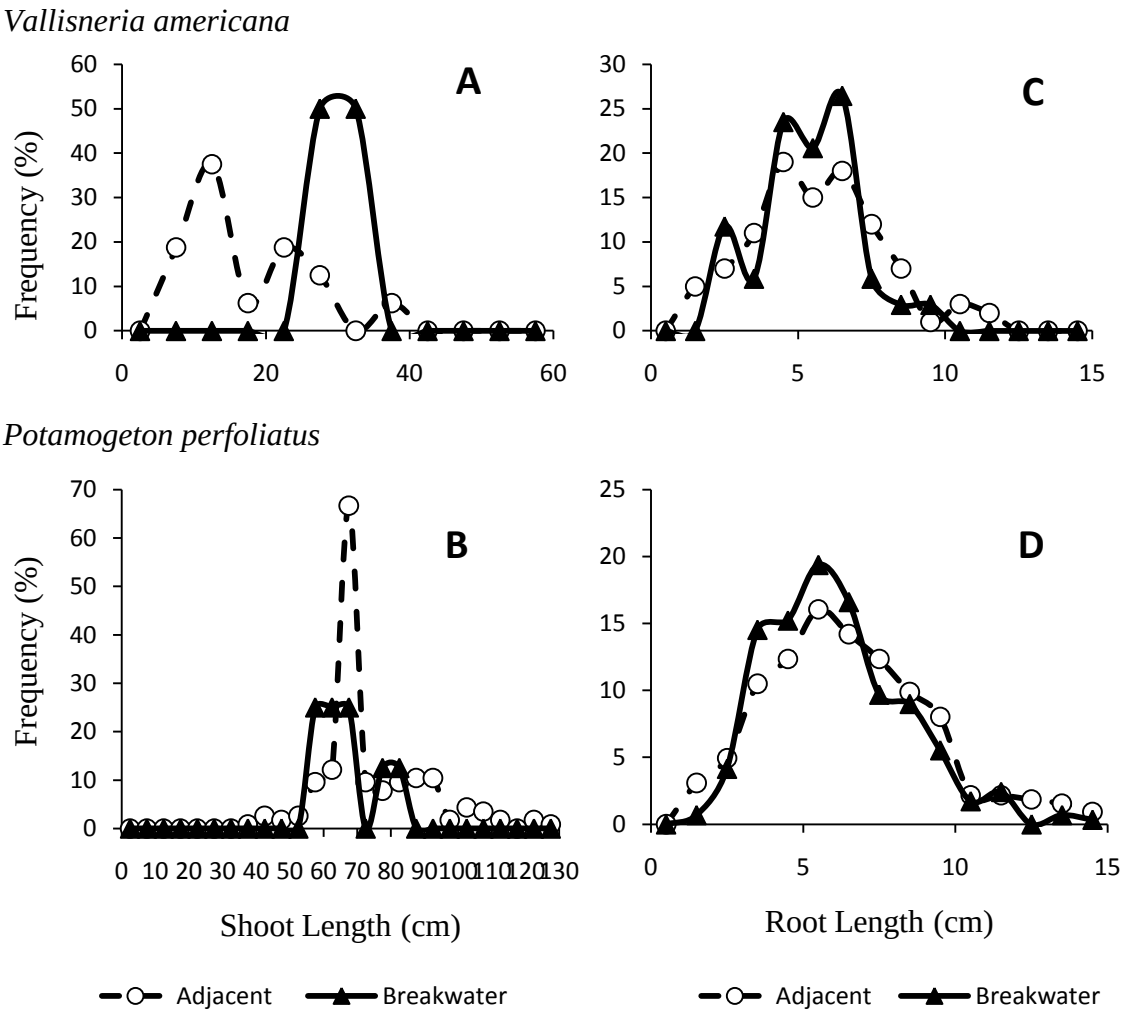

Figure HMI5. (A) Shoot- and (C) root-length frequency plots for *Vallisneria americana* and (B) shoot- and (D) root-length frequency plots for *Potamogeton perfoliatus* at the adjacent-exposed (open circles) and breakwater-protected (closed triangle) sites.

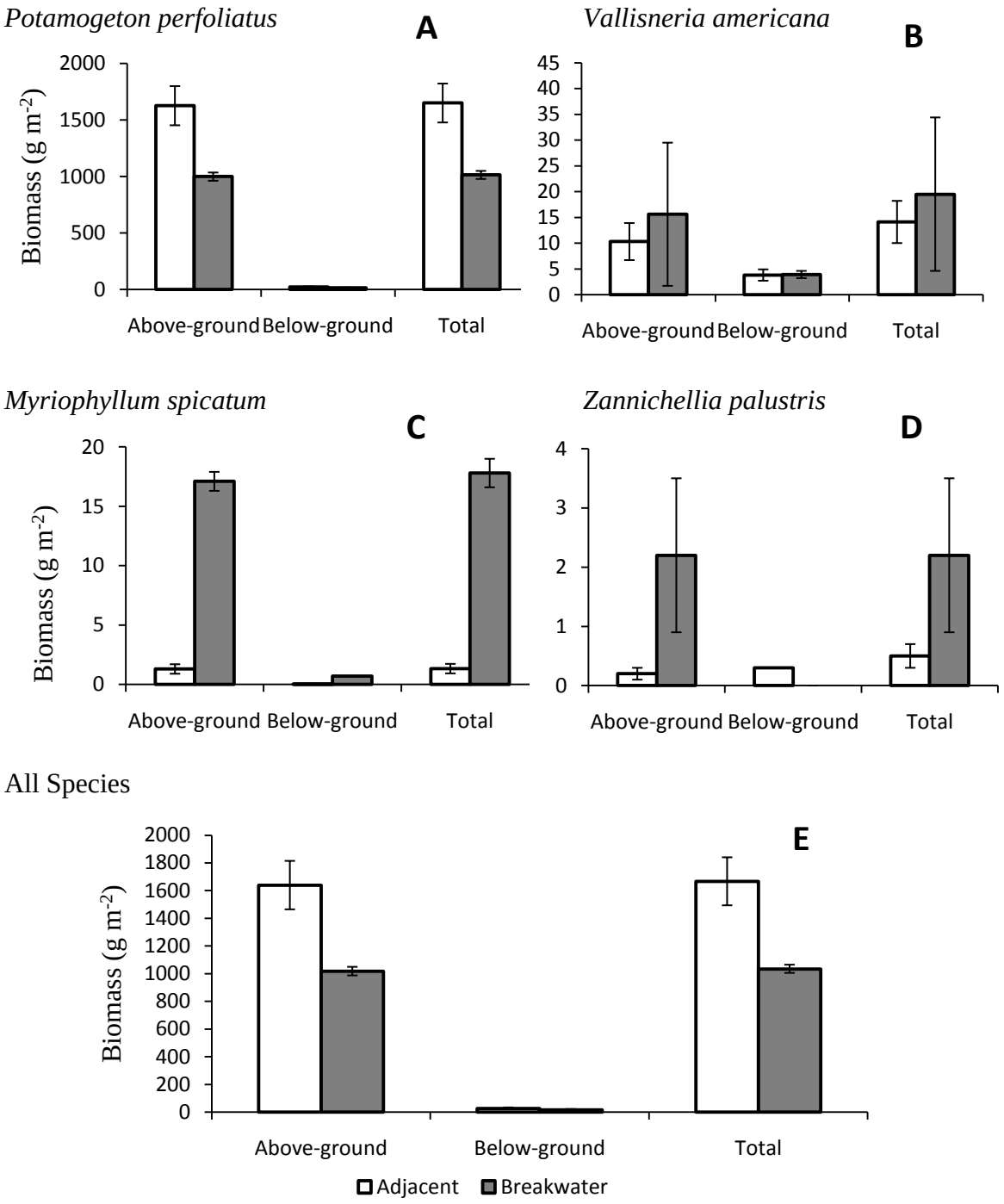

Figure HMI6. Biomass of the SAV (A) *Potamogeton perfoliatus*, (B) *Vallisneria americana*, (C) *Myriophyllum spicatum*, (D) *Zannichellia palustris*, and (E) all species of SAV at the adjacent-exposed (open bars) and breakwater-protected (closed bars) sites.

Summary of SAV data:

SAV abundance in the segment containing the Hart-Miller Island site generally increased over the observation period. At Hart-Miller, SAV also increased both in the adjacent site and the breakwater site starting 2 years post breakwater construction. Both the breakwater and adjacent sites mirror the segment totals fairly closely throughout the observation period, and % cover is similar regardless of whether or not the site sampled was protected (Figure HMI4).

Of the 4 SAV species observed at Hart-Miller Island *Potamogeton perfoliatus* is the only species to have longer shoots ($p= 0.13$) and more biomass at the adjacent-exposed site than the breakwater-protected (Table HMI2). This was the dominant species growing in the area and so when all species are combined biomass data shows that there is greater ($p= 0.81$) total biomass at the adjacent-exposed site (Figure HMI6). *V. americana* had longer shoots (sample size is too small for statistical analysis) at the breakwater-protected site than the adjacent-exposed (Figure HMI5). *P. perfoliatus* root lengths are not significantly different ($p = 0.20$) between the adjacent-exposed and breakwater sites, neither is *V. americana* roots ($p = 0.60$).

Breakwater influence on SAV is species-specific as is illustrated at Hart-Miller Island. Careful evaluation of local SAV populations should be conducted before construction of a breakwater, as to increase the success of SAV survival.

Sue Creek

Description: This semi-circular, segmented, rock-mound breakwater has 5 segments, 2 of which are attached to land. The total breakwater length is 45.6 m, with segment lengths 9±2 m (mean ± SD) and gap lengths 7±0.5 m. Average distance from shore is 5±0.4 m. This breakwater protects a forested shoreline. The adjacent-exposed site is also a forested shoreline.

Year of Construction: 1994 **Age at Sampling:** 15 years

Salinity Regime: Oligohaline

Fetch: Adjacent: 0.1±0.01 km

Breakwater: 0.1±0.1 km

Sampling Coordinates:

SUE A vbc	39º17'05.5"	76º24'59.5"
SUE A pc	39º17'05.5"	76º24'59.5"
SUE B vbc	39º17'04.4"	76º24'59.6"
SUE B pc	39º17'04.4"	76º24'59.6"
SAV A1	39º17'05.4"	76º24'59.5"
SAV A2	39º17'05.9"	76º24'59.3"
SAV A3	39º17'05.2"	76º24'59.4"
SAV A4	39º17'05.5"	76º24'59.4"
SAV A5	39º17'04.9"	76º24'59.2"
SAV B1	39º17'04.1"	76º24'59.9"
SAV B2	39º17'02.7"	76º24'59.9"
SAV B3	39º17'03.9"	76º24'59.1"
SAV B4	39º17'04.7"	76º24'59.4"
SAV B5	39º17'04.7"	76º24'59.3"

Table SUE1. Latitude and longitude of vibracores (vbc), pushcores (pc), and SAV cores taken in the adjacent-exposed ("A") and breakwater-protected ("B") Sites at Sue Creek.

Figure SUE1. Aerial photo of the breakwater at Sue Creek, MD.

Sediment Data:

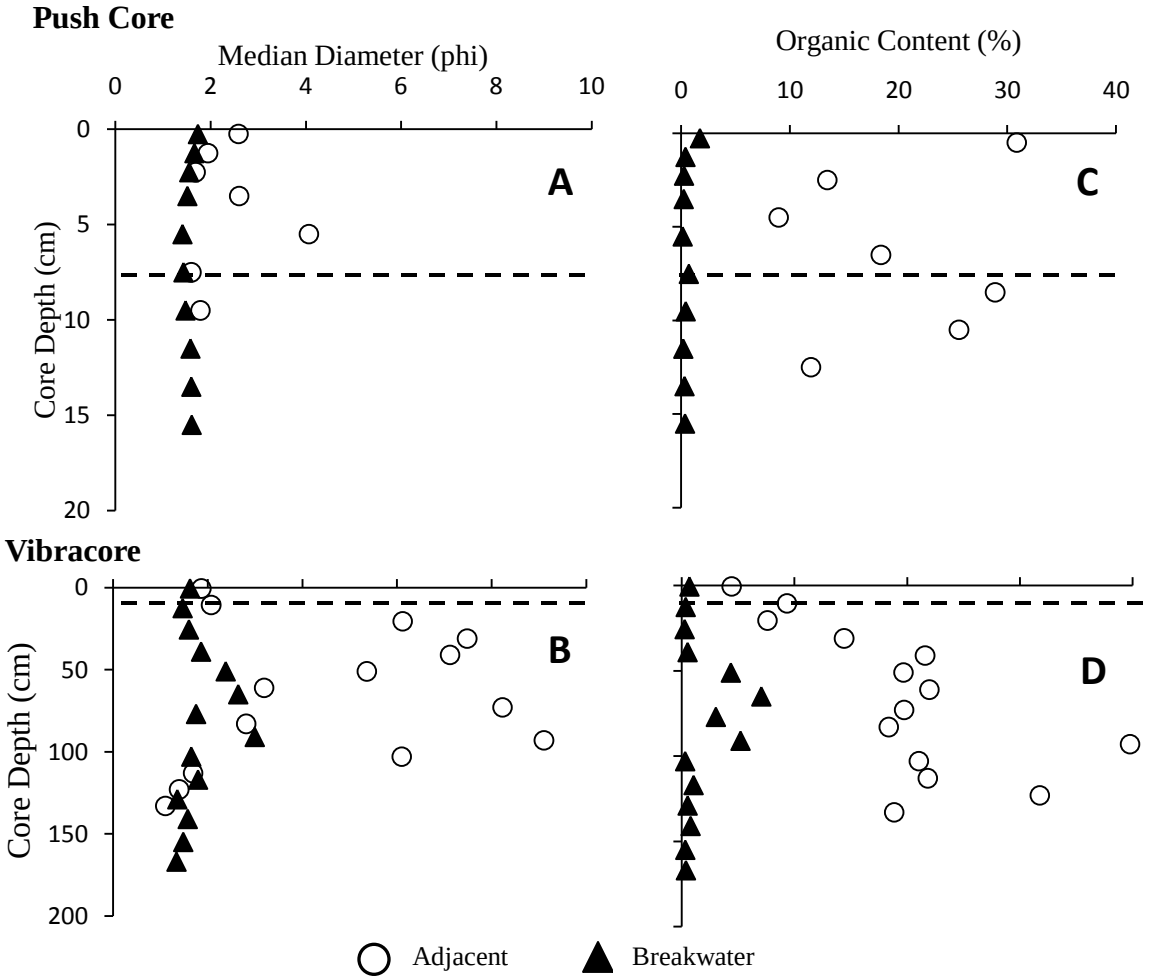

Figure SUE2. Sediment grain size (median diameter) collected with a push core (A) or vibracore (B) at the adjacent-exposed (open circles) and breakwater-protected (closed triangles) sites. Sediment organic content collected with a push core (C) or vibracore (D) at the adjacent-exposed and breakwater-protected sites. The dashed line represents the interpreted depth of breakwater appearance (8 cm).

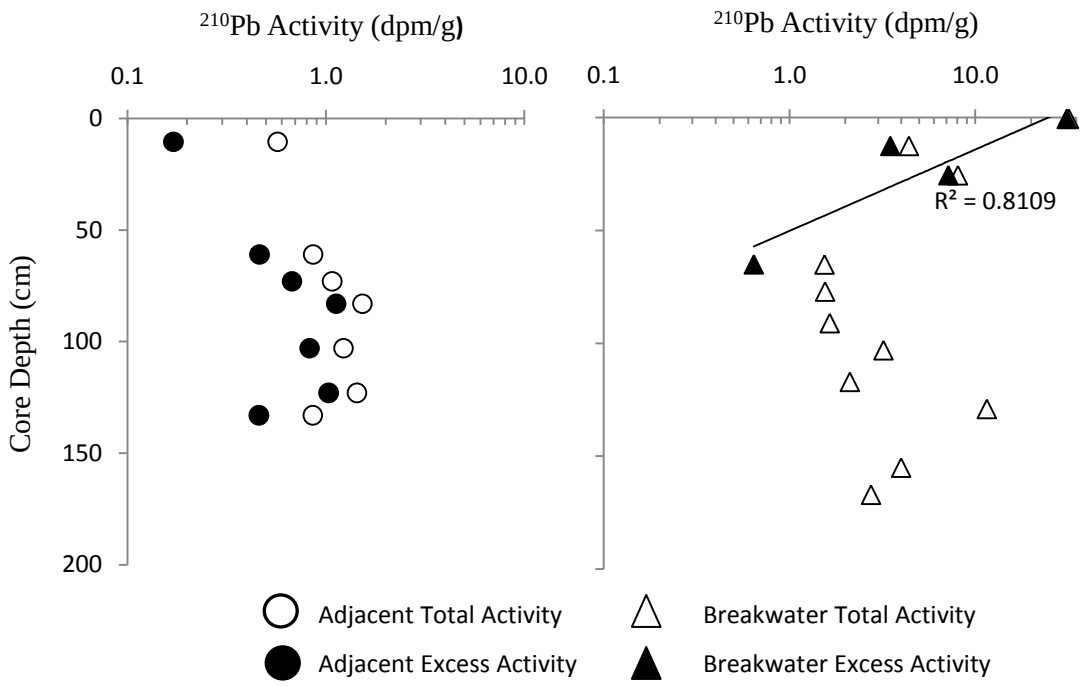

Figure SUE3. ^{210}Pb profiles at the adjacent-exposed (A) and breakwater-protected (B) sites. Activities at both sites have been normalized to the mud content to remove the effect of grain-size variations. At the adjacent-exposed site, normalized activities increase with depth to ~100 cm, and then are relatively uniform. A minimum rate of >1.5 cm/y can be calculated for this core. At the breakwater-protected site, normalized activities decrease logarithmically with depth and an accumulation rate of 0.5 cm/y can be calculated.

Summary of sediment data:

Surficial sediment (upper 10 cm) at the adjacent-exposed site is finer ($p = 0.02$) and more organic ($p < 0.0001$) than at the breakwater-protected site. The adjacent-exposed site has an average median diameter of 2.3±0.4 phi (203.1 µm) and an average organic content of 20.1±3.6%. Surficial sediment at the breakwater-protected site has an

average median diameter of 1.5±0.1 phi (353.6 µm) and an average organic content of 0.6±0.2%.

^{210}Pb activities at both sites are normalized to the mud content to remove the effect of grain-size variations. At the adjacent-exposed site, normalized activities increase to ~100 cm then are fairly uniform. Only a minimum accumulation rate can be calculated at this site and is >1.5 cm/y. At the breakwater-protected site, normalized activities decrease logarithmically with depth and the calculated accumulation rate is 0.5 cm/y, representing the pre-construction sedimentation rate.

At the breakwater-protected site, there is no obvious change in either the grain-size or organic-content vibracore profile. It is assumed that there is also no significant change in the sedimentation rate, and so the post-construction rate would be equal to the pre-construction rate. If the post-construction rate (0.5 cm/y) is applied to the breakwater age (15 y), then the depth of breakwater influence is 8 cm.

SAV Data:

Table SUE2. Characteristics of the SAV *Myriophyllum spicatum* and *Vallisneria americana* growing at the adjacent-exposed and breakwater-protected sites, values are reported as mean ±SE.

Location	Species	Shoot Length (cm)	Root Length (cm)	Above-ground Biomass ($g\ m^{-2}$)	Below-ground Biomass ($g\ m^{-2}$)	Total Biomass ($g\ m^{-2}$)	Ratio Above-/ Below-ground Biomass
Adjacent-exposed	*Myriophyllum spicatum*	54.2± 3.21	12.1± 0.3	386.2± 114.3	14.8± 4.7	401.1± 118.8	27.0± 6.8
Breakwater-protected	*Myriophyllum spicatum*	68.9± 5.4	12.6± 0.4	569.8± 182.7	10.3± 3.2	580.1±1 82.0	99.6± 61.8
Adjacent-exposed	*Vallisneria americana*	37.5± 2.6	6.4± 0.3	65.7± 7.2	5.9± 2.4	71.6± 4.8	13.8± 6.7
Breakwater-protected	*Vallisneria americana*	44.2± 2.7	4.2± 1.2	45.7	1.0	46.7	45.7

Vallisneria americana

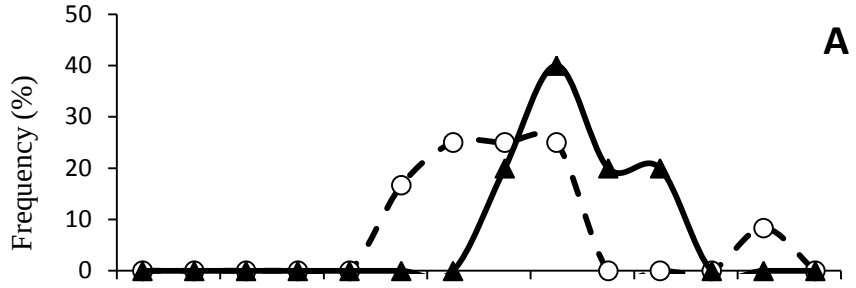

Myriophyllum spicatum

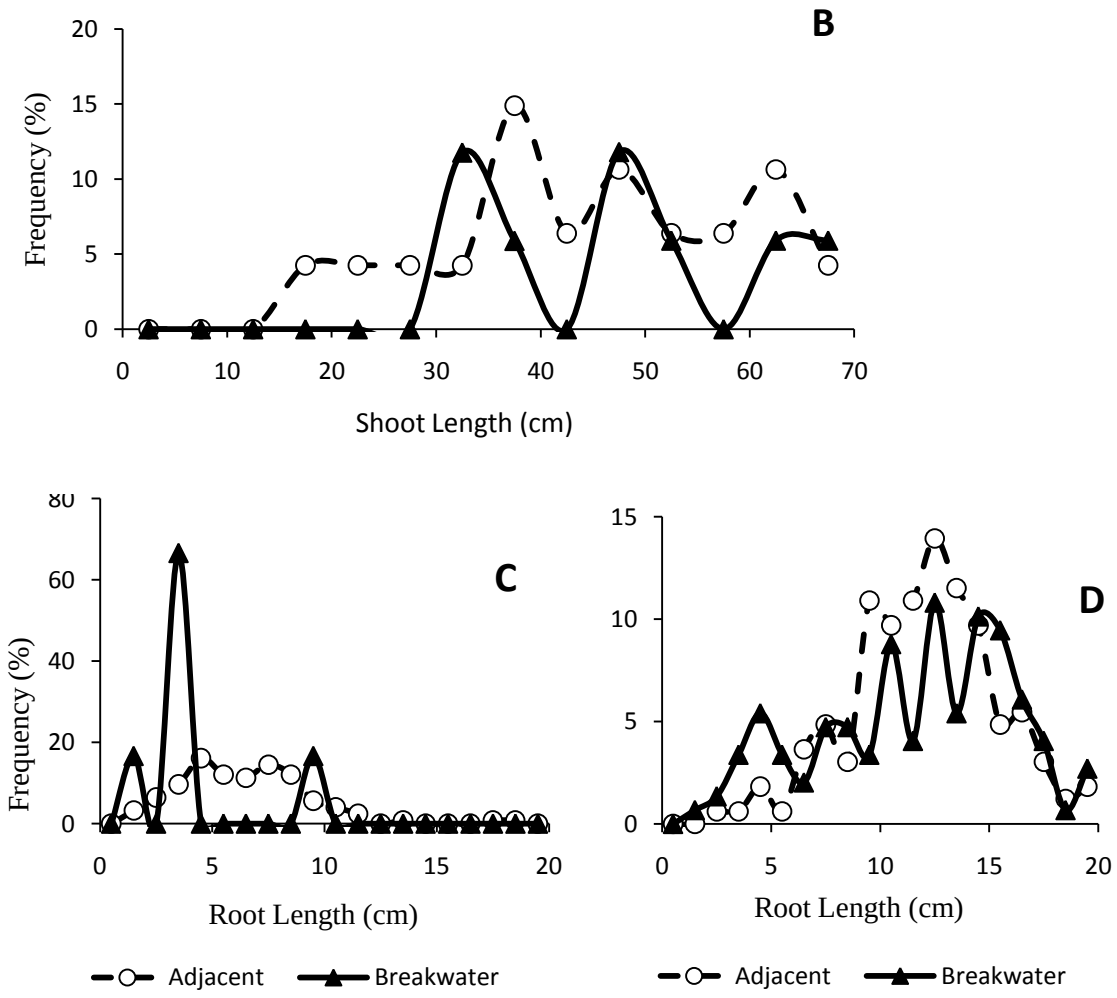

Figure SUE5. (A) Shoot- and (C) root-length frequency plots for *Vallisneria americana* and (B) shoot- and (D) root-length frequency plots for *Myriophyllum spicatum* at the adjacent-exposed (open circles) and breakwater-protected (closed triangle) sites.

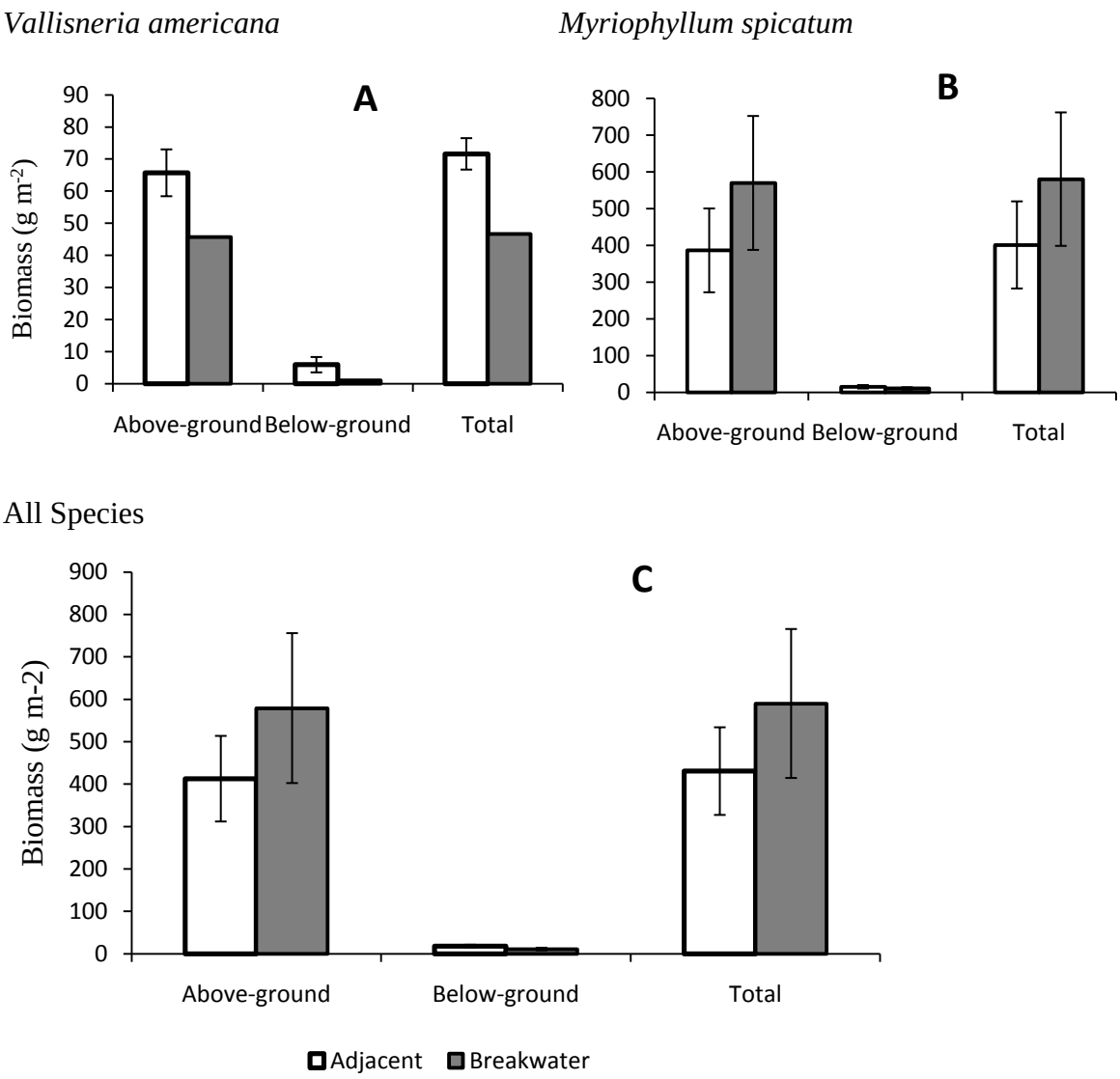

Figure SUE6. Biomass of the SAV (A) Vallisneria americana, (B) Myriophyllum spicatum, and (C) all species of SAV at the adjacent-exposed (open bars) and breakwater-protected (closed bars) sites.

Summary of SAV data:

SAV total biomass was similar (p= 0.46) at the adjacent-exposed and breakwater-protected sites. *M. spicatum* shoots are longer (p = 0.02) at the breakwater-protected site

than at the adjacent-exposed site, however root lengths of this species are not different ($p = 0.32$) between sites. *V. americana* shoot lengths are similar ($p = 0.10$) at the adjacent-exposed and breakwater-protected sites. Unlike *M. spicatum*, roots were significantly longer ($p = 0.02$) at the adjacent-exposed site. This illustrates that SAV response to sediments and the presence of a breakwater are species-specific and can differ between them.

Red Eyed Yacht Club

Description: This semi-circular, segmented, rock-mound breakwater has 6 segments which are parallel to a curved shoreline. The total breakwater length is 85.2 m, with segment lengths 13±1 m (mean ± SD) and gap length 9±1 m. Average distance from shore is 8±1 m. This breakwater protects a forested shoreline.

Year of Construction: 1994 **Age at Sampling:** 15 years

Salinity Regime: Oligohaline

Fetch: Adjacent: 0.2±0.1 km

Breakwater: 0.2±0.1 km

Sampling Coordinates:

REYC A vbc	39º17'09.5"N	76º24'49.9"W
REYC A pc	39º17'09.5"N	76º24'49.9"W
REYC B vbc	39º17'09.6"N	76º24'49.4"W
REYC B pc	39º17'09.6"N	76º24'49.4"W
REYC B pc	39º17'09.6"N	76º24'49.4"W
SAV A1	39º17'09.1"N	76º24'49.4"W
SAV A2	39º17'09.2"N	76º24'49.5"W
SAV A3	39º17'09.4"N	76º24'49.4"W
SAV A4	39º17'09.2"N	76º24'49.8"W
SAV A5	39º17'09.5"N	76º24'49.7"W
SAV B1	39º17'06.5"N	76º24'49.6"W
SAV B2	39º17'06.4"N	76º24'49.6"W
SAV B3	39º17'06.4"N	76º24'49.3"W
SAV B4	39º17'06.8"N	76º24'48.8"W
SAV B5	39º17'06.9"N	76º24'48.7"W

Table REYC1. Latitude and longitude of vibracores (vbc), pushcores (pc), and SAV cores taken in the adjacent-exposed ("A") and breakwater-protected ("B") sites at Red Eyed Yacht Club.

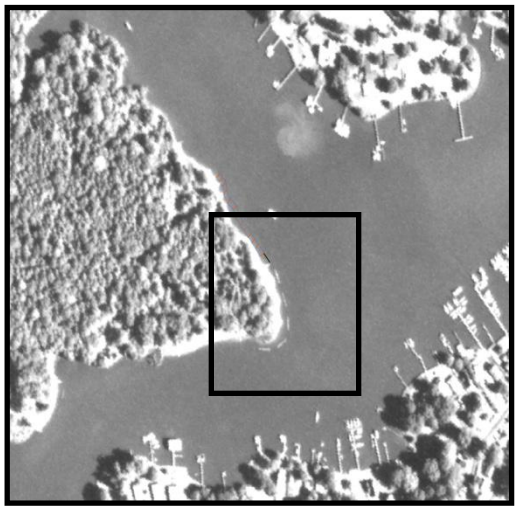

Figure REYC1. Aerial photo of the breakwater at Red Eyed Yacht Club, MD.

Sediment Data:

Push Core

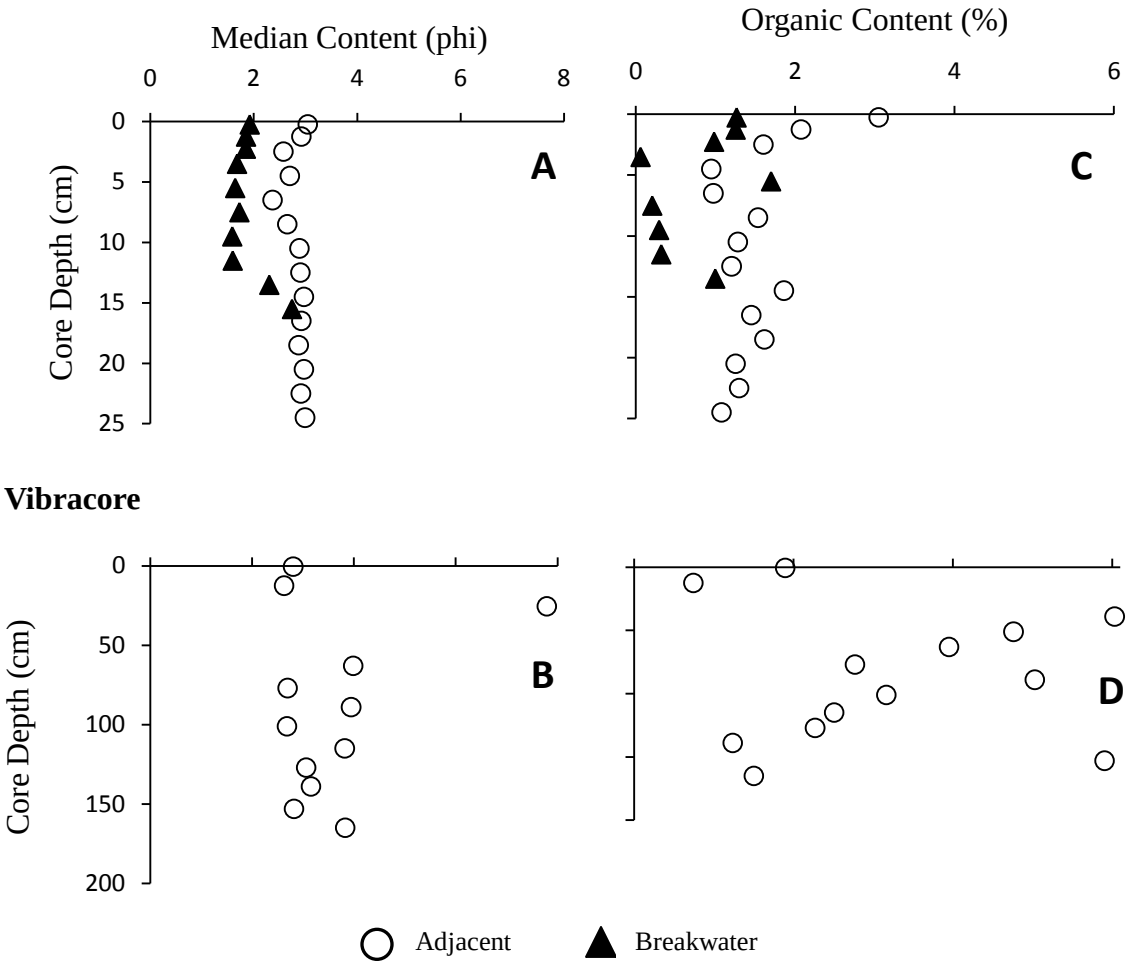

Figure REYC2. Sediment grain size (median diameter) collected with a push core (A) or vibracore (B) at the adjacent-exposed (open circles) and breakwater-protected (closed triangles) sites. Sediment organic content collected with a push core (C) or vibracore (D) at the adjacent-exposed and breakwater-protected sites. The dashed line represents the interpreted depth of breakwater appearance (16 cm). A vibracore was not collected at the breakwater-protected site

Summary of sediment data

Surficial sediment (upper 10 cm) at the adjacent-exposed site are finer ($p < 0.0001$) and more organic ($p = 0.03$) than those at the breakwater-protected site. The adjacent-exposed site has an average median diameter of 2.7±0.1 phi (153.9 μm) and an average organic content of 1.7±0.3%. Surficial sediment at the breakwater-protected site has an average median diameter of 1.7±0.1 phi (307.8 μm) and an average organic content of 0.9±0.2%.

A vibracore was not collected at the breakwater-protected site, precluding ^{210}Pb analyses. ^{210}Pb was also not measured at the adjacent-exposed site.

The vibracore at the breakwater-protected site was prevented by the presence of impenetrable landscaping fabric. This fabric was likely emplaced when the breakwater was installed, thus providing a baseline from which to measure post-construction sedimentation. The push core captured 16 cm of sediment on top of the fabric, providing the depth of breakwater influence. The pre-construction accumulation rate can be derived by dividing this depth by the breakwater age (15 y) and is 1.1 cm/y. Because a vibracore was not collected at the breakwater-protected site, and so pre-construction sediments were not sampled, potential changes in sediment character or accumulation rate due to the breakwater cannot be determined.

SAV Data:

Table REYC2. Characteristics of the SAV *Myriophyllum spicatum* growing at the adjacent-exposed and breakwater-protected sites, values are reported as mean ±SE.

Location	Species	Shoot Length (cm)	Root Length (cm)	Above-ground Biomass (g m^{-2})	Below-ground Biomass (g m^{-2})	Total Biomass (g m^{-2})	Ratio Above-/ Below-ground Biomass
Adjacent-exposed	*Myriophyllum spicatum*	58.1± 8.7	12.2± 0.6	632.1± 96.3	10.0± 2.5	642.1± 96.3	153.3± 97.1
Breakwater-protected	*Myriophyllum spicatum*	33.5± 3.5	11.1± 0.3	257.1± 109.7	15.7± 1.5	272.8± 110.5	15.3± 6.3

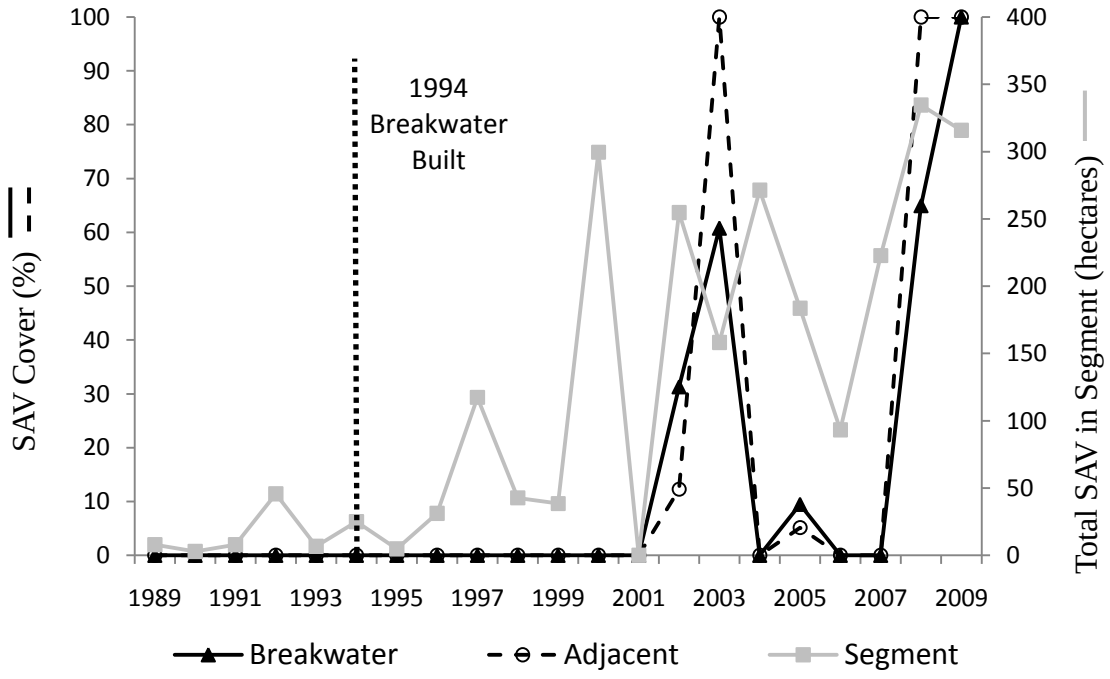

Figure REYC4. SAV % cover plotted against the total SAV in the bay segment as determined by VIMS aerial photography from 5 years prior to breakwater installation to present day.

Myriophyllum spicatum

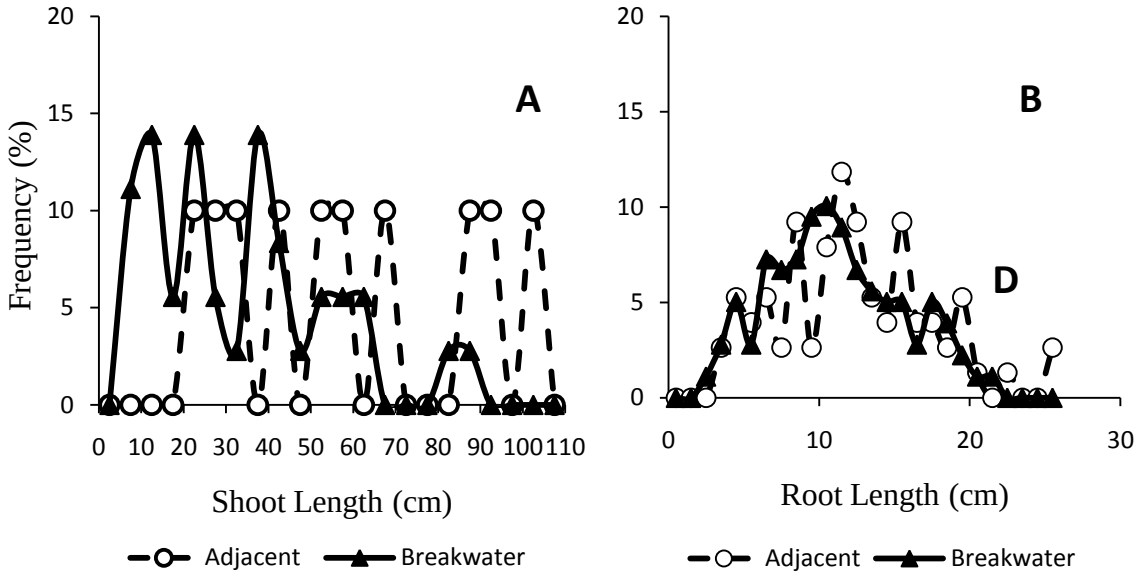

Figure REYC5. (A) Shoot- and (B) root-length frequency plots for *Myriophyllum spicatum* at the adjacent-exposed (open circles) and breakwater-protected (closed triangle) sites.

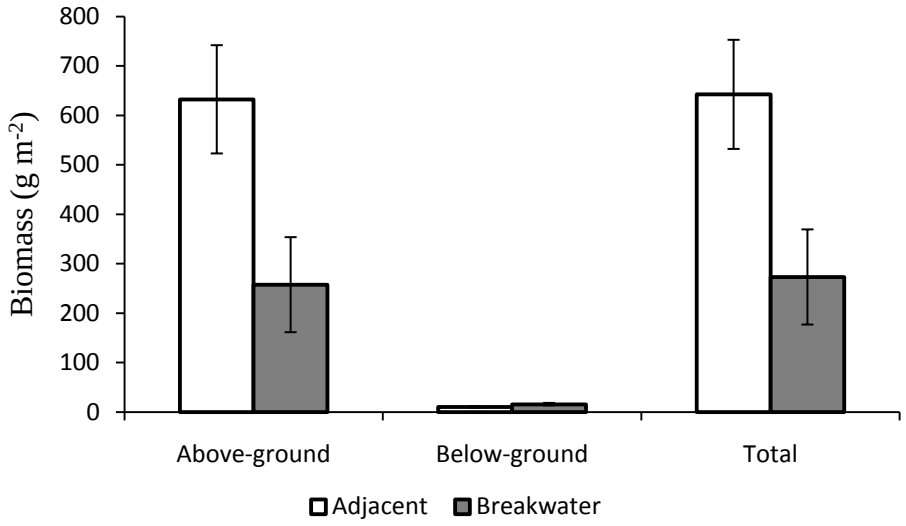

Figure REYC6. Biomass of the SAV *Myriophyllum spicatum* at the adjacent-exposed (open bars) and breakwater-protected (closed bars) sites.

Summary of SAV data:

SAV abundance in the segment containing the Red Eyed Yacht Club site generally increased over the observation period. At Red Eyed Yacht Club, SAV % cover also increased both in the adjacent site and the breakwater site starting 7 years after the breakwater was built. Both the breakwater and adjacent sites mirror the segment totals and are fairly similar to each other throughout the observation period.

M. spicatum total biomass is greater ($p = 0.04$) at the adjacent-exposed site than at the breakwater-protected. Shoot length was longer ($p = 0.01$) at the adjacent-exposed site as well, although root lengths between sites did not differ ($p = 0.08$).

Taylors Island

Description: The breakwater at Taylors Island is a linear, segmented, rock-mound structure measuring 395.7 m in length. It consists of 6 segments, with an average segment length of 36±1 m (mean ± SD) and an average gap length of 40±26 m. The largest gap is located in the middle with 3 segments on either side. The breakwater protects a marsh and is 161±57 m offshore. The adjacent-exposed shoreline is also a marsh.

Year of Construction: 2008 **Age at Sampling:** 1 year

Location: Mesohaline

Fetch: Adjacent: 7.4±1.9 km

Breakwater: 11.6±4.5 km

Sampling Coordinates:

TAY A vbc	38º25'13.5"N	76º17'08.2"W
TAY A pc	38º25'13.5"N	76º17'08.2"W
TAY B vbc	38º25'24.8"N	76º17'24.8"W
TAY B pc	38º25'24.8"N	76º17'24.8"W
No SAV		

Table TAY1. Latitude and longitude of vibracores (vbc), pushcores (pc), and SAV cores taken in the adjacent-exposed ("A") and breakwater-protected ("B") sites at Taylors Island.

Figure TAY1. Aerial photograph of the breakwater at Taylors Island, MD.

Sediment data:

Push core

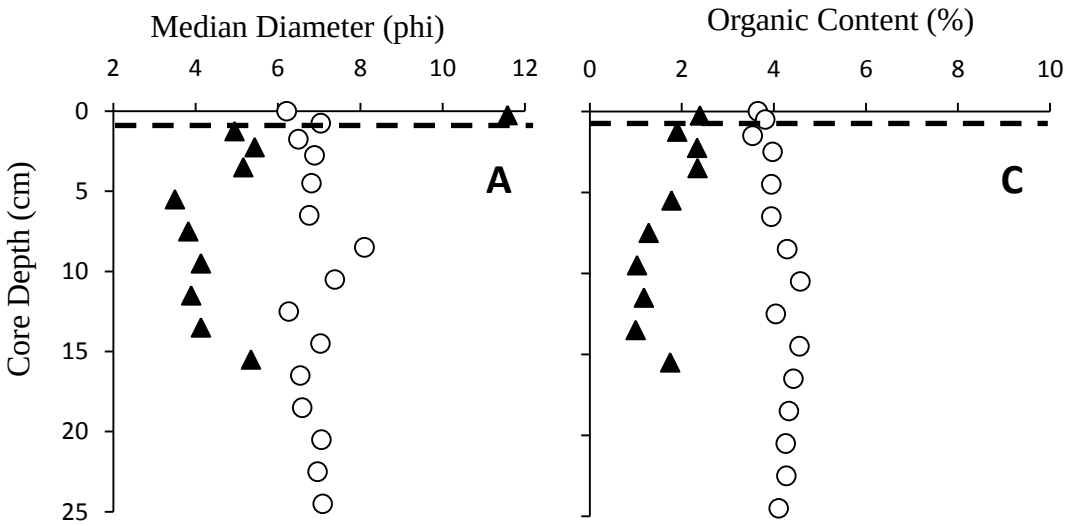

Vibracore

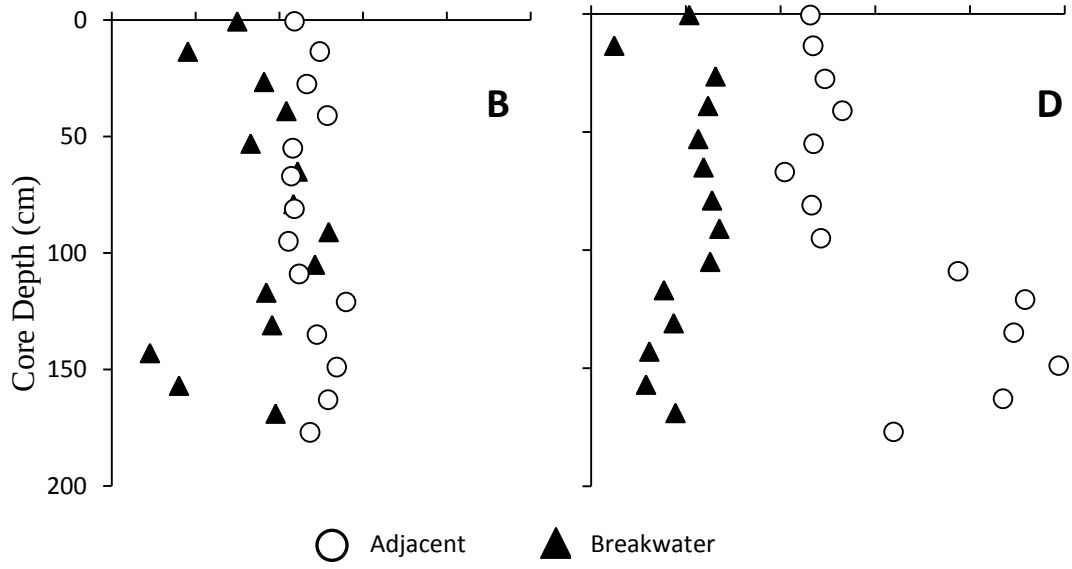

Figure TAY2. Sediment grain size (median diameter) collected with a push core (A) or vibracore (B) at the adjacent-exposed (open circles) and breakwater-protected (closed triangles) sites. Sediment organic content collected with a push core (C) or vibracore (D) at the adjacent-exposed and breakwater-protected sites. The dashed line represents the interpreted depth of breakwater appearance (1 cm).

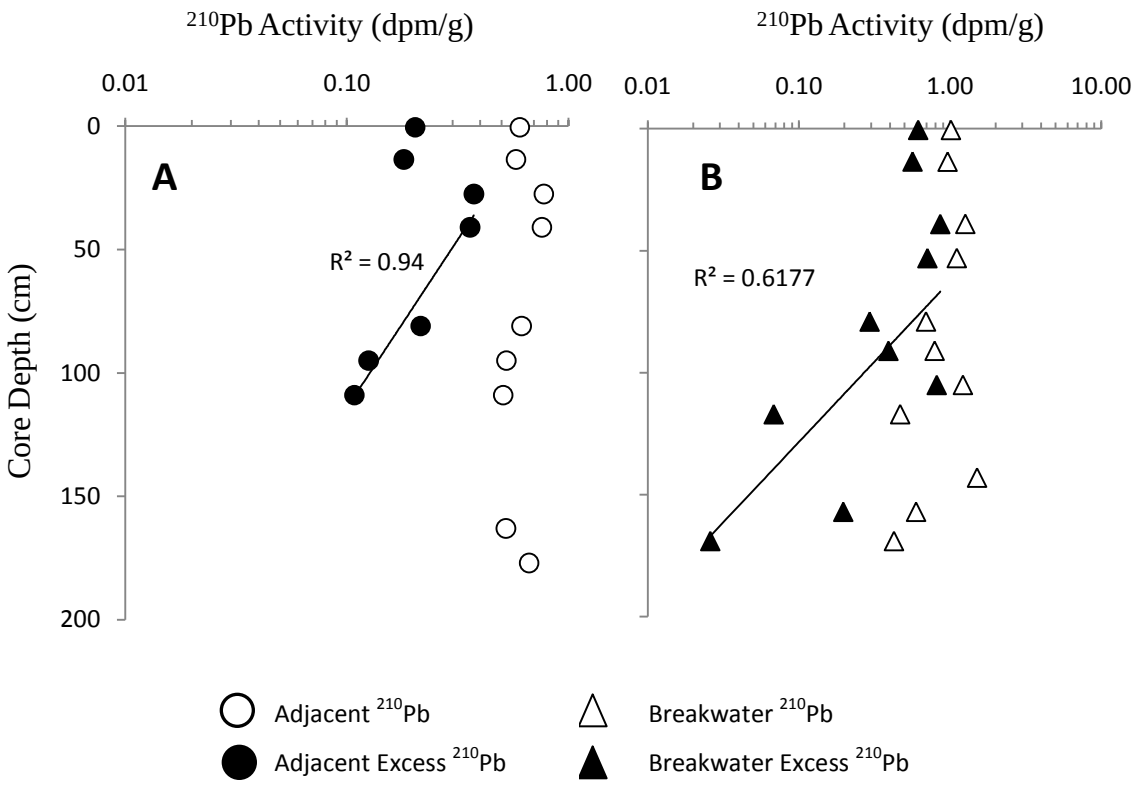

Figure TAY3. ^{210}Pb profiles at the adjacent-exposed (A) and breakwater-protected (B) sites. Excess activities at both sites decrease logarithmically with depth, indicating steady-state sedimentation. The calculated sediment accumulation rate is 2.0 cm/y at the adjacent-exposed site and 1.4 cm/y at the breakwater-protected site.

Summary of sediment data

There was no significant difference ($p = 0.07$) between the adjacent-exposed average median diameter of surficial (upper 10 cm) sediment (6.9±0.2 phi, 8.4 µm) and the breakwater-protected (5.5±1.1 phi, 22.1 µm). Average organic content of surficial sediment was significantly higher ($p < 0.0001$) at the adjacent-exposed site than at the breakwater-protected site, 3.9±0.1% and 1.9±0.2%, respectively.

Excess ^{210}Pb activities decrease logarithmically with depth and the calculated accumulation rate is 2.0 cm/y at the adjacent-exposed site and 1.4 cm/y at the breakwater-protected site. The latter represents the pre-construction sedimentation rate.

Sediment in the upper 1 cm of the breakwater-protected push-core grain-size profile is much finer than the rest of the core, indicating sedimentation since breakwater construction. With an interpreted depth of breakwater influence of 1 cm, the post-construction sedimentation rate is 1 cm/y. However, because this breakwater is very young, the post-construction rate should be used with caution.

SAV Data:

No SAV was present at the adjacent-exposed or breakwater-protected sites.

Tangier Island

Description: This linear, segmented, rock-mound breakwater has 2 segments which are parallel to the shoreline. The total breakwater length is 95.3 m, with segment lengths 31±1 m (mean ± SD) and gap length 31 m (only 1 gap). Average distance from shore is 24±1 m. This breakwater protects a retreating marsh covered by a layer of sand. The shoreline at the adjacent-exposed shoreline was also marsh covered with a layer of sand.

Year of Construction: 2007 **Age at Sampling:** 2 years

Salinity Regime: Mesohaline

Fetch: Adjacent: 7.8±2.0 km

Breakwater: 12.0±3.2 km

Sampling Coordinates:

TAN A vbc	37º50'04.0"	75º58'38.9"
TAN A pc	37º50'04.0"	75º58'38.9"
TAN B vbc	37º50'05.8"	75º58'43.2"
TAN B pc	37º50'05.8"	75º58'43.2"
SAV A	None	
SAV B1	37º50'05.6"	75º58'42.5"
SAV B2	37º50'05.0"	75º58'40.6"
SAV B3	37º50'05.9"	75º58'43.1"
SAV B4	37º50'05.5"	75º58'42.6"
SAV B5	37º50'05.4"	75º58'42.5"

Table TAN1. Latitude and longitude of vibracores (vbc), pushcores (pc), and SAV cores taken in the adjacent-exposed ("A") and breakwater-protected ("B") sites at Tangier Island. Note that SAV cores were not collected at the adjacent-exposed site, as SAV was not present at this site in 2009.

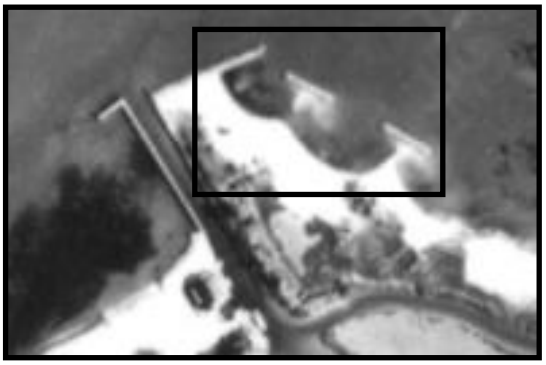

Figure TAN1. Aerial photo of the breakwater at Tangier Island, VA.

Sediment Data:

Push Core

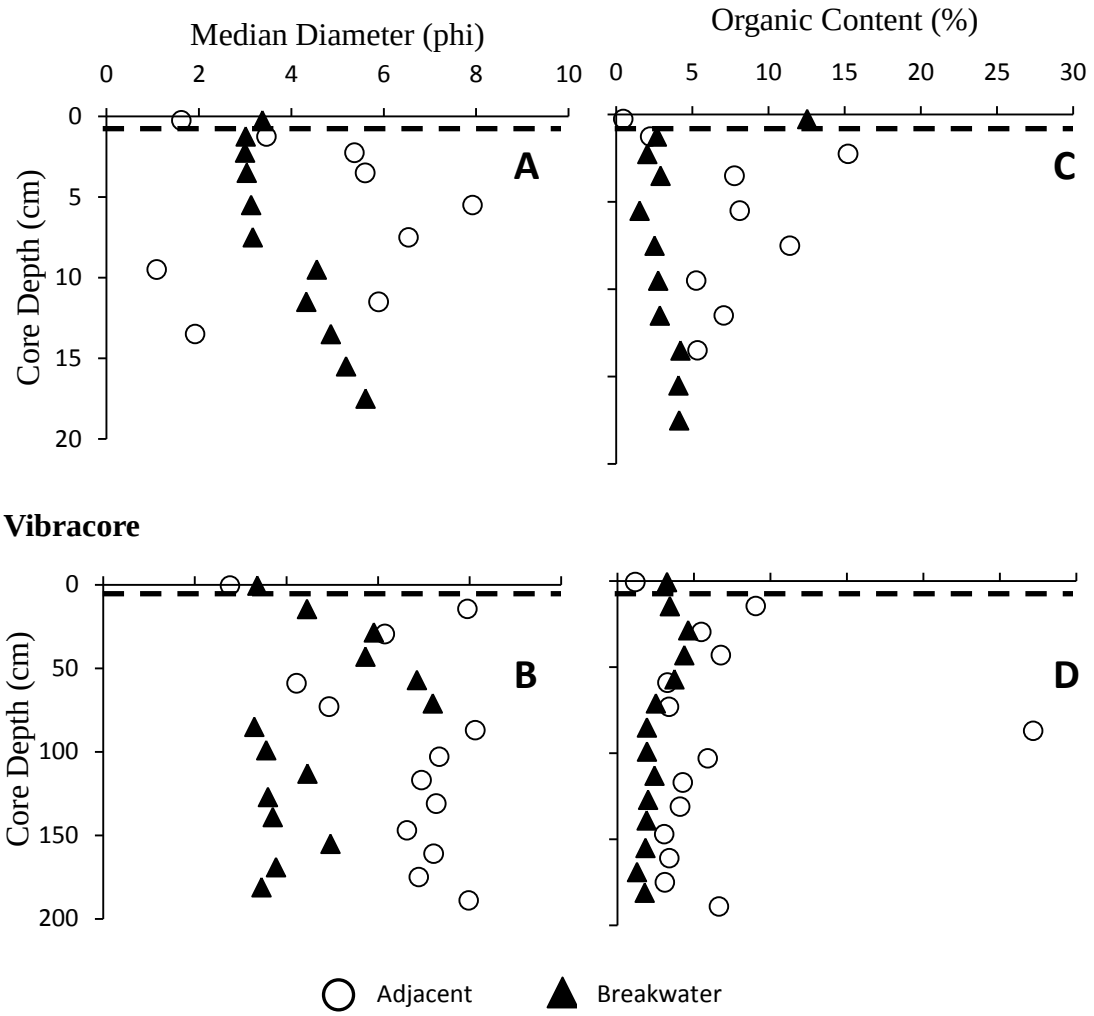

Figure TAN2. Sediment grain size (median diameter) collected with a push core (A) or vibracore (B) at the adjacent-exposed (open circles) and breakwater-protected (closed triangles) sites. Sediment organic content collected with a push core (C) or vibracore (D) at the adjacent-exposed and breakwater-protected sites. The dashed line represents the interpreted depth of breakwater appearance (1 cm).

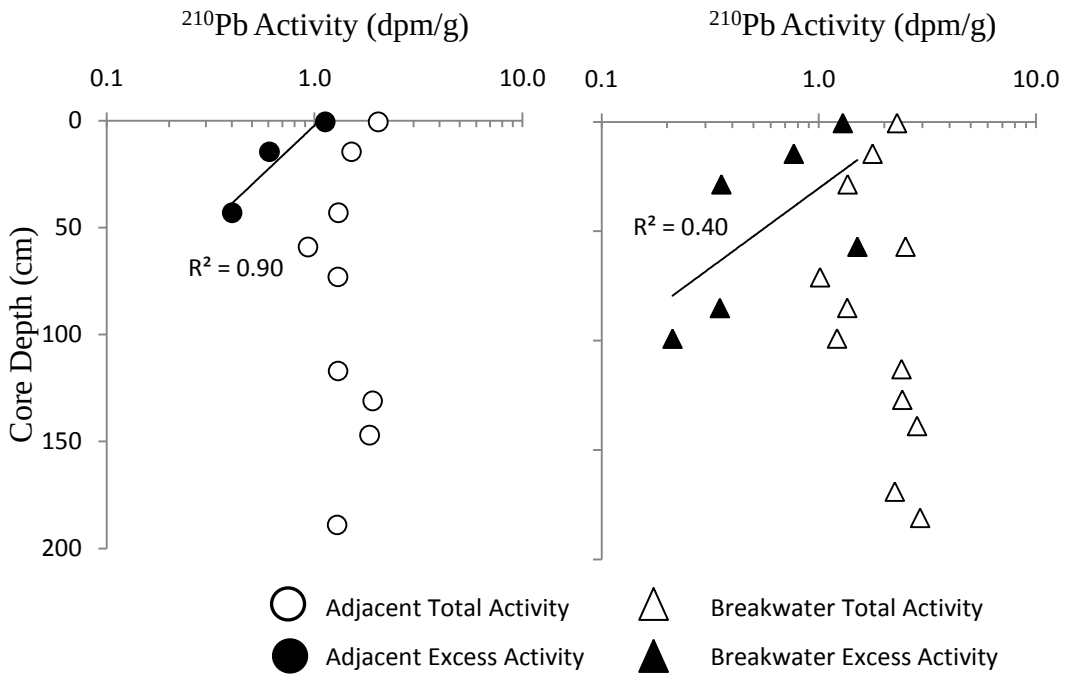

Figure TAN3. ^{210}Pb profiles at the adjacent-exposed (A) and breakwater-protected (B) sites. Activities at both sites have been normalized to the mud content to remove the effect of grain-size variations. Excess normalized activities at both sites decrease logarithmically with depth, indicating steady-state sedimentation. The calculated sediment accumulation rate is 1.4 cm/y at the adjacent-exposed site and 2.1 cm/y at the breakwater-protected site.

Summary of sediment data:

Surficial sediment (upper 10 cm) at the adjacent-exposed site has an average median diameter of 4.5±1.0 phi (44.2 µm) and an average organic content of 7.2±1.9%. Surficial sediment at the breakwater-protected site has an average median diameter of 3.3±0.2 phi (101.5 µm) and an average organic content of 3.9±1.5%. The adjacent-

exposed site is finer ($p = 0.25$) and more organic ($p = 0.19$) than the breakwater-protected.

^{210}Pb activities at both sites are normalized to the mud content to remove the effect of grain-size variations. Excess normalized activities decrease logarithmically with depth and the calculated accumulation rate is 1.4 cm/y at the adjacent-exposed site and 2.1 cm/y at the breakwater-protected site. The latter represents the pre-construction sedimentation rate.

At the breakwater-protected site, organic content in the upper 1 cm is much higher than in the rest of the push-core profile. This likely reflects the influence of the breakwater, and so 1 cm is the interpreted depth of breakwater appearance. The corresponding post-construction sedimentation rate is 0.5 cm/y. However, the breakwater at this site is very young, and so the post-construction sedimentation rate is biased by recent sedimentary conditions.

SAV Data:

Table TAN2. Characteristics of the SAV species *Ruppia maritima* and *Zostera marina* growing at the adjacent-exposed and breakwater-protected sites, values are reported as mean ±SE.

Location	Species	Shoot Length (cm)	Root Length (cm)	Above-ground Biomass (g m^{-2})	Below-ground Biomass (g m^{-2})	Total Biomass (g m^{-2})	Ratio Above- / Below-ground Biomass
Adjacent-exposed	None						
Breakwater-protected	*Ruppia maritima*	11.5± 0.2	7.4± 0.3	36.5± 10.7	21.1± 10.0	57.6± 20.3	3.8± 2.2
Breakwater-protected	*Zostera marina*	16.5± 0.6	5.2± 0.2	63.0± 13.4	25.2± 6.5	88.2± 19.9	2.5± 0.1

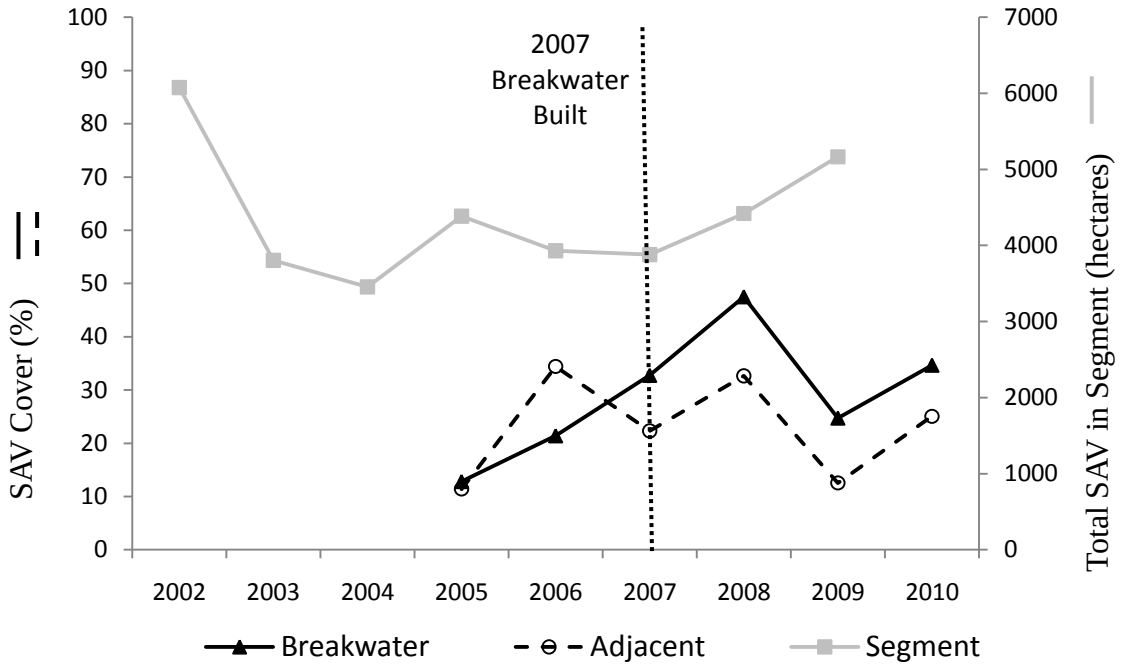

Figure TAN4. SAV % cover plotted against the total SAV in the bay segment as determined by VIMS aerial photography from 4 years prior to breakwater installation to present day.

Ruppia maritima

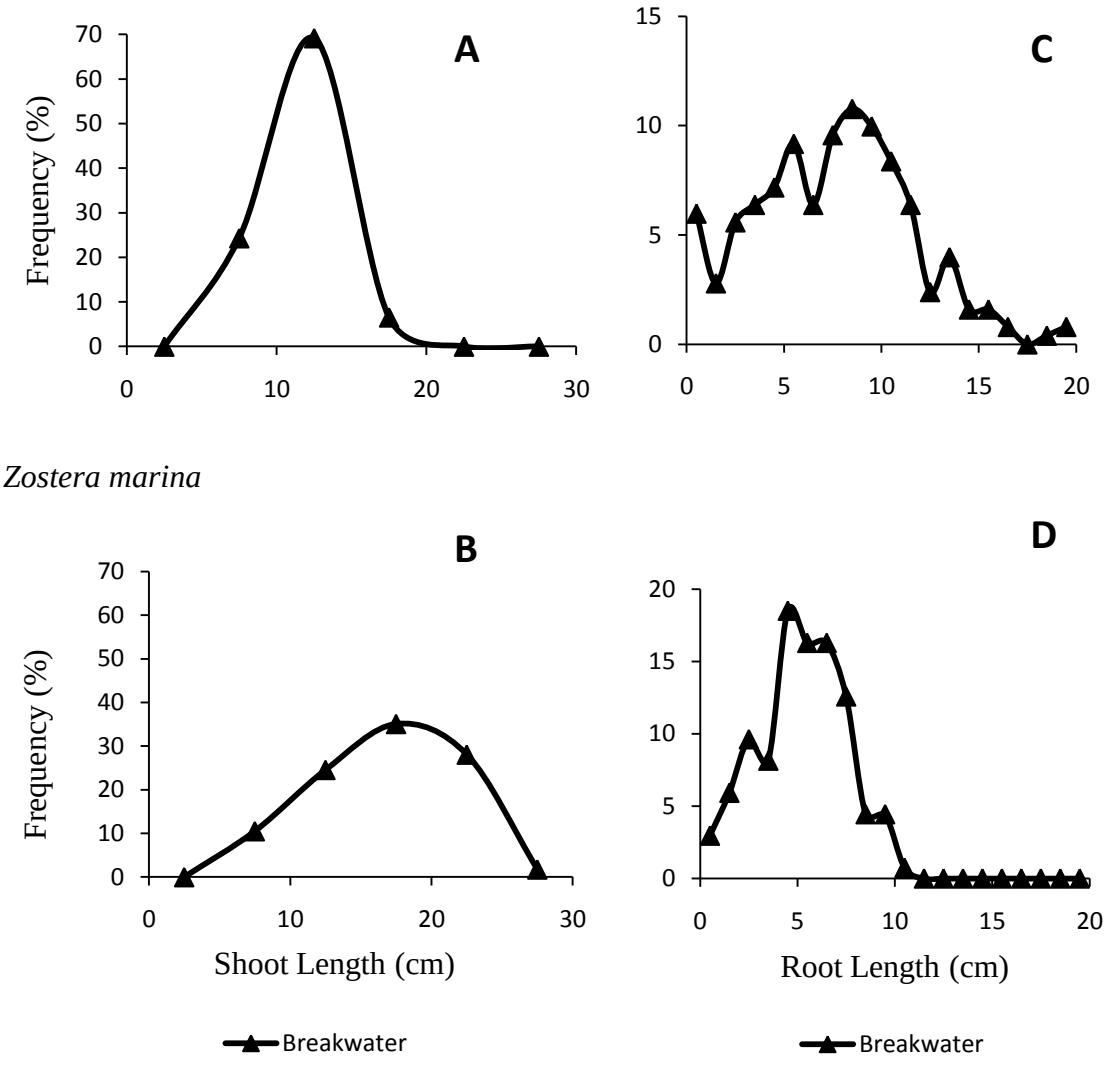

Zostera marina

Figure TAN5. (A) Shoot- and (C) root-length frequency plots for *Ruppia maritima* and (B) shoot- and (D) root-length frequency plots for *Zostera marina* at the adjacent-exposed (open circles) and breakwater-protected (closed triangle) sites.

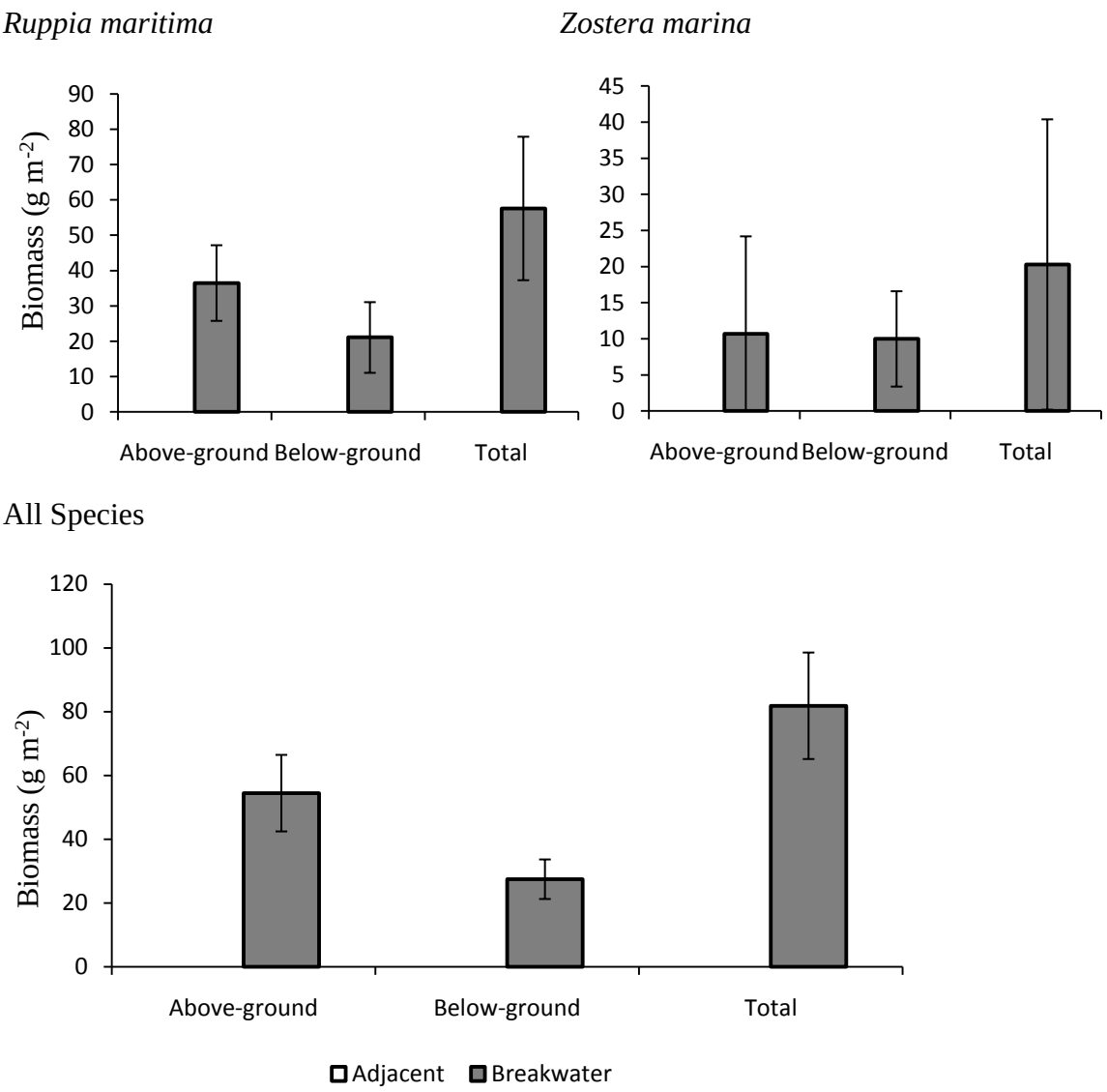

Figure TAN6. Biomass of the SAV (A) *Ruppia maritima*, (B) *Zostera marina*, and (C) all species of SAV at the adjacent-exposed (open bars) and breakwater-protected (closed bars) sites.

Summary of SAV data:

SAV abundance in the segment containing the Tangier Island site was fairly stable over the observation period. At Tangier, SAV % cover appeared to be increasing until just after breakwater installation, then decreased, but may have been recovering in 2010. *R. maritima* and *Z. marina* were collected in the breakwater-protected area, but were not present at the adjacent-exposed area, likely due to the fact that the sediments were compacted peat. It has been shown that these SAV do not colonize compacted peat (Wicks et al., 2009). At this location the breakwater is beneficial to SAV.

Mayo North

Description: Mayo North has a linear, segmented, rock-mound breakwater oriented parallel to the sandy shoreline. The northernmost segment of this 16 segment structure is curved and attached to the shoreline. This was historically a groin field, but it was converted into a segmented breakwater in 2000, with a total length of 696.4 m. Average segment length is 21±2 m, and average gap length is 23±2 m. The average distance from the shoreline is 49±8 m. Adjacent-exposed and breakwater-protected shorelines are sandy beach.

Year of Construction: 2000 **Age at Sampling:** 9 years

Salinity Regime: Mesohaline

Fetch: Adjacent: 8.4±2.0 km

Breakwater: 7.9±2.0 km

Sampling Coordinates:

MayNA vbc	38º52'42.3"N	76º29'53.6"W
MayNA pc	38º52'42.3"N	76º29'53.6"W
MayNB vbc	38º52'52.7"N	76º29'40.7"W
MayNB pc	38º52'52.7"N	76º29'40.7"W
No SAV		

Table MayN1. Latitude and longitude of vibracores (vbc), pushcores (pc), and SAV cores taken in the adjacent-exposed ("A") and breakwater-protected ("B") sites at Mayo North. Note that SAV cores were not collected as SAV was absent in 2009.

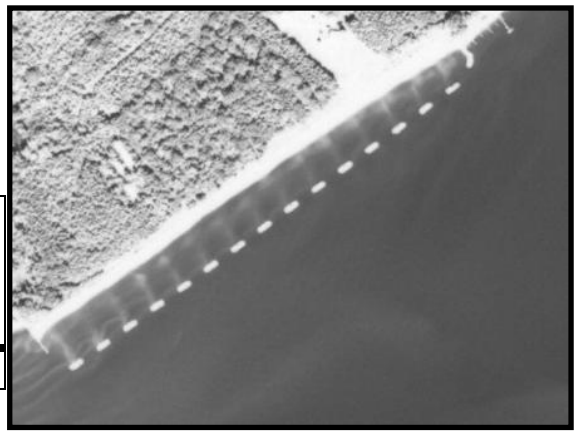

Figure MayN1. Aerial photograph of the breakwater at Mayo North, MD.

Sediment Data:

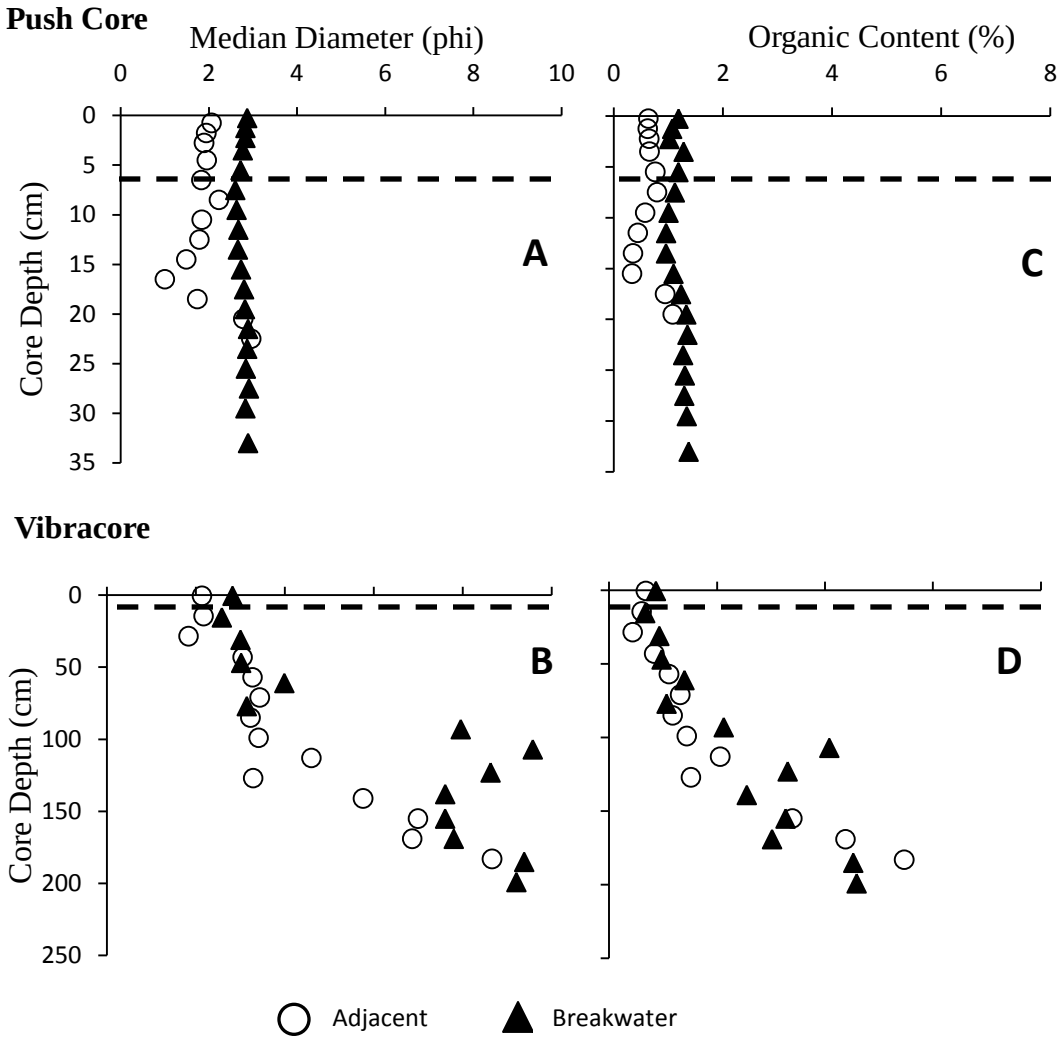

Figure MayN2. Sediment grain size (median diameter) collected with a push core (A) or vibracore (B) at the adjacent-exposed (open circles) and breakwater-protected (closed triangles) sites. The dashed line represents the interpreted depth of breakwater appearance (6 cm). Sediment organic content collected with a push core (C) or vibracore (D) at the adjacent-exposed and breakwater-protected sites.

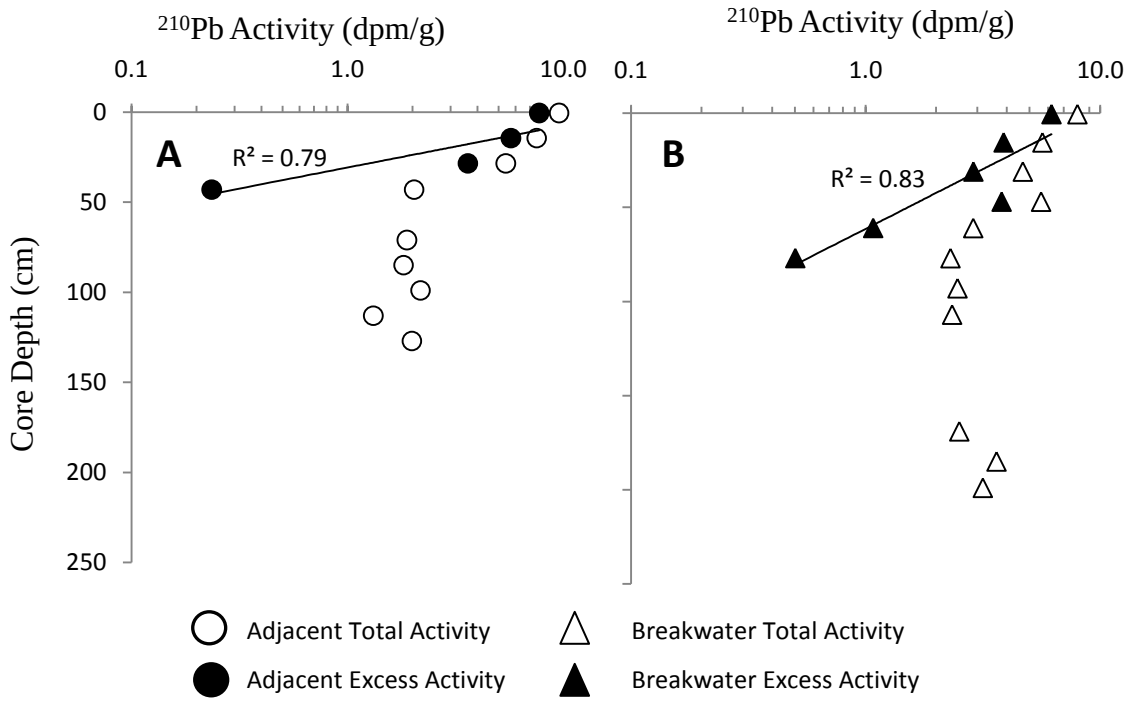

Figure MayN3. ^{210}Pb profiles at the adjacent-exposed (A) and breakwater-protected (B) sites. The calculated sediment accumulation rate is 0.4 cm/y at the adjacent-exposed site, and 0.7 cm/y at the breakwater-protected site. Activities at both sites have been normalized to the mud content to remove the influence of grain-size due to the strong coarsening upward trend in the vibracore grain-size profiles.

Summary of sediment data

Surficial sediment (upper 10 cm) at the adjacent-exposed site is coarser ($p < .0001$) and less organic ($p < .0001$) than the breakwater-protected site. The adjacent-exposed site has an average median diameter of 2.0±0.1 phi (250.0 µm) and an average organic content of 0.7±0.04%. Surficial sediment at the breakwater-protected site has an average median diameter of 2.8±0.04 phi (143.6 µm) and an average organic content of 1.1±0.04%.

The ^{210}Pb profiles at both sites have activities that decrease logarithmically with depth, indicating steady-state sedimentation. Activities in both profiles have been normalized to the mud content, which removes the influence of grain size. Both sites have a strong coarsening upward trend in the vibracore grain-size profiles, which causes an apparent decrease in ^{210}Pb activity upwards if activities are not normalized. The accumulation rate at the adjacent-exposed site is 0.4 cm/y. The pre-construction rate at the breakwater-protected site is derived from the ^{210}Pb profile and is 0.7 cm/y.

There is no apparent change in sediment character (grain size, organic content) in either the push- or vibracore profiles at the breakwater-protected site. Since there is no obvious signature of breakwater influence, the sedimentation rate is assumed to also remain unchanged by the presence of the breakwater. Thus, the post-construction sedimentation rate is assumed to be equal to the pre-construction rate (0.7 cm/y) and the depth of breakwater influence is calculated by multiplying this rate by the breakwater age (9 y) to yield a depth of 6 cm.

SAV Data:

No SAV was present at the adjacent-exposed or breakwater-protected sites at Mayo North.

Mayo South

Description: The segmented, rock-mound breakwater at Mayo South is semi-circular at the south end, linear at the north end, and is oriented parallel to the sandy shoreline. This breakwater is 513.4 m long and consists of 12 segments. These segments have an average length of 25±1 m (mean ± SD), and gaps average 20±1 m long. The average distance from shore is 49±7 m. This shoreline was protected by a groin field before breakwater construction in 1998.

Year of Construction: 1998

Age at Sampling: 11 years

Salinity Regime: Mesohaline

Fetch: Adjacent: 5.9±1.5 km

Breakwater: 6.5±1.6 km

Sampling Coordinates:

MayS A vbc	38º52'35.7"N	76º30'7.0"W
MayS A pc	38º52'35.7"N	76º30'7.0"W
MayS B vbc	38º52'25.9"N	76º30'15.6"W
MayS B pc	38º52'25.9"N	76º30'15.6"W
No SAV		

Table MayS1. Latitude and longitude of vibracores (vbc), pushcores (pc), and SAV cores taken in the adjacent-exposed ("A") and breakwater-protected ("B") sites at Mayo South. Note that SAV cores were not collected as SAV was absent in 2009.

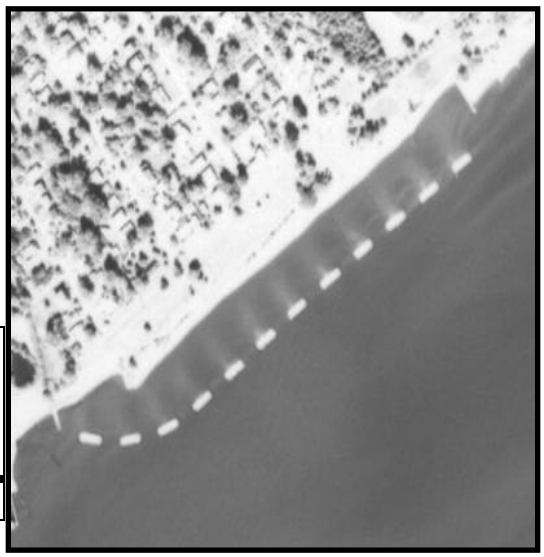

Figure MayS1. Aerial photograph of the breakwater at Mayo South, MD.

Sediment Data:

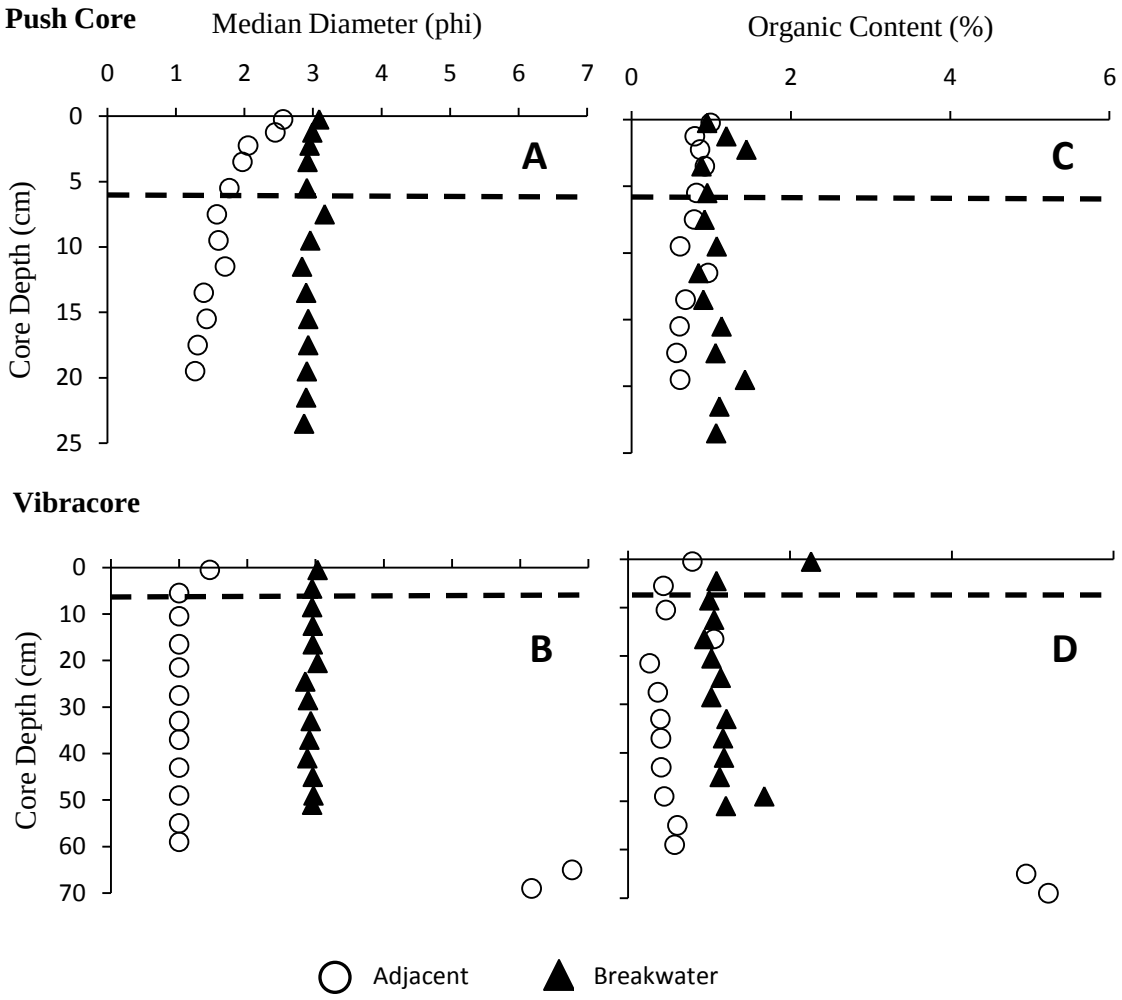

Figure MayS2. Sediment grain size (median diameter) collected with a push core (A) or vibracore (B) at the adjacent-exposed (open circles) and breakwater-protected (closed triangles) sites. The dashed line represents the interpreted depth of breakwater appearance (6 cm). Sediment organic content collected with a push core (C) or vibracore (D) at the adjacent-exposed and breakwater-protected sites.

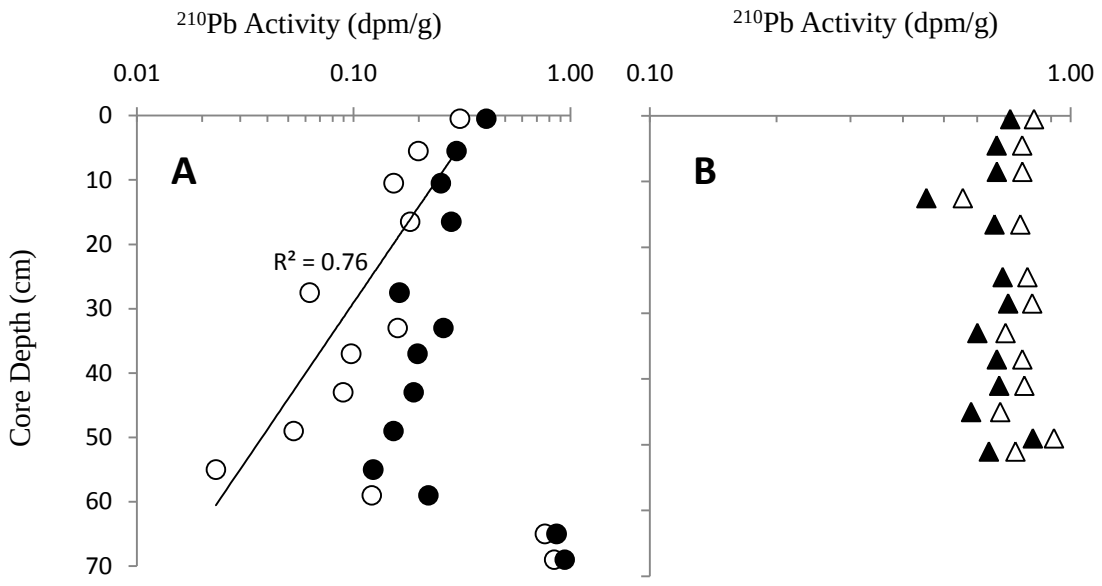

Figure MayS3. ^{210}Pb profiles at the adjacent-exposed (A) and breakwater-protected (B) sites. The calculated sediment accumulation rate is 0.9 cm/y at the adjacent-exposed site. At the breakwater-protected site, activities are uniform through the profile, so only a minimum accumulation rate of >0.5 cm/y can be calculated, by noting the presence of excess ^{210}Pb at the base of the core (sediments <100 y old).

Summary of sediment data

Surficial sediment (upper 10 cm) at the adjacent-exposed site is coarser ($p < 0.0001$) and less organic ($p = 0.01$) than the breakwater-protected. The adjacent-exposed site has an average median diameter of 2.0±0.1 phi (250.0 µm) and an average organic content of 0.8±0.1%. Surficial sediment at the breakwater-protected site has an average median diameter of 3.0±0.04 phi (125.0 µm) and an average organic content of 1.1±0.1%.

^{210}Pb activities at the adjacent-exposed site decrease logarithmically with depth, indicating steady-state sedimentation. Activities are relatively high at the base of the core, corresponding to an increase in grain size. These activities are not included in the best-fit regression line. The accumulation rate at the adjacent-exposed site is 0.9 cm/y. Activities at the breakwater-protected site are uniform through the core, so only a minimum accumulation rate of >0.5 cm/y can be calculated. The depth-integrated ^{210}Pb inventory at this site is 113.9 dpm/cm^2, greater than the atmospherically supported inventory of 25 dpm/cm^2 (Kim et al., 2000), supporting the interpretation of net sediment accumulation.

There is no apparent change in sediment character (grain size, organic content) in either the push- or vibracore profiles at the breakwater-protected site. Since there is no obvious signature of breakwater influence, the sedimentation rate is assumed to also remain unchanged by the presence of the breakwater. Thus, the post-construction sedimentation rate is assumed to be equal to the pre-construction rate (0.5 cm/y) and the depth of breakwater influence is calculated by multiplying this rate by the breakwater age (11 y) to yield a depth of 6 cm. Since the accumulation rate is a minimum estimate, the depth of breakwater influence should also be regarded as a minimum estimate.

SAV Data:

No SAV was present at the adjacent-exposed or breakwater-protected sites at Mayo South.

Bishops Head

Description: This semi-circular, segmented, rock-mound breakwater has 4 segments, 2 of which are attached to land. The total breakwater length is 188.1 m, with segment lengths 34±9 m (mean ± SD) and gap lengths 16±6 m. Average distance from shore is 50±14 m. This breakwater protects an eroding marsh and a man-made, sandy pocket-beach area. The adjacent-exposed shoreline is eroding marsh.

Year of Construction: 1997 **Age at Sampling:** 11 years

Salinity Regime: Mesohaline

Fetch: Adjacent: 4.3±1.4 km

Breakwater: 6.4±2.0 km

Sampling Coordinates:

BH A vbc	38º13'16.5"N	76º02'23.5"W
BH A pc	38º13'16.5"N	76º02'23.5"W
BH B vbc	38º13'15.1"N	76º02'20.2"W
BH B pc	38º13'15.1"N	76º02'20.2"W
SAV A1	38º13'15.6"N	76º02'24.4"W
SAV A2	38º13'15.5"N	76º02'24.1"W
SAV A3	38º13'15.2"N	76º02'23.9"W
SAV A4	38º13'14.9"N	76º02'23.8"W
SAV A5	38º13'14.9"N	76º02'24.2"W
SAV BW1	38º13'14.7"N	76º02'19.2"W
SAV BW2	38º13'14.9"N	76º02'19.4"W
SAV BW3	38º13'14.8"N	76º02'20.4"W
SAV BW4	38º13'13.7"N	76º02'18.1"W
SAV BW5	38º13'13.3"N	76º02'17.4"W
Extra BW bag	38º13'14.2"N	76º02'20.0"W

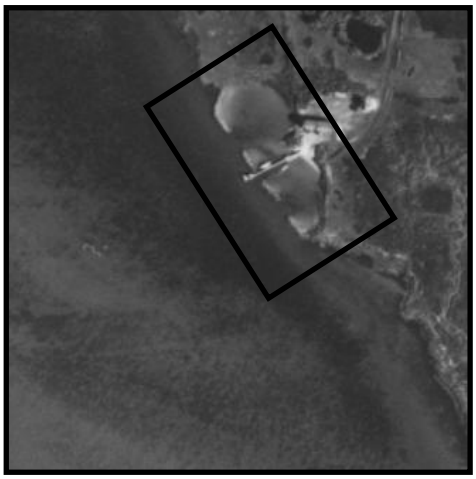

Figure BH1. Aerial photo of the breakwater at Bishops Head, MD.

Table BH1. Latitude and longitude of vibracores (vbc), pushcores (pc), and SAV cores taken in the adjacent-exposed ("A") and breakwater-protected ("B") sites at Bishops Head.

Sediment Data:

Push Core

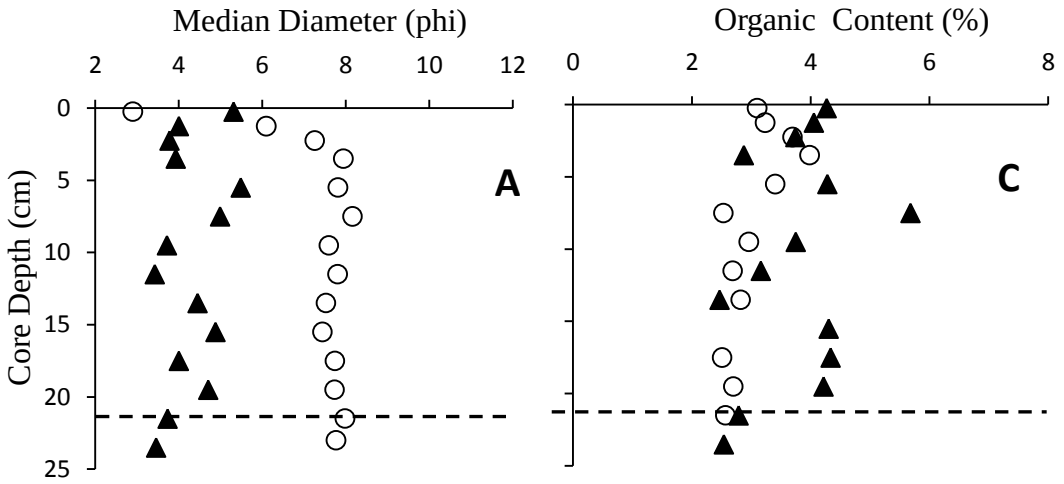

Vibracore

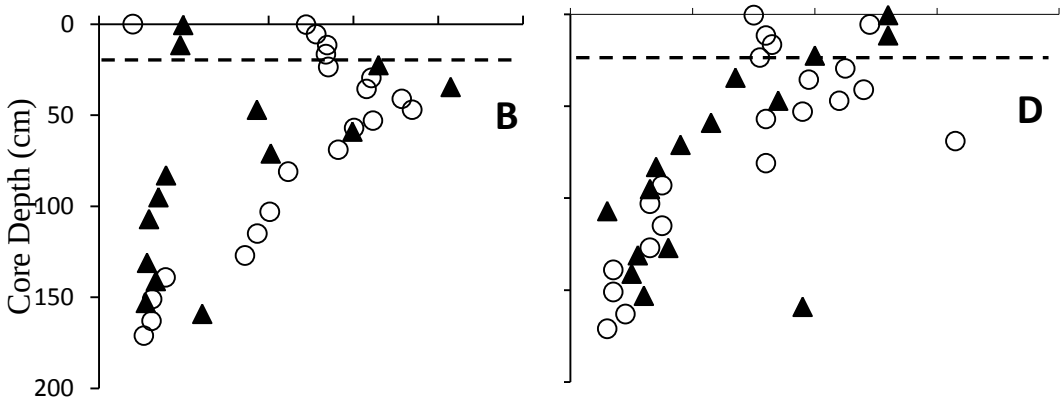

Figure BH2. Sediment grain size (median diameter) collected with a push core (A) or vibracore (B) at the adjacent-exposed (open circles) and breakwater-protected (closed triangles) sites. The dashed line represents the interpreted depth of breakwater appearance. Sediment organic content collected with a push core (C) or vibracore (D) at the adjacent-exposed and breakwater-protected sites.

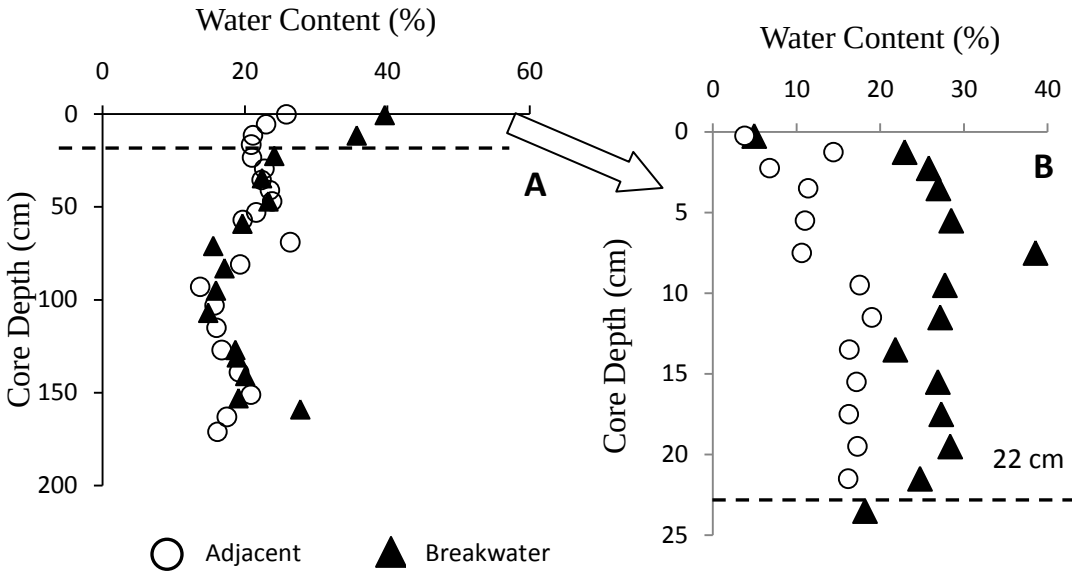

Figure BH3. Vibracore (A) and push-core (B) sediment water content. Note that the water-content profiles for the adjacent-exposed and breakwater-protected sites coincide for most of the core but diverge at 22 cm – determined from the high-resolution push-core profile.

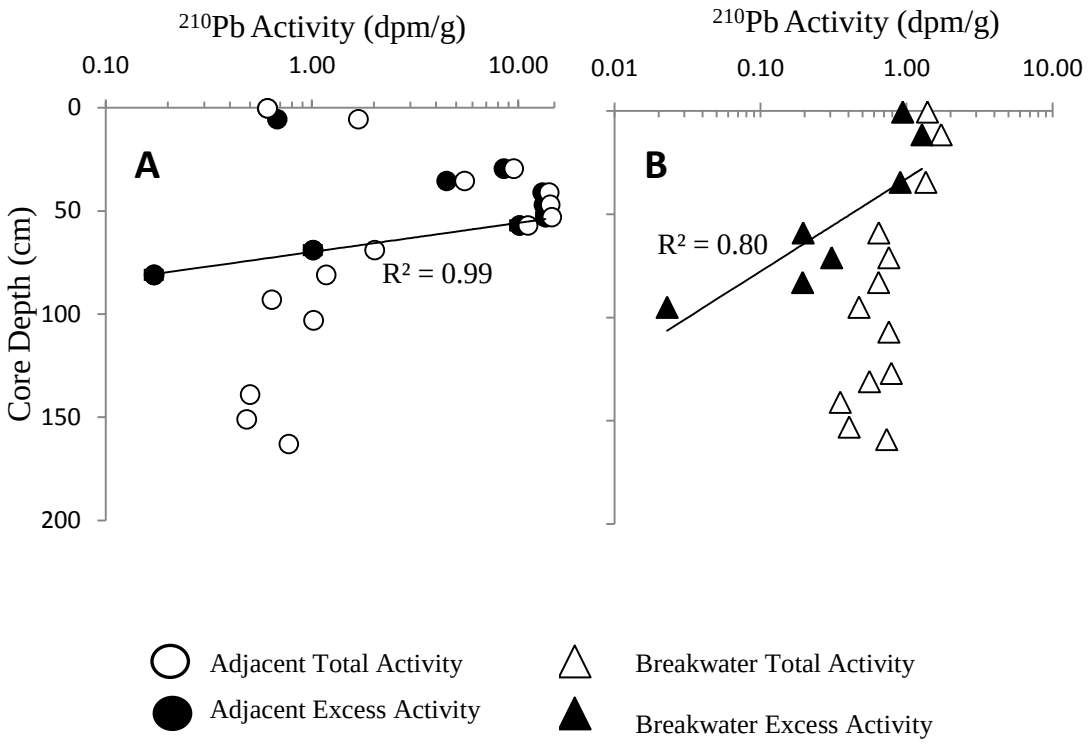

Figure BH4. ^{210}Pb profiles at the adjacent-exposed (A) and breakwater-protected (B) sites. The calculated sediment accumulation rate is 0.4 cm/y at the adjacent-exposed site and 1.1 cm/y at the breakwater-protected site. Note that the latter represents the pre-construction sedimentation rate. Also note that the x-axis scale differs between plots for visual clarity.

Summary of sediment data

Surficial (top 10 cm) sediment at the adjacent-exposed site was muddy (average median diameter of surficial sediment 6.8±0.7 phi, 9.0 μm), organic (3.3±0.2%), and relatively compacted (water content 10.8±0.2%). The sediment accumulation rate at this site was 0.4 cm/y, and a 5-cm thick layer of uniform ^{210}Pb activity (i.e., surface mixed layer) was present at top of the core. ^{137}Cs was observed ~40 cm deep in the core,

resulting in an accumulation rate of 0.7 cm/y, suggesting a possible recent (last ~50 y) increase in sedimentation at this site. Surficial sediment in the breakwater-protected area was also muddy (average median diameter 4.5±0.3 phi, 44.2 μm), but significantly ($p = 0.01$) coarser than that at the adjacent-exposed site, and significantly ($p = 0.04$) more organic (4.1±0.3%), and relatively unconsolidated (water content 25.1±0.5%).

Changes likely induced by breakwater installation can be determined by examining down-core profiles of grain size, organic content, and water content in the breakwater-protected area. While there is an historic upward fining, as well as an associated upward increase in organic content, in the vibracore grain-size profile, sediment becomes coarser in the upper portion of the profile. This change is less obvious in the organic-content profile, which appears to continue the historic trend of increasing organic content. This is probably because post-construction sediment, while coarser-grained, is still primarily muddy. There is also an increase in water content post-construction at the breakwater-protected site; examining the high-resolution push-core profile indicates that this change occurs at 22 cm. Thus, the depth of breakwater appearance is interpreted to be 22 cm.

The sediment accumulation rate, determined from ^{210}Pb measurements, at the adjacent-exposed site was 0.4 cm/y, and the pre-construction breakwater accumulation rate was 1.1 cm/y. The depth of breakwater appearance can be divided by the breakwater age at the time of sampling (11 y) to yield the post-construction rate of 2.0 cm/y. However, since samples were taken at the end of summer (August 2008) and thus likely after a relatively quiescent period, some of the 22-cm, some of this post-construction layer could be eroded during energetic winter storms.

Thus, the effect of breakwater installation on sediments at Bishops Head appears to be an increase in grain size (decreasing phi units), no change in organic content, increase in water content, and increase in sedimentation rate.

SAV data:

Table BH2. Characteristics of the SAV *Ruppia maritima* growing at the adjacent-exposed and breakwater-protected sites, values are reported as mean ±SE.

Location	Species	Shoot Length (cm)	Root Length (cm)	Above-ground Biomass ($g\ m^{-2}$)	Below-ground Biomass ($g\ m^{-2}$)	Total Biomass ($g\ m^{-2}$)	Ratio Above-/ Below-ground Biomass
Adjacent-exposed	*Ruppia maritima*	9.9± 0.2	4.8± 0.2	55.4± 17.9	36.4± 9.6	91.7± 26.8	1.8± 0.4
Breakwater-protected	*Ruppia maritima*	11.9± 0.3	5.3± 0.2	181.2± 91.8	52.6± 12.4	233.8± 103.0	2.8± 0.7

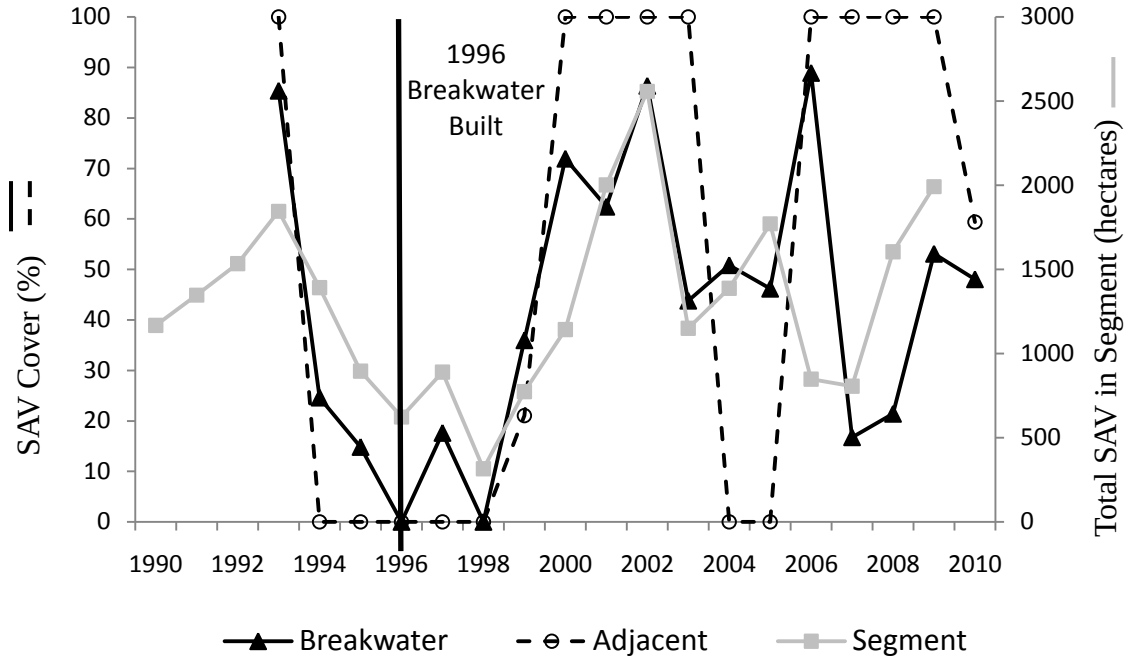

Figure BH5. SAV % cover plotted against the total SAV in the bay segment as determined by VIMS aerial photography from 6 years prior to breakwater installation to present day

Ruppia maritima.

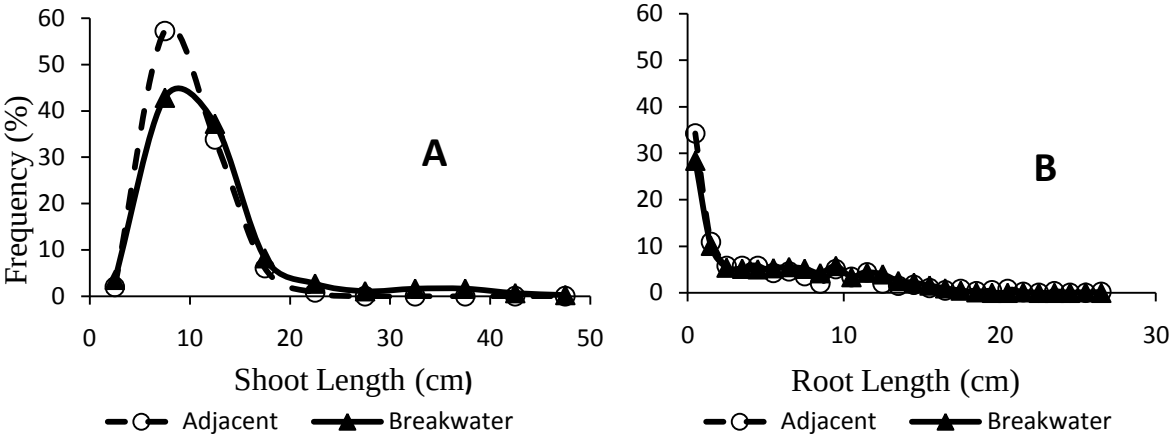

Figure BH6. (A) Shoot- and (B) root-length frequency plots for *Ruppia maritima* at the adjacent-exposed (open circles) and breakwater-protected (closed triangle) sites.

Ruppia maritima

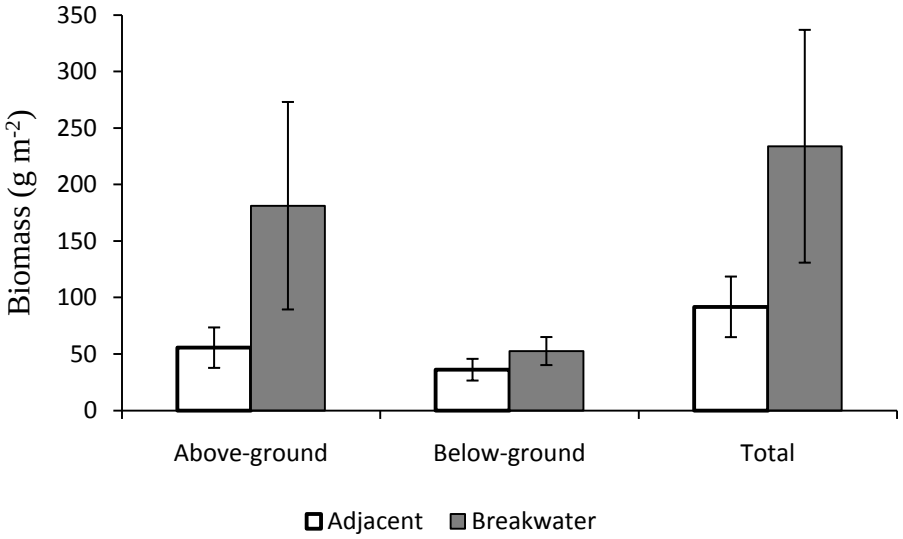

Figure BH7. Biomass of the SAV *Ruppia maritima* at the adjacent-exposed (open bars) and breakwater-protected (closed bars) sites.

Summary of SAV data

SAV coverage in the breakwater and adjacent sites at Bishops Head generally mirrored the total SAV in the segment, but more extreme increases and decreases were observed in the adjacent-exposed site (Figure BH5). *Ruppia maritima* growing at Bishops Head had longer shoots ($p = 0.001$), roots ($p = 0.07$;Table BH2; Figure BH6), and greater biomass ($p = 0.17$; Figure BH7) in the breakwater-protected area than the plants located in the adjacent exposed site. This difference due to the presence of long reproductive shoots in the breakwater-protected site but not at the adjacent-exposed site. The ratio of above- to below-ground biomass was 1.8 in the adjacent-exposed site and 2.8 in the breakwater-protected site (Table BH2). This may be a response to the greater organic-

matter content and reduced wave energy at the breakwater-protected site that reduces the likelihood of being uprooted. It also must be noted that the adjacent-exposed sediment cores were taken in a different location than the SAV cores, as the area of the sediment cores had no SAV present due to sediments consisting of compacted peat. SAV could be seen growing farther offshore in aerial photos, so the adjacent-exposed SAV samples were collected from this area.

Hoopers Island

Description: This linear, segmented, rock-mound breakwater has 5 segments, 1 of which is attached to land. The total breakwater length is 363.5 m, with segment lengths 49±2 m (mean ± SD) and gap lengths 25±1 m. Average distance from shore is 46±13 m. This breakwater protects an eroding marsh. The adjacent-exposed shoreline is also eroding marsh.

Year of Construction: 1991 **Age at Sampling:** 14 years

Salinity Regime: Mesohaline

Fetch: Adjacent: 16.2±4.8 km

Breakwater: 16.2±4.8 km

Sampling Coordinates:

HI A vbc	38º17'20.7"	76º12'05.7"
HI A pc	38º17'20.7"	76º12'05.7"
HI B vbc	38º17'27.4"	76º12'09.0"
HI B pc	38º17'27.4"	76º12'09.0"
SAV A	None	
SAV B1	38º17'29.8"	76º12'09.7"
SAV B2	38º17'28.4"	76º12'08.7"
SAV B3	38º17'27.3"	76º12'08.1"
SAV B4	38º17'26.4"	76º12'07.8"
SAV B5	38º17'24.9"	76º12'07.3"

Table HI1. Latitude and longitude of vibracores (vbc), pushcores (pc), and SAV cores taken in the adjacent-exposed ("A") and breakwater-protected ("B") sites at Hoopers Island. Note that SAV cores were not taken in the adjacent-exposed area, as no SAV was present in summer 2009.

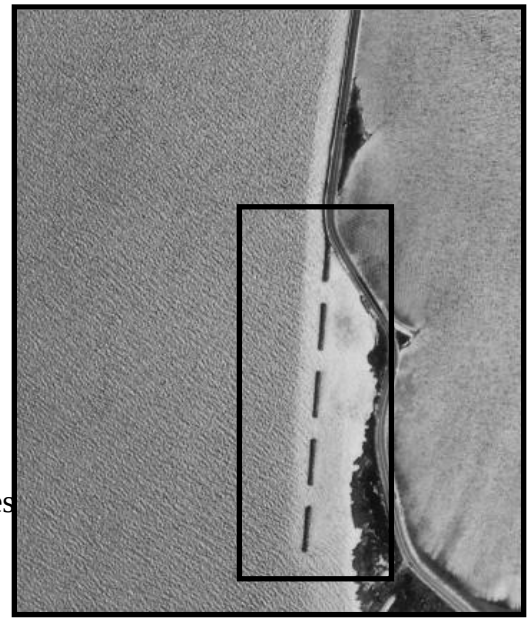

Figure HI1. Aerial photo of the breakwater at Hoopers Island, MD.

Sediment Data:

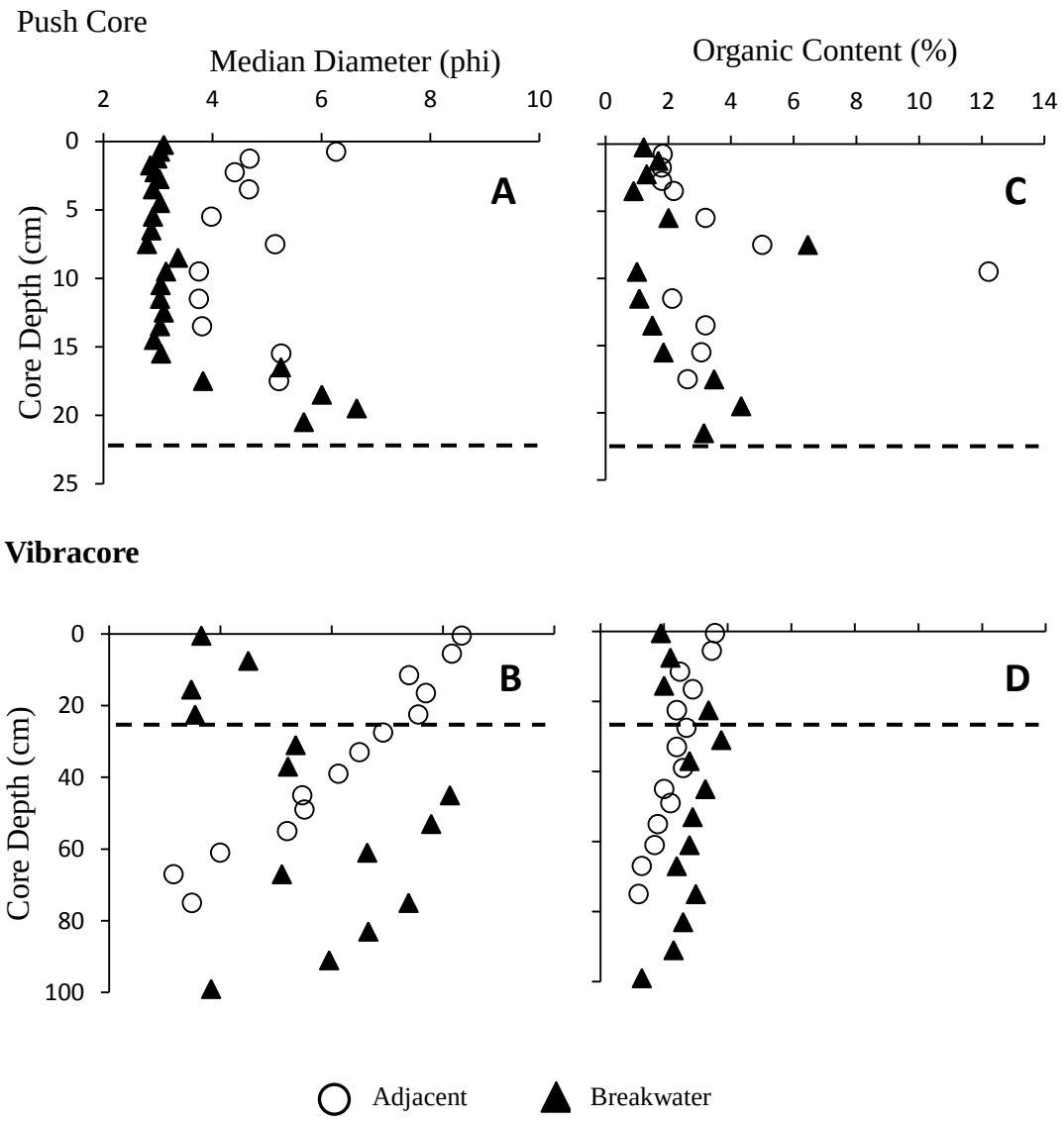

Figure HI2. Sediment grain size (median diameter) collected with a push core (A) or vibracore (B) at the adjacent-exposed (open circles) and breakwater-protected (closed triangles) sites. The dashed line represents the interpreted depth of breakwater appearance (23 cm). Sediment organic content collected with a push core (C) or vibracore (D) at the adjacent-exposed and breakwater-protected sites.

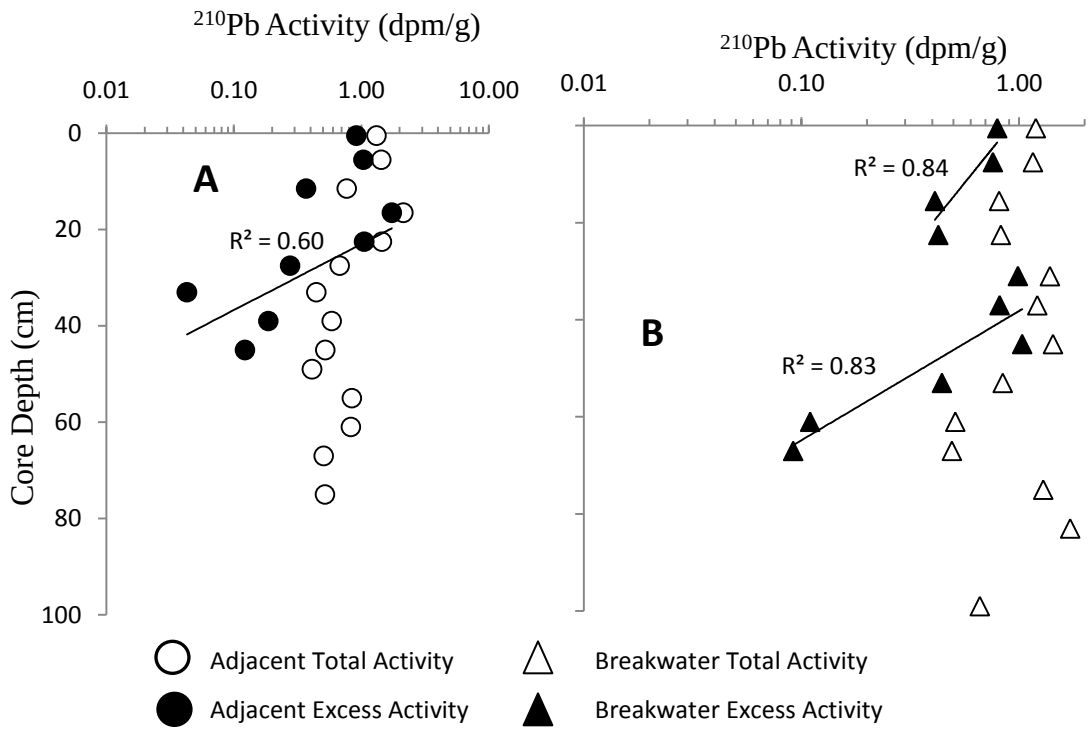

Figure HI3. ^{210}Pb profiles at the adjacent-exposed (A) and breakwater-protected (B) sites. The calculated sediment accumulation rate is 0.4 cm/y at the adjacent-exposed site. The ^{210}Pb profiles at the breakwater-protected site shows a change in slope at 23 cm – the pre-construction accumulation rate is 0.6 cm/y (lower portion of profile), increasing to 1.1 cm/y post-construction (upper portion of profile). The x-axis scale differs between plots for visual clarity.

Summary of sediment data:

Surficial (upper 10 cm) sediment at the adjacent-exposed site is finer ($p = 0.0002$) but is similar in organic content ($p = 0.24$) in comparison to the breakwater-protected site. The adjacent-exposed site has an average median diameter of 4.7±0.3 phi (38.5 µm) and average organic content of 2.6±0.5%. The breakwater-protected site is coarser (average

median diameter 3.0±0.03 phi, 125.0µm) and less organic (average organic content 2.1±0.8%).

The sediment accumulation rate at the adjacent-exposed site is 0.4 cm/y. ^{137}Cs is present at a depth of 38 cm, resulting in a sediment accumulation rate of 0.7 cm/y. The discrepancy may be due to a recent (last ~50 y) increase in accumulation rate and/or an artifact of the relatively poor regression fit from which the ^{210}Pb-derived rate is calculated. The ^{210}Pb sediment accumulation rate at the base of the breakwater-protected core is 0.6 cm/y, increasing to 1.1 cm/y (reflected by the change in slope at ~32 cm). ^{137}Cs is present at a depth of 42 cm in this core. If sediment is assumed to accumulate at 1.1 cm/y for the post-construction period (14 y) and 0.6 cm/y from construction to 1954 (first appearance of ^{137}Cs; 40 y), then the expected penetration depth would be 39.4 cm, which is similar to the observed penetration depth. The change in slope is interpreted to reflect the presence of the breakwater. Above this depth in the breakwater-protected area, sediment becomes coarser and less organic, probably due to sand-layer application during installation.

SAV Data:

Table HI2. Characteristics of the SAV *Ruppia maritima* and *Zostera marina* growing at the adjacent-exposed and breakwater-protected sites, values are reported as mean ±SE.

Location	Species	Shoot Length (cm)	Root Length (cm)	Above-ground Biomass (g m^{-2})	Below-ground Biomass (g m^{-2})	Total Biomass (g m^{-2})	Ratio Above- / Below-ground Biomass
Adjacent-exposed	*None*						
Breakwater-protected	*Ruppia maritima*	12.0± 0.2	4.9± 0.3	126.2± 33.6	42.4± 4.6	168.6± 38.1	2.9± 0.5
Breakwater-protected	*Zostera marina*	n/a	n/a	190.8± 99.5	200.7± 168.1	391.5± 267.6	1.8± 1.0

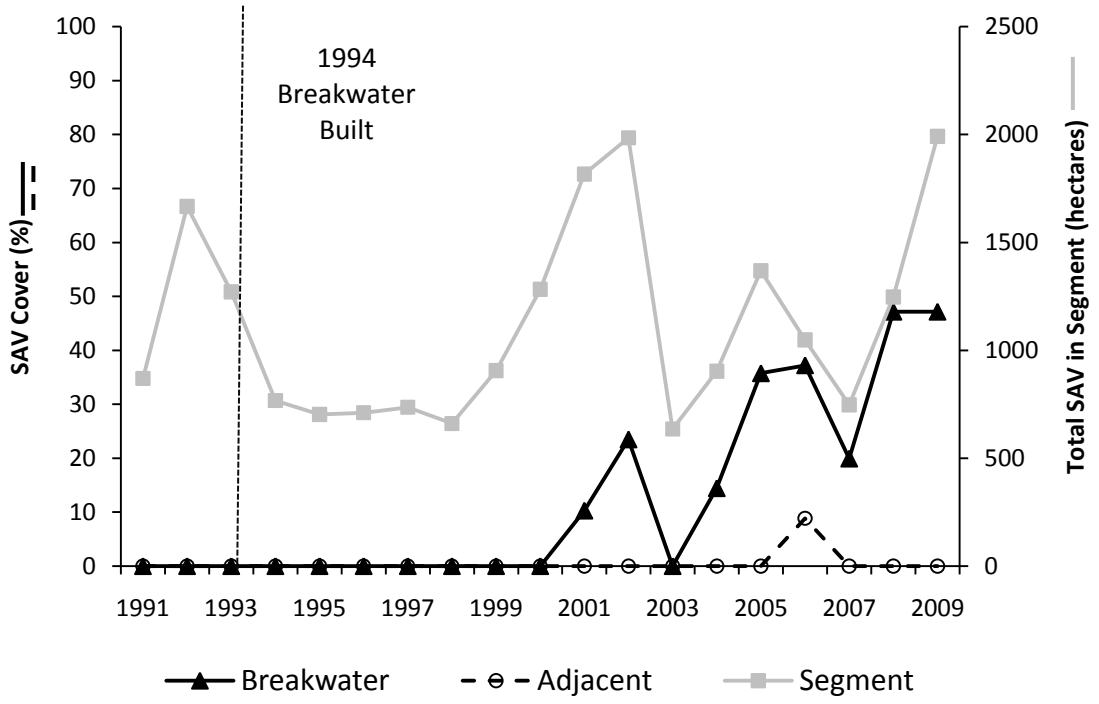

Figure HI4. SAV % cover plotted against the total SAV in the bay segment as determined by VIMS aerial photography from 3 years prior to breakwater installation to present day.

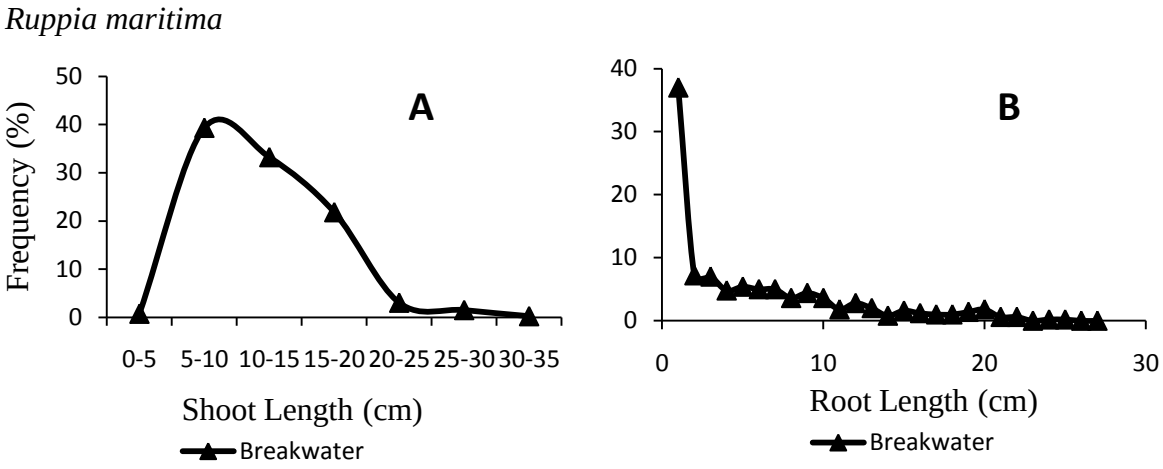

Figure HI5. (A) Shoot- and (B) root-length frequency plots for *Ruppia maritima* at the adjacent-exposed (open circles) and breakwater-protected (closed triangle) sites.

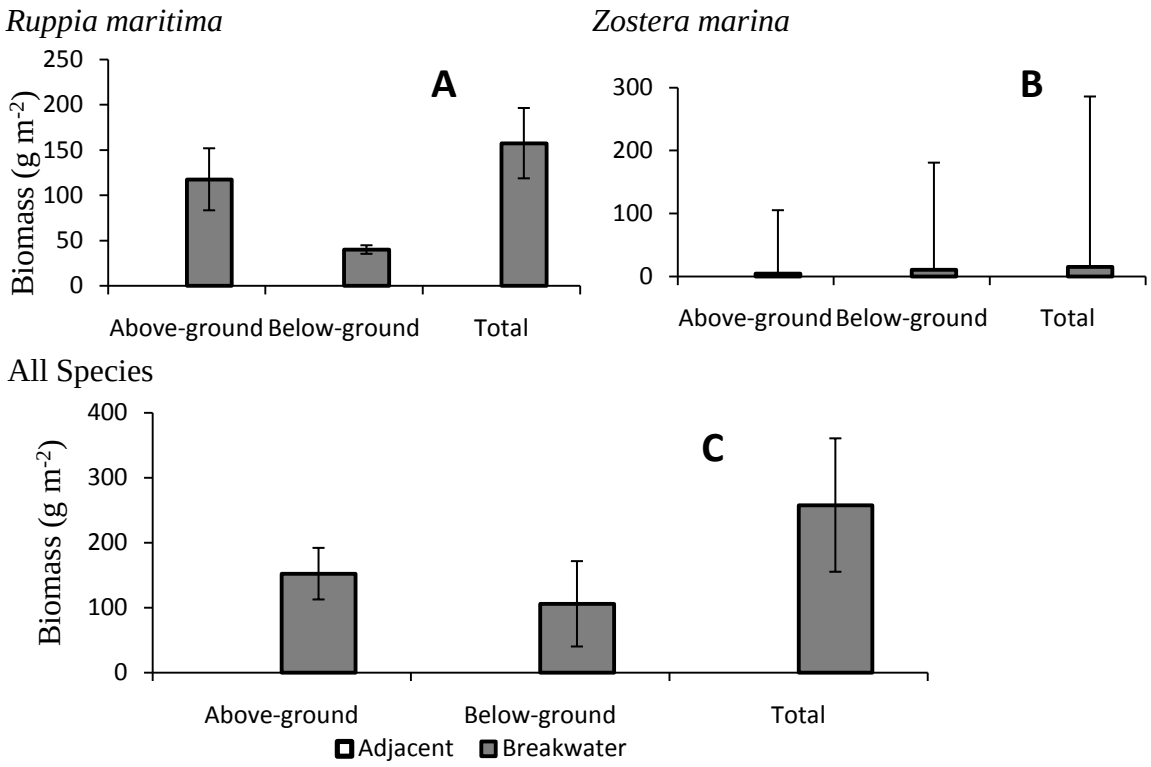

Figure HI6. Biomass of the SAV species (A) *Ruppia maritima*, (B) *Zostera marina*, and (C) all species at the adjacent-exposed (open bars) and breakwater-protected (closed bars) sites.

Summary of SAV data:

SAV abundance in the segment containing the Hoopers Island site is somewhat variable over the observation period. At Hoopers Island, SAV coverage seems to mimic the segment totals starting in 2000, with a greater response seen in the protected breakwater site. The adjacent site remains mostly unvegetated throughout the observation period (Figure HI4).

Prior to breakwater construction the sediment at Hoopers Island was compacted peat, which is not suitable for colonization of SAV (Wicks et al., 2009). However, a possible sand-layer application at time of breakwater construction facilitated a change in substrate composition, thus creating viable SAV habitat. *Ruppia maritima* and *Zostera marina* were observed growing in the breakwater-protected area and no SAV was present in the adjacent-exposed (Figure HI6). Due to the possible addition of sand, the breakwater at Hoopers Island is beneficial for SAV in the area.

Eastern Neck

Description: This semi-circular, segmented, rock-mound breakwater has 19 segments, 2 of which are attached to land. The total breakwater length is 1161.3 m, with segment lengths 25±2 m (this does not include the longest segment which is 360 m long; mean ± SD) and gap lengths 22±3 m. Average distance from shore is 57±11 m. The north end of this breakwater protects a rip rapped shoreline and the south end is an eroding sand cliff. The adjacent-exposed shoreline is rip rapped.

Y**ear of Construction:** 1993 **Age at Sampling:** 15 years

Salinity Regime: Mesohaline

Fetch: Adjacent: 6.6±1.5 km

Breakwater: 7.2±1.5 km

Sampling Coordinates:

EN A vbc	39º02'03.7"N	76º14'28.1"W
EN A pc	39º02'03.7"N	76º14'28.1"W
EN B vbc	39º02'17.5"N	76º14'27.8"W
EN B pc	39º02'17.5"N	76º14'27.8"W
SAV B1	39º02'19.1"N	76º14'27.4"W
SAV B2	39º02'18.6"N	76º14'27.4"W
SAV B3	39º02'16.0"N	76º14'27.9"W
SAV B4	39º02'15.0"N	76º14'27.3"W
SAV B5	39º02'14.3"N	76º14.27.3"W
SAV A	None	

Table EN1. Latitude and longitude of Vibracores (vbc), pushcores (pc), and SAV cores taken at the adjacent-exposed ("A") and breakwater-protected ("B") sites at Eastern Neck.

Figure EN1. Aerial photo of the breakwater at Eastern Neck Island, MD.

Sediment Data:

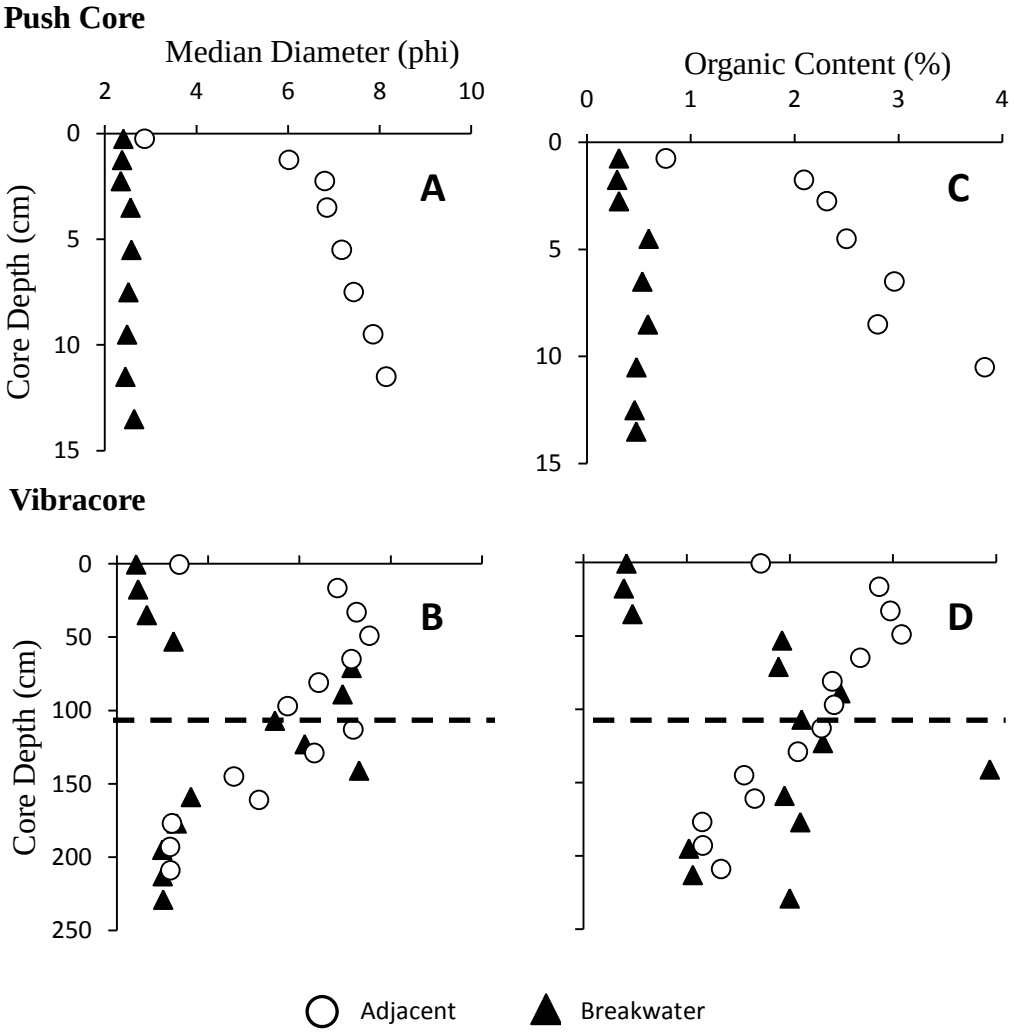

Figure EN2. Sediment grain size (median diameter) collected with a push core (A) or vibracore (B) at the adjacent-exposed (open circles) and breakwater-protected (closed triangles) sites. The dashed line represents the interpreted depth of breakwater appearance. This line is absent in the push-core profiles as these represent post-construction sediment. Sediment organic content collected with a push core (C) or vibracore (D) at the adjacent-exposed and breakwater-protected sites.

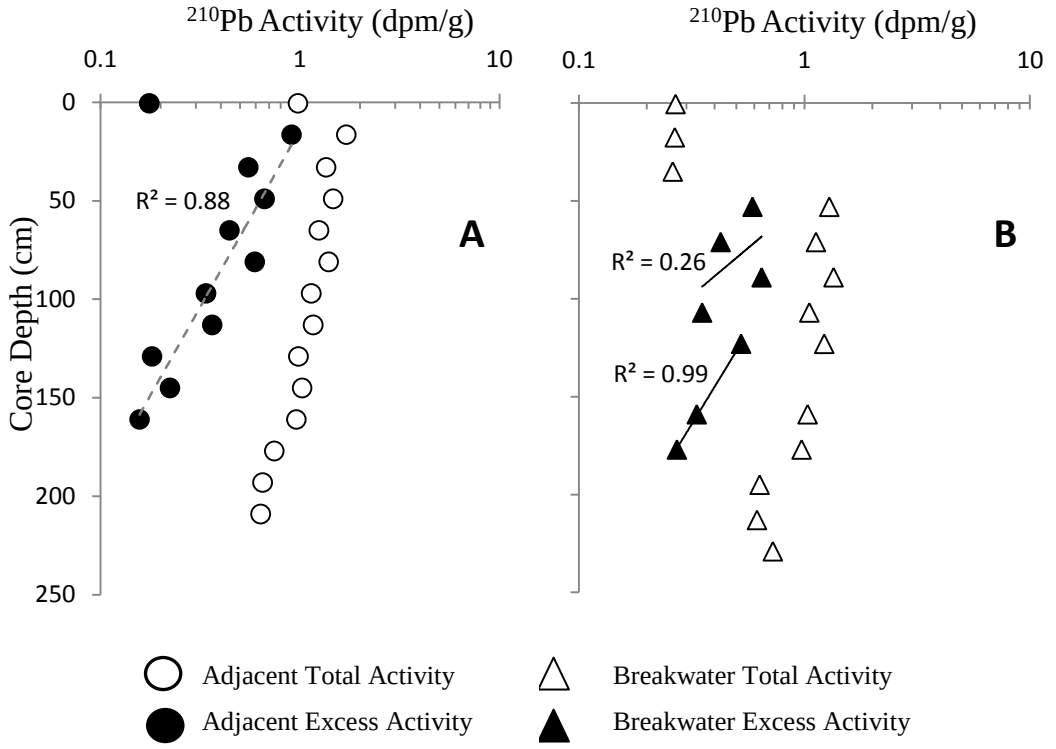

Figure EN3. ^{210}Pb profiles at the adjacent-exposed (A) and breakwater-protected (B) sites. The calculated sediment accumulation rate is 2.3 cm/y at the adjacent-exposed site. At the breakwater-protected site, there is an apparent increase in the accumulation rate, likely due to breakwater construction. The pre-construction (lower portion of profile) rate is 2.6 cm/y, similar to that observed at the adjacent-exposed, and the post-construction rate (upper portion of profile) is 4.9 cm/y.

Summary of sediment data:

The average diameter of surficial (upper 10 cm) sediments at the adjacent-exposed sites is 6.4±0.6 phi (11.8 μm), and the average organic content is 2.2±0.4%. Sediment at the breakwater-protected site is significantly ($p = 0.0001$) coarser, with an average median diameter of 2.5±0.03 phi (176.8 μm), and significantly ($p < 0.0001$) less

organic, with an average organic content of 0.4±0.1%. In the vibracore profiles, grain size is similar in the lower portion of both cores, with a relatively coarse base below 177 cm – average median diameter 3.1 phi (119.8 μm) – overlain by sediment that fines upward to an average median diameter of 7.1 phi (7.1 μm) at 65 cm. Above this depth, sediment behind the breakwater coarsens, whereas it remains relatively unchanged adjacent to the breakwater.

Adjacent to the breakwater, steady-state sedimentation dominates at a rate of 2.8 cm/y. However, there is an apparent change in accumulation rate behind the breakwater at 108 cm. The lower portion shows steady-state sedimentation and a rate of 2.6 cm/y, similar to the adjacent core. The upper portion has more variable activities, indicating episodic sedimentation, and an accumulation rate of 4.9 cm/y. At the surface of the core is a low-activity ~36-cm sand layer that is not included in the accumulation rate-calculations. This sand layer probably corresponds to that appearing between aerial photos taken in 2005 and 2007. If this sand layer is assumed to be a recent event layer with respect to ^{210}Pb, and the change in accumulation rate at 108 cm is assumed to coincide with breakwater construction, then 72 cm of sediment accumulated within the last 15 y, yielding a rate of 4.8 cm/y.

SAV Data:

Table EN2. Characteristics of the SAV *Zannichellia palustris* growing at the adjacent-exposed and breakwater-protected sites, values are reported as mean ±SE.

Location	Species	Shoot Length (cm)	Root Length (cm)	Above-ground Biomass (g m^{-2})	Below-ground Biomass (g m^{-2})	Total Biomass (g m^{-2})	Ratio Above-/ Below-ground Biomass
Adjacent-exposed	None						
Breakwater-protected	*Zannichellia palustris*	6.4± 0.1	2.9± 0.2	4.8± 1.3	2.1± 0.5	6.9± 1.8	2.2± 0.1

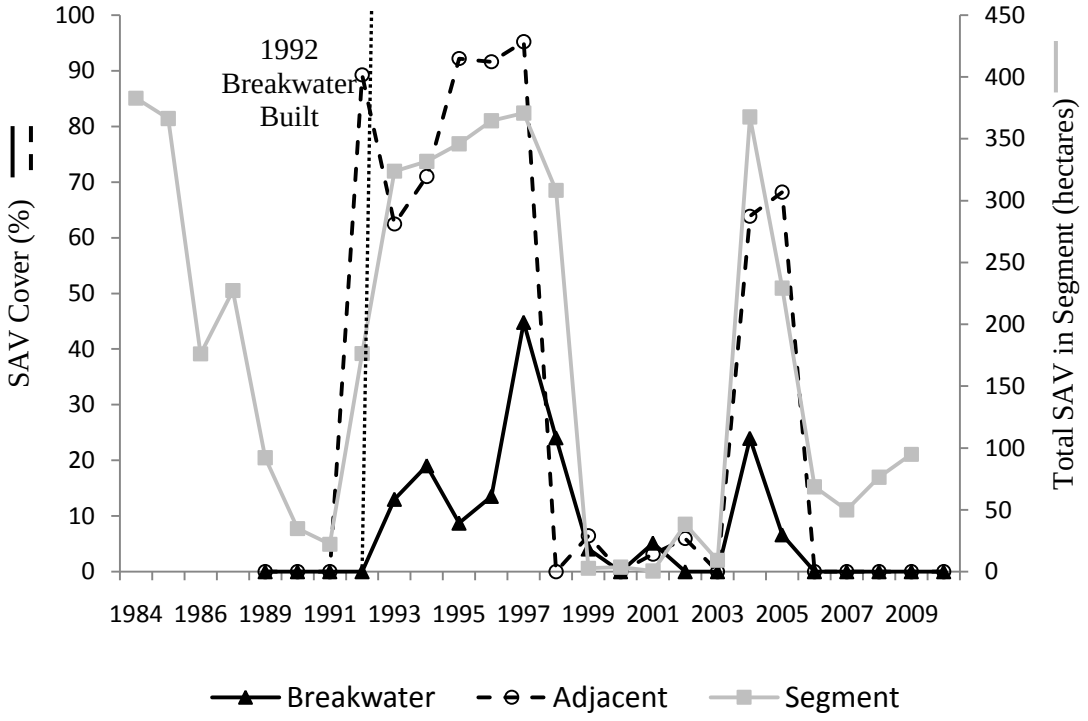

Figure EN4. SAV % cover plotted against the total SAV in the bay segment as determined by VIMS aerial photography from 7 years prior to breakwater installation to present day.

Zannichellia palustris

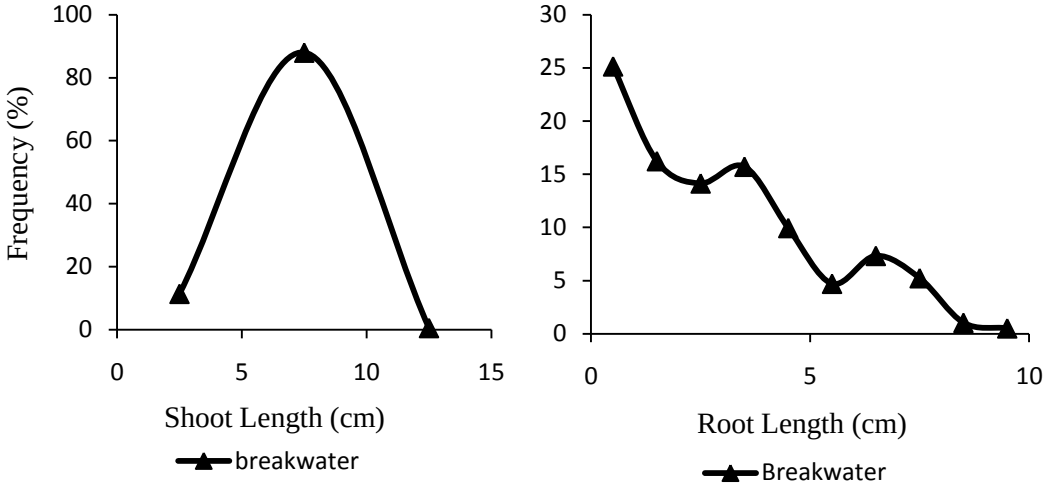

Figure EN5. (A) Shoot- and (B) root-length frequency plots for *Zannichellia palustris* at the adjacent-exposed (open circles) and breakwater-protected (closed triangle) sites.

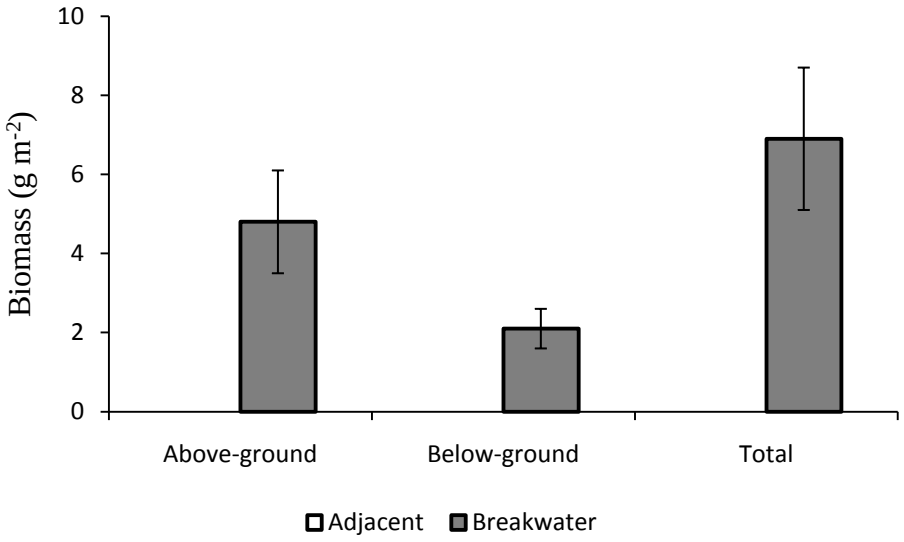

Figure EN6. Biomass of the SAV *Zannichellia palustris* at the adjacent-exposed (open bars) and breakwater-protected (closed bars) sites.

Summary of SAV data:

SAV abundance in the segment containing the Eastern Neck site was variable over the observation period. At Eastern Neck, SAV % cover generally mirrored the abundances seen in the section totals, but higher SAV % cover was usually seen in the adjacent site (Figure EN4).

It was difficult to draw conclusions about *Zannichellia palustris* due to small sample sizes, and no SAV present at the adjacent-exposed area. It is likely that the *Z. palustris* collected at the breakwater-protected site was affected by a seasonal dieback and not reduced due to the sediment characteristics. *Z. palustris* was only growing the area landward of the breakwater that had the sand event layer, SAV was absent from the portion of the breakwater that protected the rip rapped shoreline; this difference was probably due to sediment suitability. The adjacent-exposed site however, had sediments that were ~70% silt/clay, which has previously been demonstrated as unsuitable for SAV growth (Leschen et al., 2010; Koch et al., in prep).

Highland Beach

Description: The breakwater protecting Highland Beach is a linear, segmented, rock-mound breakwater consisting of 14 segments, with a total length of 804.2 m. Average segment length is 29±4 m (mean ± SD) and average gap length is 31±8 m. The breakwater is located 29±6 m from shore. The shoreline consists of a vegetated bank with rip rap at the base. Bayward of the rip rap is a sandy beach. Drain pipes protrude from the base of the bank and extend out to the breakwater segments. These drain pipes are located at almost every other breakwater segment. Water moving through the pipes is discharged bayward of the segments. The shoreline adjacent to the adjacent-exposed area is a sandy beach absent of the bank, rip rap, or drain pipes that characterize the shoreline adjacent to the breakwater-protected area. The bottom substrate in both areas had large ray pits and a resident school of rays in summer 2009.

Year of Construction: 1991

Age at Sampling: 18 years

Salinity Regime: Mesohaline

Fetch: Adjacent-exposed: 5.7±1.6 km

Breakwater-protected: 7.5±2.9 km

Sampling Coordinates:

HBA vbc	38º55'52.9"N	76º27'43.2"W
HBA pc	38º55'52.9"N	76º27'43.2"W
HBB vbc	38º56'02.6"N	76º27'34.1"W
HBB pc	38º56'02.6"N	76º27'34.1"W
No SAV		

Table HB1. Latitude and longitude of vibracores (vbc), pushcores (pc), and SAV cores taken in the adjacent-exposed ("A") and breakwater-protected ("B") sites at Highland Beach.

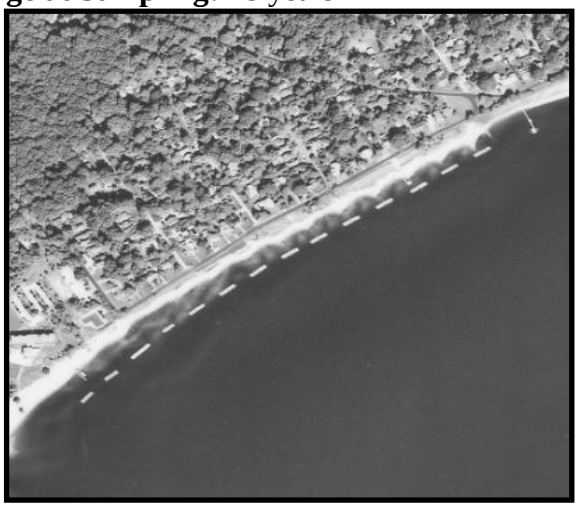

Figure HB1. Aerial photo of the breakwater breakwater at Highland Beach, MD.

Sediment Data:

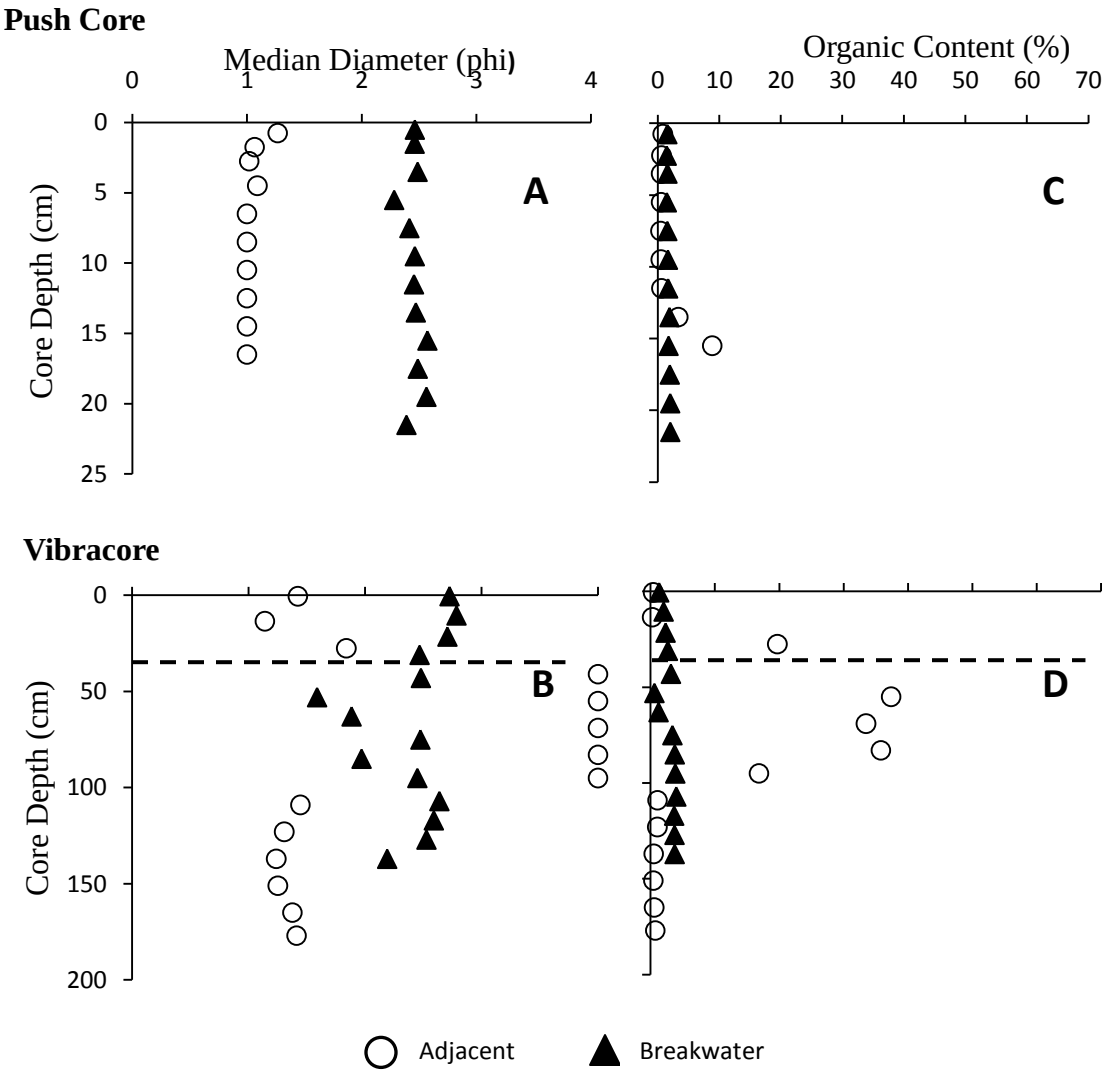

Figure HB2. Sediment grain size (median diameter) collected with a push core (A) or vibracore (B) at the adjacent-exposed (open circles) and breakwater-protected (closed triangles) sites. Sediment organic content collected with a push core (C) or vibracore (D) at the adjacent-exposed and breakwater-protected sites. In the vibracore profiles, the dashed line represents the interpreted depth of breakwater appearance (32 cm). Note that the adjacent-exposed site has a layer of highly organic, fine sediment from 40 to 96 cm in the vibracore profiles.

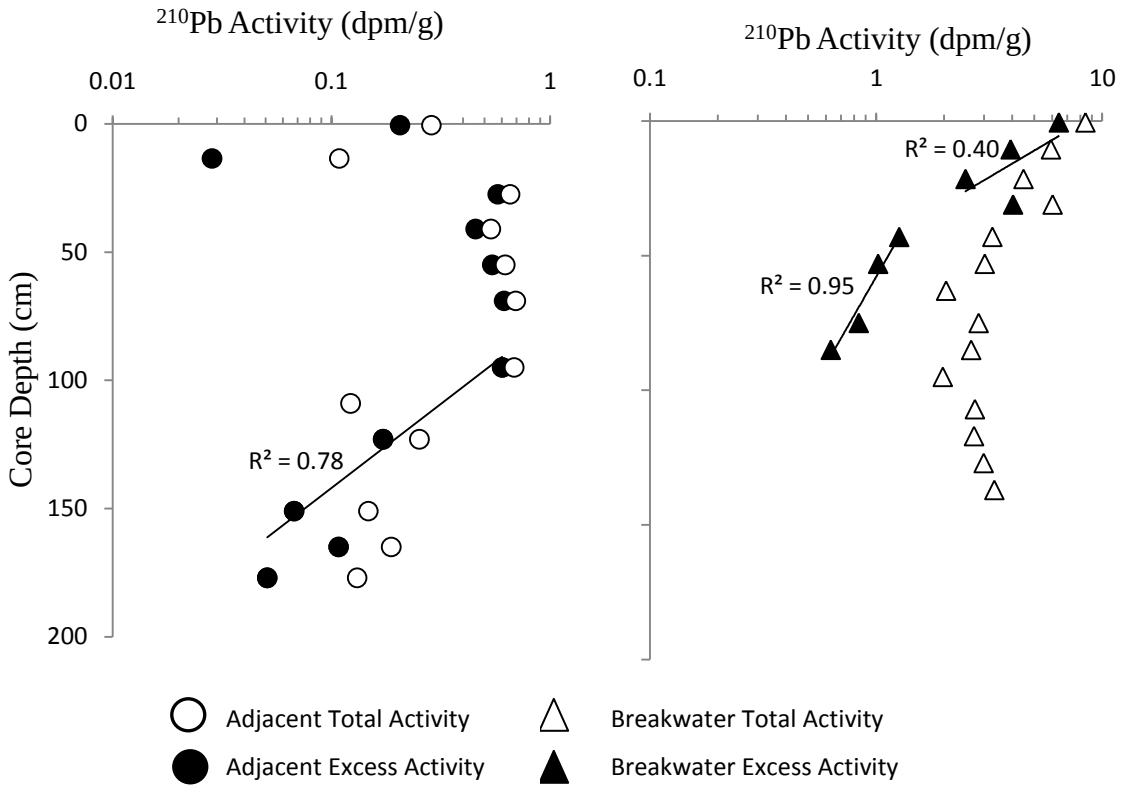

Figure HB3. ^{210}Pb profiles at the adjacent-exposed (A) and breakwater-protected (B) sites. The calculated sediment accumulation rate is 1.2 cm/y at the adjacent-exposed site. The ^{210}Pb profiles at the breakwater-protected site shows a change in slope at 32 cm – the pre-construction accumulation rate is 2.1 cm/y (lower portion of profile), decreasing to 1.7 cm/y post-construction (upper portion of profile). The x-axis scale differs between plots for visual clarity.

Summary of sediment data:

Surficial (upper 10 cm) sediment at the adjacent-exposed site has an average diameter of 1.1±0.1 phi (466.5 µm) and average organic content of 0.6±0.04%. The breakwater-protected site has finer sediments ($p < .0001$), with an average median

diameter of 2.4±0.03 phi (189.5 µm), that are more organic ($p < .0001$; average organic content 1.6±0.03%).

At the adjacent-exposed site, the ^{210}Pb profile has a thick (~100 cm) mixed layer with uniform activity, below which activities decrease logarithmically with depth. The accumulation rate calculated from this profile is 1.2 cm/y. In the breakwater-protected ^{210}Pb profile, a change in slope occurs at ~32 cm (Figure 2.4a) and is interpreted to be caused by breakwater installation. The sedimentation rate calculated for the lower portion of the profile is 2.1 cm/y, corresponding to pre-construction sedimentation. The rate for the upper portion is 1.7 cm/y, corresponding to post-construction sedimentation. This latter rate, multiplied by the breakwater age, yields a depth a 31 cm, supporting the conclusion that the change in slope is related to breakwater installation. There is little obvious change in either the grain size or organic content of post-construction material at this site (i.e., sediment above 32 cm), suggesting that the sediment source (most likely the sandy shoreline) is unchanged. The decrease in sedimentation rate may be due to reduced shoreline erosion, decreasing sediment supply. However, sediment grain size and organic content do not appear to be affected by the presence of the breakwater.

SAV Data:

No SAV was present at the adjacent-exposed or breakwater-protected sites at Highland Beach.

Gratitude

Description: This rock-mound semi-circular segmented breakwater has 3 segments, averaging 17±6 m (mean ± SD) in length with 19±1-m long gaps. The breakwater protects a small public beach and is located 13±2 m offshore. During low tides, the water directly behind the breakwater segments is very shallow. The shoreline adjacent to the adjacent-exposed site is a marsh that is protected with rip-rap.

Year of Construction: 1990 **Age at Sampling:** 19 years

Salinity Regime: Mesohaline

Fetch: Adjacent: 6.7±1.8 km

Breakwater: 6.7±1.8 km

Sampling Coordinates:

G A vbc	39º08'12.2"N	76º15'24.9"W
G A pc	39º08'12.2"N	76º15'24.9"W
G B vbc	39º08'13.7"N	76º15'24.6"W
G B pc	39º08'13.7"N	76º15'24.6"W

Table G1. Latitude and longitude of vibracores (vbc), and pushcores (pc) taken in the adjacent-exposed ("A") and breakwater-protected ("B") sites. There was no SAV observed at either site in 2009.

Figure G1. Aerial photo of the breakwater at Gratitude, MD.

Sediment Data:

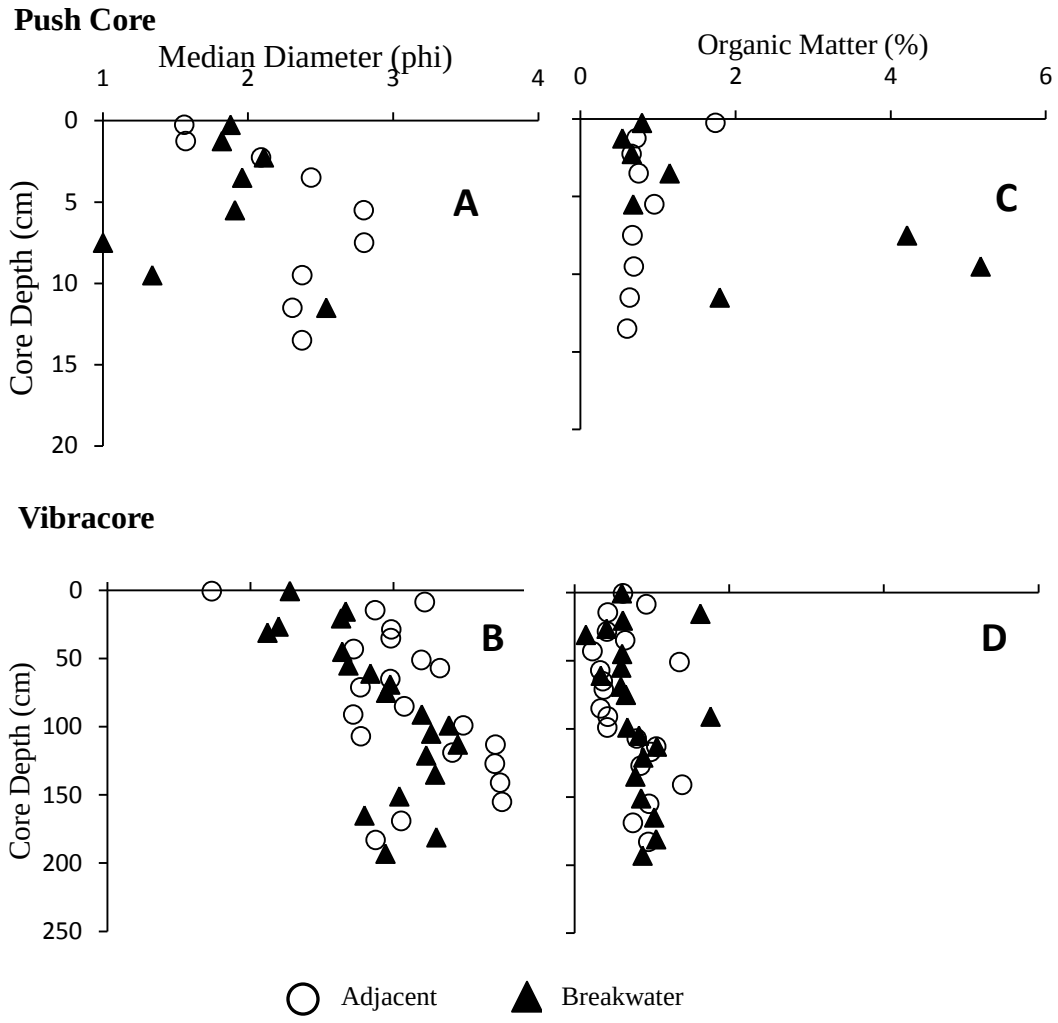

Figure G2. Sediment grain size (median diameter) collected with a push core (A) or vibracore (B) at the adjacent-exposed (open circles) and breakwater-protected (closed triangles) sites. Sediment organic content collected with a push core (C) or vibracore (D) at the adjacent-exposed and breakwater-protected sites. In the push-core profiles, the dashed line represents the interpreted depth of breakwater appearance (10 cm).

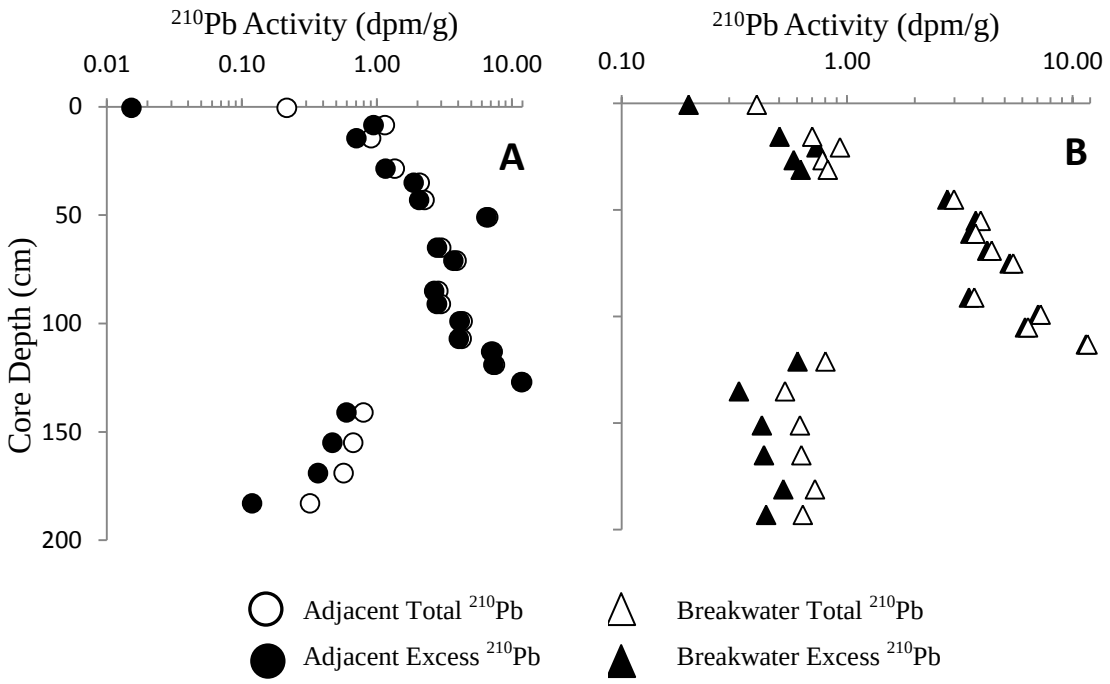

Figure G3. ^{210}Pb activity profiles at the adjacent-exposed (A) and breakwater-protected (B) sites. The calculated sediment accumulation rate is 1.9 cm/y for both the adjacent-exposed and breakwater-protected sites. Note that the latter represents the pre-construction sedimentation rate. Because activities increase with depth at both sites, accumulation rates are calculated by noting the presence of excess ^{210}Pb activity at the base of cores, corresponding to sediment <100y. Thus, the sedimentation rates should be regarded as minimum estimates. Also note that the x-axis scale differs between plots for visual clarity.

Summary of sediment data

Surface sediments (0-10 cm) did not differ significantly ($p = 0.06$) between the adjacent-exposed and breakwater-protected sites in grain size. The average median diameter at was 2.2±0.2 phi (217.6 µm) at the adjacent-exposed site and 1.7±0.2 phi (307.8 µm) at the breakwater-protected site. Average organic content was 1.0±0.1% at

the adjacent-exposed site and 1.9±0.7% at the breakwater-protected site ($p = 0.31$). At both sites, sediments have become coarser over time but organic content has remained similar, as shown in the vibracore profiles.

Decoding the sedimentary record at Gratitude is complicated. The ^{210}Pb activity profiles at the adjacent-exposed and breakwater-protected sites are remarkably similar. Both sites have a layer of increasing ^{210}Pb activity with depth. The highest ^{210}Pb activity is observed at 128 cm in the profile at the adjacent-exposed site, but only at 114 cm at the breakwater-protected site. For both sites, the increase in activity persists when activities are normalized to the mud content (data not shown), indicating that grain size is not the controlling factor but rather that changes in the initial activity of ^{210}Pb are likely responsible. Below this layer, activities return to similar values as observed at the surface of the core. Thus, the assumption of constant initial activity is violated at both sites, and accumulation rates must be calculated from the penetration depth of excess ^{210}Pb, which is at the base of both cores and yields a minimum sedimentation rate of 1.9 cm/y for both sites.

However, on the shorter time scale (~50 y) represented by ^{137}Cs, depth horizons are also offset between the adjacent-exposed and breakwater-protected sites, but in the opposite way. The penetration depth of ^{137}Cs is ~10 cm deeper at the breakwater-protected site (102 cm) than at the adjacent-exposed site (92 cm). Reconciling the penetration depths of both ^{210}Pb and ^{137}Cs would require erosion/non-deposition at the breakwater-protected site and/or increased deposition at the adjacent-exposed site between 50 and 100 years ago. Regardless of the cause, it is not linked to the presence of the breakwater, as it would have had to occur more than ~40 years before construction.

Changes in the sedimentary record associated with the presence of the breakwater can be seen in the push-core grain-size and organic-content profiles, which indicate a depth of influence of 10 cm, corresponding to observed coarsening and decrease in organic content, as well as the difference in ^{137}Cs penetration depths.

SAV Data:

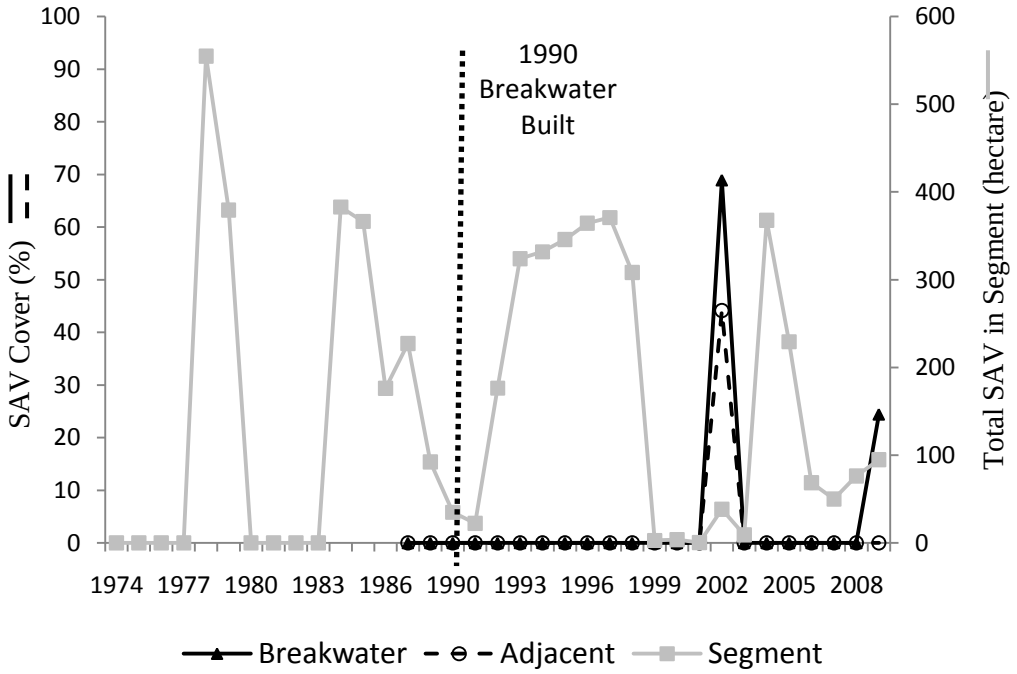

Figure G4. SAV % cover plotted against the total SAV in the bay segment as determined by VIMS aerial photography from 15 years prior to breakwater installation to present day.

Summary of SAV data:

SAV abundance in the segment containing the Gratitude site was extremely variable over the observation period. At Gratitude, SAV % cover was 0% until a small spike in 2001, mirroring a segment increase. It then dropped back to 0% in 2003. Both the adjacent and breakwater sites are relatively similar throughout, with only a minor deviation in 2009, where more SAV is seen behind the breakwater (Figure G4). SAV seen in aerial photo in 2009 was present in September, however; no SAV was present when sampling occurred in early June.

Brannock Bay

Description: The Brannock Bay rock-mound breakwater has 6 linear segments parallel to the shoreline, 3 which have filled in with marsh and are subaerially exposed. The remaining unattached segments have very shallow, warm water landward of them. Total length of the structure is 207.4 m. The mean segment length is 18±1 m (mean ± SD) and the average gap distance between segments is 13±2 m. The unattached portion of this structure is 7±7 m from the shoreline and protects a marshy shoreline with an eroding escarpment. The adjacent-exposed shoreline is hardened with a sea wall.

Year of Construction: 1989 **Age at Sampling:** 19 years

Salinity Regime: Mesohaline

Fetch: Adjacent: 5.1±1.6 km

Breakwater: 5.3±1.6 km

Sampling Coordinates:

BB A vbc	38º34'56.4"N	76º16'14.9"W
BB A pc	38º34'56.5"N	76º16'15.0"W
BB B vbc	38º34'55.9"N	76º16'16.4"W
BB B pc	38º34'55.9"N	76º16'16.3"W
SAV A1	38º34'55.7"N	76º16'15.6"W
SAV A2	38º34'55.7"N	76º16'15.6"W
SAV A3	38º34'58.1"N	76º16'12.2"W
SAV A4	38º34'57.8"N	76º16'12.0"W
SAV A5	38º34'56.2"N	76º16'15.3"W
SAV B1	38º34'54.1"N	76º16'19.3"W
SAV B2	38º34'54.7"N	76º16'18.2"W
SAV B3	38º34'54.7"N	76º16'18.1"W
SAV B4	38º34'55.3"N	76º16'17.3"W
SAV B5	38º34'55.5"N	76º16'16.6"W

Figure BB1. Aerial photo of the breakwater in Brannock Bay, MD.

Table BB1. Latitude and longitude of vibracores (vbc), pushcores (pc), and SAV cores taken in the adjacent-exposed ("A") and breakwater-protected ("B") sites in Brannock Bay.

Sediment Data:

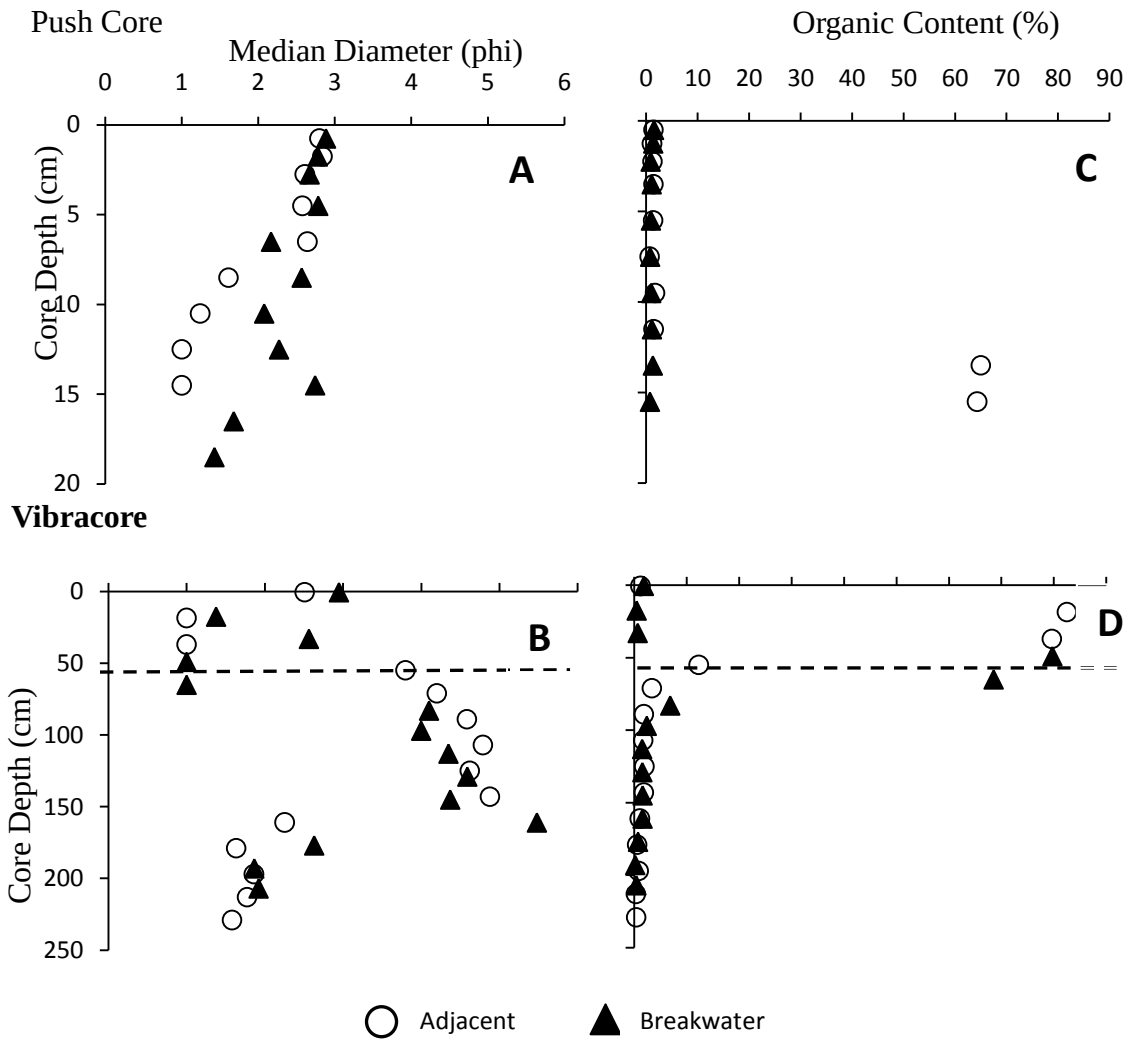

Figure BB2. Sediment grain size (median diameter) collected with a push core (A) or vibracore (B) at the adjacent-exposed (open circles) and breakwater-protected (closed triangles) sites. Sediment organic content collected with a push core (C) or vibracore (D) at the adjacent-exposed and breakwater-protected sites. The dashed line represents the interpreted depth of breakwater appearance. Note that because it is below the penetration depth of the push cores, it is not shown in (A) or (C).

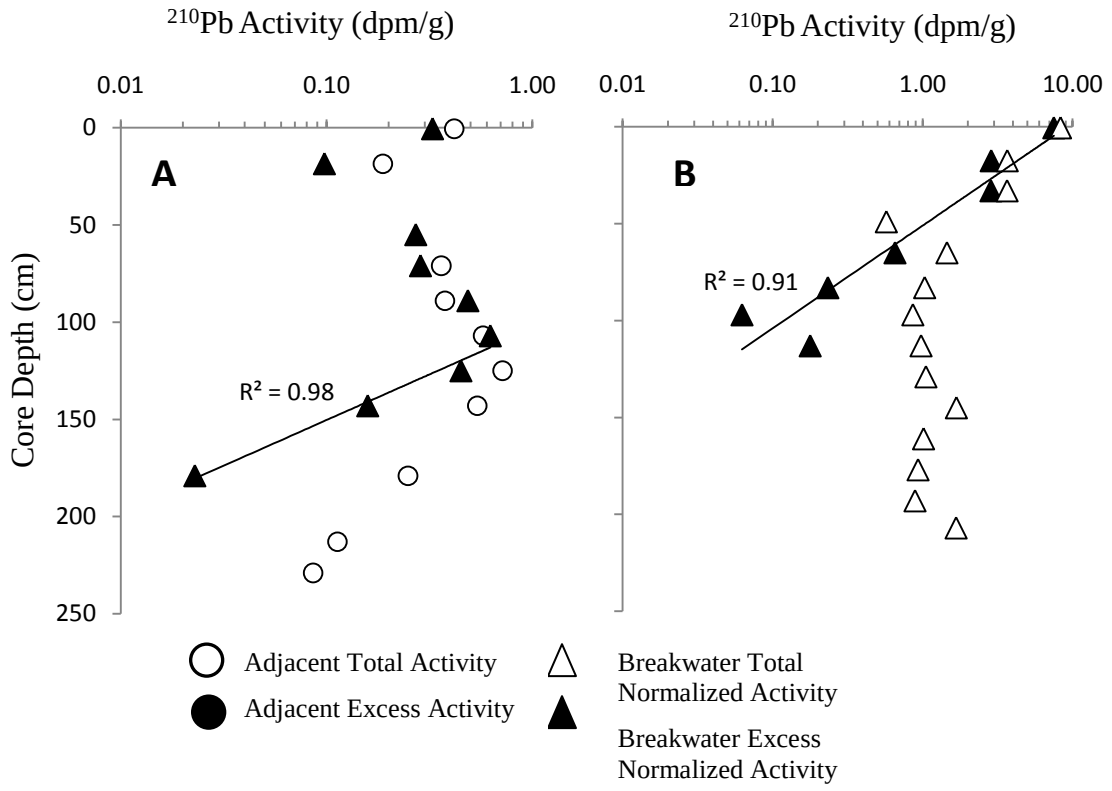

Figure BB3. ^{210}Pb profiles at the adjacent-exposed (A) and breakwater-protected (B) sites. The calculated sediment accumulation rate is 0.9 cm/y at the adjacent-exposed site and 1.0 cm/y at the breakwater-protected site. Because the mud content changes throughout the core at the breakwater-protected site, and since ^{210}Pb attaches preferentially to fine-grained (mud) particles, ^{210}Pb activities for each depth horizon in this core were normalized to the corresponding mud content prior to the accumulation-rate calculation.

Summary of sediment data

Push-core grain-size data showed a similar, fining-upward trend ($p = 0.41$) at both the adjacent-exposed and breakwater-protected sites. Sediment fined from coarse sand at

the base to fine sand at the top of the core. The average median diameter of surficial sediment (0-10 cm) at both sites was classified by fine sand (adjacent-exposed, 2.5±0.2 phi (153.9 μm); breakwater-protected, 2.6±0.1 phi (164.9 μm). Surficial organic content is also similar at both sites ($p = 0.29$) – 1.3±0.1% at the adjacent-exposed site, and 1.1±.1% at the breakwater-protected site.

Comparison of trends in the vibracore sediment-character (grain size, organic content) data revealed that both sites have experienced the same sedimentological changes over time; however, they are offset 30 cm, with layers displaced deeper in the breakwater-protected core. While there are no obvious changes in sediment character that can be attributed to breakwater construction, the distinct, but offset, layering present in both the grain-size and organic-content profiles indicates that 30 cm of sediment has likely deposited since breakwater construction.

The ^{210}Pb profile at the adjacent-exposed site had a thick (116 cm), uniform-activity layer overlying the region of logarithmic decay, and the sediment accumulation rate at this site was 0.9 cm/y. This uniform-activity layer was not present at the breakwater-protected site; the ^{210}Pb profile at this site indicates steady-state sedimentation and an accumulation rate of 1.0 cm/y. This rate represents the pre-construction sedimentation rate; the post-construction rate is 1.6 cm/y – derived by attributing the 30-cm offset to deposition following breakwater installation 19-y ago. ^{137}Cs activities were measured at this location; however, activities were near or below the detection limit at both adjacent-exposed and breakwater-protected sites. For example, ^{137}Cs was present at 83 cm but not at 79 cm. Thus, ^{137}Cs was not used to calculate accumulation rates for this location.

Breakwater installation in Brannock Bay does not appear to have affected the character (grain size, organic content) of post-construction sediment, but did increase the rate of sedimentation in the breakwater-protected area.

SAV data:

Table BB2. Characteristics of the SAV *Ruppia maritima* growing at the adjacent-exposed and breakwater-protected sites. Values are reported as mean ± SE.

Location	Species	Shoot Length (cm)	Root Length (cm)	Above-ground Biomass (g m^{-2})	Below-Ground Biomass (g m^{-2})	Total Biomass (g m^{-2})	Ratio Above-/ Below Ground Biomass
Adjacent-exposed	*Ruppia maritima*	3.8± 0.1	4.5± 0.2	7.3± 3.3	11.9± 4.9	19.3±8.2	0.6± 0.1
Breakwater-protected	*Ruppia maritima*	4.1± 0.1	4.7± 0.3	3.4± 0.6	2.4± 0.5	5.8±0.9	1.6± 0.4

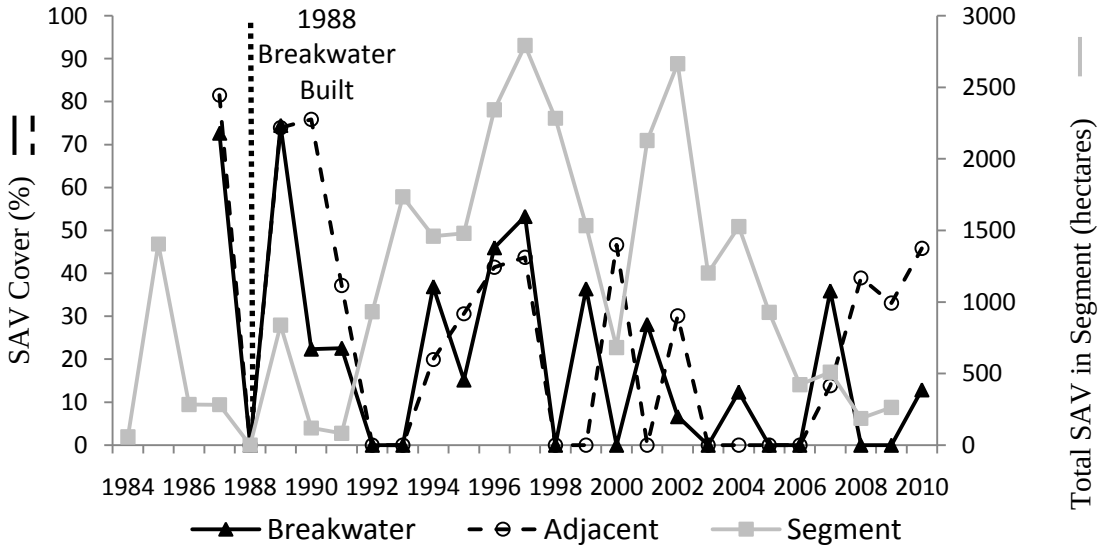

Figure BB4. SAV % cover plotted against the total SAV in the bay segment as determined by VIMS aerial photography from 4 years prior to breakwater installation to present day.

Ruppia maritima

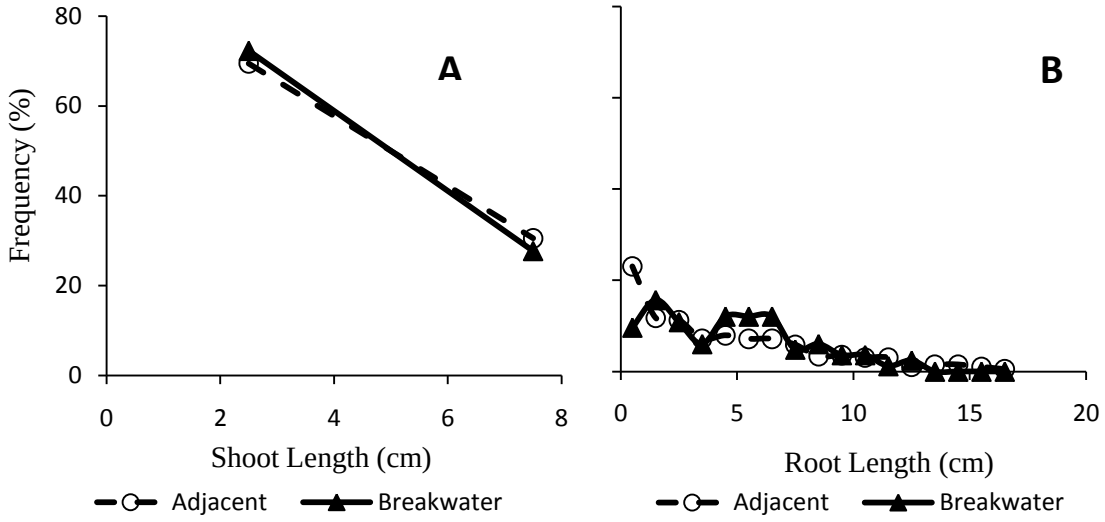

Figure BB5. (A) Shoot- and (B) root-length frequency plots for *Ruppia maritima* at the adjacent-exposed (open circles) and breakwater-protected (closed triangle). Shoot frequency data appears to have only 2 points for each site however, 131 shoots were measured at the breakwater-protected site but lengths fell into only 2 ranges (0-5 and 5-10 cm). The same was observed at the adjacent-exposed site where 382 shoots were measured.

Ruppia maritima

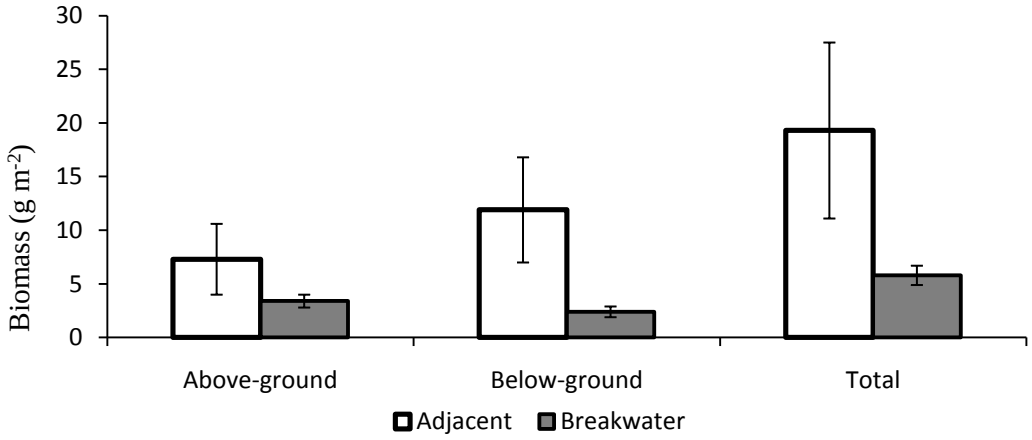

Figure BB6. Biomass of the SAV *Ruppia maritima* at the adjacent-exposed (open bars) and breakwater-protected (closed bars) sites.

Summary of SAV data

SAV abundance in the segment containing the Brannock Bay site was variable over the observation period. At Brannock Bay, SAV % cover mirrored the total SAV abundance in the segment, with very little observable difference between adjacent and breakwater sampling sites (Figure BB4).

Ruppia maritima average shoot- and root-lengths (Table BB2; Figure BB5) were similar (shoots, $p = 0.08$; roots, $p = 0.59$) at the adjacent-exposed and breakwater-protected sites. Total biomass, however; was greater ($p = 0.05$) in the adjacent-exposed site versus the breakwater-protected (Figure BB6). This could have been due to the shallowness of the water landward of the structure, some breakwater segments have already had marsh become established connecting the breakwater segments to the shoreline. At the time of sampling the water was also observed to be rather warm. This breakwater created favorable conditions for marsh to establish itself behind the breakwater – so in this case it was detrimental to SAV but beneficial to the marsh.

Cape Charles Bay Creek

Description: The rock-mound breakwater located at Cape Charles Bay Creek has 7 linear segments in a parallel orientation to the shoreline. The total breakwater length is 657.6 m, with a mean segment length of 69±1 m (mean ± SD) and gaps averaging 125±4 m. The shoreline is characterized as a sandy beach, and the breakwater is located 38±20 m off shore.

Year of Construction: 2006 **Age at Sampling:** 3 years

Salinity Region: Polyhaline

Fetch: Adjacent: 8.8±2.3 km

Breakwater: 11.9±2.9 km

Sampling Coordinates:

CCBC A vbc	37º16'53.3"N	76º00'44.1"W
CCBC A pc	37º16'53.3"N	76º00'44.1"W
CCBC B vbc	37º16'41.1"N	76º00'55.9"W
CCBC B pc	37º16'41.1"N	76º00'55.9"W
SAV A1	37º16'46.6"N	76º00'47.0"W
SAV A2	37º16'47.4"N	76º00'47.8"W
SAV A3	37º16'48.7"N	76º00'46.7"W
SAV A4	37º16'49.5"N	76º00'45.8"W
SAV A5	37º16'20.8"N	76º01'18.6"W
SAV B1	37º16'30.4"N	76º01'07.1"W
SAV B2	37º16'31.1"N	76º01'06.1"W
SAV B3	37º16'32.3"N	76º01'04.5"W
SAV B4	37º16'36.5"N	76º01'00.0"W
SAV B5	37º16'41.3"N	76º00'54.3"W
SAV B6	37º16'43.9"N	76º00'50.7"W

Figure CCBC1. Aerial photo of the breakwater at Cape Charles Public Beach, VA

Table CCBC1. Latitude and longitude of vibracores (vbc), pushcores (pc), and SAV cores taken in the adjacent-exposed ("A") and breakwater-protected ("B") sites at Cape Charles Bay Creek.

Sediment Data:

Push Core

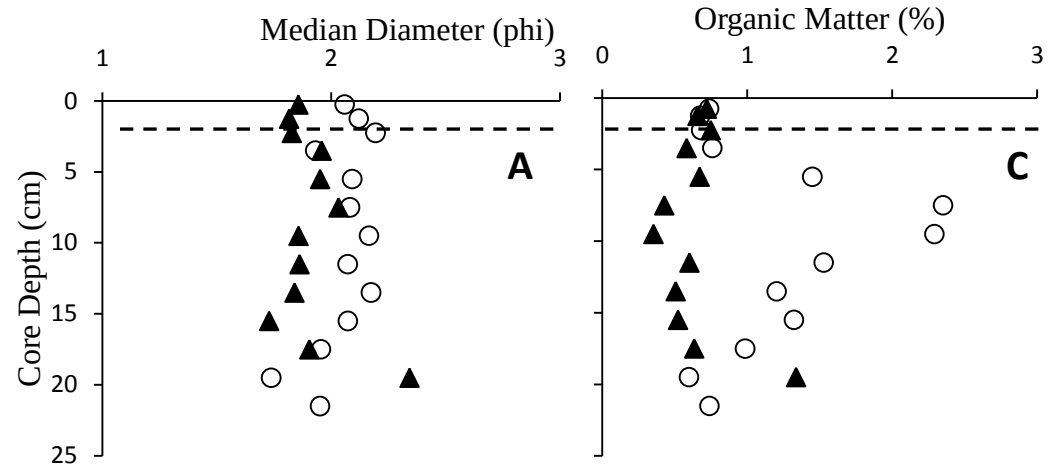

Vibracore

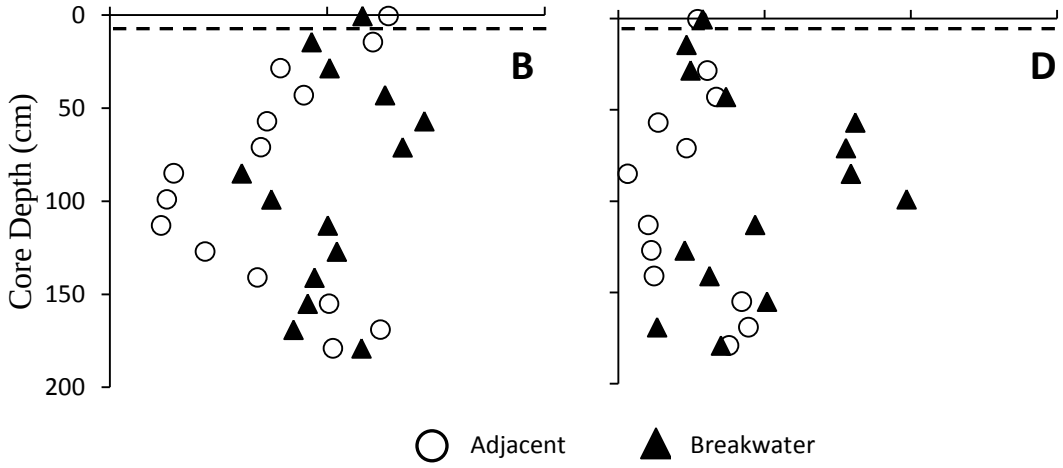

Figure CCBC2. Sediment grain size (median diameter) collected with a push core (A) or vibracore (B) at the adjacent-exposed (open circles) and breakwater-protected (closed triangles) sites. The dashed line represents the interpreted depth of breakwater appearance. Sediment organic content collected with a push core (C) or vibracore (D) at the adjacent-exposed and breakwater-protected sites.

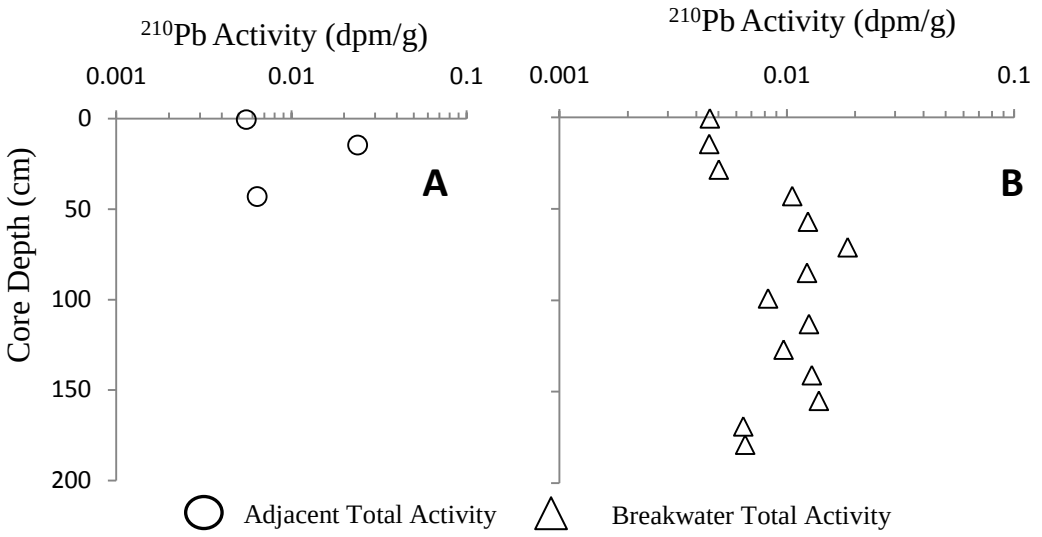

Figure CCBC3. ^{210}Pb profiles at the adjacent-exposed (A) and breakwater-protected (B) sites. At the adjacent-exposed site, only 3 samples had detectable ^{210}Pb, and activities for both sites are much lower than those measured at any other site. Excess activities are not plotted, as activities are below the supported value.

Summary of sediment data

Surficial (top 10 cm) sediment at the adjacent-exposed site was sandy (average median diameter of surficial sediment 2.1±0.04 phi, 233.3 µm) and low in organic content (1.3±0.3%). Surficial sediment in the breakwater-protected area was also sandy (average median diameter 1.9±0.04 phi, 267.9 µm), coarser ($p = 0.001$) than that at the adjacent-exposed site, and less organic (0.6±0.08%; $p = 0.04$).

Both sites are Cape Charles Bay Creek are net erosional, on a ~100-y time scale. ^{210}Pb depth-integrated inventories are below the atmospherically supported inventory (~25 dpm/cm^2; Kim et al., 2000), indicating net erosion. The inventories at the adjacent-

exposed and breakwater-protected sites are 0.42 dpm/cm^2 and 1.48 dpm/cm^2, respectively. When normalized to the mud content, which would remove the effect of dilution by coarse sediment, inventories are 1.31 dpm/cm^2 and 8.56 dpm/cm^2, respectively. The adjacent-exposed core was taken at the entrance to an inlet, and the breakwater-protected core was collected in between segments, likely explaining the erosional nature of these cores.

While pre-construction (~100-y) sedimentation at this location was net erosional, there is an increase in the median diameter of push-core sediments at the breakwater-protected site ~2.5 cm deep. If this horizon represents the depth of breakwater influence, then the post-construction rate would be 0.8 cm/y. Thus, the breakwater appears to be trapping sandy sediment in the protected area, which had previously been net erosional.

SAV Data:

Table CCBC2. Characteristics of the SAV species *Ruppia maritima* and *Zostera marina* growing at the adjacent-exposed and breakwater-protected sites, values are reported as mean ±SE.

Location	Species	Shoot Length (cm)	Root Length (cm)	Above-Ground Biomass (g m^{-2})	Below-ground Biomass (g m^{-2})	Total Biomass (g m^{-2})	Ratio Above-/ Below-Ground Biomass
Adjacent-exposed	*Ruppia maritima*	6.1± 0.1	7.6± 0.3	12.6± 5.8	10.0± 3.5	22.6± 9.0	1.1± 0.2
Breakwater-protected	*Ruppia maritima*	9.9± 0.2	8.4± 0.3	19.4± 9.7	13.7± 7.6	33.1± 17.1	1.7± 0.5
Adjacent-exposed	*Zostera marina*	9.6± 0.7	7.7± 0.8	7.2± 6.6	9.6	12.0± 11.4	1.4
Breakwater-protected	*Zostera marina*	19.2± 0.6	6.2± 0.2	66.0± 23.1	33.1± 9.9	99.2± 32.9	1.6± 0.4

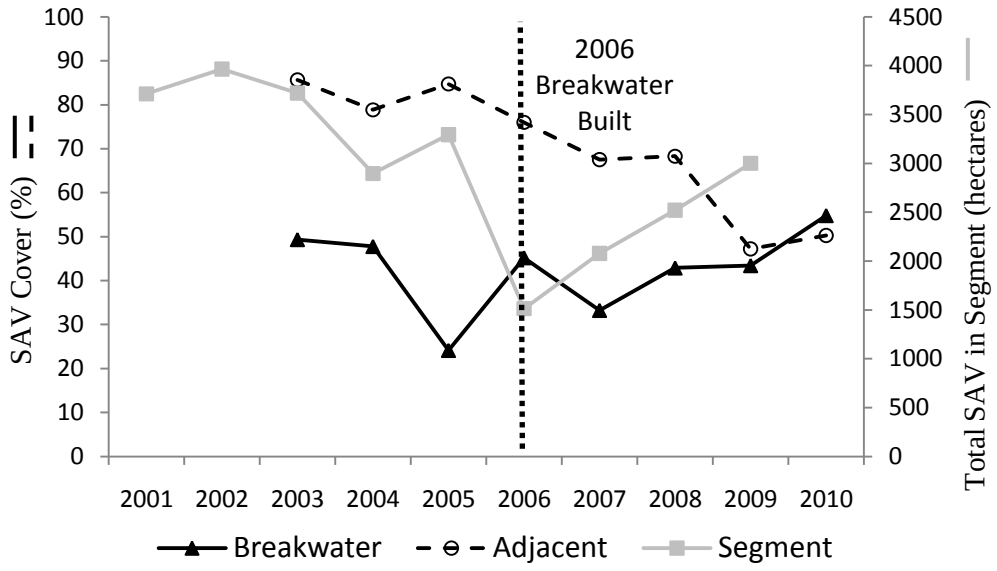

Figure CCBC4. SAV % cover plotted against the total SAV in the bay segment as determined by VIMS aerial photography from 5 years prior to breakwater installation to 2010.

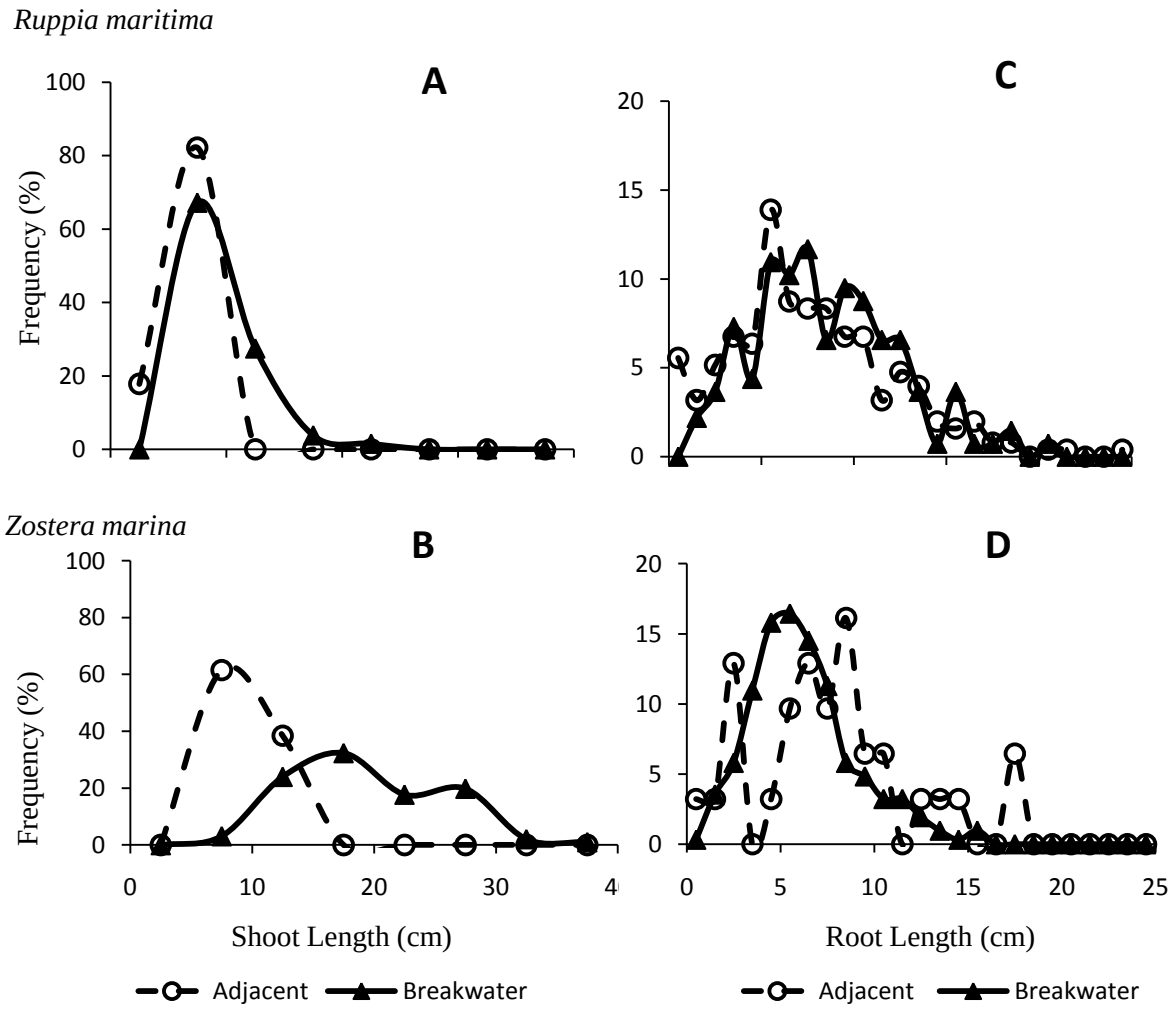

Figure CCBC5. (A) Shoot- and (C) root-length frequency plots for *Ruppia maritima* and (B) shoot- and (D) root-length frequency plots for *Zostera marina* at the adjacent-exposed (open circles) and breakwater-protected (closed triangle) sites.

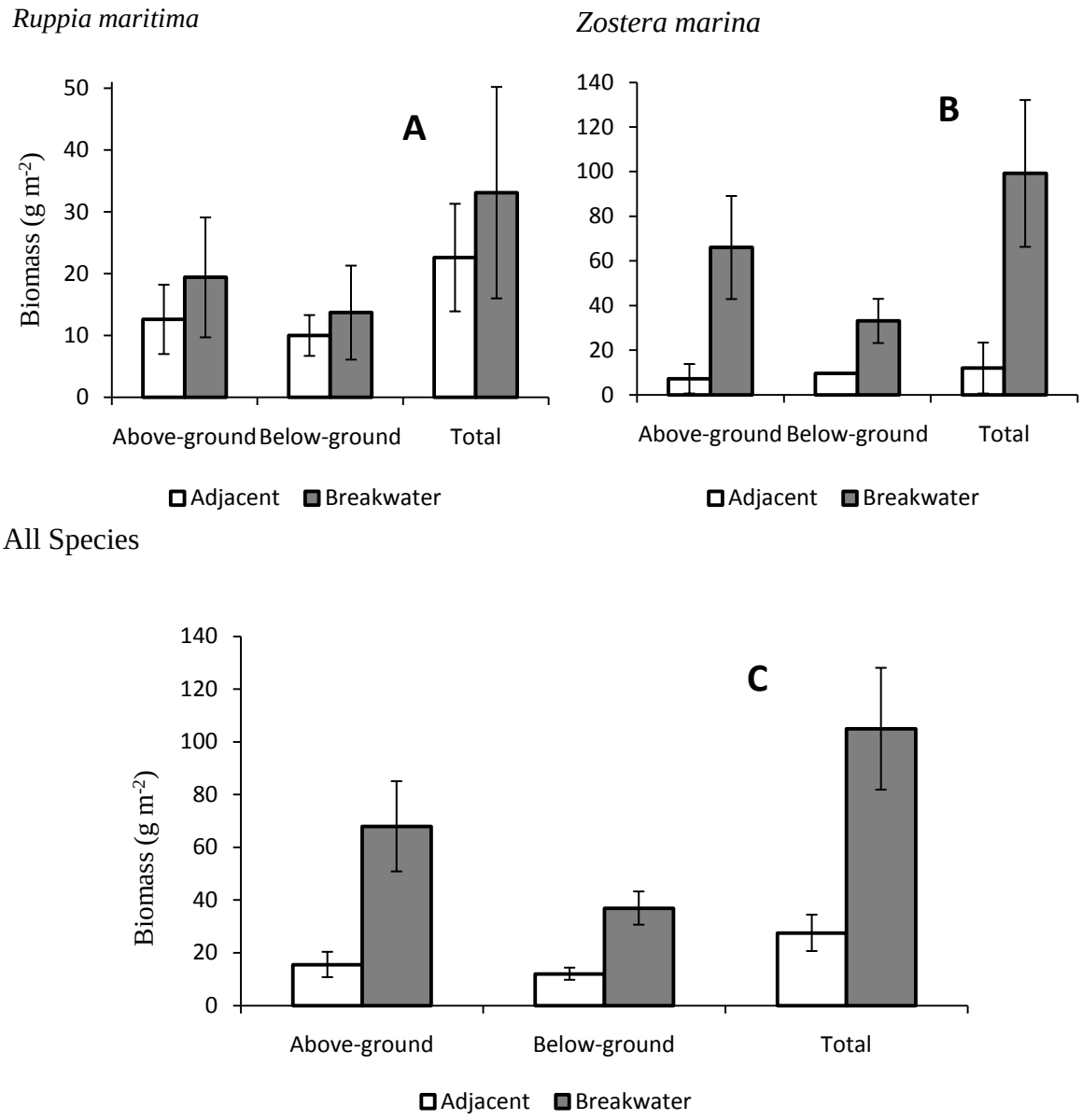

Figure CCBC6. Biomass of the SAV (A) *Ruppia maritima*, (B) *Zostera marina*, and (C) all species of SAV at the adjacent-exposed (open bars) and breakwater-protected (closed bars) sites.

Summary of SAV data:

SAV abundance in the segment containing the Cape Charles Bay Creek site decreased prior to the date of breakwater installation and then appeared to be increasing. At Bay Creek, SAV % cover decreased, in the years preceding the breakwater, similar to the segment totals. After installation, % cover in the adjacent area continued to decrease, but the area protected by the breakwater increased, again mirroring the overall segment pattern (Figure CCBC4).

Both *Ruppia maritima* and *Zostera marina* had longer shoot lengths at the breakwater-protected sites ($p < 0.0001$, for both species) than the adjacent-exposed. *R. maritima* roots were also longer at the breakwater-protected site ($p = 0.05$) than the adjacent-exposed, however *Z. marina* roots were longer ($p = 0.01$) at the adjacent-exposed site (Table CCBC2; Figure CCBC5). Total biomass was greater ($p = 0.02$) at the breakwater-protected site than the adjacent exposed. The breakwater at Cape Charles Bay Creek appears to be beneficial to the SAV in the area.

Cape Charles Public Beach

Description: This linear, segmented, rock-mound breakwater has 3 larger V-shaped segments, and 2 smaller straight segments. The total breakwater length is 412.1 m, with segment lengths 46±24 m (mean ± SD) and gap lengths 56±25 m. Average distance from shore is 38±20 m. This breakwater protects an engineered sandy beach. The adjacent-exposed site shoreline is also sandy beach.

Year of Construction: 2002 **Age at Sampling:** 7 years

Salinity Regime: Polyhaline

Fetch: Adjacent: 21.0±4.5 km

Breakwater: 18.2±3.9 km

Sampling Coordinates:

CCPB A vbc	37º16'09.5"N	76º01'26.7"W
CCPB A pc	37º16'09.5"N	76º01'26.7"W
CCPB B vbc	37º16'16.6"N	76º01'23.0"W
CCPB B pc	37º16'16.6"N	76º01'23.0"W
SAV A1	37º16'08.4"N	76º01'26.1"W
SAV A2	37º16'08.1"N	76º01'26.1"W
SAV A3	37º16'07.3"N	76º01'26.3"W
SAV A4	37º16'06.9"N	76º01'26.4"W
SAV A5	37º16'07.0"N	76º01'26.5"W
SAV B1	37º16'19.7"N	76º01'19.9"W
SAV B2	37º16'19.0"N	76º01'20.7"W
SAV B3	37º16'18.8"N	76º01'20.9"W
SAV B4	37º16'17.0"N	76º01'22.0"W
SAV B5	37º16'13.6"N	76º01'23.4"W

Table CCPB1. Latitude and longitude of vibracores (vbc), pushcores (pc), and SAV cores taken in the adjacent-exposed ("A") and breakwater-protected ("B") sites at Cape Charles Public Beach.

Figure CCPB1. Aerial photo of the breakwater at Cape Charles Public Beach, VA.

Sediment Data:

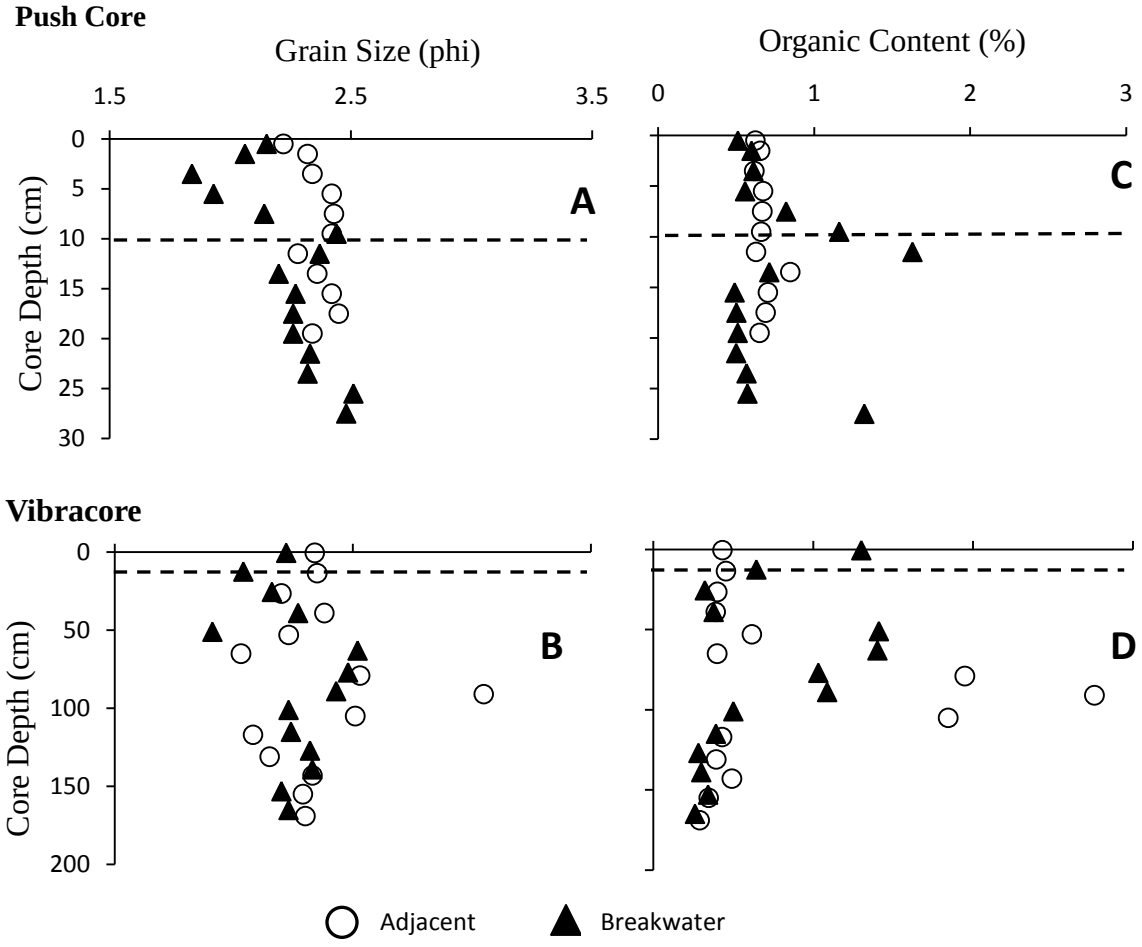

Figure CCPB2. Sediment grain size (median diameter) collected with a push core (A) or vibracore (B) at the adjacent-exposed (open circles) and breakwater-protected (closed triangles) sites. The dashed line represents the interpreted depth of breakwater appearance. Sediment organic content collected with a push core (C) or vibracore (D) at the adjacent-exposed and breakwater-protected sites.

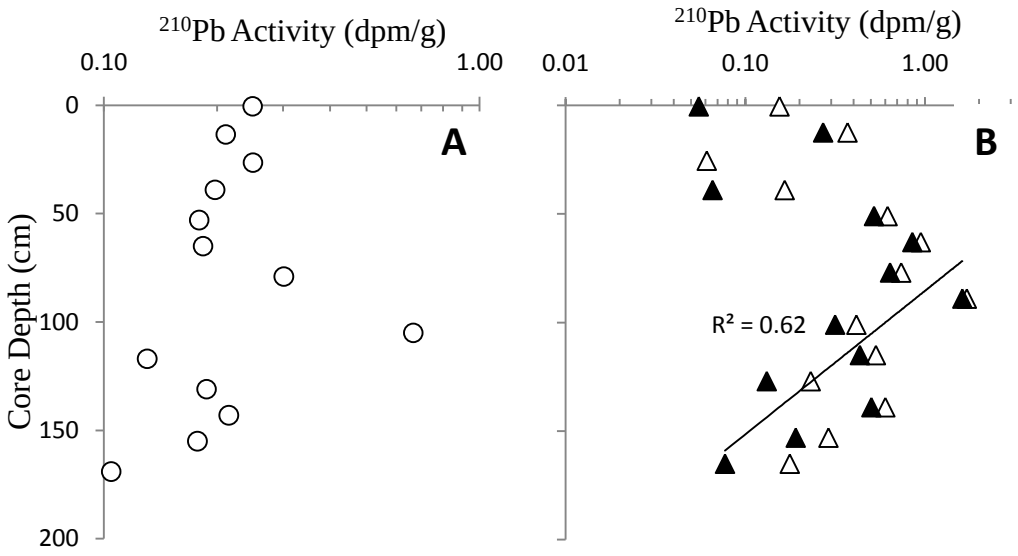

Figure CCPB3. ^{210}Pb activity profiles at the adjacent-exposed (A) and breakwater-protected (B) sites. The calculated sediment accumulation rate is 1.4 cm/y for the breakwater-protected sites, representing the pre-construction sedimentation rate. The adjacent-exposed site is erosional, indicated by its low depth-integrated inventory. Note that the x-axis scale differs between plots.

Summary of sediment data:

Surficial (top 10 cm) sediment at the adjacent-exposed site was sandy (average median diameter of surficial sediment 2.3±0.04 phi, 203.1 µm) and low in organic content (0.6±0.01%). This site is erosional, indicated by its low depth-integrated ^{210}Pb activity of 13.9 dpm/cm^2, which is below the atmospheric inventory of ~25 dpm/cm^2 (Kim et al., 2000). The depth-integrated inventory at this site is below this value, even when measured activities are normalized to the mud content (18.3 dpm/cm^2, indicating erosion. Normalizing the activities (and adjusting the corresponding supported level of

^{210}Pb) before calculating the inventory removes the potential effect of dilution by coarse particles that may not scavenge ^{210}Pb as effectively.

Surficial sediment in the breakwater-protected area was also sandy (average median diameter 2.1±0.1 phi, 233.3 μm), and significantly ($p = 0.03$) coarser than that at the adjacent-exposed site, and had similar organic content (0.7±0.2%; $p = 0.26$). The pre-construction accumulation rate for this site is 1.4 cm/y, calculated from the ^{210}Pb profile. The depth-integrated ^{210}Pb inventory, when normalized for mud content, is 43.2 dpm/cm^2, which is above the atmospheric inventory and supports the interpretation of net sedimentation.

The depth of breakwater influence is most clearly indicated in the push-core grain-size profile, where sediment coarsens above 10 cm. Dividing this depth by the breakwater age at the time of sampling (7 y) yields a post-construction rate of 1.4 cm/y, equal to the pre-construction rate. Thus, the effect of breakwater construction on sediments at Cape Charles Public Beach appears to be an increase in grain size (decreasing phi units), and no change in organic content or sedimentation rate.

SAV Data:

Table CCPB2. Characteristics of the SAV *Ruppia maritima* and *Zostera marina* growing at the adjacent-exposed and breakwater-protected sites, values are reported as mean ±SE.

Location	Species	Shoot Length (cm)	Root Length (cm)	Above-ground Biomass ($g\ m^{-2}$)	Below-ground Biomass ($g\ m^{-2}$)	Total Biomass ($g\ m^{-2}$)	Ratio Above-/ Below-ground Biomass
Adjacent-exposed	*Ruppia maritima*	7.5± 0.1	8.8± 0.3	15.9± 9.1	17.3± 8.7	33.2± 17.5	1.4± 0.5
Breakwater-protected	*Ruppia maritima*	7.8± 0.2	7.8± 0.2	38.1± 1.1	34.0± 7.8	72.1± 8.9	1.2± 0.2
Adjacent-exposed	*Zostera marina*	21.9± 0.9	6.5± 0.1	125.6± 78.7	105.3± 47.3	230.9± 123.6	1.2± 0.2
Breakwater-protected	*Zostera marina*	21.4± 1.2	7.1± 0.1	221.9± 60.0	152.9± 52.9	374.8± 46.6	2.6± 1.6

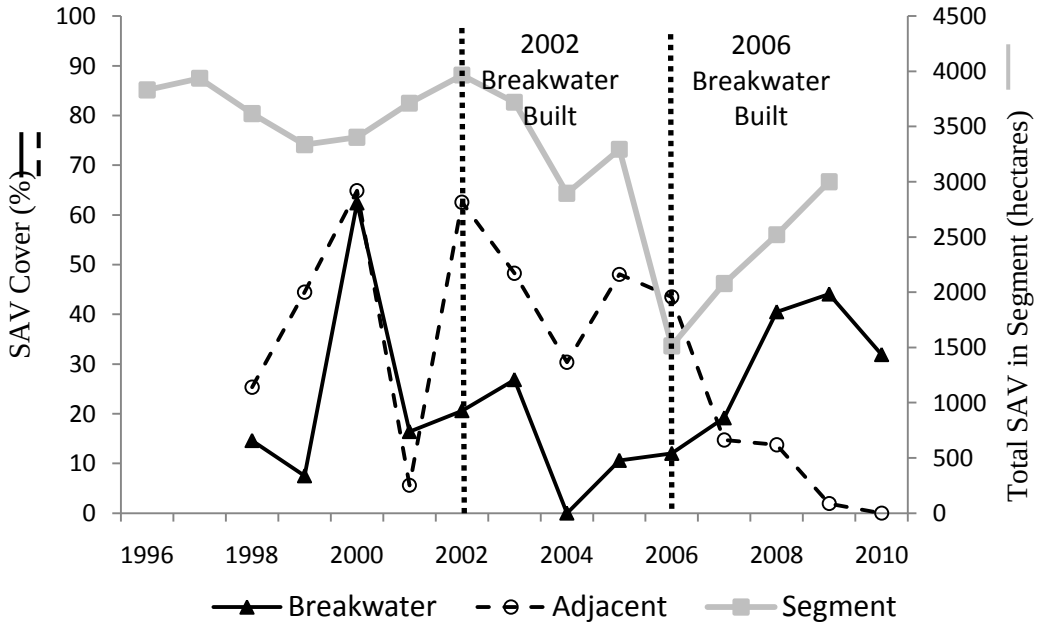

Figure CCPB4. SAV % cover plotted against the total SAV in the bay segment as determined by VIMS aerial photography. Two breakwaters were installed on different dates at this site as indicated by the vertical dotted lines on the figure.

Ruppia maritima

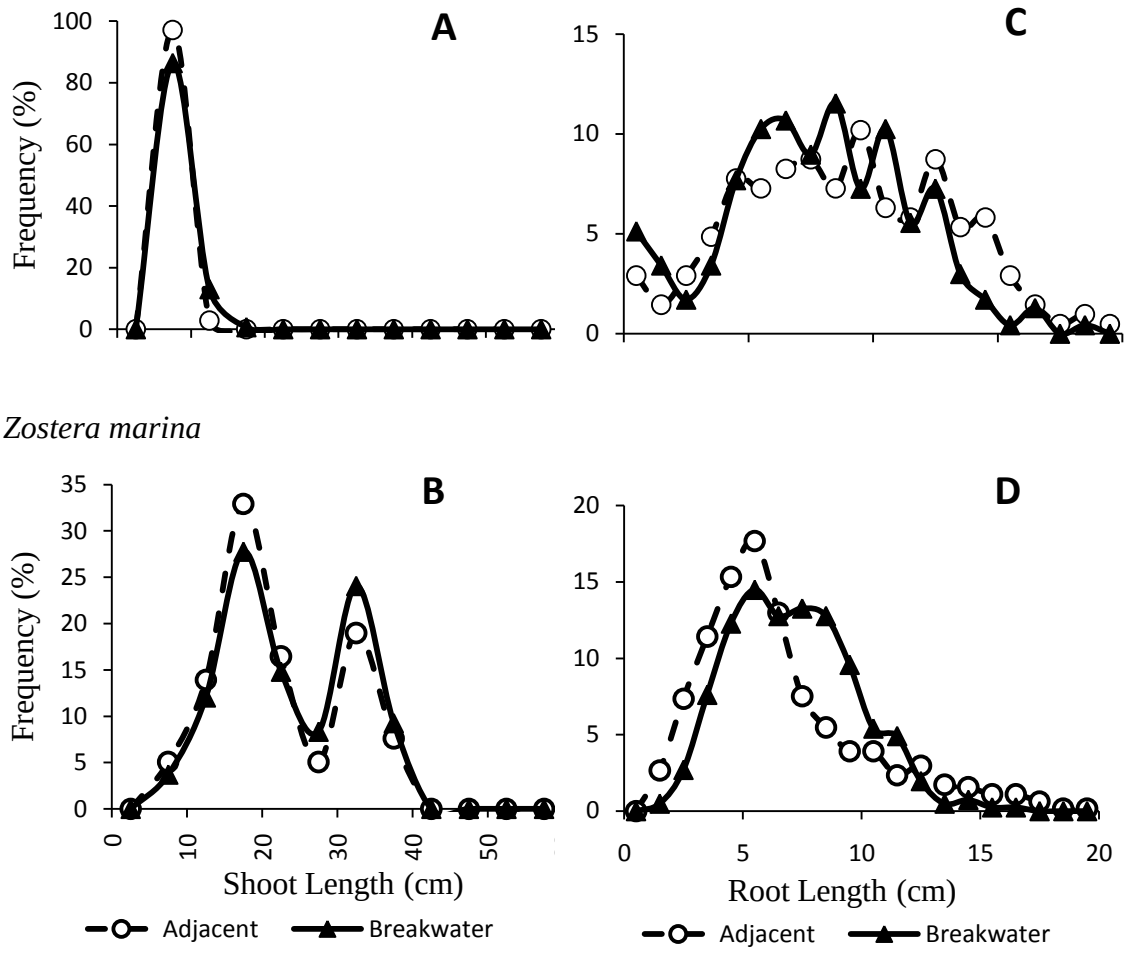

Zostera marina

Figure CCPB5. (A) Shoot- and (C) root-length frequency plots for *Ruppia maritima* and (B) shoot- and (D) root-length frequency plots for *Zostera marina* at the adjacent-exposed (open circles) and breakwater-protected (closed triangle) sites.

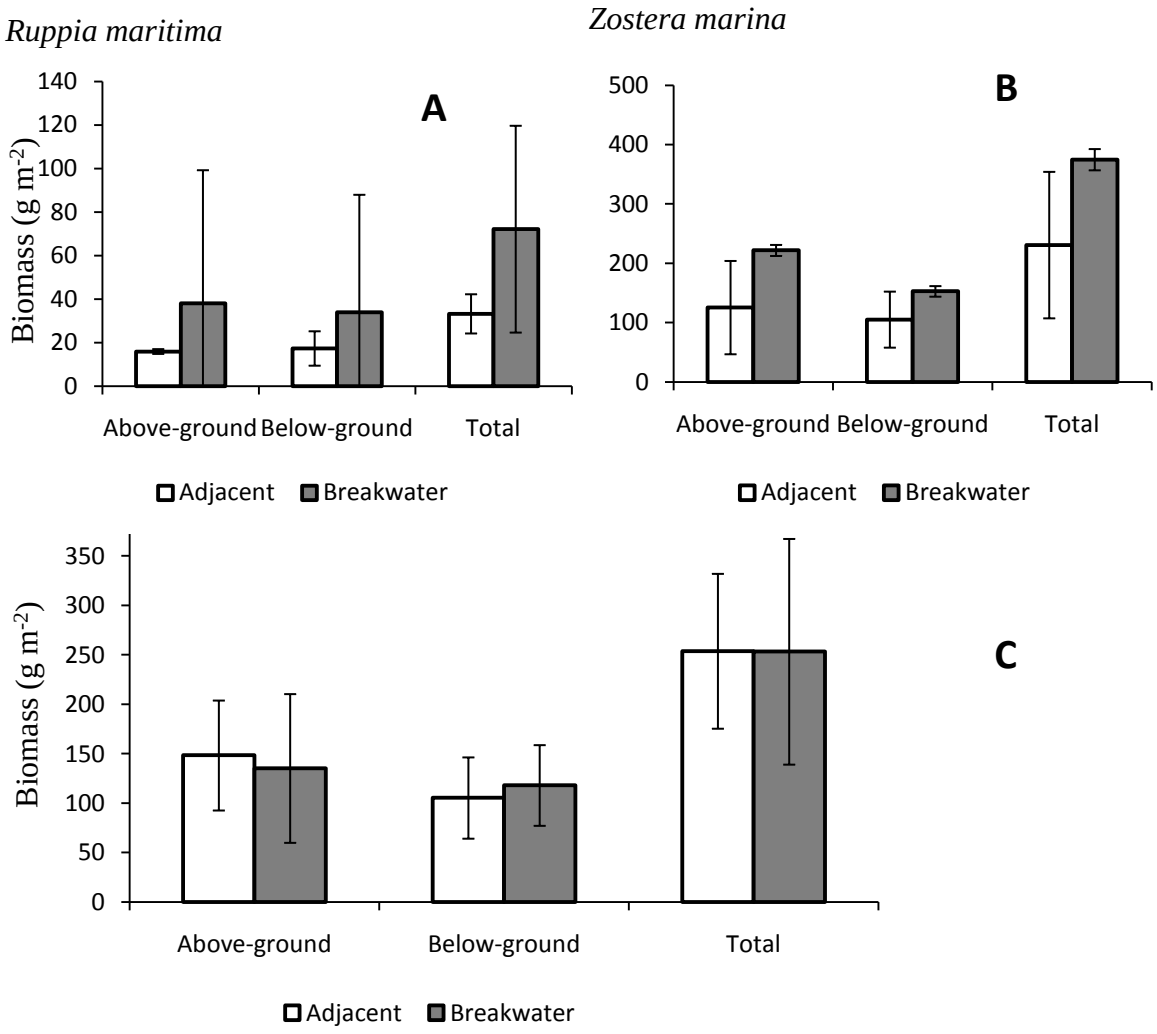

Figure CCPB6. Biomass of the SAV (A) *Ruppia maritima* (B) *Zostera marina* and (C) all species of SAV at the adjacent-exposed (open bars) and breakwater-protected (closed bars) sites.

Summary of SAV data:

SAV abundance in the segment containing the Cape Charles Public Beach site was variable over the observation period, generally decreasing until 2006 then increasing

from 2006 to 2010. Prior to the first breakwater installation in 2002 the adjacent and breakwater sites were fairly similar. SAV % cover dropped in both sites after installation, but was more pronounced in the breakwater site from 2002 to 2006. In 2006 a second breakwater was installed and the pattern switches, with the adjacent area declining and the breakwater area increasing, mirroring the segment totals (Figure CCPB4).

Ruppia maritima ($p = 0.36$) and *Zostera marina* ($p = 0.26$) shoot lengths did not differ between the breakwater-protected and adjacent-exposed sites. *R. maritima* roots however were longer ($p = 0.01$) at the adjacent-exposed site, while *Z. marina* roots were longer ($p < .0001$) at the breakwater-protected site. Total biomass was similar at the breakwater-protected area than at the adjacent-exposed ($p = 1.00$). Other than longer shoot growth at the breakwater-protected site the breakwater at Cape Charles Public Beach appeared to have no effect on SAV in the area.

Mobjack Bay

Description: This linear, segmented, rock-mound breakwater has 6 segments that are oriented parallel to the shoreline. The total breakwater length is 58.8 m, with average segment length 7±2 m (mean ± SD) and average gap length 3±0.5 m. Average distance from shore is 9±3 m. This breakwater protects a small marsh transitioning into a lawn. The adjacent-exposed shoreline is also a marsh transitioning into a lawn.

Year of Construction: 2002 **Age at Sampling:** 7 years

Salinity Regime: Polyhaline

Fetch: Adjacent: 1.6±0.6 km

Breakwater: 2.1±0.9 km

Sampling Coordinates:

MB A vbc	37º25'05.6"N	76º24'21.4"W
MB A pc	37º25'05.6"N	76º24'21.4"W
MB B vbc	37º25'04.4"N	76º24'23.4"W
MB B pc	37º25'04.4"N	76º24'23.4"W
SAV A1	37º25'05.6"N	76º24'22.1"W
SAV A2	37º25'05.7"N	76º24'22.0"W
SAV A3	37º25'05.7"N	76º24'22.0"W
SAV A4	37º25'05.7"N	76º24'21.8"W
SAV A5	37º25'05.8"N	76º24'21.7"W
SAV B1	37º25'05.9"N	76º24'23.9"W
SAV B2	37º25'05.5"N	76º24'23.6"W
SAV B3	37º25'05.5"N	76º24'23.6"W
SAV B4	37º25'05.4"N	76º24'24.1"W
SAV B5	37º25'05.5"N	76º24'24.1"W

Table MB1. Latitude and longitude of vibracores (vbc), pushcores (pc), and SAV cores taken in the adjacent-exposed ("A") and breakwater-protected ("B") sites at Mobjack Bay.

Figure MB1. Aerial photograph of the breakwater at Mobjack Bay, VA

Sediment Data:

Push Core

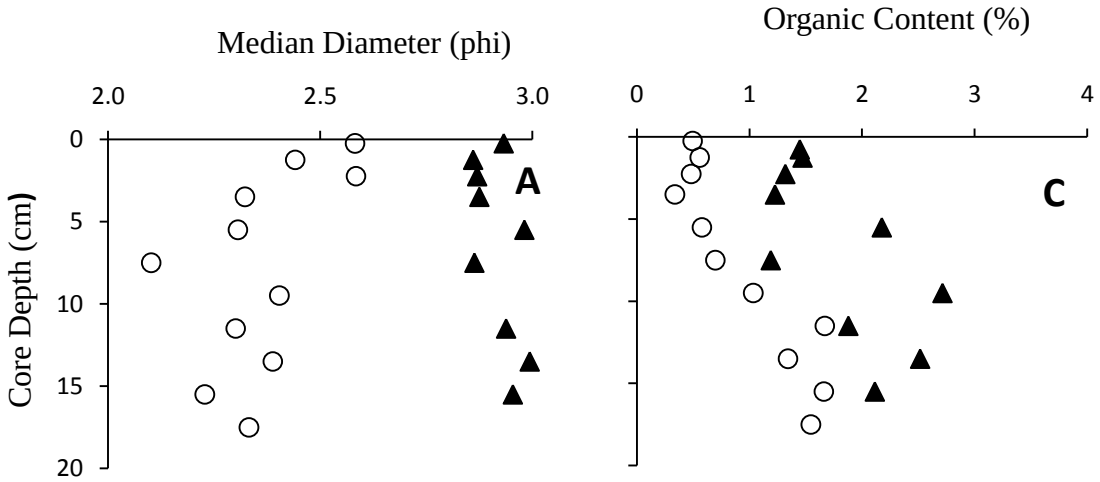

Vibracore

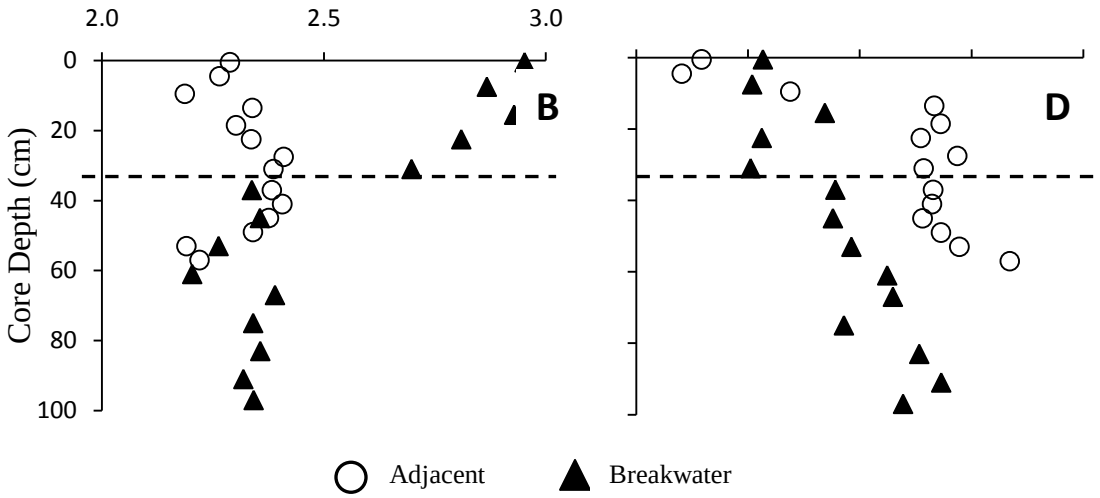

Figure MB2. Sediment grain size (median diameter) collected with a push core (A) or vibracore (B) at the adjacent-exposed (open circles) and breakwater-protected (closed triangles) sites. Sediment organic content collected with a push core (C) or vibracore (D) at the adjacent-exposed and breakwater-protected sites. The dashed line represents the interpreted depth of breakwater appearance (32 cm).

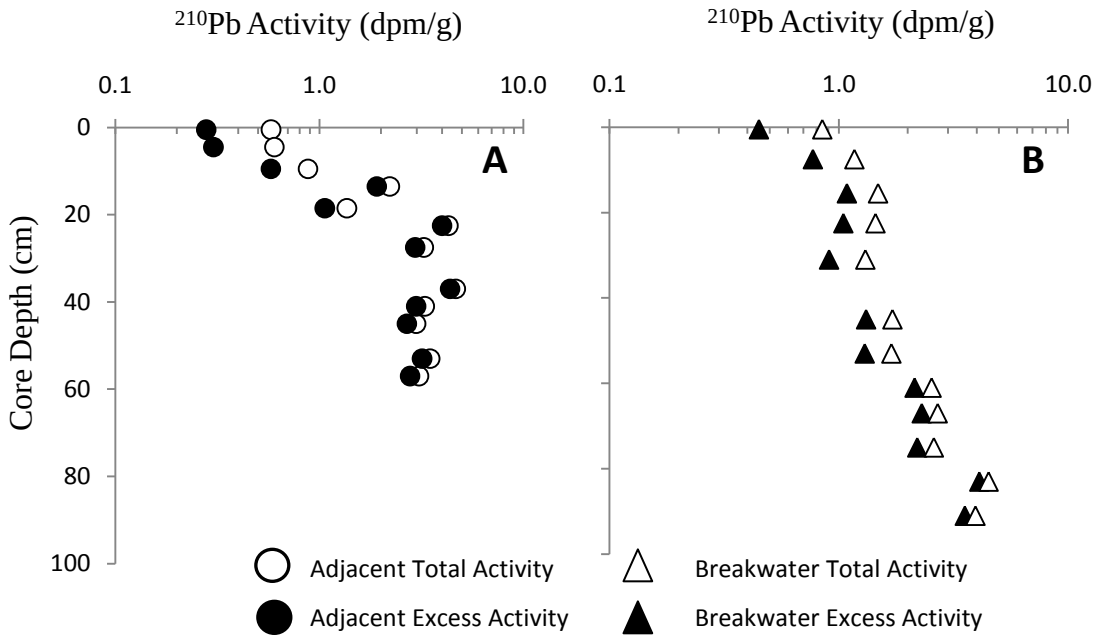

Figure MB3. ^{210}Pb profiles at the adjacent-exposed (A) and breakwater-protected (B) sites. At both sites, activities increase with depth and only minimum accumulation rates can be calculated. These rates are >0.6 cm/y for the adjacent-exposed site and >0.9 cm/y for the breakwater-protected site.

Summary of sediment data:

Surficial sediment (upper 10 cm) at the adjacent-exposed site has an average median diameter of 2.4±0.1 phi (189.5 µm) and an average organic content of 0.6±0.1%. Surficial sediment at the breakwater-protected site has an average median diameter of 2.9±0.1 phi (134.0 µm) and an average organic content of 1.6±0.2%. Statistically the adjacent-exposed site was coarser ($p < 0.0001$) and less organic ($p = 0.0001$) than the breakwater-protected site.

The ^{210}Pb profiles at both sites increase with depth. At the adjacent-exposed site, most of this increase occurs above ~20cm, and activities are fairly uniform below this

depth. Grain size is relatively uniform throughout the core, suggesting that the initial activity of ^{210}Pb has changed, and only a minimum accumulation rate of >0.6 cm/y can be calculated. At the breakwater-protected site, activities decrease throughout the core. Above 32 cm, the decrease may be related to changes in grain size; however, below this depth, grain size is fairly uniform. This suggests that, like the adjacent-exposed site, the initial activity of ^{210}Pb has changed and only a minimum accumulation rate of >0.9 cm/y can be calculated.

There is an abrupt change in the grain-size profile at the breakwater-protected site at 32 cm. Sediment fines upward above this depth but is relatively uniform below it. There is also a decrease in organic content above this depth that is more subtle. These changes are likely due to the presence of the breakwater, and so the interpreted depth of breakwater appearance is 32 cm. The corresponding post-construction sedimentation rate can be calculated by dividing this depth by the breakwater age (7 y) and is 4.6 cm/y.

SAV data:

Table MB2. Characteristics of the SAV *Ruppia maritima* growing at the adjacent-exposed and breakwater-protected sites, values are reported as mean ±SE.

Location	Species	Shoot Length (cm)	Root Length (cm)	Above-ground Biomass (g m^{-2})	Below-ground Biomass (g m^{-2})	Total Biomass (g m^{-2})	Ratio Above-/ Below-ground Biomass
Adjacent-exposed	*Ruppia maritima*	22.8± 0.6	7.7± 0.3	151.6± 18.7	12.7± 2.3	164.3± 20.3	13.1± 2.2
Breakwater-protected	*Ruppia maritima*	17.4± 0.7	5.3± 0.3	67.2± 13.9	9.4± 2.3	76.6± 16.2	7.5± 0.8

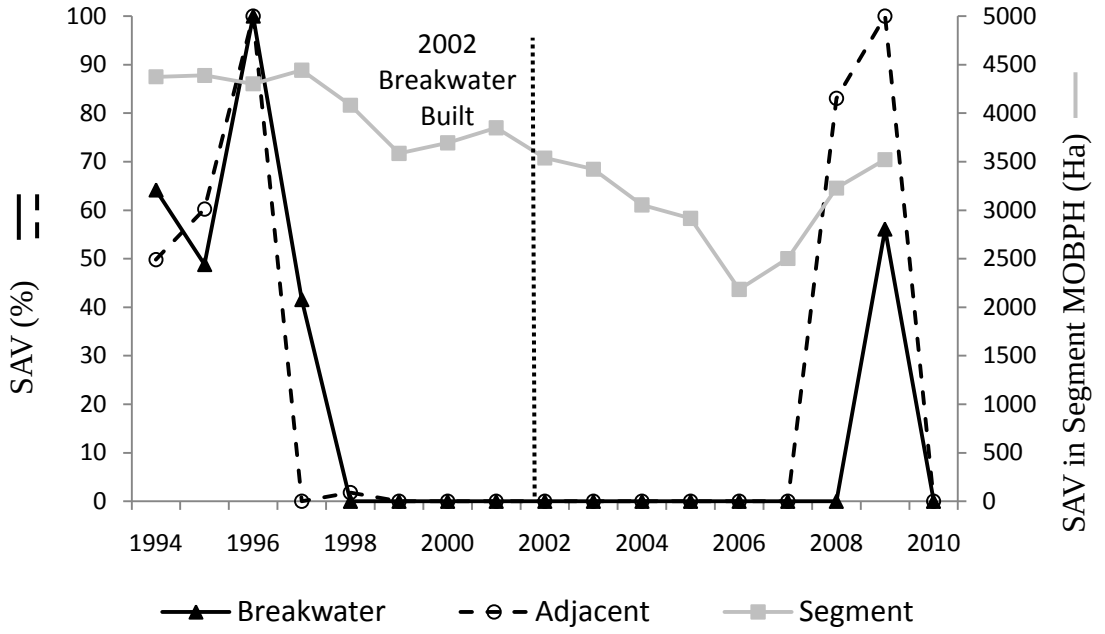

Figure MB4. SAV % cover plotted against the total SAV in the bay segment as determined by VIMS aerial photography from 8 years prior to breakwater installation to 2010.

Ruppia maritima

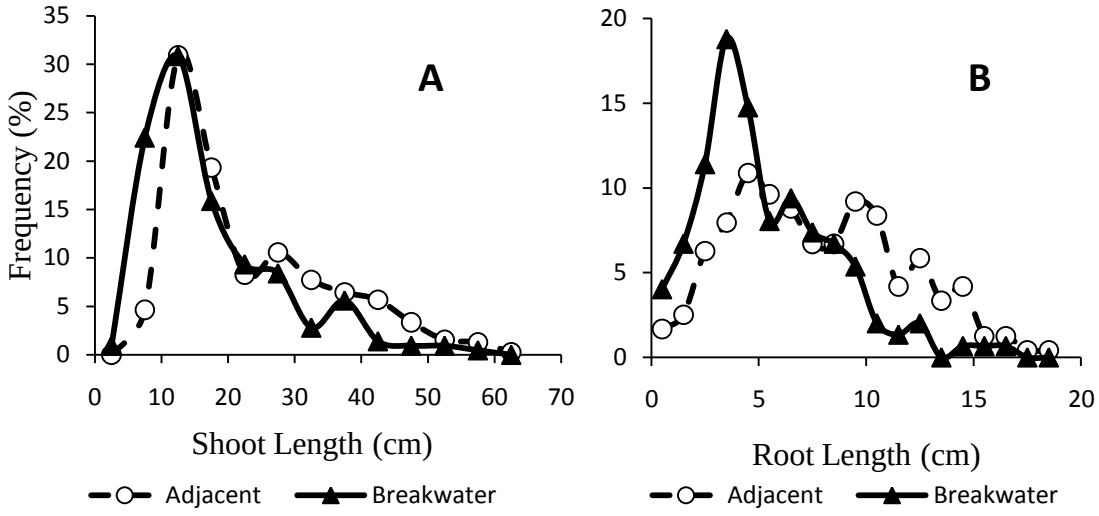

Figure MB5. (A) Shoot- and (B) root-length frequency plots for *Ruppia maritima* at the adjacent-exposed (open circles) and breakwater-protected (closed triangle) sites.

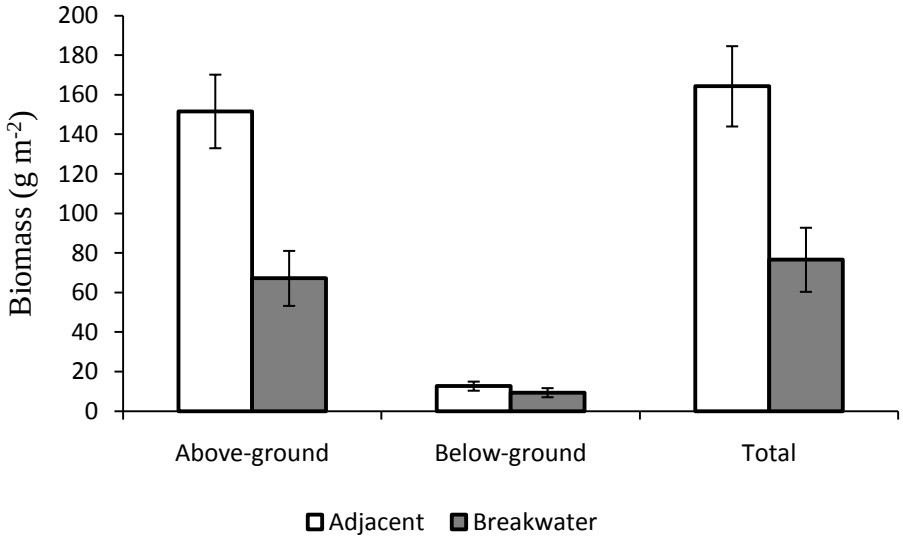

Figure MB6. Biomass of the all species of SAV at the adjacent-exposed (open bars) and breakwater-protected (closed bars) sites.

Summary of SAV data:

SAV abundance in the segment containing the Mobjack Bay site declined fairly consistently from 1984-2006 then it increased from 2007-2009. At Mobjack Bay, SAV was absent in both the adjacent and breakwater sampling sites until 2007 when grass appeared in the adjacent site. After breakwater installation SAV was only noted in the breakwater site in 2009. When SAV was observed in the sampling areas, it was higher in the adjacent section.

R. maritima biomass is greater ($p = 0.01$) at the adjacent-exposed site than at the breakwater-protected. Shoot- and root- length are also longer ($p < 0.0001$ and $p < 0.0001$, respectively) at the adjacent-exposed site than at the breakwater-protected site.

Mobjack Bay 5 (MOB5)

Description: The segmented, rock-mound breakwater at MOB5 has 4 segments and is 207.0 m long. It is linear and oriented parallel to a curved, sandy shoreline. Average segment length is 20±2 m (mean ± SD) and average gap length is 43±30 m. The structure is located 12±3 m from the shoreline. The segments are not evenly spaced, but rather are in sets of 2 with a larger gap (containing a boat pier) in the middle. The shoreline at both the breakwater-protected and adjacent-exposed sites is a manicured lawn transitioning into rip rap and then marsh.

Year Constructed: 2001 **Age at Sampling:** 8 years

Salinity Regime: Polyhaline

Fetch: Adjacent: 0.9±0.2 km

Breakwater: 0.9±0.2 km

Sampling Coordinates:

MOB5 A vbc	37º24'55.1"N	76º26'36.1"W
MOB5 A pc	37º24'55.1"N	76º26'36.1"W
MOB5 B vbc	37º24'55.6"N	76º26'38.6"W
MOB5 B pc	37º24'55.6"N	76º26'38.6"W
NO SAV		

Table MOB5.1. Latitude and longitude of vibracores (vbc), pushcores (pc), and SAV cores taken in the adjacent-exposed ("A") and breakwater-protected ("B") sites at Mobjack Bay 5.

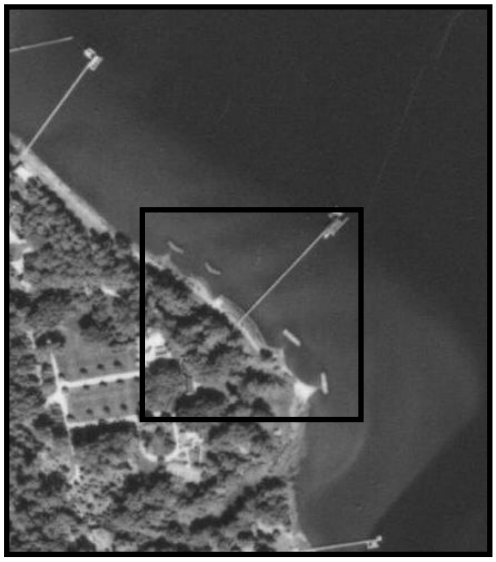

Figure MOB5.1. Aerial photograph of the breakwater at Mobjack Bay 5, VA.

Sediment Data:

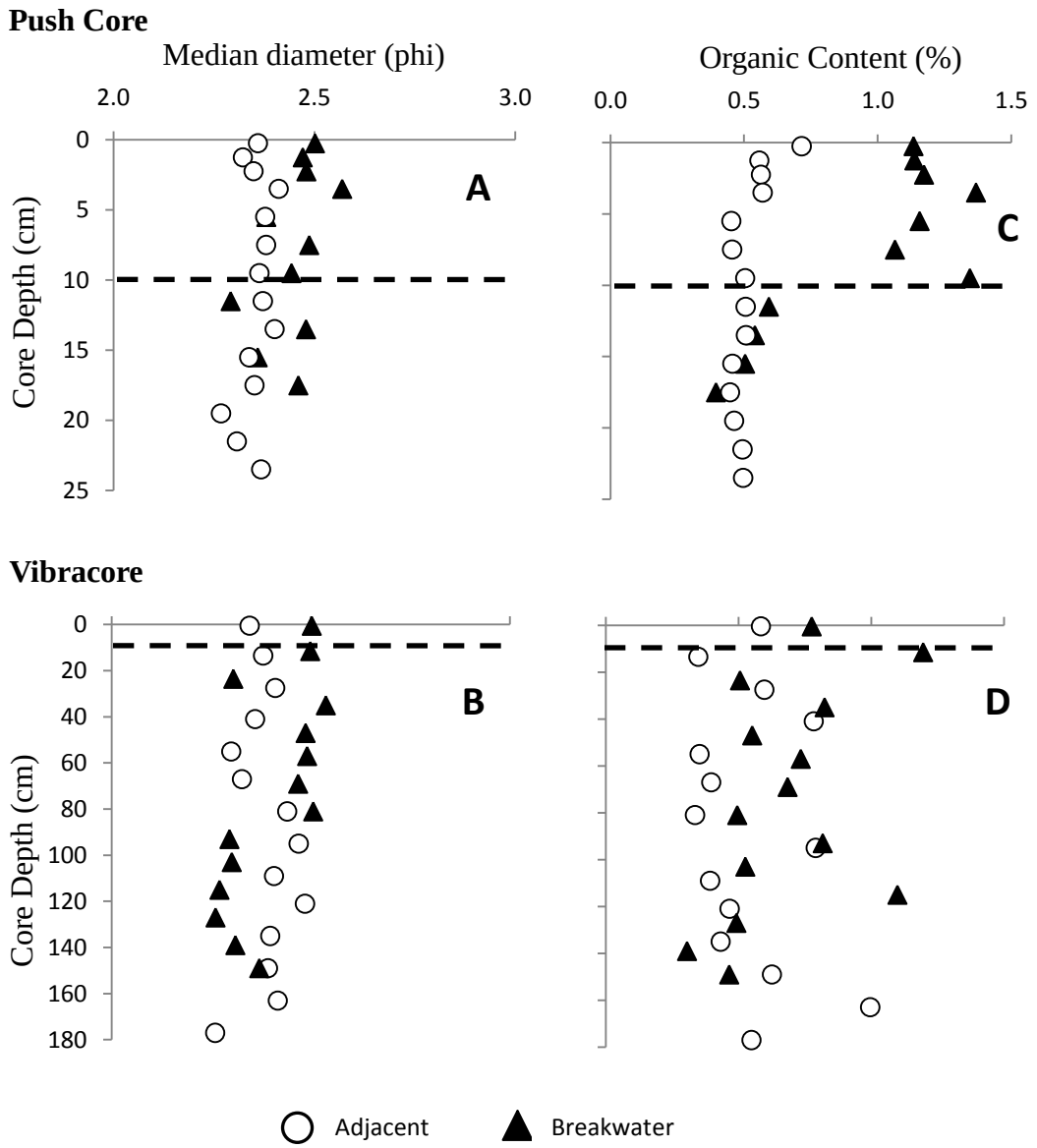

Figure MOB5.2. Sediment grain size (median diameter) collected with a push core (A) or vibracore (B) at the adjacent-exposed (open circles) and breakwater-protected (closed triangles) sites. Sediment organic content collected with a push core (C) or vibracore (D) at the adjacent-exposed and breakwater-protected sites. The dashed line represents the interpreted depth of breakwater appearance (10 cm).

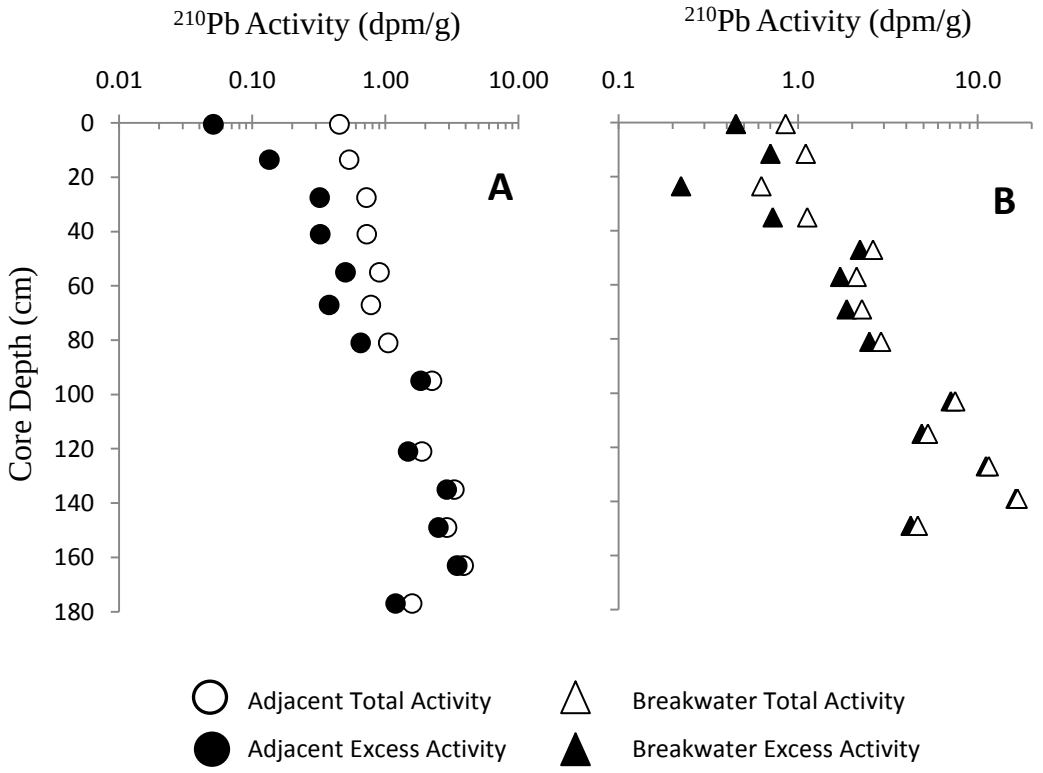

Figure MOB5.3. ^{210}Pb profiles at the adjacent-exposed (A) and breakwater-protected (B) sites. At both sites, activities increase with depth and only minimum accumulation rates can be calculated. These rates are >1.8 cm/y for the adjacent-exposed site and >1.5 cm/y for the breakwater-protected site.

Summary of sediment data:

Surficial sediment (upper 10 cm) at the adjacent-exposed site is similar in grain size to the breakwater-protected, however is statistically different ($p = 0.001$) and is less organic ($p < 0.0001$) than the breakwater-protected site. The adjacent-exposed site has an average median diameter of 2.4±0.01 phi (189.5 µm) and an average organic content of 0.5±0.3%. Surficial sediment at the breakwater-protected site has an average median diameter of 2.5±0.02 phi (176.8 µm) and an average organic content of 1.2±0.04%.

The ^{210}Pb profiles at both sites increase with depth. However, grain size is relatively uniform throughout both cores, suggesting that the initial activity of ^{210}Pb has changed. Thus, only minimum accumulation rates can be calculated and are >1.8 cm/y at the adjacent-exposed site and >1.5 cm/y at the breakwater-protected site. At the breakwater-protected site, this represents the pre-construction sedimentation rate.

The most obvious change in push-core profiles is a shift toward sediment with higher organic content above 10 cm. This is likely due to the presence of the breakwater, and so the interpreted depth of breakwater appearance is 10 cm. The corresponding post-construction sedimentation rate can be calculated by dividing this depth by the breakwater age (8 y) and is 1.3 cm/y. Thus, the effect of the breakwater at this location is no change in grain size, increase in organic content, and decrease in sedimentation rate.

SAV Data:

No SAV was present at the adjacent-exposed or breakwater-protected sites at Mobjack Bay 5.

Mobjack Bay 7 (MOB7)

Description: This linear, segmented, rock-mound breakwater has 2 segments which are parallel to the shoreline. The total breakwater length is 69.2 m, with segment lengths 24±1 m (mean ± SD) and gap length 24 m. Average distance from shore is 14±4 m. This breakwater protects a sandy beach. The adjacent-exposed site is also a sand beach at the base of a sea wall.

Year of Construction: 2001 **Age at Sampling:** 8 years

Salinity Regime: Polyhaline

Fetch: Adjacent: 1.1±0.2 km

Breakwater: 1.0±0.2 km

Sampling Coordinates:

MOB7 A vbc	37º21'49.4"N	76º27'39.6"W
MOB7 A pc	37º21'49.4"N	76º27'39.6"W
MOB7 B vbc	37º21'50.5"N	76º27'40.5"W
MOB7 B pc	37º21'50.5"N	76º27'40.5"W
SAV A1	37º21'49.4"N	76º27'39.0"W
SAV A2	37º21'49.2"N	76º27'39.0"W
SAV A3	37º21'49.1"N	76º27'38.7"W
SAV A4	37º21'49.0"N	76º27'38.6"W
SAV A5	37º21'48.9"N	76º27'38.7"W
SAV B1	37º21'50.7"N	76º27'40.7"W
SAV B2	37º21'50.8"N	76º27'40.6"W
SAV B3	37º21'50.8"N	76º27'40.7"W
SAV B4	37º21'51.0"N	76º27'40.9"W
SAV B5	37º21'51.6"N	76º27'41.7"W

Table MOB7.1. Latitude and longitude of vibracores (vbc), pushcores (pc), and SAV cores taken in the adjacent-exposed ("A") and breakwater-protected ("B") sites at Mobjack Bay 7.

Figure MOB7.1. Aerial photo of the breakwater at Mobjack Bay7, VA

Sediment Data:

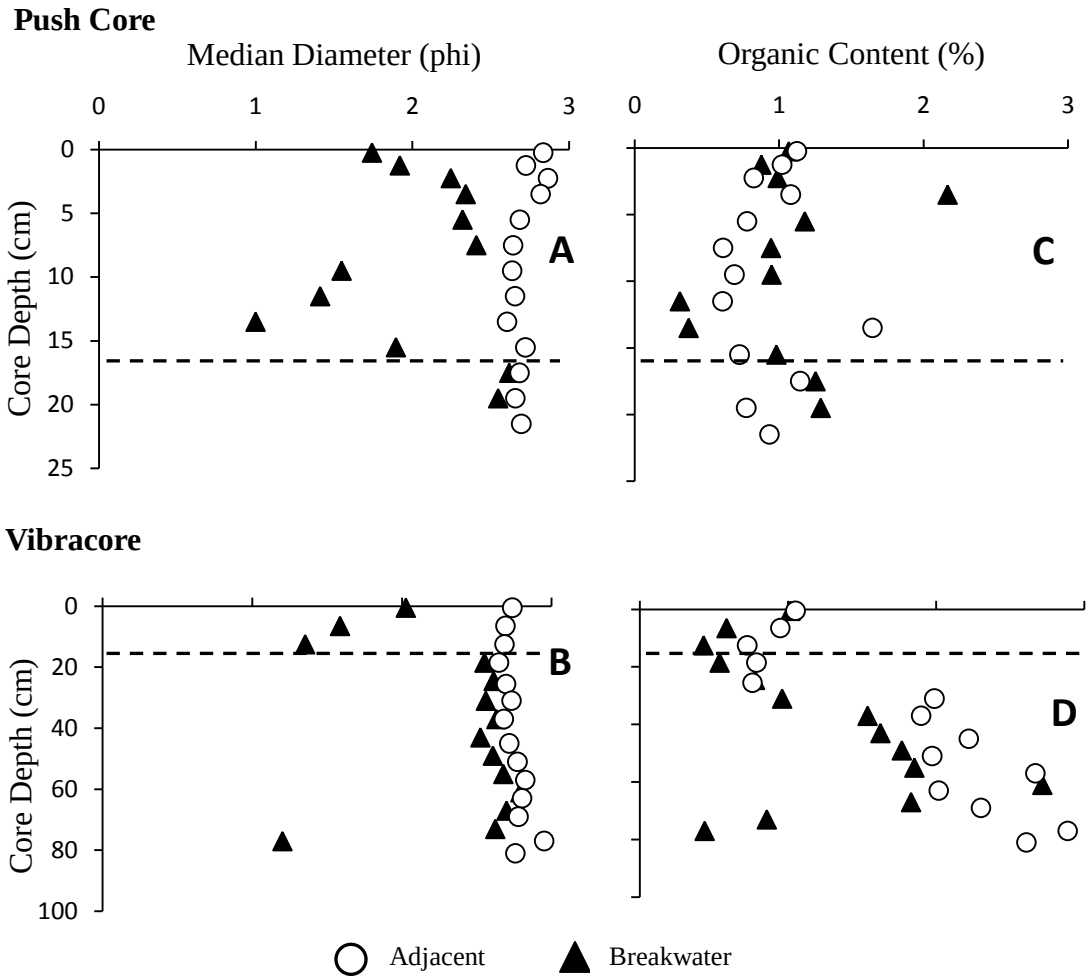

Figure MOB7.2. Sediment grain size (median diameter) collected with a push core (A) or vibracore (B) at the adjacent-exposed (open circles) and breakwater-protected (closed triangles) sites. Sediment organic content collected with a push core (C) or vibracore (D) at the adjacent-exposed and breakwater-protected sites. The dashed line represents the interpreted depth of breakwater appearance (16 cm).

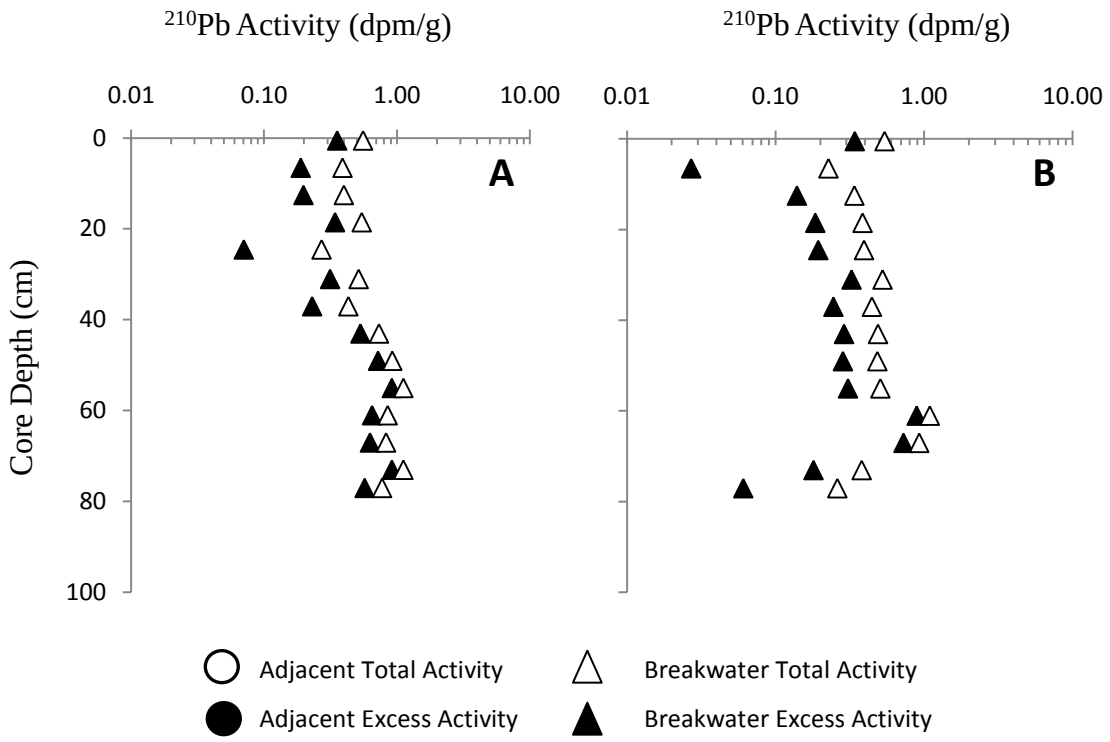

Figure MOB7.3. ^{210}Pb profiles at the adjacent-exposed (A) and breakwater-protected (B) sites. At both sites, activities increase with depth and only minimum accumulation rates can be calculated. These rates are >0.8 cm/y for the adjacent-exposed site and also >0.8 cm/y for the breakwater-protected site.

Summary of sediment data

Surficial sediment (upper 10 cm) at the adjacent-exposed site has finer ($p = 0.0003$) but similar organic content ($p = 0.10$) than the breakwater-protected site. The adjacent-exposed site has an average median diameter of 2.7±0.04 phi (153.9 µm) and an average organic content of 0.9±0.1%. Surficial sediment at the breakwater-protected site has an average median diameter of 2.1±0.1 phi (233.3 µm) and an average organic content of 1.2±0.2%.

The ^{210}Pb profiles at both sites increase with depth. However, grain size is relatively uniform throughout both cores, suggesting that the initial activity of ^{210}Pb has changed. Thus, only minimum accumulation rates can be calculated and are >0.8 cm/y at both the adjacent-exposed and breakwater-protected sites. At the breakwater-protected site, this represents the pre-construction sedimentation rate.

There is an increase in grain size in both the push- and vibracore profiles. This occurs above 16 cm, which is the interpreted depth of breakwater influence. The corresponding post-construction sedimentation rate can be calculated by dividing this depth by the breakwater age (8 y) and is 2.0 cm/y. Thus, the effect of the breakwater at this location is an increase in grain size, no change in organic content, and increase in sedimentation rate. However, note that the post-construction rate is a minimum estimate.

SAV data:

Table MOB7.2. Characteristics of the SAV *Ruppia maritima* growing at the adjacent-exposed and breakwater-protected sites, values are reported as mean ±SE.

Location	Species	Shoot Length (cm)	Root Length (cm)	Above-ground Biomass (g m^{-2})	Below-ground Biomass (g m^{-2})	Total Biomass (g m^{-2})	Ratio Above-/ Below-ground Biomass
Adjacent-exposed	*Ruppia maritima*	11.2± 0.5	4.9± 0.3	17.1± 9.1	3.8± 1.3	20.9± 10.3	4.8± 1.5
Breakwater-protected	*Ruppia maritima*	9.2± 0.4	5.5± 0.3	10.9± 1.7	4.4± 0.8	15.3± 2.3	2.7± 0.5

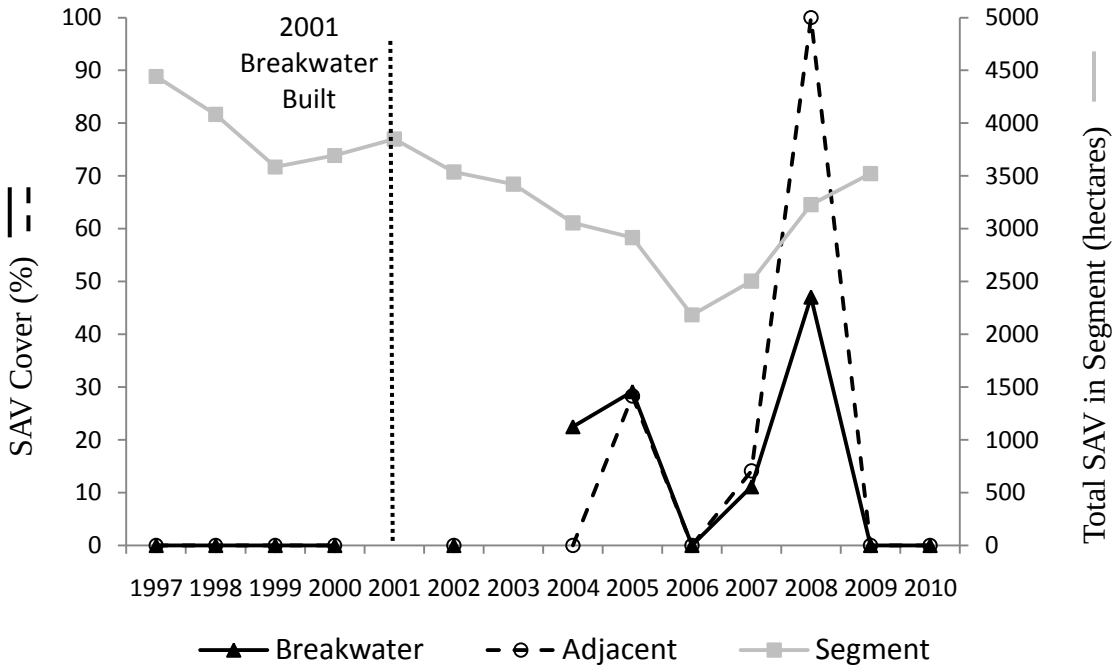

Figure MOB7.4. SAV % cover plotted against the total SAV in the bay segment as determined by VIMS aerial photography from 4 years prior to breakwater installation to 2010.

Ruppia maritima

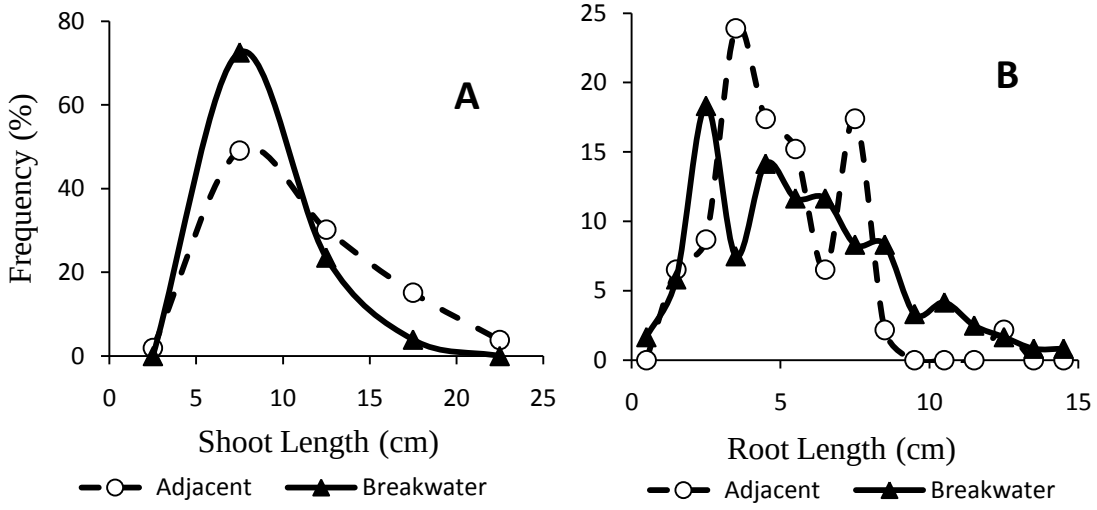

Figure MOB7.5. (A) Shoot- and (B) root-length frequency plots for *Ruppia maritima* at the adjacent-exposed (open circles) and breakwater-protected (closed triangle) sites.

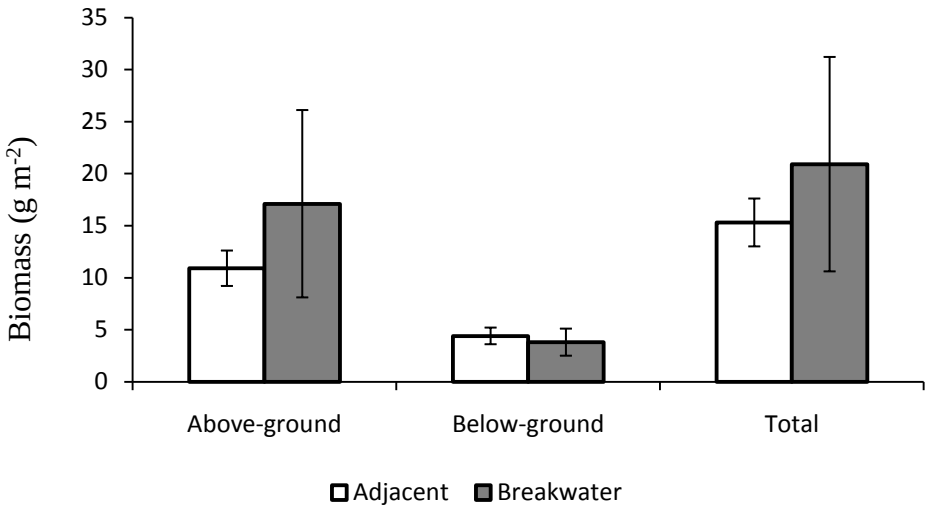

Figure MOB7.6. Biomass of the SAV *Ruppia maritima* at the adjacent-exposed (open bars) and breakwater-protected (closed bars) sites.

Summary of SAV data:

SAV abundance in the segment containing the Mobjack Bay 7 declined fairly consistently from 1987-2006 then it increased from 2007-2009. At Mobjack Bay 7, SAV was absent in both the adjacent and breakwater sampling sites until 2004 when grass appeared in the breakwater site. From 2006 to 2008 SAV % cover increased in both the adjacent and breakwater sites, with more SAV being noted in the adjacent compared to the breakwater site. In 2009 both areas declined and returned to 0%.

Biomass at the adjacent-exposed and breakwater-protected sites is similar ($p = 0.99$). Shoot lengths at the adjacent-exposed site are longer ($p = 0.002$) than at the breakwater-protected site, however root lengths were similar ($p = 0.57$) between the two sites.

Yorktown

Description: This slightly semi-circular, segmented, rock-mound breakwater has 5 segments, with the southernmost segment attached to the shoreline. The total breakwater length is 209.9 m, with average segment length 27±6 m and average gap length 24±5 m. Average distance from shore is 35±10 m. This breakwater protects a sandy beach. The adjacent-exposed site shoreline was a grassy bank that with rip rap at the base.

Year of Construction: 1993 **Age at Sampling:** 16 years

Salinity Regime: Polyhaline

Fetch: Adjacent: 4.8±1.8 km

Breakwater: 3.6±1.6 km

Sampling Coordinates:

YT A vbc	37º12'58.8"N	76º28'19.8"W
YT A pc	37º12'58.8"N	76º28'19.8"W
YT B vbc	37º12'56.7"N	76º28'14.5"W
YT B pc	37º12'56.7"N	76º28'14.5"W
No SAV		

Table YT1. Latitude and longitude of vibracores (vbc), pushcores (pc), and SAV cores taken in the adjacent-exposed ("A") and breakwater-protected ("B") sites at Yorktown. Note that SAV cores were not collected, as SAV was not present in summer 2009.

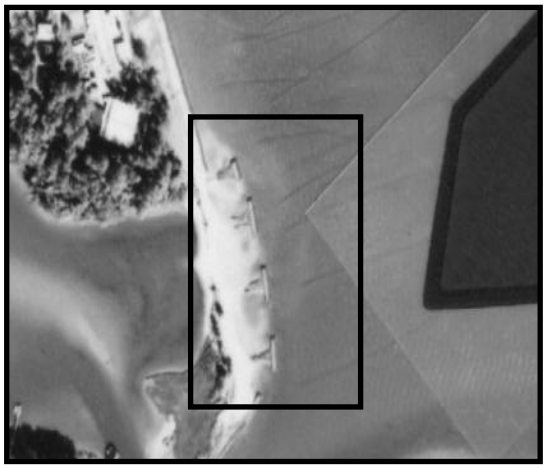

Figure YT1. Aerial photo of the breakwater at Yorktown, VA.

Sediment Data:

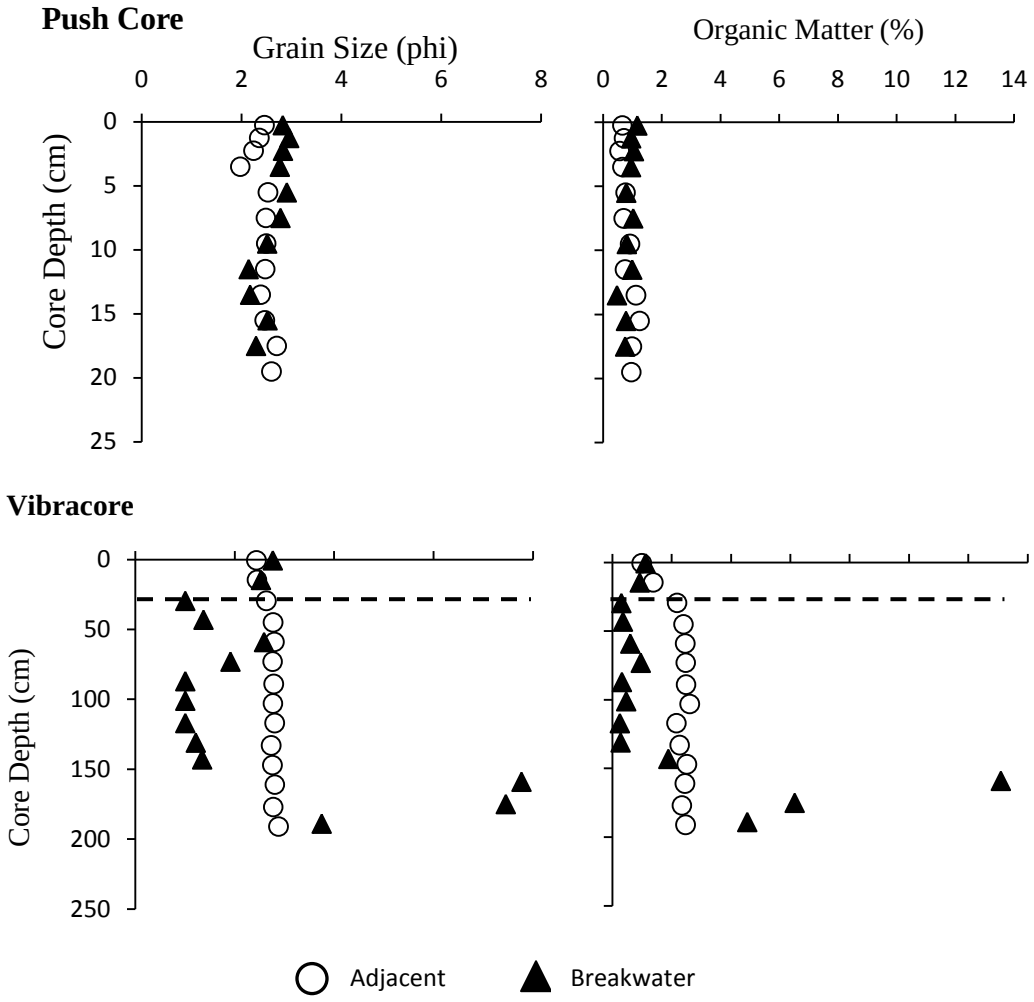

Figure YT2. Sediment grain size (median diameter) collected with a push core (A) or vibracore (B) at the adjacent-exposed (open circles) and breakwater-protected (closed triangles) sites. Sediment organic content collected with a push core (C) or vibracore (D) at the adjacent-exposed and breakwater-protected sites. The dashed line represents the interpreted depth of breakwater appearance (29 cm).

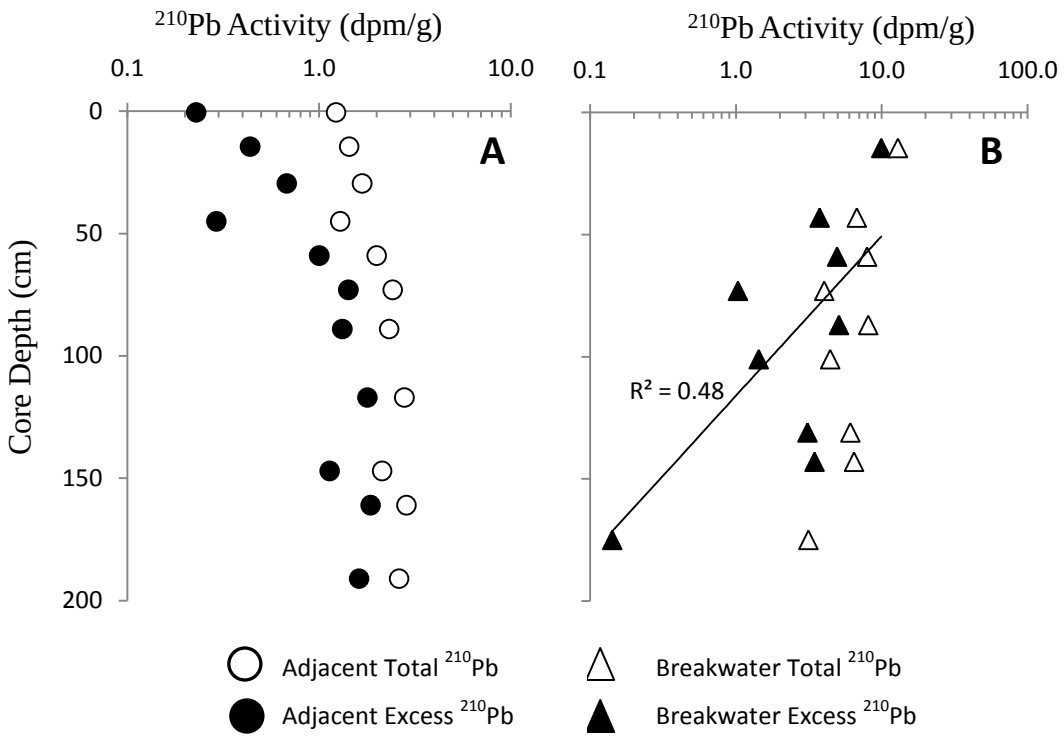

Figure YT3. ^{210}Pb profiles at the adjacent-exposed (A) and breakwater-protected (B) sites. Excess activities at the adjacent-exposed site increase with depth, and only a minimum accumulation rate of >2.0 cm/y can be calculated. Excess activities at the breakwater-protected site decrease logarithmically with depth, indicating steady-state sedimentation. The calculated sediment accumulation rate is 1.8 cm/y.

Summary of sediment data:

Surficial (upper 10 cm) sediment at the adjacent-exposed site is coarser ($p = 0.001$) and less organic ($p = 0.002$) than the breakwater-protected site. The adjacent-exposed site has an average median diameter of 2.4±0.1 phi (189.5 µm) and an average organic content of 0.7±0.1%. Surficial sediment at the breakwater-protected site has an

average median diameter of 2.8±0.1 phi (143.6) and an average organic content of 1.0±0.1%.

Excess ^{210}Pb activities increase with depth at the adjacent-exposed site, and only a minimum accumulation rate of >2.0 cm/y can be calculated. Excess activities at the breakwater-protected site decrease logarithmically with depth and the calculated accumulation rate is 1.8 cm/y, representing the pre-construction sedimentation rate.

Sediment in the upper 29 cm of the breakwater-protected vibracore grain-size profile is finer than the rest of the core, indicating sedimentation since breakwater construction. With an interpreted depth of breakwater influence of 29 cm, the post-construction sedimentation rate is 1.8 cm/y, which is unchanged from the pre-construction rate. Thus, under the influence of the breakwater at this site, grain size decreases, and organic content and sedimentation rate are not affected.

SAV Data:

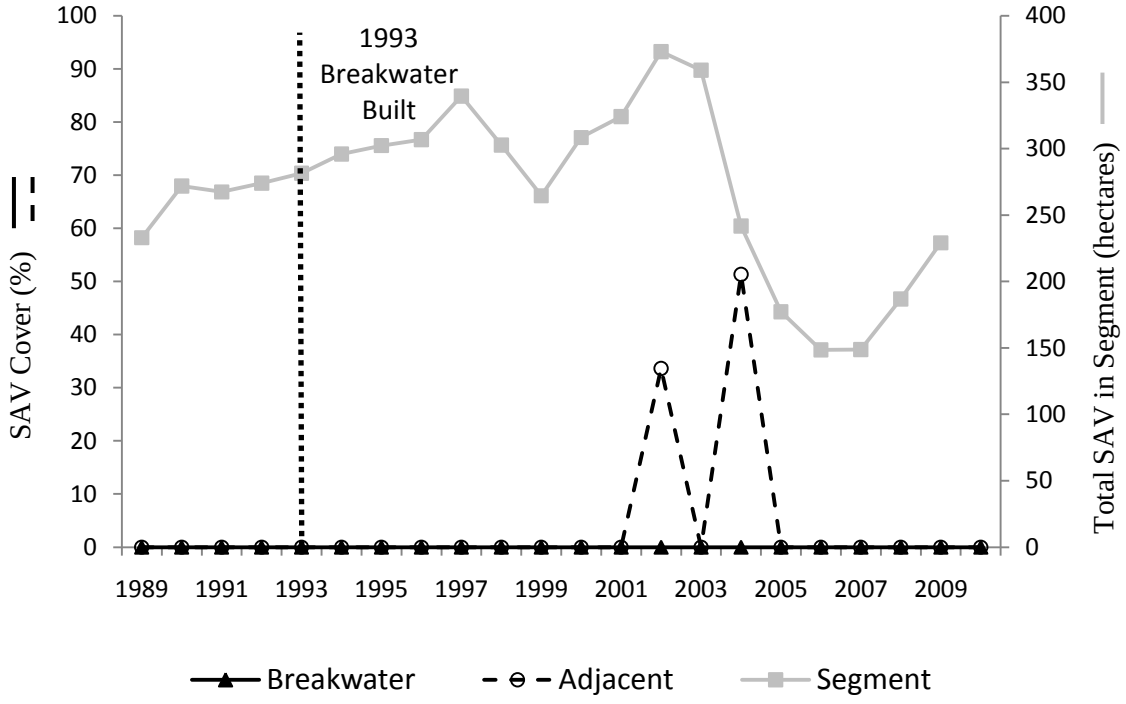

Figure YT4. SAV % cover plotted against the total SAV in the bay segment as determined by VIMS aerial photography from 4 years prior to breakwater installation to 2010.

Summary of SAV data:

SAV abundance in the segment containing the Yorktown site was fairly stable over the observation period, though it did see a decrease between 2002 and 2007. At Yorktown, SAV % cover was only noted during this interval where the overall segment totals were decreasing, and only in the adjacent site. No SAV was present at time of sampling.

Mobjack Bay 3 (MOB3)

Description: This linear, segmented, gabion basket (wire mesh cage filled with rock) breakwater has 8 segments, which are parallel to a curved shoreline. The total breakwater length is 167.0 m, with segment lengths 8±0.5 m (mean ± SD) and gap lengths 14±2 m. Average distance from shore is 15±4 m. This breakwater protects a sandy beach. The adjacent-exposed shoreline is also a sandy beach.

Year of Construction: 1992 **Age at Sampling:** 17 years

Salinity Regime: Polyhaline

Fetch: Adjacent: 1.4±0.4 km

Breakwater: 7.7±5.2 km

Sampling Coordinates:

MOB3 A vbc	37º23'41.0"N	76º25'1.8"W
MOB3 A pc	37º23'41.0"N	76º25'1.8"W
MOB3 B vbc	37º23'45.4"N	76º25'04.8"W
MOB3 B pc	37º23'45.4"N	76º25'04.8"W
SAV A1	37º23'41.2"N	76º25'04.9"W
SAV A2	37º23'41.1"N	76º25'02.1"W
SAV A3	37º23'41.0"N	76º25'01.6"W
SAV A4	37º23'40.8"N	76º25'01.7"W
SAV A5	37º23'40.5"N	76º25'01.0"W
SAV B1	37º23'47.0"N	76º25'04.9"W
SAV B2	37º23'46.5"N	76º25'04.6"W
SAV B3	37º23'45.9"N	76º25'04.8"W
SAV B4	37º23'44.6"N	76º25'04.5"W
SAV B5	37º23'42.1"N	76º25'03.2"W

Table MOB3.1. Latitude and longitude of vibracores (vbc), pushcores (pc), and SAV cores taken in the adjacent-exposed ("A") and breakwater-protected ("B") sites at Mobjack Bay 3.

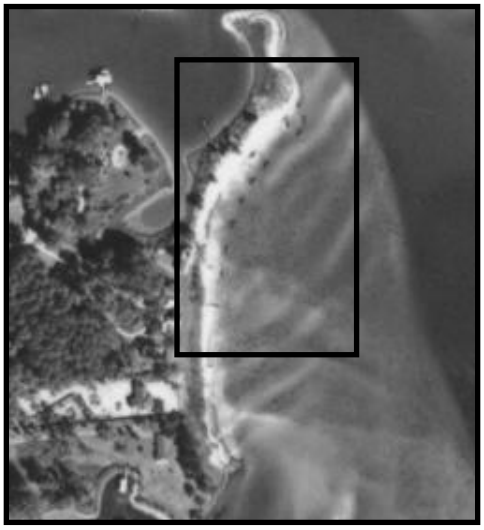

Figure MOB3.1. Aerial photo of the breakwater at Mobjack Bay 3, VA.

Sediment Data:

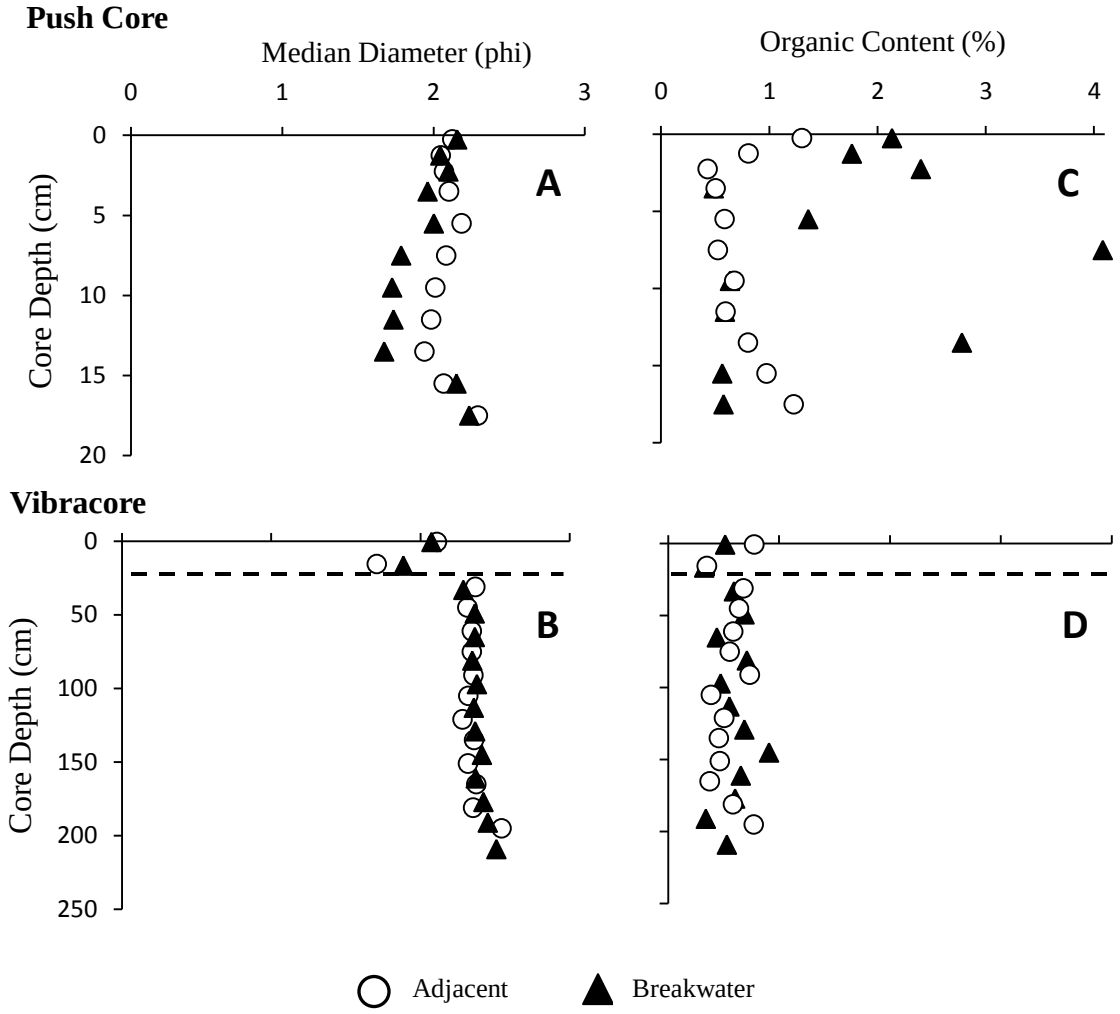

Figure MOB3.2. Sediment grain size (median diameter) collected with a push core (A) or vibracore (B) at the adjacent-exposed (open circles) and breakwater-protected (closed triangles) sites. Sediment organic content collected with a push core (C) or vibracore (D) at the adjacent-exposed and breakwater-protected sites. The dashed line represents the interpreted depth of breakwater appearance (32 cm).

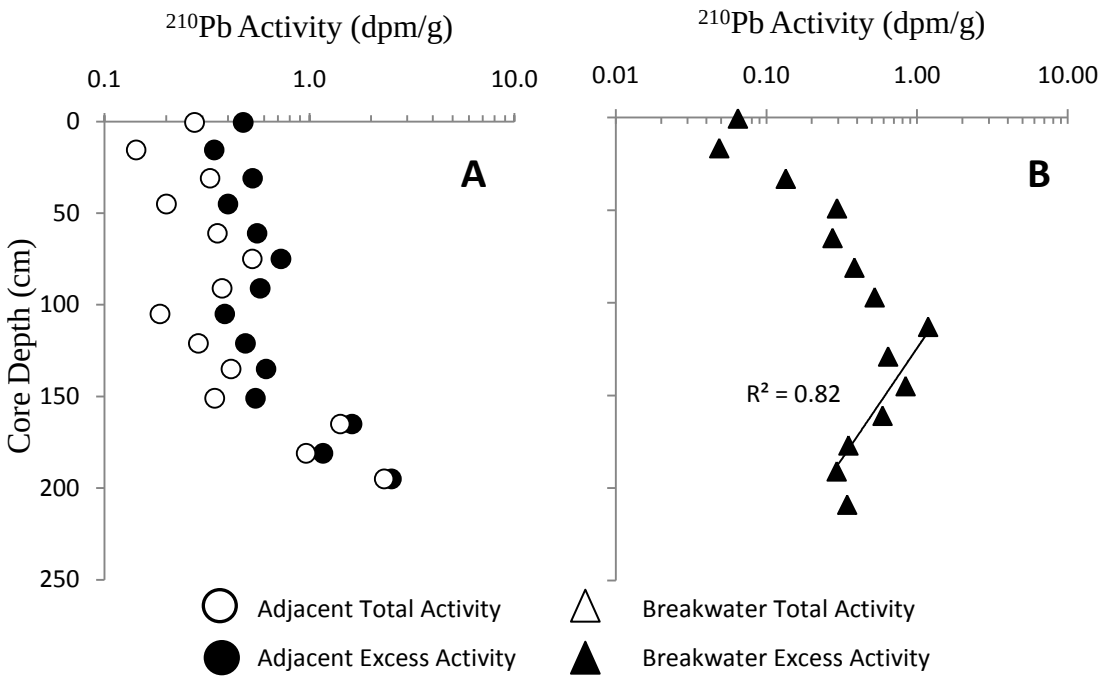

Figure MOB3.3. ^{210}Pb profiles at the adjacent-exposed (A) and breakwater-protected (B) sites. At the adjacent-exposed site, activities increase with depth and only a minimum accumulation rate of 2.0 cm/y can be calculated. Activities also increase with depth at the breakwater-protected site; however, this trend reverses at ~100 cm and the calculated sediment accumulation rate is 1.9 cm/y. Note that the x-axis varies between the plots.

Summary of sediment data:

Surficial sediment (upper 10 cm) at the adjacent-exposed site has similar grain size as the breakwater-protected site ($p = 0.08$), but is less organic ($p = 0.03$). The adjacent-exposed site has an average median diameter of 2.1±0.02 phi (233.3 µm) and an average organic content of 0.7±0.1%. Surficial sediment at the breakwater-protected site

has an average median diameter of 2.0±0.1 phi (250.0 μm) and an average organic content of 1.8±0.5%.

At the adjacent-exposed site, ^{210}Pb activities increase with depth. This increase is not due to grain-size changes, as the median diameter of vibracore sediments varies little, but is likely due to changes in the initial activity of sediments. Thus, only a minimum accumulation rate of 2.0 cm/y can be calculated for this site. At the breakwater-protected site, activities also increase with depth to ~100 cm; however, under this layer, activities decrease logarithmically with depth and an accumulation rate of 1.9 cm/y can be calculated, which is the pre-construction sedimentation rate.

Sediment character (grain size, organic content) in either the push- or vibracore profiles at the breakwater-protected site vary little, with the exception of some coarsening toward the top of the vibracore. If the sedimentation rate is assumed to remain unchanged by the presence of the breakwater, the post-construction sedimentation rate would also be 1.9 cm/y, and the depth of breakwater influence (calculated by multiplying this rate by the breakwater age of 17 y) would be 32 cm. The coarsening in the vibracore profile occurs between 17 and 45 cm and is likely related to breakwater construction.

SAV Data:

Table MOB3.2. Characteristics of SAV *Ruppia maritima* and *Zostera marina* growing at the adjacent-exposed and breakwater-protected sites, values are reported as mean ±SE.

Location	Species	Shoot Length (cm)	Root Length (cm)	Above-ground Biomass (g m^{-2})	Below-ground Biomass (g m^{-2})	Total Biomass (g m^{-2})	Ratio Above-/ Below-ground Biomass
Adjacent-exposed	*Ruppia maritima*	12.5± 0.4	5.3± 0.1	71.0± 10.6	20.0± 1.1	91.0± 10.6	3.6± 0.5
Breakwater-protected	*Ruppia maritima*	15.0± 0.6	5.7± 0.1	86.2± 14.8	20.7± 2.0	106.9± 16.4	4.1± 0.4
Adjacent-exposed	*Zostera marina*	n/a	n/a	2.5± 1.6	0	2.5± 1.6	n/a
Breakwater-protected	*Zostera marina*	15.8± 0.6	6.9± 0.5	4.5± 1.2	10.7	6.7± 3.1	0.7

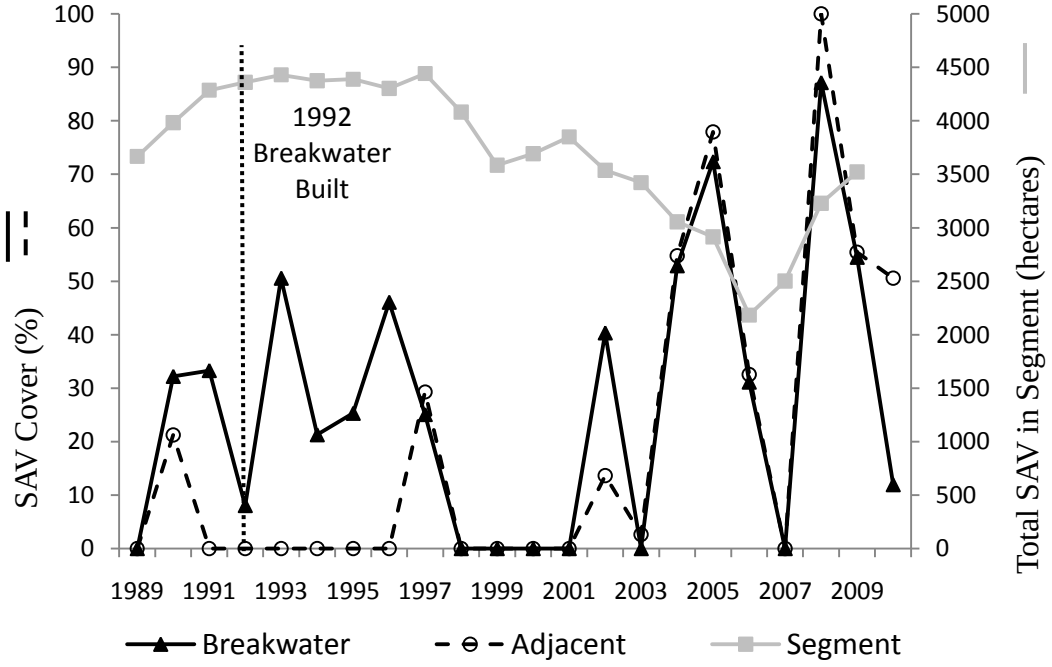

Figure MOB3.4. SAV % cover plotted against the total SAV in the bay segment as determined by VIMS aerial photography from 3 years prior to breakwater installation to 2010.

Ruppia maritima

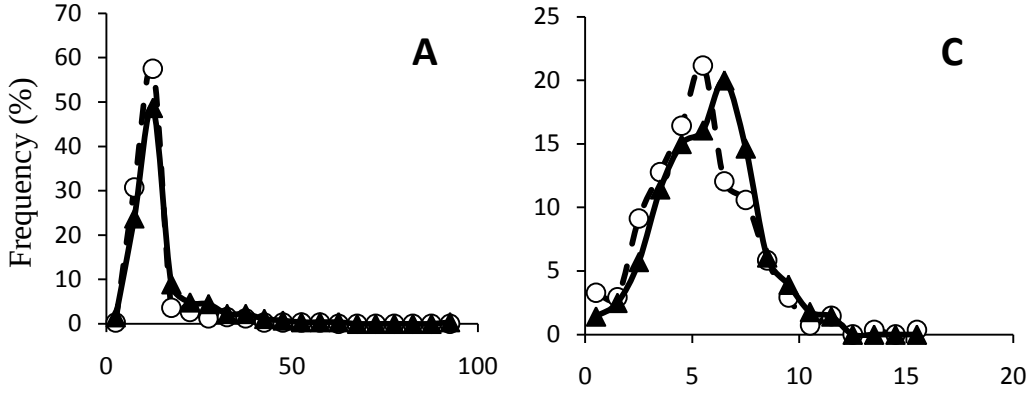

Zostera marina

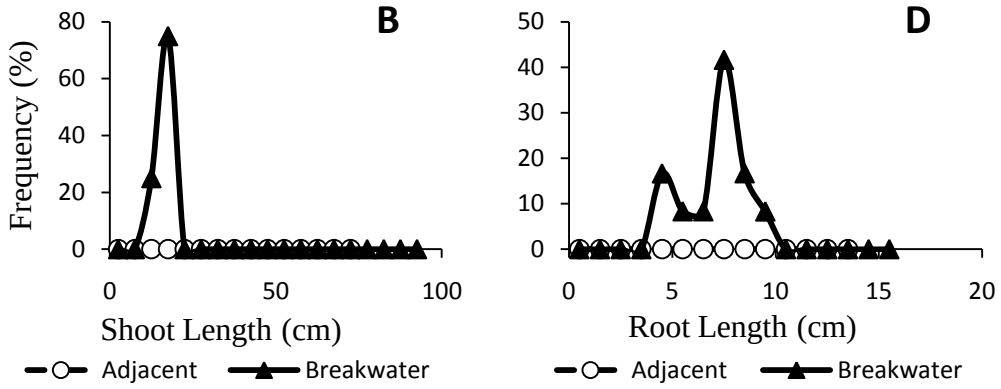

Figure MOB3.5. (A) Shoot- and (C) root-length frequency plots for *Ruppia americana* and (B) shoot- and (D) root-length frequency plots for *Zostera marina* at the adjacent-exposed (open circles) and breakwater-protected (closed triangle) sites.

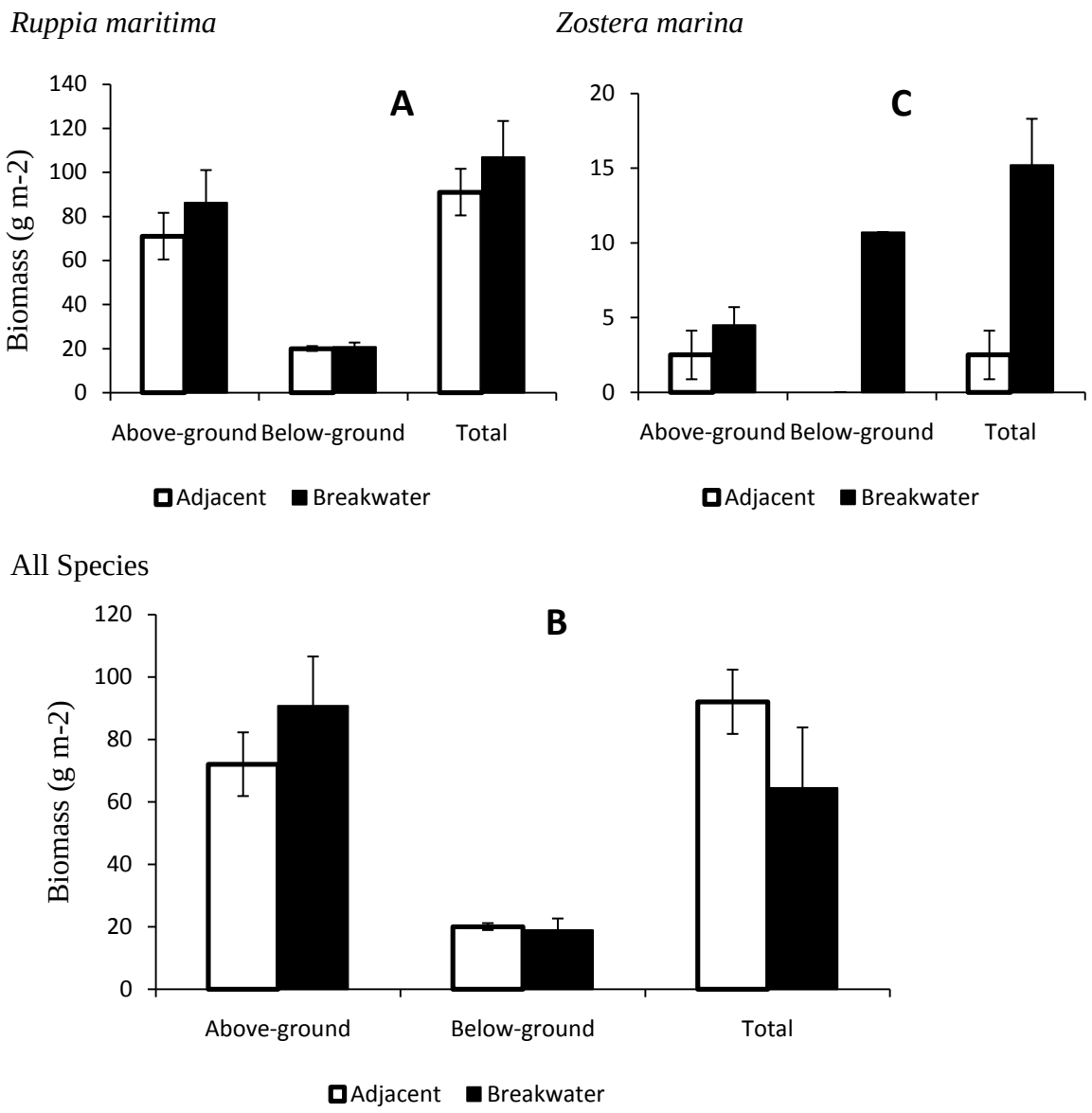

Figure MOB3.6. Biomass of the SAV species (A) *Ruppia maritima*, (B) *Zostera marina*, and (C) all species of SAV at the adjacent-exposed (open bars) and breakwater-protected (closed bars) sites.

Summary of SAV data:

SAV abundance in the segment containing the Mobjack 3 site declined fairly consistently from 1984-2006 then it increased from 2007-2009. At Mobjack 3, SAV % cover did not mirror the segment patterns. SAV % cover was higher in the breakwater sampling site in the years following breakwater installation, but after 1997 there was little observable difference between the adjacent and the breakwater sites.

SAV total biomass was greater at the breakwater-protected site than the adjacent-exposed area however, not significantly ($p = 0.44$). Shoot- and root- lengths for *R. maritima* were significantly longer at breakwater-protected site than at the adjacent-exposed site ($p = 0.003$ and $p = 0.02$, respectively). *Z. marina* shoots and roots were unable to be measured, as no intact shoots/roots were collected.

Schley

Description: This linear, segmented, gabion basket (wire mesh cage filled with rock) breakwater has 6 segments which are parallel to the shoreline; they are submerged at high tide. The total breakwater length is 117.4 m, with segment lengths 7±2 m (mean ± SD) and gap length 15±1 m. Average distance from shore is 12±3 m. This breakwater protects a marsh. The shoreline of the adjacent-exposed site is also marsh.

Year of Construction: 1991 **Age at Sampling:** 18 years

Salinity Regime: Polyhaline

Fetch: Adjacent: 0.7±0.2 km

Breakwater: 0.9±0.2 km

Sampling Coordinates:

SCH B vbc	37º23'16.0"	76º27'16.1"
SCH B pc	37º23'16.0"	76º27'16.1"
SCH A vbc	37º23'15.4"	76º27'11.0"
SCH A pc	37º23'15.4"	76º27'11.0"
SAV B1	37º23'16.4"	76º27'16.9"
SAV B2	37º23'17.3"	76º27'16.1"
SAV B3	37º23'16.2"	76º27'16.1"
SAV B4	37º23'15.6"	76º27'15.3"
SAV B5	37º23'15.5"	76º27'14.0"
SAV A1	37º23'15.9"	76º27'10.7"
SAV A2	37º23'15.6"	76º27'10.9"
SAV A3	37º23'15.7"	76º27'11.1"
SAV A4	37º23'15.7"	76º27'11.0"
SAV A5	37º23'15.3"	76º27'11.2"

Table SCH1. Latitude and longitude of vibracores (vbc), pushcores (pc), and SAV cores taken in the adjacent-exposed ("A") and breakwater-protected ("B") sites at Schley.

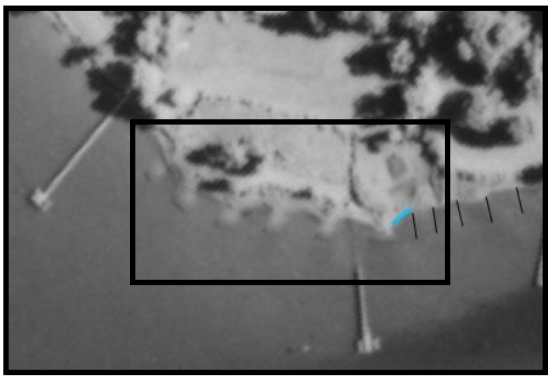

Figure SCH1. Aerial photo of the breakwater at Schley, VA.

Sediment Data:

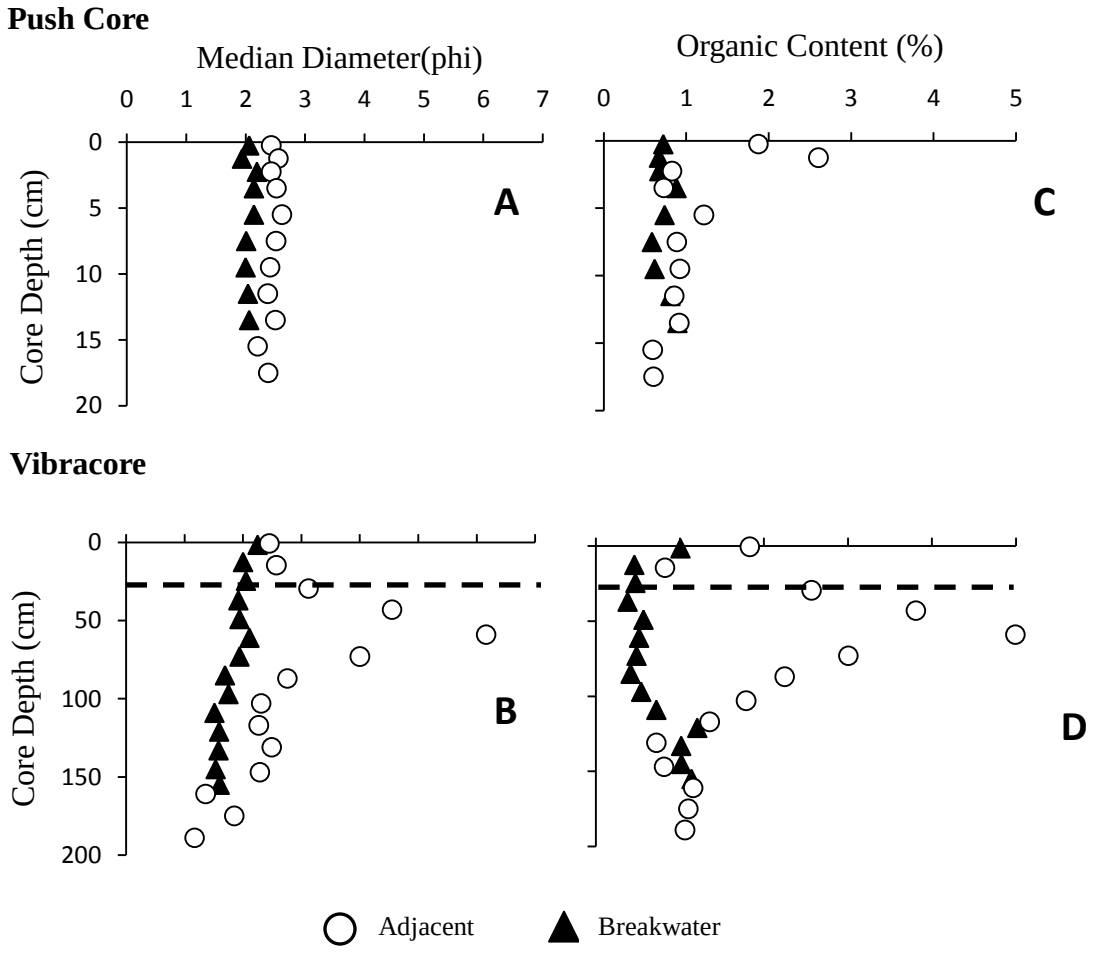

Figure SCH2. Sediment grain size (median diameter) collected with a push core (A) or vibracore (B) at the adjacent-exposed (open circles) and breakwater-protected (closed triangles) sites. Sediment organic content collected with a push core (C) or vibracore (D) at the adjacent-exposed and breakwater-protected sites. The dashed line represents the interpreted depth of breakwater appearance (29 cm).

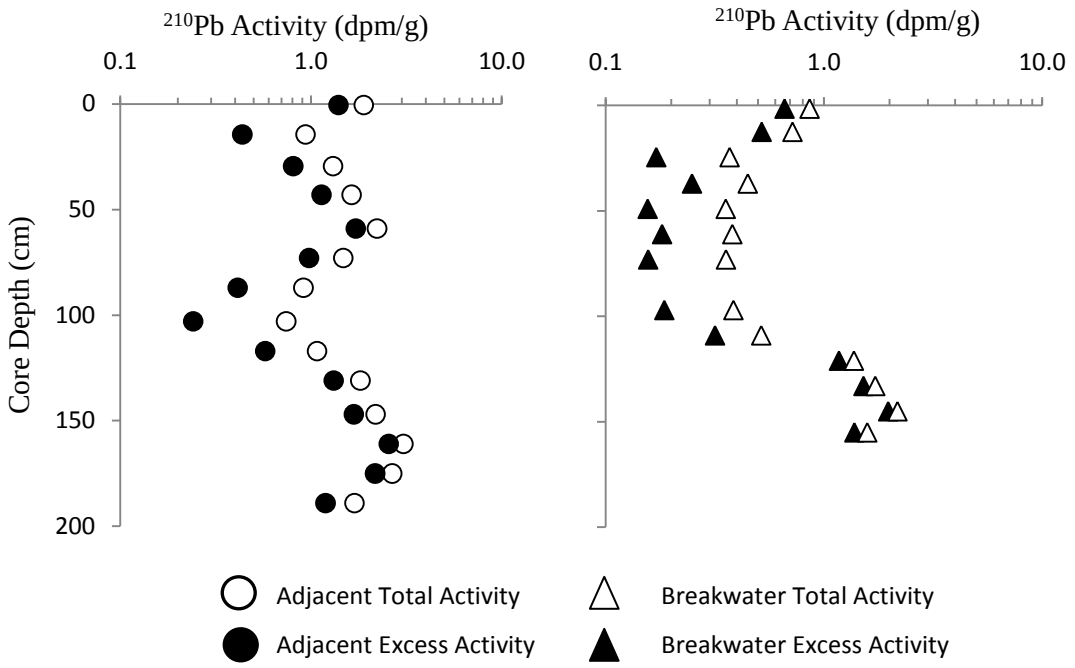

Figure SCH3. ^{210}Pb profiles at the adjacent-exposed (A) and breakwater-protected (B) sites. At both sites, activities are variable with depth and only minimum accumulation rates can be calculated. These rates are >1.9 cm/y for the adjacent-exposed site and >1.6 cm/y for the breakwater-protected site.

Summary of sediment data

Surficial sediment (upper 10 cm) at the adjacent-exposed site has an average median diameter of 2.5±0.03 phi (176.8 μm) and an average organic content of 1.3±0.3%. Surficial sediment at the breakwater-protected site has an average median diameter of 2.1±0.03 phi (233.3 μm) and an average organic content of 0.7±0.04%. Grain size is statistically finer ($p < 0.0001$) and more organic ($p = 0.02$) at the adjacent-exposed site than the breakwater-protected site.

The ^{210}Pb profiles at both sites have variable activities with depth. However, grain size is relatively uniform throughout both cores, except for a fine and organic layer 30-90-cm deep in the adjacent-exposed vibracore profile. However, ^{210}Pb activities are variable above and below this layer, suggesting that while this layer may be affected by grain size, the rest of the profile is not. Thus, the initial activity of ^{210}Pb has likely changed, and only a minimum accumulation rate of >1.9 cm/y can be calculated for the adjacent-exposed site. At the breakwater-protected site, ^{210}Pb activities are also variable and the minimum sediment accumulation rate if >1.6 cm/y, representing the pre-construction sedimentation rate.

At the breakwater-protected site, there is no obvious change in either the grain-size or organic-content vibracore profile. It is assumed that there is also no significant change in the sedimentation rate, and so the post-construction rate would be equal to the pre-construction rate. If the post-construction rate (>1.6 cm/y) is applied to the breakwater age (18 y), then the depth of breakwater influence is >29 cm. Note that this is a minimum estimate.

SAV Data:

Table SCH2. Characteristics of the SAV *Ruppia maritima* growing at the adjacent-exposed and breakwater-protected sites, values are reported as mean ±SE.

Location	Species	Shoot Length (cm)	Root Length (cm)	Above-ground Biomass (g m^{-2})	Below-ground Biomass (g m^{-2})	Total Biomass (g m^{-2})	Ratio Above-/ Below-ground Biomass
Adjacent-exposed	*Ruppia maritima*	21.2± 0.6	8.4± 0.3	86.6± 8.6	9.5± 0.9	96.2± 9.1	9.2± 0.9
Breakwater-protected	*Ruppia maritima*	15.4± 0.4	9.1± 0.3	43.3± 11.7	11.2± 2.3	54.5± 13.3	4.1± 1.1

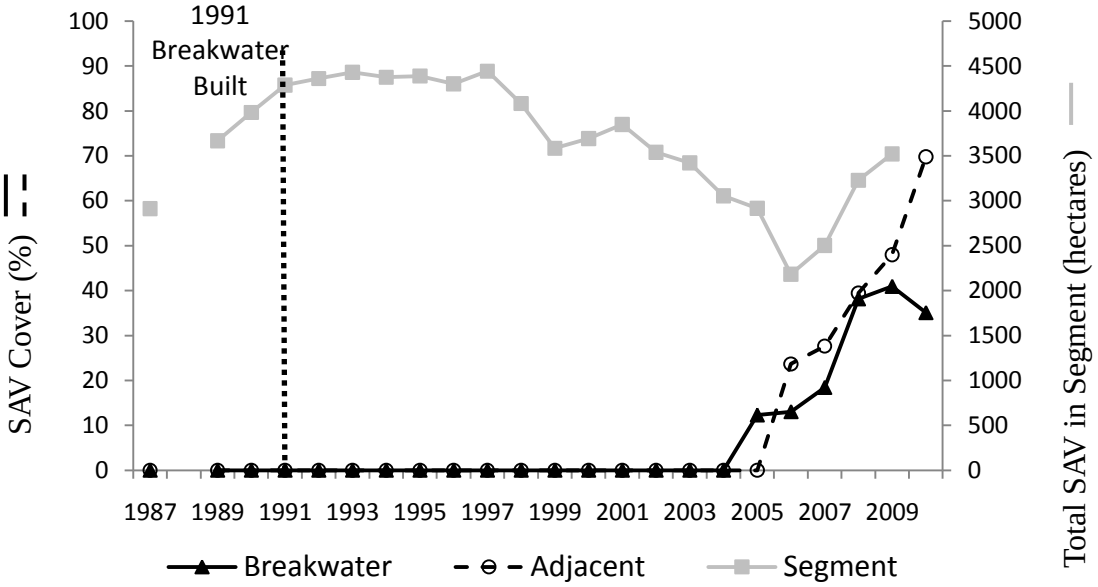

Figure SCH4. SAV % cover plotted against the total SAV in the bay segment as determined by VIMS aerial photography from 4 years prior to breakwater installation to 2010.

Ruppia maritima

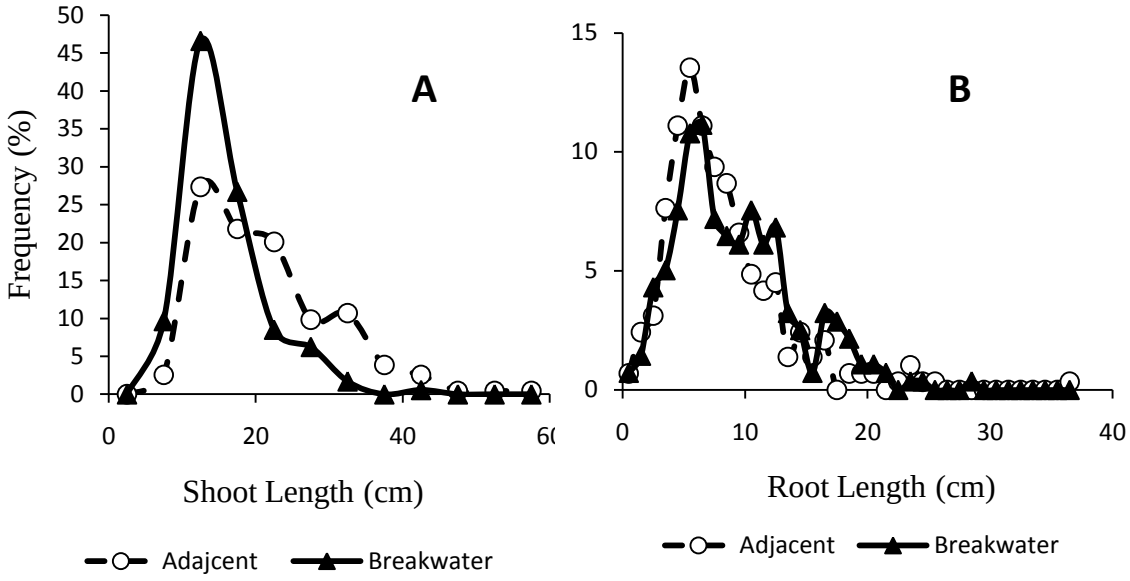

Figure SCH5. (A) Shoot- and (B) root-length frequency plots for *Ruppia maritima* at the adjacent-exposed (open circles) and breakwater-protected (closed triangle) sites.

Ruppia maritima

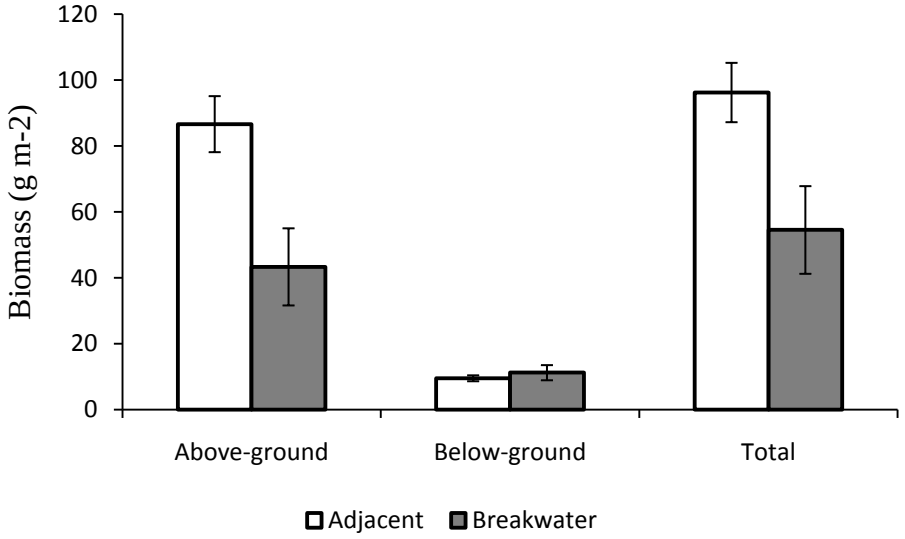

Figure SCH6. Biomass of the all species of SAV at the adjacent-exposed (open bars) and breakwater-protected (closed bars) sites.

Summary of SAV data:

SAV abundance in the segment containing the Schley site declined fairly consistently from 1987-2006 then it increased from 2007-2009. At Schley, SAV was absent in both the adjacent and breakwater sampling sites until 2005 when grass appeared in the breakwater site, 14 years after breakwater installation. This increase coincided with the increase in overall segment totals. Though % cover is fairly similar, higher % cover is noted in the adjacent site when compared with the breakwater site from 2005-2010.

R. maritima total biomass is greater ($p = 0.03$) at the adjacent-exposed site than at the breakwater-protected. Shoot length is longer ($p < 0.0001$) at this site as is root length ($p = 0.02$).

REFERENCES

Ailstock, M. S., D. J., Shafer and A.D. Magoun, A.D. 2010. Effects of Planting Depth, Sediment Grain Size, and Nutrients on *Ruppia maritima* and *Potamogeton perfoliatus* Seedling Emergence and Growth. Restoration Ecology 18: 574-583.

Airoldi, L., M. Abbiati, M.W. Beck, S.J. Hawkins, P.R. Jonsson, D. Martin, P.S. Moschella, A. Sundelof, R.C. Thompson, and P. Aberg. 2005. An ecological perspective on the deployment and design of low-crested and other hard coastal defense structures. Coastal Engineering 52: 1073-1087.

Aller, R. C. and J. K. Cochran. 1976. Th-234-U-238 disequilibrium in near-shore sediment - particle reworking and diagenetic time scales. Earth and Planetary Science Letters 29: 37-50.

Annotated Code of Maryland's Environmental Article Section 16-201, 2008.

Arnold, R.R., J.C. Cornwell, W.C. Dennison, and J.C. Stevenson. 2000. Sediment-based reconstruction of submersed aquatic vegetation distribution in the Severn River, a sub-estuary of Chesapeake Bay. Journal of Coastal Research 16: 188-195.

Asaeda, T., L. Rajapakse, and M. Kanoh. 2009. Fine sediment retention as affected by annual shoot collapse: *Sparganium erectum* as an ecosystem engineer in a lowland stream 26: 1153-1169.

Bacchiocchi, F., and L. Airoldi. 2003. Distribution and dynamics of epibiota on hard structures for coastal protection. Estuarine, Coastal and Shelf Science 56: 1157-1166.

Barko, J.W., and R.M. Smart. 1983. Effects of organic matter additions to sediment on the growth of aquatic plants. Journal of Ecology 71: 161-175.

Barko, J.W., and R.M. Smart. 1986. Sediment-related mechanisms of growth limitation in submersed macrophytes. Ecology 67: 1328-1340.

Batiuk, R.A., R.J. Orth, K.A. Moore, W.C. Dennison, J.C. Stevenson. 1992. Chesapeake Bay submerged aquatic vegetation habitat requirements and restoration targets: a technical synthesis. Virginia Institute of Marine Science report CBP/TRS-83/92.

Berman, M.R., H. Berquist, S. Dewing, J. Glover, C.H. Hershner, T. Rudnicky, D.E. Schatt, and K. Skunda. 2000. Mathews County shoreline situation report. Special Report in Applied Marine Science and Ocean Engineering 364, Comprehensive Coastal Inventory Program, Virginia Institute of Marine Science.

Birben, A.R., I.H. Ozolcer, S. Karasu, and M.I. Komurcu. 2007. Investigation of the effects of offshore breakwater parameters on sediment accumulation. Ocean Engineering 34: 284-302.

Bird, E.C.F. 1993. Submerging coasts: the effects of rising sea level on coastal environments. Wiley, Chichester.

Bos, A.R., T.J.Bouma, T.J., de Kort, G.L.J., and van Katwijk, M.M. 2007. Ecosystem engineering by annual intertidal seagrass beds: sediment accretion and modification. Estuarine, Coastal and Shelf Science 74: 344-348.

Bruland, K.W., M. Koide, and E.D. Goldberg. 1974. The comparative marine geochemistries of Lead 210 and Radium 226. Journal of Geophysical Research 79: 3083-3086.

Brush, G.S., E.A. Martin, R.S. Defries, and C.A. Rice. 1982. Comparisons of Pb-210 and pollen analysis for determining rates of estuarine sediment accumulation. Quaternary Research 18: 196-217.

Bulleri, F. and M.G. Chapman. 2010. The introduction of coastal infrastructure as a driver of change in marine environments. Journal of Applied Ecology 47: 26-35.

Busch, K.E., R.R. Golden, T.A. Parham, L.P. Karrh, M.J. Lewandowski, and M.D. Naylor. 2010. Large-Scale *Zostera marina* (eelgrass) Restoration in Chesapeake Bay, Maryland, USA. Part I: A Comparison of Techniques and Associated Costs. Restoration Ecology 18: 490-500.

Caffrey, J.M., and W.M. Kemp. 1991. Seasonal and special patterns of oxygen production, respiration and root-rhizome release in *Potamogeton perfoliatus* L. and *Zostera marina* L. Aquatic Botany 40:109-128.

Capone, D.G., and R.P. Kiene. 1988. Comparison of microbial dynamics in marine and freshwater sediments: Contrasts in anaerobic carbon catabolism. Limnology and Oceanography 33: 725-749.

Chasten, M.A., J.D. Rosati, and J.W. McCormick. 1994. Engineering design guidance for detached breakwaters and shoreline stabilization structures. United States Army Corps of Engineers. Technical Report CERC-93-19.

Chesapeake Bay Program, 2004. Chesapeake Bay Program Analytical Segmentation Scheme: revisions, decisions, and rationales 1983-2003. Available at http://www.chesapeakebay.net/content/publications/cbp_13272.pdf.

Chesapeake Bay Program, Tidal Sediment Task Force of the Sediment Work Group, 2005. Sediment in the Chesapeake Bay and management issues: tidal erosion processes. CBP-TRS276-05.

Church, J.A., and N.J. White. 2006. 20th century acceleration in global sea-level rise. Geophys Research Letters. doi: 10.1029/2005GL024826.

Corona, A., L.A. Soto, and A.J. Sanchez. 2000. Epibenthic amphipod abundance and predation efficiency of the pink shrimp *Farfantepenaeus duorarum* (Burkenroad, 1939) in habitats with different physical complexity in a tropical estuarine system. Journal of Experimental Marine Biology and Ecology 253: 33-48.

Dalal, V.P., J.E. Baker, and R.P. Mason. 1999. Environmental assessment of Poplar Island dredge material placement site, Talbot County, Maryland. Estuaries 22: 770-784.

Davis, J.L.D., L.A. Levin, and S.M. Walther. 2002. Artificial armored shorelines: sites for open-coast species in Southern California Bay. Marine Biology 140: 1249-1262.

Davis, G.H. 1987. Land subsidence and sea level rise on the Atlantic coastal plain of the United States. Environmental Geology and Water Science 10: 67-80.

Dennison, W.C., R.J. Orth, K.A. Moore, J.C. Stevenson, V. Carter, S. Kollar, P.W. Bergstrom, and R.A. Batiuk. 1993. Assessing water quality with submersed aquatic vegetation. Bioscience 43: 86-94.

Dibb, J.E. and D.L. Rice. 1989a. Temporal and special distribution of Beryllium-7 in the sediments of the Chesapeake Bay. Estuarine, Coastal and Shelf Science 28: 395-400.

Dibb, J.E. and D.L. Rice. 1989b. The geochemistry of Beryllium-7 in Chesapeake Bay. Coastal and Shelf Science 28: 379-394.

Duarte, C.M. 1991. Seagrass depth limits. Aquatic Botany 40: 363-377.

Erftemeijer, P.L.A. and E.W. Koch. 2001. Chapter 18: Sediment geology methods for seagrass habitat. In: Global seagrass research methods. F.T. Short and R.G. Coles (eds) Elsevier Science B.V. 345-367.

Fonseca, M.S., J.S. Fisher, J.C. Zieman, and G.W. Thayer. 1981. Influence of the seagrass, *Zostera marina* L., on current flow. Estuarine, Coastal and Shelf Science 15: 351-364.

Fonseca, M.S., and J.S. Fisher. 1986. A comparison of canopy friction and sediment movement between four species of seagrass with reference to their ecology and restoration. Marine Ecology Progress Series 29: 15-22.

Fonseca, M.S., and J.A. Cahalan. 1992. A preliminary evaluation of wave attenuation by four species of seagrass. Estuarine, Coastal and Shelf Science 35: 565-576.

French, P.W. 1997. Coastal and Estuarine Management. Routledge, London.

Gacia, E., T.C. Granata, and C.M. Duarte. 1999. An approach to measurement of particle flux and sediment retention within seagrass (*Posidonia oceanica*) meadows. Aquatic Botany 65: 255-268.

Gacia, E., and C.M Duarte. 2001. Sediment retention by Mediterranean *Posidonia oceanica* meadow: the balance between deposition and resuspension. Estuarine, Coastal and Shelf Science 52: 505-514.

Gambi, M.C., A.R.M. Nowell, and P.A. Jumars. 1990. Flume observations on flow dynamics in *Zostera marina* (eelgrass) beds. Marine Ecology Progress Series 61: 159-169.

Goodbred, S.L. and S.A. Kuehl. 1998. Floodplain processes on the Bengal Basin and the storage of Ganges-Brahmaputra river sediment: an accretion study using Cs-137 and Pb-210 geochronology. Sedimentary Geology 121: 239-258.

Hardaway, C.S., and J.R. Gunn. 2010. Design and performance of headland bays in Chesapeake Bay, USA. Coastal Engineering 57: 203-212.

Heilman, M.A., and R.G. Carlton. 2001. Methane oxidation associated with submersed vascular macrophytes and its impact of plant diffusive methane flux. Biogeochemistry 52: 207-224.

Hendriks, I.E., T. Sintes, T.J. Bouma, and C.M. Duarte. 2008. Experimental assessment and modeling evaluation of the effects of the seagrass *Posidonia oceanica* on flow and particle trapping. Marine Ecology Progress Series 356: 163-173.

Hengst, A., J. Melton, and L. Murray. Estuarine restoration of submersed aquatic vegetation: the nursery bed effect. Restoration Ecology 18: 605-614.

Hicks, S.D., H.A. Debaugh, and L.E. Hickman. 1983. Sea level variation for the United States 1955-1980. U.S. Dept of Commerce, NOAA, Rockville, MD.

Hobbs, C.H., J.P. Halka, R.T. Kerhin, and M.J. Carron. 1992. Chesapeake Bay sediment budget. Journal of Coastal Research 8: 292-300.

Holdahl, S.R., and N.L. Morrison. 1974. Regional investigations of vertical crustal movements in the U.S., using precise relevelings and mareograph data. Tectonophysics 23: 373-390.

Inman, M. 2010. Working with water. Nature Reports Climate Change. Published online: 6 April 2010. doi:10.1038/climate.2010.28

Infantes, E., J. Terrados, A. Orfila, B. Canellas, and A. Alvarez-Ellacuria. 2009. Wave energy and the upper depth limit distribution of *Posidonia oceanica*. Botanica Marina 52: 419-427.

Jaeger, J.M., C.A. Nittrouer, N.D. Scott, and J.D. Milliman. 1998. Sediment accumulation along a glacially impacted mountainous coastline: north-east Gulf of Alaska. Basin Research 10: 155-173.

James, T.R., M.J. Chimney, B. Sharfstein, D.R. Engstrom, S.P. Schottler, T. East, and K. Jin. 2008. Hurricane effects on shallow lake ecosystem, Lake Okeechobee, Florida (USA). Fundamental and Applied Limnology 172: 273-287.

Jones, J.I., J.W. Eaton, and K. Hardwick. 2000. The influence of periphyton on boundary layer conditions: pH microelectrode investigation. Aquatic Botany 67: 191-206.

Karrh, L. 2000. Effects of breakwaters on submerged vegetation. Maryland Department of Natural Resources, pp. 1-44.

Kearney, M.S., and J.C. Stevenson. 1991. Island land loss and marsh vertical accretion rate evidence for historical sea-level changes in Chesapeake Bay. Journal of Coastal Research 7: 403-415.

Kearney, M.S., A.S. Rogers, J.R.G. Townshend, J.C. Stevenson, J. Stevens, E. Rizzo, and K. Sundberg. 2002. Landsat imagery shows decline of coastal marshes in Chesapeake and Delaware Bays. Eos, Transactions, American Geophysical Union 83: 177-178.

Kemp, W.M., R. Batiuk, R. Bartleson, P. Bergstrom, V. Carter, C.L. Gallegos, W. Hunley, L. Karrh, E.W. Koch, J.M. Landwehr, K.A. Moore, L. Murray, M. Naylor, N.B. Rybicki, J.C. Stevenson, and D.J. Wilcox. 2004. Habitat requirements for submerged aquatic vegetation in Chesapeake Bay: Water quality, light regime, and physical-chemical factors. Estuaries 27: 363-377.

Kemp, W. M., R. Batiuk, R. Bartleson, P. Bergstrom, V. Carter, C.L. Gallegos, W. Hunley, L. Karrh, L., E.W. Koch, J.M. Landwehr, K.A. Moore, L. Murray, M. Naylor, N.B. Rybicki, J.C Stevenson, and D.J. Wilcox. 2004. Habitat requirements for submerged aquatic vegetation in Chesapeake Bay: water quality, light regime, and physical-chemical factors. Estuaries 27: 363-377.

Kenworthy, W.J., J.C Zieman, and G.W. Thayer. 1982. Evidence for the influence of seagrass on the benthic Nitrogen cycle in a coastal plain estuary near Beaufort, North Carolina (USA). Oecologia 54: 152-158.

Kerhin, R.T., J.P. Halka, D.V Wells, E.L. Hennessee, P.J. Blakeslee, N. Zoltan, and R.H. Cuthbertson. 1988. Chesapeake Bay Earth Science Study (CBESS): Physical properties of surficial sediments, Chesapeake Bay, Maryland. Maryland Geological Survey.

Kim, G., N. Hussain, J.R. Scudlark, and T.M. Church. 2000. Factors influencing the atmospheric depositional fluxes of stable Pb, Pb-210, and Be-7 into Chesapeake Bay. Journal of Atmospheric Chemistry 36: 65-79.

Kleeberg, A., J. Kohler, T. Sukhodolova, and A. Sukhodolov. 2010. Effects of aquatic macrophytes on organic matter depositions, resuspension and phosphorus entrainment in a lowland river. Freshwater Biology 55: 326-345.

Koch, E.W. 1994. Hydrodynamics, diffusion-boundary layers and photosynthesis of the seagrass *Thalassia testudinum* and *Cymodocea nodosa*. Marine Biology 118: 767-776.

Koch, E.W. and S. Beer. 1996. Tides, light and the distribution of *Zostera marina* in Long Island Sound, USA. Aquatic Botany 53: 97-107.

Koch, E.W. 1999. Sediment resuspension in a shallow *Thalassia testudinum* banks ex Konig bed. Aquatic Botany 65: 269-280.

Koch, E.W. 2001. Beyond light: Physical, geological, and geochemical parameters as possible submersed aquatic vegetation habitat requirements. Estuaries 24: 1-17.

Koch, E.W., L.P. Sanford, S.N. Chen, D.J. Shafer, and J.M. Smith. 2006. Waves in Seagrass Systems: Review and Technical Recommendations. Army Corps of Engineers Technical report ERDC TR-06-15.

Koch, E.W., M.S. Ailstock, D.M. Booth, D.J. Shafer, and A.D. Magoun. 2010. The Role of Currents and Waves in the Dispersal of Submersed Angiosperm Seeds and Seedlings. Restoration Ecology 18: 584-595.

Komar, P. D., and S.M. Shih. 1993. Cliff erosion along the Oregon coast: a tectonic-sea level imprint plus local controls by beach processes. Journal of Coastal Research 9: 747-765.

Krause-Jensen, D., J. Carstensen, S.L. Nielsen, T. Dalsgaard, P.B. Christensen, H. Fossing, and M.B. Rasmussen. 2011. Sea bottom characteristics affect depth limits of eelgrass *Zostera marina* 425: 91-102.

Kreiling, R.M., Y. Yin, and D.T. Gerber. 2007. Abiotic influences on the biomass of *Vallisneria americana* Michx in the upper Mississippi River. River Research and Applications 23: 343-349.

Langland, M. and T. Cronin (eds.) 2003. A summary report of sediment processes in Chesapeake Bay and watershed. Water-Resources Investigations Report 03-4123.

Larsen, I.L. and N.H. Cutshall. 1981. Direct determination of ^{7}Be in sediments. Earth and Planetary Science Letters 54: 379-384.

Lathrop, R.G. Jr., and J.A. Bognar. 1997. Monitoring Habitat loss and alteration in the Barnegat Bay region, eds. Filmlin, G.E. Jr., and M.J. Kennish, The Barnegat Bay Ecosystem Workshop. Cooperative Extension of Ocean County, Toms River, N.J. pp. 243-253.

Lazzari, M.A., and B.Z. Stone. 2006. Use of submerged aquatic vegetation as habitat by young-of-the-year epibenthic fishes in shallow Maine nearshore waters. Estuarine Coastal and Shelf Science 69: 591-606.

Leschen, A.S., K.H. Ford, and N.T. Evans. 2010. Successful eelgrass (*Zostera marina*) restoration in a formerly eutrophic estuary (Boston Harbor) supports the use of a multifaceted watershed approach to mitigating eelgrass loss. Estuaries and Coasts 33: 1340-1345.

Living Shoreline Summit Steering Committee. 2006. Proceedings of the 2006 Living Shoreline Summit, Chesapeake Bay, CRC Publ. No. 08-164.

Loreau, M., S. Naeem, and P. Inchausti. 2002. Biodiversity and Ecosystem Functioning – Synthesis and Perspectives. Oxford University Press, Oxford.

Ma, H.G., H. Townsend, X.S. Zhang, M. Sigrist, and V. Christensen. 2010. Using fisheries ecosystem model with water quality model to explore trophic and habitat impacts on a fisheries stock: A case study of the blue crab population in the Chesapeake Bay. Ecological Modeling 221: 997-1004.

Makkay, K., F.R. Pick, and L. Gillespie. 2008. Predicting diversity versus community composition of aquatic plants at the river scale. Aquatic Botany 88: 338-346.

Marcus, W.A. and M.S. Kearney. 1991. Upland and coastal sediment sources in Chesapeake Bay estuary. Annals of the Association of American Geographers 81: 408-424.

Martin, M., F. Bertasi, M.A. Colangelo, M. de Vries, M. Frost, S.J. Hawkins, E. Macpherson, P.S. Moschella, M.P. Satta, R.C. Thompson, and V.U. Ceccherelli. 2005. Ecological impact of coastal defense structures on sediment and mobile fauna: Evaluating and forecasting consequences of unavoidable modifications of native habitats. Coastal Engineering 52: 1027-1051.

Martins, G.M., A.F. Amaral, F.M. Wallenstein, and A.I. Neto. 2009. Influence of a breakwater on nearby rocky intertidal community structure. Marine Environmental Research 67: 237–245.

McKee, B. A., C.A. Nittrouer, D.J. DeMaster. 1983. Concepts of sediment deposition and accumulation applied to the continental shelf near the mouth of the Yangtze River. Geology 11: 631-633.

Mills, W.B., C. Chung, and K. Hancock. 2005. Predictions of relative sea-level change and shoreline erosion over the 21st century on Tangier Island, Virginia. Journal of Coastal Research 21: 36-51.

Moore, K.A., E.C. Shields, and J.C. Jarvis. 2010. The Role of Habitat and Herbivory on the Restoration of Tidal freshwater submerged Aquatic Vegetation Populations. Restoration Ecology 18: 596-604.

Moschella, P.S., M. Abbiati, P. Aberg, L. Airoldi, J.M. Anderson, F. Bacchiocchi, F. Bulleri, G.E. Dinesen, M. Frost, E. Gacia, L. Granhag, P.R. Jonsson, M.P. Satta, A. Sundelof, R.C. Thompson, and S.J. Hawkins. 2005. Low-crested defense structures as artificial habitats for marine life: using ecological criteria in design. Coastal Engineering 52: 1053-1071.

Neelamani, S., and N. Sandhya. 2004. Wave reflection, run-up, run-down and pressures on plane, denated and serrated seawalls. Coastal Engineering Journal 46: 141-169.

Newbolt, C.H., G.R. Hepp, and C.W. Wood. 2008. Characteristics of Sediments Associated with Submersed Plant Communities in the Lower Mobile River Delta, Alabama. Journal of Aquatic Plant Management 46: 107-113.

Nishihara, G.N., and J.D. Ackerman. The effect of hydrodynamics on the mass transfer of dissolved inorganic carbon to the freshwater macrophyte *Vallisneria americana*. Limnology and Oceanography 51:2734-2745.

Nittrouer, C.A., R.W. Sternberg, R. Carpenter, and J.T. Bennett. 1979. The use of Pb-210 geochronology as a sedimentological tool: application to the Washington continental shelf. Marine Geology 31: 297-326.

Nordstrom, K.F., U. Gamper, G. Fontolan, A. Bezzi, and N.L. Jackson. 2009. Characteristics of coastal dune topography and vegetation in environments recently modified using beach fill and vegetation plantings, Veneto, Italy. Environmental Management 44: 1121-1135.

Olsen, C.R., I.L. Larsen, P.D. Lowry, and N.H. Cutshall. 1986. Geochemistry and deposition of ^{7}Be in river-estuarine and coastal waters. Journal of Geophysical Research 91: 896-908.

Orth, R.J., and K.A. Moore. 1983. Chesapeake Bay: an unprecedented decline in submerged aquatic vegetation. Science 222: 51-53.

Orth, R.J., and K.A. Moore. 1984. Distribution and abundance of submerged aquatic vegetation in Chesapeake Bay: a historical perspective. Estuaries 7: 531-540.

Orth, R.J., R.A. Batiuk, P.W. Bergstrom, and K.A. Moore. 2002. A perspective on two decades of policies and regulations influencing the protection and restoration of submerged aquatic vegetation in Chesapeake Bay, USA. Bulletin of Marine Science 71: 1391-1403.

Orth, R.J., T.J.B. Carruthers, W.C. Dennison, C.M. Duarte, J.W. Fourqurean, K.L. Jr. Heck, A.R. Hughes, G.A. Kendrick, W.J. Denworthy, S. Olyarnik, F.T. Short, M. Waycott, and S.L. Williams. 2006. A global crisis for seagrass ecosystems. Bioscience 56: 987-996.

Orth, R.J., and S.R. Marion. 2008. Restoration of eelgrass communities in Chesapeake Bay with seeds: The emerging issues. Final Report. National Oceanic and Atmospheric Administration. Award Number NA03NMF4570250463.

Orth, R.J., D.J. Wilcox, J.R. Whiting, L.S. Nagey, A.L. Owens, and A.K. Kenne. 2009. 2008 distribution of submerged aquatic vegetation in Chesapeake Bay and Coastal Bays. Special Scientific Report 152. Virginia Institute of Marine Science, Gloucester Point, USA.

Orth, R.J., M.R. Williams, S.R. Marion, D.J. Wilcox, T.J.B. Carruthers, K.A. Moore, W.C. Dennison, N. Rybicki, P. Bergstrom, R.A. Batiuk. 2010. Long-Term Trends in Submersed Aquatic Vegetation (SAV) in Chesapeake Bay, USA, Related to Water Quality. Estuaries and Coasts 33: 1144-1163.

Palinkas, C.M. and E.W. Koch, in review. Sediment accumulation rates and SAV distributions in the mesohaline Chesapeake Bay, USA. Estuaries and Coasts.

Palinkas, C. M., E. W. Koch, N. Barth. 2010. Sedimentation adjacent to naturally eroding and breakwater-protected shorelines in Chesapeake Bay. IOP Conference Series: Earth and Environmental Science 9: doi:10.1088/1755-1315/9/1/012012.

Palinkas, C.M. and C.A. Nittrouer. 2006. Clinoform sedimentation along the Apennine shelf, Adriatic Sea. Marine Geology 234: 245-260.

Palinkas, C.M., C.A. Nittrouer, R.A. Wheatcroft, and L. Langone. 2005. The use of ^{7}Be to identify event and seasonal sedimentation near the Po River delta, Adriatic Sea. Marine Geology 222-223: 95-112.

Pan, G., B. Yang, D. Wang, H. Chen, B. Tian, M. Zhang, X. Yuan, J. Chen. 2011. In-lake algal bloom removal and submerged vegetation restoration using modified local soils. Ecological Engineering 37: 302-308.

Peterson, C.H., R.A. Jr. Luettich, F. Micheli, and G.A. Skilleter. 2004. Attenuation of water flow inside seagrass canopies of differing structure. Marine Ecology Progress Series 268: 81-92.

Rosenzweig, M.S. 1994. On the life history, systematic and ecology of Ruppia maritima L. (Potamogetonaceae) in lower Chesapeake Bay. Doctoral Thesis Dissertation pp 1-172.

Rybicki, N.B., and J.M. Landwehr. 2007. Long-term changes in abundance and diversity of macrophyte and waterfowl populations in an estuary with exotic macrophytes and improving water quality. Limnology and Oceanography 52: 1195-1207.

Sagova-Mareckova, M., A. Petrusek, and J. Kvet. 2009. Biomass production and nutrient accumulation in *Sparganium emersum* Rehm. After sediment treatment with mineral and organic fertilizers in the three mesocosm experiments. Aquatic Ecology 43: 903-913.

Sand-Jensen, K., C. Prahl, and H. Stockholm. 1982. Oxygen release from roots of submerged aquatic macrophytes. Oikos 38: 349-354.

Sanford, L. P., S.E. Suttles, and J.P. Halka. 2001. Reconsidering the physics of the Chesapeake Bay estuarine turbidity maximum. Estuaries 24: 655-669.

Schanz, A., and H. Asmus. 2003. Impact of hydrodynamics on development and morphology of intertidal seagrasses in the Wadden Sea. Marine Ecology Progress Series 261: 123-134.

Shafer, D., and P. Bergstrom. 2010. An introduction to a special issue on large-scale submerged aquatic vegetation restoration research in the Chesapeake Bay: 2003-2008. Restoration Ecology 18: 481-489.

Short, F.T. 1987. Effects of sediment nutrients on seagrasses: Literature review and mesocosm experiment. Aquatic Botany 27: 41-57.

Short, F.T., B. Polidoro, S.R. Livingstone, K.E. Carpenter, S. Bandeira, J.S. Bujang, H.P. Calumpong, T.J.B. Carruthers, R.G. Coles, W.C. Dennison, P.L.A. Erftemeijer, M.D. Fortes, A.S. Freeman, T.G. Jagtap, A.M.H. Kamal, G.A. Kendrick, W.J. Kenworthy, Y.A. La Nafie, I.M. Nasution, R.J. Orth. 2001. Extinction risk assessment of the world's seagrass species. Biological Conservation 144:1961-1971.

Silva, J.F., R.W. Duck, and J.B. Catarino. 2009. Nutrient retention in the sediments and the submerged aquatic vegetation of the costal lagoon of the Ria de Aveiro, Portugal. Journal of Sea Research 62: 276-285.

Smith, K.A., E.W. North, F. Shi, S. Chen, R.R. Hood, E.W. Koch, and R.I.E. Newell. 2009. Modeling the effects of oyster reefs and breakwaters on seagrass growth. Estuaries and Coasts 32: 748-757.

Sokal, R. R. and F. J. Rohlf. 1995. Biometry: the principles and practice of statistics in biological research. 3rd edition. W. H. Freeman and Co.: New York. 887 pp. ISBN: 0-7167-2411-1.

Sommerfield, C.K. and C.A. Nittrouer. 1999. Modern accumulation rates and sediment budget for the Elf shelf: a flood-dominated depositional environment. Marine Geology 154: 227-241.

Sommerfield, C.K., C.A. Nittrouer, and C.R. Alexander. 1999. ^{7}Be as a tracer of flood sedimentation on the northern California continental margin. Continental Shelf Research 19: 335-361.

Stamos, D.G. and M.R. Hajj. 2001. Reflection and transmission of waves over submerged breakwaters. Journal of Engineering Mechanics 127: 99-105.

Steward, J.S., R.W. Virnstein, L.J. Morris, and E.F. Lowe. 2005. Setting Seagrass Depth, Coverage and Light Targets for the Indian River Lagoon System, Florida. Estuaries 28: 923-935.

Titus, J.G., R.A. Park, S.P. Leatherman, J.R. Weggel, M.S. Greene, P.W. Mausel, S. Brown, G. Gaunt, M. Trehan, and G. Yohe. 1991. Greenhouse effect and sea level rise: The cost of holding back the sea. Coastal Management 19: 171-204.

Titus, J.G. and V.K. Narayanan. 1995. The probability of sea level rise. United States Environmental Protection Agency, Office of Policy, Planning, and Evaluation (2122), EPA 230-R-95-008, Washington, DC, 186 pp.

Titus, J.G. and C. Richman. 2001. Maps of lands vulnerable to sea level rise: modeled elevations along the US Atlantic and Gulf coasts. Climate Research 18: 205-228.

US Army Corps Coastal Engineering Manual. 2008. EM 1110-2-1100, pp. 1-2059.

Ward, L.G., W.M. Kemp, and W.R. Boynton. 1984. The influence of waves and seagrass communities on suspended particulates in an estuarine embayment. Marine Geology 59: 85-103.

Waycott, M., C.M. Duarte, T.J.B. Carruthers, R.J. Orth, W.C. Dennison, S. Olyarnik, A. Calladine, J.W. Fourqurean, K.L. Heck, A.R. Hughes, G.A. Kendrick, W.J. Kenworthy, F.T. Short, and S.L. Williams. 2009. Accelerating loss of seagrass across the globe threatens coastal ecosystems. Proceedings of the National Academy of Sciences of the United States of America 106: 12377-12381.

Wicks, E.C., E.W. Koch, J.M. O'Neil, and K. Elliston. 2009. Effects of sediment organic content and hydrodynamic conditions on the growth and distribution of *Zostera marina*. Marine Ecology Progress Series 378: 71-80.

Widdows, J., N.D. Pope, M.D. Brinsley, H. Asmus, and R.M. Asmus. 2008. Effects of seagrass beds (*Zostera noltii* and Z. marina) on near-bed hydrodynamics and sediment resuspension. Marine Ecology Progress Series 358: 125-136.

Winkel, A., and J. Borum. 2009. Use of sediment CO2 by submersed rooted plants. Annals of Botany 103: 1015-1023.

Wray, R.D., S.P. Leatherman, and R.J. Nicholls. 1995. Historic and future land loss of upland and marsh islands in the Chesapeake Bay, Maryland, U.S.A. Journal of Coastal Research 11: 1195-1203.

Yarbro, L.A., P.R. Carlson, T.R. Fisher, J.P. Canton, and W.M. Kemp. 1983. A sediment budget for the Choptank River estuary in Maryland, USA. Estuarine, Coastal and Shelf Science 17: 307-323.

Ye, C., H. Yu, H. Kong, X. Song, G. Zou, Q. Xu, and J. Liu. 2009. Community collocation of four submerged macrophytes on two kinds of sediments in Lake Taihu, China. Ecological Engineering 35: 1656-1663.

Zhang, C.Y. and X.L. Feng. 2011. Natural and human-induced effects on grain size of surface sediments along the Lianyungang muddy coast, China. Chinese Journal of Oceanology and Limnology 29: 387-397.